



The  
University  
Of  
Sheffield.

---

Integrated Cell and Bioprocess Engineering  
for Rapid and Intensive Continuous  
Production of Biopharmaceuticals

---

A thesis submitted in partial fulfilment of the requirements for the degree  
of Doctor of Philosophy

The University of Sheffield  
Department of Chemical & Biological Engineering

September 2020

**William Morgan-Evans**

Supervised by David. C James & Adam. J Brown  
Sponsored by CPI

---

## DECLARATION

I, William Morgan-Evans, confirm that the Thesis is my own work. I am aware of the University's Guidance on the Use of Unfair Means. This work has not previously been presented for an award at this, or any other, university.

---

## ABSTRACT

---

Continuous upstream processing is becoming increasingly popular for the industrial production of biopharmaceuticals. Despite this, cell line and process development remains reliant on batch-wise experimentation to acquire data; this approach is time consuming, costly and labour intensive as the demands put upon these processes increase. A shift to continuous experimentation, with perfusion utilised to keep cells sustained for longer periods with continual testing, may alleviate these demands. However, the lack of small-scale, high throughout perfusion systems makes this difficult to achieve. For the commercial systems that are available, the cell retention technology employed is frequently not compatible with familiar labware, instead requiring dedicated equipment for successful operation. This makes adoption with existing development protocols challenging.

Microcarriers have been used previously to adhere CHO cells in suspension culture. Microcarriers are easily handled, scalable and compatible with many vessel formats. Their use as a potential cell retention device has been greatly overlooked. Commercial microcarriers are available, but they often require attachment proteins for cell adhesion, despite the discouragement of animal-derived products in biopharmaceutical processing. The work here has developed an in-house, microsphere-based cell retention device for a suspension-adapted, IgG-producing CHO cell line. Polyethylenimine, an animal origin-free, inexpensive cationic polymer, has been shown to enable the attachment of these cells to vessel surfaces. Alongside this, acrylic-based polyHIPE microspheres with diameters from 270 to 1100  $\mu\text{m}$  have been fabricated at negligible cost. A novel monomer, mono-2-(methacryloyloxy)ethyl succinate, has been included from 2 to 16 % to give the resulting materials increasing carboxyl functionality. These carboxyls have both increased the stability of microspheres in solution and enabled the rapid adsorption of polyethylenimine.

Cell loading, where high cell density suspensions are forced to interact with microspheres, has been introduced as a technique for guaranteed cell retainment. With this method, 30–100 million cells per mL of microspheres were retained within an hour, depending upon conditions used. To demonstrate the versatility of the cell retention device, a pseudo-continuous culture was performed for over 30 days using Erlenmeyer flasks, with continual IgG production demonstrated. A simple perfusion system, employing these microspheres within a modified spinner flask, was also tested. It has been shown here that sophisticated cell retention technology is not necessary for effective retainment of CHO cells. Because of this, continuous processing has been performed in the laboratory without costly equipment or prior experience. It is hoped the data obtained may inspire others to explore continuous operations for the pre-clinical development of biopharmaceuticals.

---

## ACKNOWLEDGEMENTS

---

The data presented in this thesis are, of course, the outcome of my own work, but none of it would have been obtained without the training, expertise, help and encouragement given to me by colleagues at the University of Sheffield. The page here gives credit to these very people.

To start, I would like to thank Jags Pandhal, who acknowledged my email (an incredibly rare event in academia) and kindly guided me to David James, who would later become my supervisor. I wish to thank David for the opportunity in letting me carry out this work, as well as for his tutelage throughout the project. The skills, knowledge and experience I have gained are invaluable and are a direct consequence of his trust in letting me do this project. A thank you, also, to CPI, who sponsored my project, offered me advice and allowed me to use their facilities.

A big thank you to the entire DCJ group, a fantastic team of investigators, who were not afraid to offer their thoughts and ideas when lab presentation time came around! Particular thanks go to Devika Khalsi, who taught me the ways of CHO cell culture from the very beginning; Dr Jaffe, for the discussions and laughs, and Joe Cartwright, for answering my many questions over the years. A nod and thumbs up to James Grinham, a fine technician, problem-solver and friend. I shall miss our early morning lab chats.

The majority of the work was carried out in the Department of Chemical and Biological Engineering, but a considerable amount was also done at the Department of Materials Science and Engineering. The latter housed the Kroto Research Institute; it was here that the biomaterials team kindly took me in and taught me the wonders of polymer fabrication. I thank Fred Claeysens for allowing me to use the labs and learn from the many experts in his group. Particular thanks go to Hossein Bahmaee, who first showed me how to make a polyHIPE; Colin Sherborne, one of the most relentless researchers I've met and a polyHIPE pioneer, and Sam Pashneh-Tala, probably the most resourceful researcher in the university, and the very definition of an engineer.

My time at Sheffield was nothing but a pleasure.

*A big thanks to you all!*

---

To my mother and father — but especially to my mother, who once asked if I have to kill hamsters...

This page intentionally left blank

---

# TABLE OF CONTENTS

---

Abstract	III
Acknowledgements	IV
List of Abbreviations	X
List of Figures	XVII
List of Tables	XVII
Introduction and Thesis Layout	XVIII
<b>1</b>   Literature Review	
I.1 Biologics	I
I.1.1 Biologics Industry	I
I.1.2 Therapeutic Antibodies	2
I.1.3 Indications for Therapeutic Antibodies	6
I.1.4 Expression Systems	8
I.1.5 Chinese Hamster Ovary Cells	II
I.1.6 Stable and Transient Transfection	13
I.1.7 Chemically Defined Bioprocessing	14
I.2 Continuous Bioprocessing	17
I.2.1 Biologics in Batch	17
I.2.2 Perfusion and Continuous Upstream Operations	18
I.2.3 Cell Retention for Perfusion	22
I.2.4 Current Technologies For Continuous Upstream R&D	24
I.3 Polymerised High Internal Phase Emulsions	25
I.3.1 An Introduction to PolyHIPEs	25
I.3.2 Chemistry of PolyHIPEs	27
I.3.3 PolyHIPEs as Cell Culture Scaffolds	29
I.3.4 Commercial PolyHIPE Case Study: <i>Alvetex</i>	30
I.3.5 PolyHIPE Functionalisation	32
I.3.6 PolyHIPE Microspheres	33
I.3.7 Alternative Methods of Microsphere Fabrication	35
I.3.8 Commercial Microcarriers	36
<b>2</b>   Materials and Methods	
2.1 Cell Culture	41
2.1.1 CHO Cell Line Routine Maintenance	41
2.1.2 HEK-293 Cell Line Routine Maintenance	42
2.2 Adhesion Substrates	42
2.2.1 PrestoBlue Cell Viability Reagent for Cell Adherence	42
2.2.2 ValitaTITER for IgG Titre Determination	43
2.2.3 Coating and Screening of Adhesion Substrates	44

---

2.2.4	Adherent Culture Imaging and Growth Tests	46
2.2.5	Adherence Capability for Cell Loading	47
2.2.6	Adhesion Assays	48
2.2.7	Dissociation and Regrowth from Adhesion Substrates	50
2.2.8	Animal Origin-free Dissociation	51
2.2.9	Simple Glucose Concentration Determination	52
2.2.10	Adherent Culture and Mild Hypothermia	53
2.2.11	Cell Loading and Mild Hypothermia	53
2.3	Cell Pausing	55
2.3.1	Temperature Check for Cell Pausing	55
2.3.2	Suspension Pausing and Regrowth	56
2.3.3	Adherent Pausing Imaging	56
2.3.4	Adherent Pausing and Dissociation	57
2.4	PolyHIPE Materials Development	58
2.4.1	Routine HIPE and PolyHIPE Fabrication	58
2.4.2	Scanning Electron Microscopy for PolyHIPES	60
2.4.3	Toluidine Blue Assay Development	61
2.4.4	Carboxyl Functionality Assay using Toluidine Blue	61
2.4.5	Fabrication of PolyHIPE Microspheres	63
2.4.6	Co-Flow Fabrication of Microspheres	64
2.4.7	T-Junction Fabrication of Microspheres	65
2.4.8	T-Junction Fabrication of 'Smaller' Microspheres	66
2.4.9	Pump Speed and Flow Rate of Carrier Phase	66
2.5	Microsphere Applications	67
2.5.1	Microsphere Washing, PEI Adsorption and Sterilisation	67
2.5.2	Syringe Pump Microsphere Loading	68
2.5.3	Microsphere Cell Growth in T-Flasks	69
2.5.4	Peristaltic Pump Microsphere Loading	69
2.5.5	Microsphere Loading using Ambr15 Bioreactors	71
2.6	Pseudo-Continuous Systems	71
2.6.1	Validation of Cedex Bio Analyser	71
2.6.2	Suspension Cell Culture and Mild Hypothermia	72
2.6.3	Pseudo-Continuous Culture using Erlenmeyer Flasks	72
2.7	Perfusion System Development	74
2.7.1	Perfusion System Ideas	74
2.7.2	Perfusion System Set Up	74
2.7.3	Perfusion System Operation	75

---

<b>3</b>	<b> </b>	<b>Adhesion Substrates</b>	
3.1		Introduction to Adhesion Substrates	77
3.1.1		Identification and Testing of Adhesion Substrates	78
3.1.2		Adhesion Assays	94
3.1.3		Dissociation from PEI Substrates	100
3.1.4		PEI Adherence and Mild Hypothermia	107
3.1.5		Conclusions	116
<b>4</b>	<b> </b>	<b>Cell Pausing</b>	
4.1		Introduction to Cell Pausing	119
4.1.1		Suspension Cell Pausing	120
4.1.2		Adherent Cell Pausing	128
4.1.3		Conclusions	133
<b>5</b>	<b> </b>	<b>PolyHIPE Microsphere Technology</b>	
5.1		Introduction to PolyHIPE Materials Development	135
5.1.1		Building in Carboxyl Functionality	136
5.1.2		Co-Flow Fabrication of Microspheres	145
5.1.3		T-Junction Fabrication of Microspheres using Glycerol	159
5.1.4		Conclusions	167
5.2		Introduction to Microsphere Applications	169
5.2.1		PEI Adsorption to Microspheres	170
5.2.2		Cell Loading and Microsphere Cell Growth	172
5.2.3		Ambr15 Bioreactor Cell Loading	185
5.2.4		Conclusions	188
<b>6</b>	<b> </b>	<b>Continuous Bioprocessing Systems</b>	
6.1		Introduction to Pseudo-Continuous Systems	191
6.1.1		Cedex Bio Analyzer and Mild Hypothermic Culture	193
6.1.2		Pseudo-Continuous Systems using Erlenmeyer Flasks	202
6.1.3		Conclusions	214
6.2		Introduction to Continuous Systems	216
6.2.1		Packed-Bed Perfusion	216
6.2.2		Spinner Flask-based Perfusion	225
6.2.3		Conclusions	234
<b>7</b>	<b> </b>	<b>Conclusions and Future Work</b>	
7.1		Conclusions and Evaluation	237
7.2		Future Work	240
		References	247

---

## LIST OF ABBREVIATIONS

---

*Acronyms, initialisms and shorthands used within this thesis*

ATF	Alternating tangential flow
ATP	Adenosine triphosphate
BBS	Borate buffer saline
BHK	Baby hamster kidney
CD CHO	Chemically defined CHO (medium)
CDR	Complementary-determining region
CG	Collagen
CHO	Chinese hamster ovary
CHO-S	Chinese hamster ovary (suspension-adapted)
DHFR	Dihydrofolate reductase
DNA	Deoxyribonucleic acid
DPBS	Dulbecco's phosphate buffer saline
EDTA	Ethylenediaminetetraacetic acid
EHA	2-Ethylhexyl acrylate
ELISA	Enzyme-linked immunosorbent assay
EMA	European medicines agency
Fab	Antigen binding fragment
Fc	Crystallisable fragment
FBS	Foetal bovine serum
FDA	Food and drug administration
FN	Fibronectin
Fv	Variable fragment
GFP	Green fluorescent protein
GS	Glutamine synthetase
HBSS	Hank's balanced salt solution
HEK	Human embryonic kidney
HER2	Human epidermal growth factor receptor 2
HIPE	High internal phase emulsion
HIV	Human immunodeficiency virus
IBOA	Isobornyl acrylate
ID	Internal diameter
Ig(A, D, E, G, M)	Immunoglobulin(A, D, E, G, M)
IL	Interleukin
INN	International nonproprietary name
LM	Laminin
mAb	Monoclonal antibody
MAES	Mono-2-(methacryloyloxy)ethyl succinate
MSX	Methionine sulfoximine
MTX	Methotrexate

---

MW	Molecular weight
pAb	Polyclonal antibody
PB	PrestoBlue
PBS	Phosphate buffered saline
PDL	Poly-D-lysine
PEI	Polyethylenimine
PLO	Poly-L-ornithine
PolyHIPE	Polymerised high internal phase emulsion
PolyLIPE	Polymerised low internal phase emulsion
PolyMIPE	Polymerised medium internal phase emulsion
PTFE	Polytetrafluoroethylene
PVA	Polyvinyl alcohol
PVC	Polyvinyl chloride
qGLT	Cell-specific L-glutamine consumption rate
qP	Cell-specific productivity
RFU	Relative fluorescence unit
rpm	Revolutions per minute
RT	Room temperature
SBTI	Soybean trypsin inhibitor
scFv	Single-chain variable fragment
SD	Standard deviation
SEM	Scanning electron microscopy
TBO	Toluidine blue
TFF	Tangential flow filtration
TMPTA	Trimethylolpropane triacrylate
TNF	Tumour necrosis factor
UV	Ultraviolet
VEG-F	Vascular endothelial growth factor
VN	Vitronectin

This page intentionally left blank

---

## LIST OF FIGURES

---

- FIGURE 1.1 Schematic of an IgG Antibody 4
- FIGURE 1.2 Schematic detailing the four cell culture modes, categorised as either batch, semi-continuous or continuous operation 21
- FIGURE 1.3 Scanning electron micrographs showing the structure differences between *Alvetex Scaffold* and *Alvetex Strata* 31
- FIGURE 2.1 Schematic detailing the workflow of using adhesion substrates on multiwell plates for CHO cell adhesion with subsequent analysis 45
- FIGURE 2.2 Schematic detailing the generation of an acrylic HIPE followed by the fabrication of a PolyHIPE via photopolymerisation 59
- FIGURE 2.3 Skeletal formulae of the acrylate monomers employed for the fabrication of polyHIPE monoliths and microspheres 60
- FIGURE 2.4 Schematic detailing the workflow of generating uniform polyHIPE discs, with increasing amounts of MAES, for the carboxyl functionality assay using TBO 62
- FIGURE 3.1 Screen for optimal coating concentration for animal origin and chemically defined adhesion substrates 79
- FIGURE 3.2 Comparisons of adherent CHO cell growth using animal origin and chemically defined adhesion substrates on three base material types 83
- FIGURE 3.3 Micrographs of adhered CHO cells after overnight seeding using animal origin and chemically defined adhesion substrates 88
- FIGURE 3.4 Comparisons of cell loading capability, for CHO and HEK cell lines, using polyethylenimine, poly-D-lysine and fibronectin substrates 89
- FIGURE 3.5 Standard curves for CHO cells adhered to polyethylenimine substrates using dissociation, PrestoBlue, crystal violet and neutral red assays 96
- FIGURE 3.6 Photographs of crystal violet and neutral red stains for CHO cells adhered to polyethylenimine substrates 98
- FIGURE 3.7 Trypsinisation of CHO cells adhered to polyethylenimine, poly-D-lysine and fibronectin substrates, followed by growth back in suspension culture 102

- 
- FIGURE 3.8 Differing trypsinisation exposure times on CHO cells adhered to polyethylenimine substrates, followed by growth in suspension culture and one subsequent subculture 105
- FIGURE 3.9 Dissociation, using animal origin-free reagents, of CHO cells adhered to polyethylenimine substrates, followed by growth in suspension culture 107
- FIGURE 3.10 'Standard curve' to assess suitability of a blood sugar monitoring device for determination of glucose concentration in CD CHO medium, and demonstration of its use in actual cell culture 109
- FIGURE 3.11 Effect of mild hypothermia on the growth and glucose consumption of CHO cells adhered to polyethylenimine substrates 110
- FIGURE 3.12 Effect of mild hypothermia on the growth, viability and adherence of CHO cells adhered to polyethylenimine and laminin substrates 112
- FIGURE 3.13 Effect of temperature on daily metabolite and substrate concentrations and IgG titre of CHO cells adhered to polyethylenimine substrates 115
- FIGURE 4.1 Effect of temperature, during cell pausing, on CHO cell viability and glucose consumption 121
- FIGURE 4.2 Effect of temperature and pausing duration on subsequent regrowth of CHO cells in suspension culture using TubeSpin vessels 124
- FIGURE 4.3 Effect of temperature and pausing duration on subsequent regrowth of CHO cells in suspension culture using Erlenmeyer flasks 127
- FIGURE 4.4 Effect of temperature, for cell pausing purposes, on the morphology of CHO cells adhered to polyethylenimine and fibronectin substrates 129
- FIGURE 4.5 Effect of temperature, for cell pausing, on dissociation of CHO cells adhered to polyethylenimine and fibronectin substrates and the effect of pre-warming on paused adherent cells 131
- FIGURE 5.1 Absorbance spectra of TBO at a range of molarities 140
- FIGURE 5.2 TBO uptake for polyHIPE materials fabricated using MAES monomer 143
- FIGURE 5.3 Scanning electron micrographs for polyHIPE materials fabricated using MAES monomer 144
-

- 
- FIGURE 5.4 Schematic detailing the bespoke system employed for the fabrication of polyHIPE microspheres 146
- FIGURE 5.5 Diameter and surface porosity analysis of MAES polyHIPE microspheres fabricated using co-flow orientation and four different carrier phase compositions 150
- FIGURE 5.6 Morphology analysis of MAES polyHIPE microspheres fabricated using co-flow orientation and four different carrier phase compositions 151
- FIGURE 5.7 Scanning electron micrographs showing the physical collapse eventually experienced by MAES polyHIPE microspheres fabricated using 3 % PVA carrier phase 156
- FIGURE 5.8 Diameter and morphology analysis of MAES polyHIPE microspheres fabricated using the T-junction orientation and 80 % glycerol carrier phase 161
- FIGURE 5.9 Diameter and morphology analysis of MAES polyHIPE microspheres fabricated using the T-junction orientation and 80 % glycerol carrier phase at four different process conditions 164
- FIGURE 5.10 Evidence of by-product when fabricating MAES polyHIPE microspheres using the T-junction orientation and 80 % glycerol carrier phase 166
- FIGURE 5.11 Photographs of MAES polyHIPE microspheres in storage using acetone and after adsorption with polyethylenimine 172
- FIGURE 5.12 Breakthrough curves for CHO cells loaded onto PEI-adsorbed MAES polyHIPE microspheres 175
- FIGURE 5.13 Microsphere CHO seeding and cell growth on PEI-adsorbed MAES polyHIPE microspheres in T-25 flasks 179
- FIGURE 5.14 Computer-aided design and laser cutting of the perfusion plate 181
- FIGURE 5.15 Cell loading onto PEI-adsorbed MAES polyHIPE and Cytopore microspheres with the use of a multidrive peristaltic pump 183
- FIGURE 5.16 Cell loading onto PEI-adsorbed polyHIPE MAES microspheres using ambr15 bioreactors 187
- FIGURE 6.1 Validation of the Cedex Bio Analyzer, using controls and serial dilutions 196
- FIGURE 6.2 Demonstration of the Cedex Bio Analyzer for determination of metabolites and substrates within actual cell culture medium 197
-

- 
- FIGURE 6.3 Mild hypothermia of CHO cells using two temperatures within a biphasic culture, with daily determination of metabolites, substrates and IgG titre 199
- FIGURE 6.4 First attempt at pseudo-continuous culture of CHO cells using PEI-adsorbed MAES polyHIPE microspheres for 25 days 204
- FIGURE 6.5 Metabolite and substrate analysis of the first attempt at pseudo-continuous culture of CHO cells using PEI-adsorbed MAES polyHIPE microspheres for 25 days 208
- FIGURE 6.6 Second attempt at pseudo-continuous culture of CHO cells using PEI-adsorbed MAES polyHIPE microspheres for 31 days 210
- FIGURE 6.7 Micrographs and photographs of the second attempt at pseudo-continuous culture of CHO cells using PEI-adsorbed MAES polyHIPE microspheres for 31 days 212
- FIGURE 6.8 Metabolite and substrate analysis of the second attempt at pseudo-continuous culture of CHO cells using PEI-adsorbed MAES polyHIPE microspheres for 31 days 213
- FIGURE 6.9 Schematic detailing the packed-bed perfusion system 218
- FIGURE 6.10 Photographs of the packed-bed perfusion system using 1.0 mL columns 220
- FIGURE 6.11 Photographs of the packed-bed perfusion system using 2.5 mL columns 223
- FIGURE 6.12 Computer-aided design and 3D printing of bespoke frit holders 227
- FIGURE 6.13 Photographs of the modified spinner flask and the spinner flask-based perfusion system 228
- FIGURE 6.14 Cells retained during intermittent agitation at the beginning of an attempt at the operation of the spinner flask-based perfusion system with visual evidence of adhered cells after 8 days 230
- FIGURE 6.15 An attempt at the operation of the spinner flask-based perfusion system using a spinner flask and PEI-adsorbed MAES polyHIPE microspheres for 35 days 232
- FIGURE 6.16 Visual evidence of cell retention on microspheres at the end of the operation of the spinner flask-based perfusion system 234

---

## LIST OF TABLES

---

TABLE 1.1	Targets and indications for a selection of assorted commercial mAb therapeutics	6
TABLE 1.2	Selection of assorted therapeutic proteins produced using CHO cells	12
TABLE 1.3	FDA-approved mAb therapeutics manufactured using perfusion technology	19
TABLE 1.4	Commercial microcarrier products and their properties	37
TABLE 2.1	Densities of components for polyHIPE fabrication	59
TABLE 2.2	HIPE formulations for polyHIPEs with varying EHA and MAES percentages	61
TABLE 2.3	HIPE formulation for EHA/MAES polyHIPE microspheres	64
TABLE 3.1	Cost comparison of all adhesion substrates used	86
TABLE 3.2	Costs of available polyethylenimines from Polysciences US	92
TABLE 3.3	Costs of available polylysines from Sigma-Aldrich UK	93

---

## INTRODUCTION AND THESIS LAYOUT

---

Despite the growing trend towards perfusion operation in the industrial manufacture of monoclonal antibodies, the availability of commercial perfusion technology for pre-clinical antibody development — which ideally would be multi-parallel, high throughput and small-scale — remains limited. For products that are available, the high cost, relatively large scale and perceived difficulty of operating such equipment may hinder adoption. This is particularly true for academic laboratories and small research and development companies where budgets, knowledge of specialised equipment and available time to learn new techniques can be limited. Similarly, the incompatibility of common cell retention devices with familiar labware makes implementation into cell development protocols challenging. This further strengthens the perception that continuous processing is a complex concept not worthy of integration into future projects.

Spherical microparticles, or microspheres, offer a possible alternative as a versatile, easy-to-use and inexpensive cell retention device. Microcarriers, which are essentially microspheres designed for cell culture purposes, have been employed successfully for over fifty years as a means to culture anchorage-dependent cells in suspension. The physical nature of these spherical materials means there is the potential to achieve large surface-area-to-volume ratios with a consequential ability to adhere a very large number of cells within a small working volume. Critical to their possible use as cell retention devices, microcarriers can be retained within familiar vessel formats such as plates, flasks, bottles and columns — this versatility meaning usage is not restricted to dedicated equipment. Using microcarriers as a way to retain cells may make the use of continuous processing simpler and easier to perform, even for laboratories with limited experience in this area. Commercial microcarriers are available as solid, microporous and macroporous structures, with the latter being particularly suitable for perfusion operation where the flow of continuous medium exchange possibly requires pressure considerations.

The addition of sera in culture medium to facilitate cell attachment, and thus ensure cell retention, is generally advised by manufacturers of microcarrier products. Whilst sera supplements such as foetal bovine serum are indeed routinely added to media destined for adherent cell culture, the use of animal origin products in biopharmaceutical processing is increasingly discouraged by regulators on traceability and contamination grounds. There thus exists several areas of potential investigation; first, an attempt at the creation of a cell retention device which utilises microsphere technology, but without the requirement for animal origin products and second, an attempt to demonstrate a continuous upstream system, which any laboratory could use, with this new retention technology.

---

The work presented in this thesis aimed to create a continuous upstream processing system for small-scale antibody development. This project was unique within the laboratory — it was the first time the continuous culture of cells had seriously been attempted, and to add further challenge, the project stipulated that the continuous system employed had to be developed and constructed entirely in-house. This system first required a cell retention device which, likewise, had to be fabricated within the laboratory. The first half of the project focused upon the development of this cell retention device, namely functionalised microspheres which did not require serum to function. This involved the screening of potential adhesion substrates and the fabrication and optimisation of specialised polyHIPE materials. The second part focused upon the use of this newly developed cell retention device for continuous culture purposes. This involved the design and attempted operation of both pseudo-continuous and perfusion culture systems.

The thesis is divided into 7 chapters. It is recommended that readers work their way through the chapters in the order that they are presented, as each builds upon earlier work presented in the preceding one. The chapters are as follows;

#### CHAPTER 1 - LITERATURE REVIEW

Presents a review of the current literature on the biologics industry, polyHIPE materials and continuous bioprocessing, as well as a brief history of each.

#### CHAPTER 2 - MATERIALS AND METHODS

Describes the materials and methods, in full detail, used for all experimental work in this thesis. Sections are presented in the general order in which the results are later shown.

#### CHAPTER 3 - ADHESION SUBSTRATES

The first results chapter, presenting data obtained at the beginning of the project and focusing on the search for an inexpensive, chemically defined adhesion substrate. An adhesion substrate is defined here as a reagent which can be coated to a base material, such as polystyrene, and consequently used to enhance the attachment of cells to these materials. It was expected the successful substrate would later be employed in the cell retention device.

#### CHAPTER 4 - CELL PAUSING

The second results chapter, presenting data obtained during a brief side project which explored cell ‘pausing’, a technique where cells are stored at severe hypothermic, but not cryogenic, temperatures for prolonged periods. Such work explored the pausing of suspended and adhered CHO cells, with potential application for the cell retention device in any future work.

---

#### CHAPTER 5 - POLYHIPE MICROSPHERE TECHNOLOGY

The third results chapter, presenting data obtained in the middle of the project and focusing upon the fabrication and development of polyHIPE microspheres. A polyHIPE is a type of highly porous, scaffold-like material, generated using an emulsion, and can be readily fabricated with relatively simple equipment. The microspheres fabricated would become the physical component of the cell retention device, with the adhesion substrate identified in chapter 3 being the chemical component.

#### CHAPTER 6 - CONTINUOUS BIOPROCESSING SYSTEMS

The fourth and final results chapter, presenting data obtained towards the end of the project and focusing upon the creation and demonstration of pseudo-continuous and perfusion systems. For the former, medium is periodically exchanged by the operator, whilst the latter describes actual continual medium exchange. For both, the cell retention device created as described in chapters 3 and 5 is employed.

#### CHAPTER 7 - CONCLUSIONS AND FUTURE WORK

Summarises the main findings of the work presented in this thesis, with evaluations and final thoughts on the project. The chapter ends with realistic and achievable ideas for future work, taking into account the data obtained from all four results chapters.

---

# Chapter 1

---

## LITERATURE REVIEW

---

### OVERVIEW

This chapter aims to provide a review of the literature to date surrounding biologics, continuous bioprocessing and polyHIPE materials. For biologics, it focuses on the economies of the industry, the dominance of therapeutic antibodies and the continuing ascent of CHO cells. For continuous bioprocessing, it explains the persistence of batch processing, the potential benefits of perfusion culture and explores the current cell retention technology available. Finally, for polyHIPEs, it describes what these unique porous materials are and how they are made, as well as cell culture applications currently demonstrated. Brief and relevant history has also been included, where appropriate, to add context to this thesis.

### I.I BIOLOGICS

#### I.I.I BIOLOGICS INDUSTRY

The extraction, modification and consumption of products from biological systems for energy, medicine and food is nothing new, and has benefited humankind for many thousands of years. This technology, especially in respect to therapeutic products, was rapidly modernised in the closing decades of the twentieth century and led to the introduction of biologically-derived pharmaceuticals. These therapeutic macromolecules, typically produced using recombinant DNA, allowed developers to harness biologically-derived products in ways not possible before. These biologically-derived pharmaceuticals, or biopharmaceuticals, are now viewed as belonging to a wider group of biological therapeutic products, known as biologics. Whilst exact definitions vary, a biologic can generally be described as any therapeutic product derived in part, or wholly, from biological sources; either by their production, or extraction, from these living systems, which themselves may be modified for this purpose. Encompassing a growing range of products, biologics are diverse in physical nature and mode of treatment; vaccines, tissues, proteins, nucleic acids and cellular components, as well as all associated treatments using these products, may be considered biologics.

Biologics can be differentiated from traditional pharmaceuticals, often termed ‘small molecule’ drugs for comparison, by their vastly more complex molecular structures,

typically having molecular weights many order of magnitudes greater. Traditional drugs, due to their relative structural simplicity, are not reliant on living systems and can be synthesised solely using defined reactions within chemical processes. Despite the frequent comparisons with ‘older’ pharmaceuticals, some biologics already have a notable history within medicine. The first smallpox vaccine, developed in part by Edward Jenner in the late 18th century (Riedel, 2005) and building on earlier variolation practices, was indeed a biologic if the above definition given is followed. Human blood donated for transfusion is a biologic, which in its current treatment practice has been performed for over a hundred years (Schmidt et al., 2002). Penicillin-based antibiotics produced using *Penicillium* moulds — first achieved industrially in the 1940s — are biologics by virtue of their fungal source, despite their small molecular weights (Gaynes, 2017).

The shift from traditional to biological-derived pharmaceuticals is well reported. Market approvals for biologics, relative to small molecule drugs, increased steadily throughout the 1980s and 1990s (Kinch, 2015). In 2016, 25 % of the pharmaceutical market was held by biologics, up from 16 % in 2006 (Kent et al., 2017). Within the biologics market itself, approvals from 2015 to 2018 saw a doubling when compared to the five-yearly pace historically reported (Walsh, 2018). The scope of biologics is not just expansive, but also innovative and disruptive; between 1986 and 2014, almost twice the proportion of newly approved biologics by the FDA were considered first-in-class — the first to use a novel mechanism of treatment — when compared to small molecule drugs (Miller et al., 2015). The authors also reported 47 % of biologics in this period received orphan drug status (for treatment of rare diseases in which dedicated drug development is usually not deemed sufficiently profitable to pursue), in contrast to 21 % of traditional pharmaceuticals.

### I.1.2 THERAPEUTIC ANTIBODIES

Therapeutic proteins are a leading class of biopharmaceuticals. Being one of the four biomacromolecule groups, proteins hold extensive function within the human body, including biocatalysis, metabolism, immunity and cellular structure, as well as intracellular communication, signalling and transportation. Their ubiquitous nature thus mean proteins have huge potential as therapeutic agents as well as being the target themselves for many therapeutics. Whilst proteins destined for medical use were traditionally extracted from humans, e.g. blood clotting factors from human plasma for haemophiliacs (Liumbruno et al., 2009), and animals, e.g. insulin from cows and pigs for diabetics (Mohan, 2002), these ‘crude’ products posed safety (White, 2010) and efficacy concerns, and were prone to quality and supply issues.

In the latter half of the 20th century, advances in genetic sequencing, molecular cloning

---

and cell culture led to the development of recombinant DNA technology (Cohen et al., 1973). This new-found ability allowed specific genetic sequences to be ligated together; the resulting recombinant DNA — essentially designed by the user — could be inserted into cultured host systems for expression. For recombinant DNA that codes for therapeutic proteins, the expressed products can be harvested and purified for medical use. As these recombinant products are effectively synthetic in origin, the production can be controlled, supply issues reduced and the likelihood of infections passing over from crude sources to patients eliminated.

Starting in 1982 with the approval of Humulin (a recombinant human insulin produced using *E. coli* culture) by Genentech and Eli Lilly (Quianzon et al., 2012), commercial recombinant proteins available today are diverse in both structure and function; examples include erythropoietin for chronic kidney disease (Casadevall et al., 2005), human growth hormone for growth deficiencies (Cai et al., 2014), the enzyme glucocerebrosidase for Gaucher disease (Starzyk et al., 2007) and a hepatitis B vaccine utilising recombinant hepatitis antigen (Shouval, 2003). From 2011 to 2016, the FDA approved a total of sixty-two recombinant proteins; of these, 48 % were monoclonal antibodies (mAbs), 19 % were coagulation products, 11 % were enzymes and the rest being fusion proteins, hormones and growth factors (Lagassé et al., 2017). It can quickly be seen that antibodies (also known as immunoglobulins owing to their central role within immunity), are the industry favourite among therapeutic proteins. An immunogen is any substance that induces an immune response, namely a humoral response whereby antibodies for that immunogen are created within the body. Immunogens will always contain one or more antigens (*antibody generating*), specific structures which antibodies will bind to. These antibodies are used to neutralise the immunogen, by various methods, via this antigen pairing. In a wider sense, an antigen can thus be described as any structure that binds to an antibody, even if that antigen does not belong to an immunogenic substance, such as a bacterium or virus particle. It then stands that an antibody can be generated outside of the body and subsequently used *in vivo* to bind specifically and with high affinity to an antigen, independently from any naturally occurring immune response.

Antibodies, frequently described as ‘Y’-shaped, are high molecular weight (150 kDa) glycoproteins typically composed of two identical heavy chains and two identical light chains. These two chain sets are joined by disulphide bridges. The heavy chain type defines the antibody isotype;  $\alpha$  (IgA),  $\delta$  (IgD),  $\epsilon$  (IgE),  $\gamma$  (IgG), and  $\mu$  (IgM). These isotypes generally differ by their resultant complexes, with IgD, IgE and IgG presenting as monomers, IgA as a dimer and IgM as a pentamer. Figure 1.1 shows a schematic of an IgG antibody, with important regions labelled. Heavy chains have a constant domain, identical in all an-

tibodies of the same isotype, and a variable domain determined by their particular B cell production. Light chains are either one of two types;  $\gamma$  and  $\kappa$ . Both types have one constant and one variable domain, and either can be found on any of the isotypes. An antibody can be divided into two regions; the Fab (antigen-binding) region at the top of the 'Y' and the Fc (crystallizable) region at the bottom. Antibodies are frequently described as modular proteins; exposing a typical IgG antibody to the enzyme papain would yield two Fab fragments (the 'arms') and one Fc fragment, each of which could then function as an independent entity.

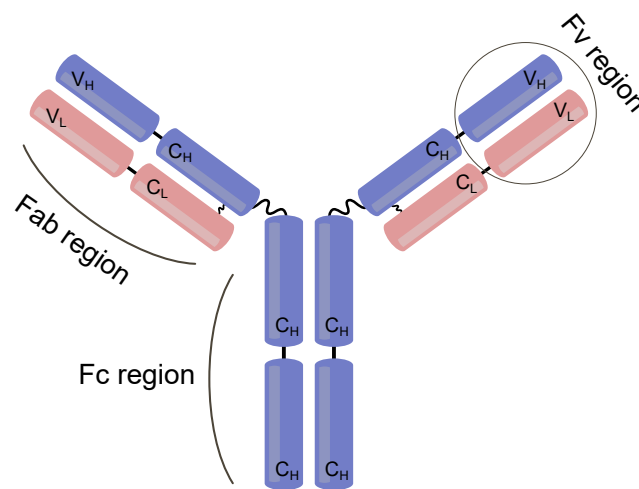


**FIGURE I.1 Schematic of an IgG antibody.** An IgG is composed of two heavy chains and two light chains, joined by disulphide bridges.  $C_H$  refers to the constant region of the heavy chain, whilst  $V_H$  refers to the variable region. The same is true for the light chain with  $V_L$  and  $C_L$ . The paratope, where the antibody binds to antigen is at the top of the arms of the 'Y', with each IgG possessing two binding sites. Other antibody isotypes will present as different complexes, due to a different number and orientation of heavy and light chains.

The Fab region is of key interest in therapeutics as it contains the paratope, the domain which binds to a specific epitope on an antigen. Each paratope is composed of six complementarity-determining regions (CDRs), three from the variable light chain and three from the variable heavy chain. Thus, a typical IgG antibody would have two paratopes with twelve CDRs in total. This highly variable region is referred to as the Fv (variable) region. The Fc region, in comparison, contains the constant region of the heavy chains and is the same for each antibody isotype. This region binds to Fc receptors on cells to initiate downstream pathways associated with the immune response. The Fab and Fc regions thus ensure antibodies can bind antigens and lead to subsequent biological activity. Being a highly researched area, the literature has a wealth of extensive reviews on antibody structure, function and application in therapeutic contexts (Awwad et al., 2018; Kubota et al., 2009; Muhammed, 2020; Wang et al., 2007).

Monoclonal antibodies (mAbs), antibodies produced recombinantly by genetically identical cells, and possessing the same specificity for a particular antigen (Nelson et al., 2000), are a dominating and growing class within the biologics market. The difference between monoclonal and polyclonal antibodies (pAbs) is apparent when considering the natural immune response within the body. Antigens may have multiple epitopes; when faced with a foreign body such as a bacterium, different B cells may recognise the same antigen, and subsequently each may produce antibodies — however, each collection of antibodies may recognise a different epitope on the antigen. This polyclonal response is thus the result of different B cell responses, and results in the production of antibodies with differing paratopes. Monoclonal antibodies, in contrast, describe all the antibodies produced by a single B-cell clone; as they are structural identical, these share the same specificity for a single epitope on an antigen.

Compared to other groups of biologics, mAbs made up over 50 % of new approvals from 2015 to 2018 (Walsh, 2018), up from almost 25 % a decade previously. Analysis of historic market approvals reveal the approval rate for mAbs to be double that of traditional pharmaceuticals (Kaplon et al., 2019), whilst mAb sales grew from almost US\$ 40 billion in 2008 to over US\$ 70 billion in 2013 (Ecker et al., 2015) — the reporting authors also predicted there would be at least 70 market approved mAb products, up from 47, in the United States and Europe by 2020. A recent review (Lu et al., 2020) indeed confirmed over 70 mAbs were now commercially available in these regions.

In 2017, of the top ten best-selling pharmaceutical products, six were mAbs (Urquhart, 2018); whilst in 2018 and 2019, seven were mAbs (Urquhart, 2019; Urquhart, 2020). Of these marketed antibody products, over fifteen have achieved elusive ‘blockbuster’ status — annual sales exceeding US\$ 1 billion — including bevacizumab, trastuzumab and rituximab (Busse et al., 2019). Adalimumab, an anti-TNF- mAb aimed at treating a range of inflammatory disorders, remains one of the best-selling pharmaceuticals of all time, with annual sales well in excess of US\$ 10 billion (Lindsley, 2018).

To date, IgG remains the most popular commercial mAb isotype (IgG1 being the most common subclass), with several Fab and scFv (single chain) fragment exceptions (Lu et al., 2020; Shoaie et al., 2019). Therapeutic antibody fragments, composed of smaller molecular weight (< 50 kDa) Fab or Fv products, allow developers to exploit the modular nature of antibodies by using only the regions that bind to antigen. Whilst their use may highly depend on clinical context, e.g. no Fc binding requirement, the general benefits of only utilising variable fragment include faster, cheaper production (via bacterial host cell expression), greater penetration into tissue inaccessible by full fragment mAbs and a reduced risk of unwanted

effects from bystander immune cells (Nelson, 2010). Indeed, the second therapeutic antibody to be approved by the FDA, abciximab, was a Fab fragment product (Marks, 2012).

### I.1.3 INDICATIONS FOR THERAPEUTIC ANTIBODIES

Inflammatory disorders and oncology remain the top indications for therapeutic mAbs; of all the mAb products listed by Lu et al. (2020), over 60 % were for either of these two disease categories, with the remainder not grouping into any obvious category. Table 1.1 lists these targets and many more for a variety of selected mAb products. Some antigens are targeted more than others, indicating the wide role they may play in disease.

The general mechanism of action for mAbs treating inflammation is through their binding

TABLE I.I Targets and indications for a selection of assorted commercial mAb therapeutics, including antibody conjugate products. Therapeutics are given their international nonproprietary name (INN). Included references are reviews detailing current targets and indications for each antibody and their clinical successes. For a list of every antibody product approved by the FDA since 1986, see Rodgers et al. (2016) or Lu et al. (2020).

mAb Therapeutic	Target(s)	Indication(s)	Reference
Adalimumab	TNF- $\alpha$	Autoimmunity	Bang et al. (2004)
Bevacizumab	VEGF-A	Cancers, macular deg.	Keating (2014)
Brolucizumab	VEGF-A	Cancers, macular deg.	Yannuzzi et al. (2019)
Certolizumab pegol	TNF- $\alpha$	Autoimmunity	Mease (2011)
Crizanlizumab	P-Selectin	Sickle cell disease	Riley et al. (2019)
Golimumab	TNF- $\alpha$	Autoimmunity	Frampton (2017)
Ibritumomab tiuxetan	CD20	Cancers, MS	Mondello et al. (2015)
Infliximab	TNF- $\alpha$	Autoimmunity	Siddiqui (2005)
Ixekizumab	IL-17A	Psoriasis	Hanley et al. (2017)
Obinutuzumab	CD20	Cancers, MS	Tobinai et al. (2017)
Ocrelizumab	CD20	Cancers, MS	Mulero et al. (2018)
Ofatumumab	CD20	Cancers, MS	O'Brien et al. (2010)
Omalizumab	IgE (Fc region)	Asthma	Lin et al. (2016)
Pertuzumab	HER2	Breast cancers	Ishii et al. (2019)
Ranibizumab	VEGF-A	Cancers, macular deg.	Chong (2016)
Rituximab	CD20	Cancers, MS	Leget et al. (1998)
Secukinumab	IL-17A	Psoriasis	Frieder et al. (2018)
Trastuzumab	HER2	Breast cancers	Gajria et al. (2011)
Trastuzumab emtansine	HER2	Breast cancers	Barok et al. (2014)
Ustekinumab	IL-12, IL- 23	Psoriasis	Benson et al. (2011)

and subsequent neutralisation of pro-inflammatory cytokines, including tumour necrosis factors (TNFs) and interleukins (ILs). Both TNFs and ILs are activated by immune cells during the inflammatory response and stimulate a host of cell signalling pathways; their over-reaction being responsible for a range of autoimmune disorders. For rheumatoid arthritis treatment, several mAbs have been employed to target specific cytokines, including tocilizumab for IL-6R, and infliximab, adalimumab and golimumab for TNF- $\alpha$  (Tanaka et al., 2014). Ustekinumab and Secukinumab have been used to treat psoriasis, neutralising IL-12 and IL-23, and IL-17A cytokines, respectively (Jeon et al., 2017). For Crohn's disease, the anti-TNF- $\alpha$  mAb, infliximab, has also been used as an anti-inflammatory treatment (Poggioli et al., 2007).

Immunotherapy, which benefits hugely from mAb products, has been employed for oncology treatment. Three mechanisms of action via the binding of mAbs to targets associated with cancerous cells are known; inhibition of receptors used by cancer for various functions required for their growth, antibody-dependent cellular cytotoxicity and complement-dependent cytotoxicity — the latter two calling on immune responses and resulting in cancer cell lysis (Kimiz-Gebologlu et al., 2018). A clinical example is trastuzumab, an anti-HER2 receptor therapeutic for the treatment of certain breast cancers, with the binding of HER2 shown to have anti-tumour effects by various mechanisms, including downregulation of pathway signalling required for tumour progression and the activation of cytotoxicity immune effects (Gajria et al., 2011).

VEGF-A, a growth factor that promotes cell proliferation through the formation of blood vessels, is a further antigen target due to its role in tumour growth. The anti-VEGF-A therapeutic, bevacizumab, has been employed to limit disease progression in colorectal (Bupathi et al., 2016), renal cell (Harshman et al., 2010) and non-small cell lung cancers (Lauro et al., 2014).

The examples given show the diversity in targets for mAb therapeutics and how antibodies can interact with structure-specific agents processes associated with disease. As targets may be involved in multiple diseases, an expansion of indications — where a drug is approved for treatment of a disease different to the one originally marketed for — is a phenomenon widely seen with commercial mAb products. Adalimumab, introduced earlier as one of the best-selling pharmaceuticals of all time, was initially approved by the FDA for rheumatoid arthritis in 2002, but has since been approved for psoriatic arthritis (2005), ankylosing spondylitis (2006), juvenile idiopathic arthritis (2008), psoriasis (2008), Crohn's disease (2010), ulcerative colitis (2012), hidradenitis suppurativa (2015) and uveitis (2018) (Lu et al., 2020). Such an increase in approvals is rather bemusing, especially when one

of its best known brand names, *Humira*, is an acronym; *human monoclonal antibody in rheumatoid arthritis*.

#### I.1.4 EXPRESSION SYSTEMS

The engineering of antibodies for therapeutic purposes has been made possible by the development of many techniques, including recombinant DNA technology, bioinformatics, phage display, and cell culture. Early methods of producing antibodies, i.e. via the immunisation of an animal host and subsequent use of hybridoma technology, has largely been eliminated. The use of expression systems, i.e. dedicated cell lines for expression of recombinant product, has taken over. This has opened up new streams of development in cell engineering, medium optimisation and upstream processing operations. The choice of cell line heavily depends upon the desired product and is an expansive area of research.

The industrial production of therapeutic proteins, including mAbs, is reliant upon expression host cell systems. These living systems, or cell lines, are selected by their capability for indefinite proliferation, genetic manipulation and reliable expression of recombinant product. Common cell types employed include bacterial, fungal, mammalian and even plant and insect cells.

*E. coli* remains the most employed bacterial host, being an extensively characterised microbial organism capable of technically simple genetic engineering; it was the expression system for many early therapeutic proteins, including insulin in 1982 (Quianson et al., 2012), human growth hormone in 1985 (Chang et al., 1987), interferon  $\alpha$ -2 in 1986 (Spiegel et al., 1986) and granulocyte colony-stimulating factor in 1991 (Vanz et al., 2008). This early adoption is immediately obvious when considering what bacterial systems offer; inexpensive medium requirements, quick growth rates, rapid product expression, high titres and process scalability. Being prokaryotic organisms (with no nucleus or membrane-bound organelles), their primitive physiologies mean they are capable of growing indefinitely in culture, under ideal conditions, without the need for prior biological manipulation. This contrasts with mammalian cells, which require immortalisation to divide continually and not suffer from drastic genetic changes or eventual senescence. This immortalisation may arise naturally, e.g. isolating a cell from cancerous tissue, as with HeLa cells (Lucey et al., 2009), or it may be acquired artificially, e.g. from the introduction of an adenoviral gene, as with the immortalisation of human embryonic kidney (HEK) cells (Shaw et al., 2002).

Despite their process advantages and early success, the frequently reported drawback for bacterial systems is the lack of suitable post-translational modifications of expressed product. Performed following (or in some cases during) protein synthesis within the Golgi ap-

paratus and endoplasmic reticulum — organelles which bacteria do not possess — these describe numerous covalent and enzymatic changes to the product including glycosylation, phosphorylation, ubiquitination and methylation amongst many others. More structurally complex proteins, when produced using *E. coli*, may also suffer from misfolding and consequent degradation or aggregation into inclusion bodies; this generally being a result of the lack of post-translational modifications which contribute to proper protein folding (Baneyx et al., 2004). Whilst bacteria are biologically capable of modifying their proteins during or after translation (Macek et al., 2019), these chemical changes are of a different nature to that found in eukaryotes and so give little clinical benefit to therapeutics destined for the human body. However, certain therapeutic antibody fragments may still be made using bacteria. Ranibizumab, an anti-VEGF-A Fab product, is commercially produced using *E. coli*; the fragment has no Fc region and thus lacks any glycosylation sites, but has indeed been used successfully for the treatment of macular degeneration (Zou et al., 2011).

Glycosylation is the most desired post-translational modification within commercial biopharmaceuticals. N-linked glycosylation, the most common type, describes the attachment of a sugar moiety (or glycan) to the nitrogen atom of an asparagine residue. For IgG molecules, this occurs at asparagine residue 297 in the heavy chain of the Fc region. This modification is deemed essential for effector functions, the result of Fc region binding to suitable receptors and thus is closely tied to the therapeutic efficacy of the final protein product (Hossler et al., 2009). Due to the nature of the modification process, different types and quantities of glycans can be added, ultimately resulting in a pool of seemingly identical mAb products, but each with varying efficacies (Walsh et al., 2006). In addition, the presence of, or lack of, glycans may also affect solubility, stability and aggregation of the antibody (Higel et al., 2016; Zheng et al., 2011). These effects have subsequently led to regulatory bodies insisting that glycoform profiles for therapeutic proteins be reproducible and kept within defined limits.

The demand for correctly folded, glycosylated proteins, starting in the late 1980s with tissue plasminogen activator (Collen et al., 2004) and erythropoietin (Kalantar-Zadeh, 2017), as well as for large molecular weight (>50 kDa) antibodies, has meant that mammalian cells gradually surpassed bacteria as the most employed expression system. Up to 1989, 66 % of approved biopharmaceuticals were produced using non-mammalian cells; from 2015 to 2018, that had decreased to 21 % of new approvals, with 79 % now using mammalian (Walsh, 2018). The ability to produce more complex proteins has consequently led to greater returns. Of the top proteins sold in 2007, two thirds of the revenue came from products made using mammalian systems, whilst the rest came from those made using other cell lines such as bacterial and yeast systems (Zhu, 2012).

The use of mammalian cells however brings process challenges, including low cell densities, genomic stability issues, reduced titres and variations in expressed product. These are generally the result of the greater genetic, phenotypic and metabolic complexities of animal-origin cells, and the specialised culture requirements that these systems demand. Mammalian culture times are also typically longer than bacterial cultures and require greater expense to run — the latter being partly responsible for the high drug costs seen with mAbs produced today. However, due to the clinical necessity of therapeutic proteins having post-translational modifications — especially glycosylation — these issues have largely been rectified, accepted or at least made tolerable by optimisation over the past three decades.

Beginning with  $100 \text{ mgL}^{-1}$  in the late 1980s, product titres have now reached an excess of  $5 \text{ gL}^{-1}$  for mammalian systems (Kunert et al., 2016). The mode of operation has contributed in part to this, with extended fed-batch runs, involving periodic feeding to keep substrates high, boosting cell densities and consequent titres when compared to simpler, shorter batch cultures. The culture environment has likewise been optimised, with increased sophistication, e.g. online monitoring, in the way bioreactors control key parameters (Pais et al., 2014; Zhao et al., 2015), as well as tailored media formulations (Jerums et al., 2005) being used. Finally, advancements in vector design, including the engineering of genetic elements such as promoter and selection markers (Ludwig, 2006) and improved cell development techniques have ensured the generation of high producing, fast growing cell lines.

Mammalian cell lines employed for therapeutic protein production include NS0, Sp2/0, baby hamster kidney (BHK), Chinese hamster ovary (CHO), Vero, HEK-293 and PER.C6 cells. The first four listed are of rodent origin, with Vero cells derived from a monkey and HEK-293 and PER.C6 from humans. HEK-293 and PER.C6 cells, derived from human foeti and immortalised via adenovirus transformation, have found extensive use in recombinant protein and viral production (Jäger et al., 2013; Xie et al., 2002).

NS0 and Sp2/0, both artificially immortalised murine cell lines, share a similar lineage. Both were derived from a myeloma, whose formation was induced by the injection of mineral oil into an inbred BALB/c mouse. NS0 cells, non-secreting/-synthesising, are so named as a result of their development history — the cells initially produced natural IgG1 molecules, but gradually lost this ability after successive selection and cloning steps (Barnes et al., 2000). However the final cell line retained the cellular machinery needed to produce heterologous mAbs. Sp2/0 is much the same, except hybridoma technology was used in the development process to fuse an early clone with BALB/c spleen cells (Shulman et al., 1978). As with NS0, the resulting cell line was unable to express endoge-

nous antibodies, but could be used for heterologous expression of antibody products. Therapeutic mAbs commercially produced using NS0 include ofatumumab, belimumab and raxibacumab; whilst for Sp2/0, include basiliximab, infliximab and cetuximab. Both cell lines benefit from a natural ability to grow in suspension, can be easily transfected and are adaptable to serum-free media (Yoo et al., 2002).

BHK, a cell line derived from polyoma-induced transformation of fibroblasts, themselves isolated from trypsinised kidneys of young hamsters (Macpherson, 1962), has been used to commercially produce recombinant factor VIIa (Hedner et al., 2011). Due to BHK cells susceptibility to viruses common to humans, they are also used for viral vaccine research. Lastly, CHO expression systems, with their prominence in recombinant protein production, deserve a separate section for discussion.

#### 1.1.5 CHINESE HAMSTER OVARY CELLS

CHO cells are the most popular mammalian cell expression system for the industrial production of mAb therapeutics. Dhara et al. (2018) list all FDA-approved mAb products and the expression systems employed to produce them. Using these data, 61 % of mAbs are produced using CHO cells, followed by NS0, 22 %; SP2/0, 11 %; murine hybridomas, 3 %; and *E. coli*, 3 %. From 2014 to 2018, 84 % of mAbs approved were produced using CHO cells (Walsh, 2018). CHO cells are not restricted to antibody production; the data listed by Dumont et al. (2016) show the diversity of recombinant proteins commercially produced, including cytokines, enzymes, fusion proteins, hormones and clotting factors. Indeed, another report, albeit an older one, states that nearly 70 % of all recombinant therapeutic proteins are produced using CHO cells (Jayapal et al., 2007). Table 1.2 shows an assorted list of proteins industrially made using the CHO expression system.

The reasons for the dominance of CHO have been extensively documented and are often included in the introductions of many CHO research articles. (i) Shared with many mammalian expression systems, is the ability of CHO cells for post-translational modification of expressed product and thus ensures heterologous proteins have sufficient biological activity *in vivo*, (ii) an expanding marketed product portfolio from the FDA, starting with tissue plasminogen activator in 1987, has set a precedent for regulatory approval with products made using CHO cells. Such a favourable record is appealing for companies choosing an expression system in the early stages of biopharmaceutical development. It also means a wealth of experience and knowledge is already present amongst drug researchers within many companies. (iii) Suspension adapted CHO cells lines, capable of high density growth within chemically defined medium, have been developed and can be employed for stirred tank reactor production, enabling volumetric scaling to industrial sizes. (iv) They are rela-

tively safe with respect to pathogenic agents, with many viruses infectious to humans, such as HIV, influenza viruses and the measles virus, not infectious to CHO cells. (v) Tolerance of genetic manipulation, when subjected to transient and stable transfection techniques, allows designed plasmids to be taken up, genes read and product expressed with relative ease.

TABLE I.2 A small selection of assorted therapeutic proteins currently produced using CHO cells with recombinant DNA technology. Adapted from Dumont et al. (2016).

Protein Therapeutic	Type	Company*
Adalimumab		Abbot Laboratories
Rituximab	mAb	Biogen
Trastuzumab		Genentech
Interferon beta-1a		Biogen
Darbepoetin alfa	Cytokine	Amgen
Agalsidase beta		Genzyme
Human DNase	Enzyme	Genentech
Abatacept	Fusion protein	Bristol Myers Squibb
Follitropin alfa	Hormone	Merck
Factor VIII	Clotting factor	Baxter Healthcare

\* Only one company listed; others may produce same therapeutic or a variant of it, depending upon patent status and geographical location.

Despite being frequently termed the workhorse of the biopharmaceutical industry, CHO cells were not originally intended for use as an expression system. Derived from a biopsied ovary of an inbred rodent (*Cricetulus griseus*, or Chinese hamster) in 1957, the adherent cells, described as ‘fibroblast-like’, were initially studied for genetic purposes (Tjio et al., 1958). Their relatively low chromosome number ( $2n=22$ ; compared to human cells with  $2n=46$ ), and the observation that the modal chromosome number did not vary significantly over many months of culture, suggested the new ‘Chinese hamster cells’ could be used as an in vitro model to study the effects of physical and chemical agents on chromosomes. It was soon reported these new cells were ‘particularly hardy and reliable’ (Puck et al., 1958) and appeared to have immortalised spontaneously. Their low generation time of 10 hours, deemed beneficial for experimentation, further ensured they would be continued to be studied.

Several subclones from the original cells were soon derived. CHO-K1, again adherent, but with a lower chromosome number of 20, is now regarded as an early parental cell line. Orig-

inal work on this subclone reported the consequence of mutagenesis, via exposure to either ethyl methanesulfonate or methylnitronitrosoguanidine, on the activity of the enzyme dihydrofolate reductase (DHFR) (Kao et al., 1968). DHFR converts folate to tetrahydrofolate, a precursor for the synthesis of purines, pyrimidines and glycine, regarded as essential for the survival of cells. Thus, cell mutants lacking DHFR activity had to be cultured in medium supplemented with these essential metabolites for growth. In later years it was proposed CHO mutants lacking DHFR activity could be exploited in a selection system for stable transfection purposes. A cell line, CHO-DG44, was prepared where it was made certain both gene loci for DHFR were removed via gamma radiation (Urlaub et al., 1983) — a scenario where DHFR activity could return was deemed theoretically possible in the earlier mutants.

The DHFR/MTX system, a means of selecting and amplifying a gene of interest, relies on the folate analogue, methotrexate (MTX), to inhibit the activity of DHFR. If a CHO cell successfully incorporates a vector containing both the gene of interest and a nearby gene coding for DHFR, they will survive and grow in medium lacking any essential metabolites, such as glycine, hypoxanthine and thymidine. Adding MTX, and steadily increasing the concentration, further ensures only cells expressing high copies of DHFR, and the gene of interest, ultimately survive.

Another selection mechanism, the GS/MSX system, relies instead upon CHO mutants lacking the enzyme glutamine synthetase (GS). GS converts glutamate and ammonia to glutamine, an essential amino acid required for cell survival. Growing the cells in medium without L-glutamine supplementation ensures only cells with incorporated genes coding for GS and the protein product survive and grow. Methionine sulfoximine (MSX), an analogue of glutamate, inhibits GS and as before can be applied as a selection pressure to obtain high producing transfected cells. Another cell line, CHO-K1SV, was derived from CHO-K1 and adapted for suspension culture by Lonza (Fan et al., 2013), and employs this GS/MSX system for industrial protein production. And finally, as well as CHO-K1 and CHO-DG44, a further parental cell line was developed, CHO-S, and adapted for suspension culture (Thompson et al., 1973). For a detailed overview of CHO cell lineages with further historical detail, see Lewis et al. (2013).

### 1.1.6 STABLE AND TRANSIENT TRANSFECTION

The use of mammalian expression systems is reliant upon the successful transfection of genetic material, specifically DNA (as RNA can also be transfected), for the expression of protein product. Transfection describes the process of introducing exogenous nucleic acids into mammalian cell lines. This is similar to, but should be not confused with, transfor-

mation, which instead describes the introduction of nucleic acids into bacterial and other non-mammalian systems.

Transfections may be defined as either stable or transient, depending upon the fate of the DNA (usually contained within a vector) once inside the cell. The former leads to the integration of the genetic material into the nucleus of the cell, ensuring it is replicated along with the host genome each time the cell divides. As noted in § 1.1.5, the use of a selection marker (which is likewise incorporated with the gene encoding the desired protein) ensures efficient selection of high producer cells post-transfection. This results in a new cell clone capable of indefinite expression of the protein. For transient transfection, the DNA is not integrated into the nucleus, but instead remains within the cytosol for a short time period (typically less than a week), with both the DNA copy number and the subsequently expressed product gradually diluting as cells divide. In recent years transient transfection has become an increasingly used workflow for biopharmaceutical development, particularly within pre-clinical antibody research. In contrast to stable transfection, transient transfection is both faster and cheaper, allowing rapid production and assessment of products without the commitment to stable cell generation.

Electroporation-mediated (Steger et al., 2015), polyethylenimine-mediated (Elshereef et al., 2019) and lipid-mediated (Rosser et al., 2005) transfection have been employed routinely for transient transfections. However, these have been performed almost exclusively using batchwise cultures. The key advantage of pairing transient transfection with continuous processes may have been overlooked, namely the potential for sequential transient gene expressions without any culture downtime. Indeed, such a set up could only be achieved if cells were cultured continually via a perfusion process, with a system such as this enabling even shorter antibody production times. The higher cell densities typically seen with perfusion cultures may further result in higher product titres during these transient expression cycles.

There exists no literature demonstrating this idea of continual transient transfections within a long-term continuous process, with an application of the work reported here indeed being sequential transient transfections. For a discussion on batch, semi-continuous and continuous processes, including a description of each, see § 1.2.

### **I.1.7 CHEMICALLY DEFINED BIOPROCESSING**

The successful production of a biopharmaceutical is dependent upon the harmonisation of multiple processes, both upstream and downstream, along with the correct input of raw materials and fine tuning of parameters. Due to the interconnectivity between bioprocesses

---

and biopharmaceuticals, it is often remarked the product is the process, or rather, the process defines the product (Vulto et al., 2017). This arises from the observation that seemingly trivial variations within a bioprocess can have dramatic effects on the final product. As the safety and efficacy, i.e. the critical quality attributes, depend ultimately upon the structure of the product, it is essential the overall process is reproducible batch-to-batch.

Such discussion complements the production of biosimilars. Once the patent has expired on a marketed biopharmaceutical, companies who are wishing to develop their version of this product can never expect to exactly replicate its molecular structure. They do not have access to the specific expression system, which will be a clone transfected with a specific vector and subsequently tailored using a cell line development process, and the process conditions originally used during production may be unknown. Thus, they must develop a new bioprocess with their own expression system, with the aim of replicating the safety and efficacy of the reference product as far as possible. As noted previously, this contrasts with conventional pharmaceuticals, whose structures have no molecular ambiguity and can be easily replicated with much simpler, and more widely understood, chemical reactions.

To ensure the above is followed, in recent times there has been a move towards chemically defined bioprocessing, i.e. where the components of material inputs are explicitly known, quantifiable and traceable. This is most pronounced within the upstream processes of production, where materials used must be accounted for downstream during the purification of the product. If the materials within the process are not known, then it cannot be known if they, or their derivatives, have been truly removed at the end of the process or what effect they may have had on the product.

Cell culture media has been a relatively easy target to drive this trend towards chemically defined processes. In the early days of cell culture, media was of low definition, i.e. it was a basal medium supplemented with serum, typically of bovine or even human origin. These sera, essentially biological extracts, served as a crude source of nutrients and factors for cellular functions such as attachment, growth and in the case of primary cells, differentiation. Due to their animal origin, serum products are ill-defined, prone to supply issues and may be considered unethically-sourced (van der Valk et al., 2004). For bioprocessing, the disadvantages of using such animal-derived products include batch-to-batch variability and the consequences on the product of not knowing the exact components. Even if the effects on product efficacy are mitigated, regulatory bodies continue to strongly discourage the use of animal-origin products due to the risk of pathogenic contamination, particularly with prions and viral agents, on the final product (Weinberg et al., 2005).

To overcome this, serum-free medium has been developed, eliminating the need to add

---

animal-derived extracts. Because specific animal-derived proteins, again usually of bovine origin, may still be added, protein-free medium continued the trend. A beneficial consequence of using animal origin-free medium is the design of media specific to the cell type employed, e.g. NS0 cells (Zhang et al., 2005) and Vero cells (Rourou et al., 2009), which has brought greater knowledge about particular cell line medium requirements and in turn a degree of optimisation. Chemically defined medium, where each component is known and quantified, was the next improvement. Particular types of chemically defined media may also be peptide-free and protein-free, depending upon the intended cell line, and is widely considered the most defined type possible. A popular commercial example, CD CHO from Thermo Fisher Scientific, is a chemically defined, serum-free, peptide-free and protein-free (recombinant or otherwise) formulation intended for suspension-adapted CHO cell culture (Zhu et al., 2012). The lack of recombinant proteins in this instance is a further measure to ensure no animal-origin components, as recombinant materials are themselves products of cell culture processes. Alternatives to FBS have been reviewed by Gstraunthaler (2003).

Despite the general move towards more defined media, adherent cell culture media is still frequently supplemented with foetal bovine serum (FBS), often as 10 % (v/v) of the medium. As with other sera, FBS is a variable mixture of growth factors, hormones, enzymes, fatty acids, adhesion proteins and trace elements (Brunner et al., 2010). The presence of adhesion proteins, effectively ‘sticky’ substrates that mimic the extracellular matrix of cells, act to encourage initial cell attachment and eventual spreading during culture growth. Whilst the issue of ill-defined FBS for adhesion may not seem relevant to the modern industrial production of mAbs — where cells are in suspension within chemically defined medium — it deserves discussion when adherent processes are repurposed for novel processes, e.g. in the use of microspheres as a cell retention device, as is the case in this work.

The coating of culture vessels with particular adhesion substrates, prior to cell seeding, is a common technique to facilitate cell adherence, which may then not demand the use of FBS. Adhesion substrates used however are typically animal-origin proteins, and thus of the same kind encountered in sera, such as fibronectin and vitronectin (Anwar et al., 1993; Groth et al., 1995). Even in these instances, many protocols may continue to list FBS as a supplement, likely for the benefit of serum’s other components for cell culture. Chemically defined, animal origin-free adhesion substrates do exist, generally taking the form of cationic homopolymers. The cationic character derives from their amines; functional groups which, under physiological pH, give a net positive charge and so attract the negatively-charged membrane of mammalian cells. Such an attraction ultimately causes cell adhesion. Polylysine, available as either D or L enantiomorph, is ubiquitous in the literature as a chemically defined adhesion substrate for many cell types (Ando et al., 2015; Huang et al., 2005;

Kam et al., 2001; Wei et al., 2009), and has been used since at least the 1970s (Mazia et al., 1975; Yavin et al., 1974). The high cost of polylysine however means its usage in coating a large volume of high surface area microspheres may be prohibitive. The continued usage of chemically defined medium, i.e. CD CHO, alongside the use of an animal origin-free adhesion substrate, is a key criterion for the work carried out and presented here.

## **I.2 CONTINUOUS BIOPROCESSING**

### **I.2.1 BIOLOGICS IN BATCH**

The industrial production of biologics, particularly biopharmaceuticals such as mAbs, is overwhelmingly performed using batchwise processing. Because of this, all unit operations from upstream to downstream are physically separated from one another and act independently as discrete steps. This brings two processing consequences; (i) a unit cannot begin until the preceding one has completed, resulting in idle operations, and (ii) non-value added steps such as holding tanks are necessary to transport the product between operations once it exits the bioreactor and starts purification. This presence of holding tanks, usually contained within skids, is a characteristic feature of the commercial production of biopharmaceuticals. Another is the frequent interaction between operator personnel and unit operations as the product makes its way downstream.

The use of batch production contrasts with other established processing industries such as oil and gas, small drug pharmaceuticals and food and drink, where at least some of the processes involved are carried out continuously, i.e. with integrated unit operations and with no or little downtime. There are many reasons for the continued reliance on batch for biologics; (i) the industry, in its commercialised form, is relatively young at around three decades, (ii) there is a prevailing conservative mind-set by companies to stick with what they know when confronted with new technologies, such as continuous processing equipment, (iii) this mind-set in part is due to the inherently challenging and highly regulated nature of biologics manufacturing, (iv) the product is the process, so any continuous processes would need to ideally be developed from the start, rather than retrofitted in later, and simply (v) the global market demand for biologics will never meet that of an industry such as oil and gas, so having a continuous output is not strictly necessary.

For upstream processing, i.e. the use of a bioreactor to grow a cell line to a sufficient biomass for subsequent expression of heterologous product, processes are frequently either batch or fed-batch mode. In batch, the bioreactor is a closed system, with medium and a cell seed added at the beginning and the culture allowed to commence. It is here that the classic cell culture growth curve starts; cells begin to consume substrates, acquire biomass and release

metabolites, some of which are toxic. As substrates are used up, cell culture growth evens out, and eventually, as toxic metabolites continue to accumulate and have a detrimental effect, cell death occurs. Subculturing, which is essentially the manual process of replenishing the medium with a fresh cell seed, would occur during the mid- or late-exponential phase.

All cell culture operations are at least batch, with batch highly prevalent in both research and industrial settings for the routine subculture to prolong the life of a cell line, in either suspension or adherent modes. In fed-batch, which may be referred to as a semi-continuous operation, medium and cell seed is added at the beginning as before. However, after a defined time period, specific substrates are added, or fed, at specified time points, to keep the quality of the medium at a desired level. This has the effect of boosting the biomass achieved, extending the culture time and increasing product output. Different feeding strategies mean the concentrations of particular substrates can be controlled and tailored to the needs of the specific cell line and culture.

It is widely known that fed-batch is the most popular mode of operation for commercial upstream purposes, with large-scale reactors (often >5,000 L) being employed to maximise product yield, with the wider process, taking into account downstream operations, being batchwise in nature. For both batch and fed-batch operations, the product remains in the bioreactor until the end of the culture period.

### 1.2.2 PERFUSION AND CONTINUOUS UPSTREAM OPERATIONS

There exist operations within biopharmaceutical production which may benefit considerably from fully continuous processing. Perfusion technology — the leading form of continuous upstream processing — brings tangible advantage to cell culture and recombinant protein production. These benefits are generally independent of wider process adoption of continuous technologies, e.g. continuous downstream units, and thus can be explored in isolation within research and development settings. Perfusion operations mimic the mammalian circulatory system, i.e. cultured cells experience a continual arrival of fresh medium and simultaneous exit of spent medium. In these systems, cells are physically retained, or separated from the exiting medium, by a retention device, so as to allow fresh medium to be perfused through without gradual cell loss. In practice, this takes the form of a modified bioreactor, where an inlet allows medium to be pumped in, and an outlet allows ‘old’ medium, already present in the vessel, to be pumped out along with the product. The retention device can be external or internal, depending upon the technology employed, and comes in a wide variety of formats (see § 1.2.3).

The advantages that perfusion offers over batch and fed-batch operation include; (i) vastly higher cell densities, often reaching in excess of  $1.0 \times 10^8$  cellmL<sup>-1</sup> (Clincke et al., 2013; Zamani et al., 2018), (ii) much longer culturing times due to medium replacement, and consequently no culture death, with twenty-five days and more culture reported (Bosco et al., 2017; Zhang et al., 2015), (iii) continual removal of product at the outlet, meaning products prone to degradation can be processed immediately as they exit, (iv) higher volumetric productivities, and so allowing a reduced footprint of upstream equipment within industrial sites, which in turn results in reduced capital cost and cost of goods, and finally (v) an optimal medium environment for cells, which may bring benefits for both product titre and therapeutic quality, including greater consistency in glycosylation profiles (Karst et al., 2017a; Karst et al., 2017b). Table 1.3 shows the mAb products commercially manufactured using perfusion today, with Janssen Biotech being the leading industrial player.

TABLE 1.3 FDA-approved mAb products manufactured, ordered by year of approval, using perfusion technology. Adapted from Schmidt (2017), where non-mAb biologics produced using perfusion culture are listed.

mAb Therapeutic	Year of Approval	Company
Abciximab	1994	Janssen Biotech
Infliximab	1998	Janssen Biotech
Alemtuzumab	2001	Genzyme (Sanofi)
Golimumab	2009	Janssen Biotech
Basiliximab	2009	Novartis
Ustekinumab	2009	Janssen Biotech

Process intensification is synonymous with perfusion, and is responsible for the key benefits of this technology. An intensified bioprocess describes an increased cell density culture, greater product titre with a consequent reduction in physical space requirements, i.e. higher volumetric productivities, with gL<sup>-1</sup>day<sup>-1</sup> often used as the metric. For perfusion, this means a smaller site footprint, reducing capital and operating costs and contrasts with much larger bioreactors and support equipment seen with fed-batch. Due to these reduced volumes, perfusion operations are thus seen as very much compatible with single-use technology and often are presented together (Whitford, 2015). As a theoretical example to demonstrate volumetric productivities, a single-use 50 L perfusion bioreactor could yield the same amount of product as a stainless steel 1,000 L fed-batch bioreactor (Langer, 2011).

Chen et al. (2018) identified three parameters responsible for process intensification; cell-specific productivity, viable cell density and length of 'idle' bioreactor stages, e.g. non-productive cell growth stages. Whilst perfusion remains the best way to intensify an upstream process, it is worth noting that fed-batch processes can indeed be intensified themselves. This is made possible by perfusion being used in the seed train prior to the fed-batch, as an 'N-1 seeding strategy', to rapidly generate enough cells to vastly increase the seeding density of the eventual fed-batch run, as demonstrated by Xu et al. (2020). The 'N-1' refers to the step immediately prior to the fed-batch operation, i.e. the step where cells will be grown to later become the seed. Due to this higher cell seed the fed-batch run may be completed in a shorter time period than would otherwise occur, meaning faster production cycles are possible.

Perfusion is not a new technology and, for biopharmaceutical manufacturing, actually predates the use of fed-batch processing. In the late 1980s and early 1990s, when product titres were a fraction of what they are today, and when a lot of heterologous products were inherently unstable in media, perfusion operations were solely employed (Bonham-Carter et al., 2011). However, media quality improved, more robust cell lines were developed and product titres consequently jumped, meaning familiar, scalable reactors took over and fed-batch became dominant in the industry.

Concerns relating to the adoption of perfusion operation within modern commercial processes mirror those of general continuous bioprocessing, with a survey from industry revealing process operational complexity, process development challenges and contamination risks as the biggest perceived concerns when using perfusion, as compared to fed-batch operations (Langer et al., 2014). Others have been more direct in their scepticism concerning the role of perfusion in bioprocessing today, referencing the genetic instability of cells when subjected to cultures lasting weeks at a time, the required higher costs of research and development and asking why companies, with successful batch facilities, would ever need to switch to continuous operations (Croughan et al., 2015).

However, the use of perfusion in commercial processing is growing with renewed interest. Despite perceived regulatory concerns, regulatory bodies actually encourage the uptake of perfusion processes — the first biologic manufactured using perfusion was approved by the FDA in the mid 1990s — and see it alongside other emerging initiatives such as quality by design and process analytical technology (Fisher et al., 2019). Perfusion is seen as a key technology in the factory of the future; characterised as, continuous, single-use, modular ('plug-and-play'), multiproduct, and small-scale yet intensive to meet changing market demands.

Figure 1.2 visualises the four cell culture modes, separated into batch, semi-continuous and continuous operations, and shows typical growth curves for each. All have been discussed, with the exception of chemostat culture, which is essentially perfusion but without any means of cell retention. The rate of medium going in, i.e. the dilution rate, is equal to that leaving, so metabolite and substrate concentrations, and cell number, reach a steady state. A culture at steady state will have a dilution rate equal to its growth rate, meaning the growth can be directly controlled by the rate at which medium is entering and leaving. Chemostats are not typically used with mammalian cells, where they would experience detrimental cell loss, and instead are employed for rapidly growing bacterial and fungal cultures (Basson, 2000; Lis et al., 2019). Chemostat vessels have been used with CHO cells, but solely as an experimental technique to investigate the effect of mild hypothermia on productivity, separately from the specific growth rate, which is not possible with usual batch operations (Vergara et al., 2014). Chemostats will not be discussed further here, but remain a technically simple option for continuous upstream processing.

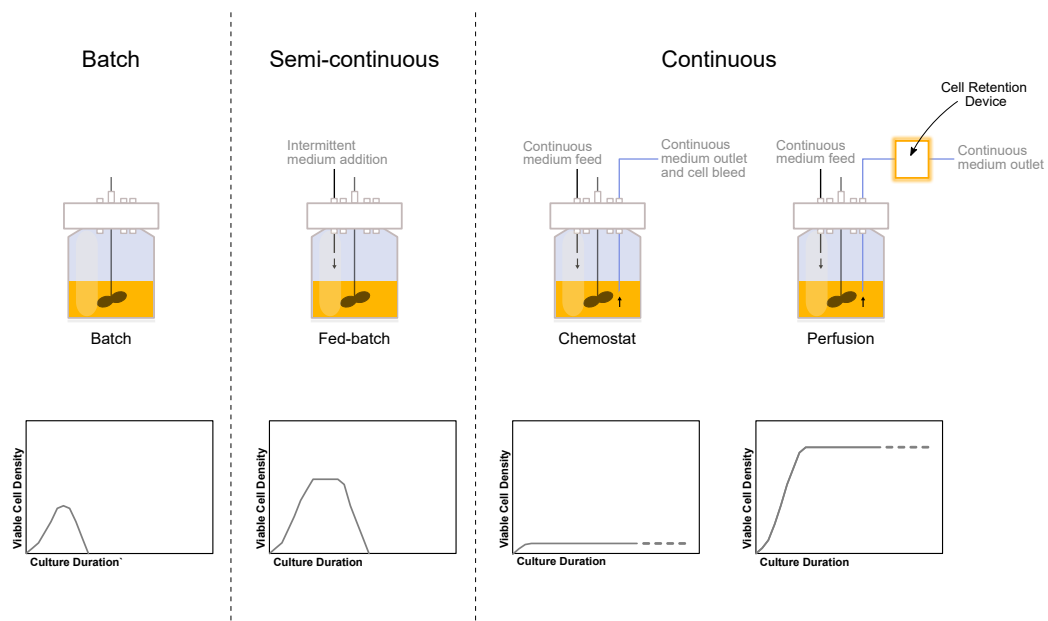


**FIGURE I.2 Schematic detailing the four cell culture modes, categorised as either batch, semi-continuous or continuous operation.** Cells can be cultured in processes defined as either batch, fed-batch, chemostat or perfusion. For batch, the culture duration is limited as medium will progressively get consumed as cells grow. Fed-batch allows an extended culture duration due to the intermittent feeding of substrates, although the culture must eventually terminate due to volume limitations within the vessel. For chemostat and perfusion, medium is continuously replenished and the culture can be sustained indefinitely. For perfusion, however, cells are retained (either internally or externally to the bioreactor) and do not get diluted out along with the medium, as is the case with a chemostat process. The choice of process will depend upon the intended application. Simplified, relative growth curves show the expected viable cell densities and typical culture durations for each of the cell culture modes.

Continuous downstream processing is also an emerging area for biopharmaceutical manufacture, albeit very much new unlike perfusion. It has not been explored in this thesis, but Zydney (2015) has reviewed current technologies for all major downstream operations. Considered together, Konstantinov et al. (2014) provides commentary on industrial continuous bioprocessing and discusses examples of hybrid set ups, e.g. a perfusion and batch downstream process, or a batch upstream and continuous downstream process, as well as fully integrated, continuous processes. Whilst the former are achievable and very much feasible, the latter may still be not be possible at certain scales, due to specific downstream equipment simply not being available as continuous units yet.

For most industry players economics will usually dictate their decision on whether to use any continuous unit operations within a commercial process. Pollock et al. (2013) have compared the economic, environmental and operational feasibility of fed-batch and two perfusion processes (one employing a spin filter cell retention device, the other an ATF cell retention device; both of which are explained further in § 1.2.3). Interestingly, the authors reported on the limitations of the spin filter process, including its low robustness, with an ATF providing the most economic benefit. However, fed-batch came out top if environmental and operational feasibility is deemed more important, owing to its lower water usage and regarded as easier to use. However, the latter may change over time as more operators are accustomed to perfusion operations or if the operations were performed by a company already familiar with continuous processing.

### 1.2.3 CELL RETENTION FOR PERFUSION

The cell retention device, or more broadly the means of cell retention, is the defining feature of any perfusion unit operation. Cell retention devices form an incredibly diverse range of equipment, and there are multiple ways, some of which are very sophisticated, to stop cells from exiting a system in a perfusion process. Some sources refer to cell retention as cell recycling, or cell separation, as this better reflects the nature of the particular retention method used. The first distinguishing factor for cell retention devices are their physical location; external devices are outside the bioreactor, whereas internal are inside. The second is their type of retainment; Voisard et al. (2003), who have produced a detailed review on cell retention devices, divides this up by size, i.e. via filtration, and by density, of the cells.

For filtration, a physical barrier is employed to stop cells from exiting with the permeate. Hollow fibre membranes are probably the most encountered within modern industrial continuous processing. These devices take the form of a cassette, or cartridge, filled with thousands of semipermeable hollow fibres. The cassette has an inlet and an outlet and is designed so that any liquid, such as medium, entering will flow through the interior of the

fibres. Cells are seeded within the extracapillary space, i.e. outside the fibres, but within the cassette. When medium is perfused through, substrates can diffuse out for cell consumption, whilst metabolites can diffuse in and exit. The pores of the fibre walls, often referenced by their molecular weight cut off, can be controlled, and so products such as antibodies can be allowed to either exit with the permeate or be retained, depending upon the application. Whitford et al. (2009) listed three fundamental characteristics of hollow fibre membranes for perfusion operations; (i) extremely high binding culture ratio to volume ratios, (ii) immobilisation of cells at a very high density, and (iii) selected porosity of the fibres, e.g. to concentrate the secreted product.

The pumping mode defines the hollow fibre membrane operation, and is sometimes referred to itself as the cell retention method. Tangential flow filtration (TFF) mode describes the flow of medium passing through the fibres, i.e. tangentially, and allowing the exchange of liquids. TFF is often contrasted with dead end filtration, where liquid is passed straight through into a filter, eventually leading to fouling of the membrane. Alternating tangential flow (ATF), designed for cell culture, has the same principle as TFF but an added diaphragm pump causes the flow of liquid to occur in both directions within the cassette, i.e. alternating, which helps to flush the membrane and further keep it from fouling.

Spin filters have been used commercially for several decades, with much of the literature on the development of the retention method dating from the 1990s (Deo et al., 1996; Yabanavar et al., 1992). Perfusion operations employing spin filters use a rotating screen filter, frequently within the bioreactor, where cells are entrapped and cultured, whilst medium enters into the vessel and exits from the inside of the filter. Cells are retained mainly due to hydrodynamic effects caused from the rotation. The rotating speed of the screen is the key parameter, with a relatively fast spin needed to prevent cell accumulation on the filter and also reduce fouling. The pore size of the screen can also be increased to prolong the process before significant fouling occurs.

Microcarriers are capable of physically adhering cells and thus offer an alternative method of cell retention, provided they themselves can be retained. A key benefit of using microcarriers is their versatility; they can be used externally or internally with almost any type of vessel, and unlike other retention devices they do not require considerable expertise to operate. Their use in perfusion processes is demonstrated in the literature, although they are certainly less encountered than hollow fibre membranes. Goldman et al. (1998) used macroporous microcarriers to retain an adherent CHO cell line within a fluidised bed system operating in perfusion mode, whilst Bleckwenn et al. (2005) used microporous microcarriers for HeLa cells, employed within a bioreactor and retained via the use of a mesh

---

screen module operating using ATF. The use of microcarriers as a bespoke cell retention devices is the overarching finding in the work presented here and will be discussed in later chapters.

#### I.2.4 CURRENT TECHNOLOGIES FOR CONTINUOUS UPSTREAM R&D

Much of the literature provided so far has focused on the use of perfusion operations within an industrial setting, i.e. for the commercial, large-scale production of biopharmaceuticals. The work presented in this thesis is not intended to be used for industrial applications, but rather as an introduction as to how continuous upstream processes could be used for small-scale research and development purposes. Commercially available perfusion systems for research and development are severely limited, which may help explain the reluctance of industry to fully adopt perfusion in their processes. The market leader, the *ambr250 High Throughput Perfusion* system, launched in 2018 by Sartorius Stedim, is designed for perfusion development and uses up to twenty-four parallel bioreactors with working volumes from 100 to 250 mL. The cell retention device, attached to each bioreactor unit, is a hollow fibre membrane with TFF operation. Each bioreactor, including the retention device, is single-use. The system is likely to be very expensive and certainly would not be affordable for most academic departments involved in perfusion research — no literature on its use from academic sources could be found — or even for start-up biologics companies. The system also possesses a large footprint and is clearly designed for industrial companies, with large labs, who intend on developing scalable perfusion operations for commercial processes.

However, many examples exist in the literature of perfusion systems developed in-house, with some even demonstrating the use of bespoke cell retention methods. Clincke et al. (2013) attached a hollow fibre membrane to a single-use 10 L wave bag bioreactor and employed either TFF or ATF for comparison, with some cultures lasting over 40 days. Cell bleeding was employed to maintain the cultures at high viability after sufficient growth. For TFF, the maximum cell density achieved was  $2.14 \times 10^8 \text{ cellmL}^{-1}$ , whilst for ATF, it was  $1.30 \times 10^8 \text{ cellmL}^{-1}$ ; the authors noting the increased viscosity when dealing with high densities caused challenges with both TFF and ATF functions.

In the same lab, Zhang et al. (2015) used a CellTank system, employing a polyester matrix (150 mL total volume) within a cassette, submerged within a 2 L bioreactor, as an internal cell retention device. Suspension-adapted CHO cells were physically entrapped within this matrix, with an inlet allowing entry of medium and an outlet from the cassette letting medium exit. Maximum cell densities achieved were above  $1.0 \times 10^7 \text{ cellmL}^{-1}$  and runs were carried out for up to 30 days. Due to the inaccessibility of the retained cells,

cell bleeds were not feasible, and instead hypothermic temperatures used to arrest cell growth, although the authors noted rapidly increasing the recirculation rate would dislodge cells from the matrix and could be used as a crude way to bleed cells. Kwon et al. (2017) utilised a novel cell retention method; namely, microfluidic channels (channels with widths measuring 600  $\mu\text{m}$  or less) in the form of spirals, fabricated using soft lithography with polydimethylsiloxane as the material. The separation effect was due to ‘inertial sorting’, with hydrodynamic forces causing the majority of cells to flow towards the inner wall and consequently into the retentate outlet at the end of the spiral. Spent medium then exits through the permeate outlet. As some cells also exit through the permeate, cell bleeding is not required to maintain a viable high cell density. Using this method eliminated any bio-fouling experienced with filter-based retention devices, such as hollow fibre membranes. The authors demonstrated this retention technique with four spirals attached, externally, to a spinner flask, with 18 days perfusion culture using CHO cells performed and a cell density of over  $2.0 \times 10^7 \text{ cell mL}^{-1}$  achieved.

As a technically simple way to mimic perfusion, semi-continuous or pseudo-continuous upstream operations have also been reported. In these instances, cells are usually settled via gravity and the medium replaced manually at set intervals to replenish substrates and remove toxic metabolites. An *ambr15*, designed for batch operation, was employed using this sedimentation strategy as a separation method (Kreye et al., 2019). For medium exchange, the agitator was switched off, cells allowed to settle for at least 30 min and 3 mL supernatant removed, with 3 mL fresh medium then added. These commands were programmed in, allowing the *ambr* system to automatically carry out medium exchange. This was performed for 45 days using a human cell line, with over  $1.0 \times 10^7 \text{ cell mL}^{-1}$  achieved, with the authors favourably comparing results to that performed using a standard ATF perfusion process. Gagliardi et al. (2019) demonstrated a relatively more sophisticated approach, again using the *ambr15* system but instead employing offline centrifugation via an external centrifuge (separate from the *ambr15* system) equipped with a custom holder for the *ambr15* vessels. In contrast to relying on cell sedimentation via gravity, this method ensured cells were only in suboptimal conditions for a minimum time period. Both these reports show that a pseudo-continuous set up can be achieved for laboratories that do not wish to employ cell retention devices.

### I.3 POLYMERISED HIGH INTERNAL PHASE EMULSIONS

#### I.3.1 AN INTRODUCTION TO POLYHIPES

A high internal phase emulsion, or HIPE, is defined as an emulsion with an internal, or droplet, phase volume ratio of 0.74 or greater, i.e. 74 % of the total emulsion volume is

---

comprised of droplets dispersed within an external phase. Usually this internal phase is water and the external, or continuous, phase is 'oil' (or rather some hydrocarbon monomer with sufficient hydrophobicity), creating a water-in-oil HIPE, and so requires a surfactant for a stable emulsion to occur. These water-in-oil HIPEs are typically white, viscous paste-like liquids. A polymerised high internal phase emulsion, or polyHIPE, may be formed when the external phase of the emulsion is cured, i.e. polymerised, and thus hardens to form a polymeric material. The water droplets can be dried to leave a highly porous (74 % or greater void space) plastic, described as scaffold-like, permeable and with varying degrees of interconnectivity. This interconnectivity describes the pores (also known as voids) and their open connections to one another via pore throats (or windows) and is the defining characteristic for polyHIPE materials. Foudazi (2021) has provided an in-depth discussion on the formation of this interconnected structure during the polymerisation of HIPEs.

Curing can be achieved through heat or radiation exposure, and may take less than a minute or many hours to complete, depending upon the monomers used, the presence of an initiator, the volumes used and the polymerisation mechanism. Because the pores are the direct result of the space previously filled by water droplets, a polyHIPE is considered an example of emulsion templating, with the water technically acting as a porogen (pore-generating) for the final material. However, the morphology of a polyHIPE may be different to that exactly seen in its preceding HIPE, due to coalescence of droplets immediately before or during polymerisation, as well as the effects of Ostwald ripening if the HIPE is stored for extended periods (Barbetta et al., 2009).

The criterion of a 74 % internal phase volume for a HIPE is not arbitrary; 0.74048 is the maximum fraction of space, or packing density, that equally sized spheres, of any specified size, can fill within any volume of space — known as the Kepler conjecture (Hales et al., 2017). Because HIPEs can exist with internal phase ratios many times greater than 0.74, it thus stands that the water droplets contained in the internal phase are not uniform in size, but deformed and irregular, which explains the seemingly randomly sized voids observed in subsequent polyHIPE structures. Polymerised medium high internal phase emulsions, or polyMIPes, with 30 to 74 % internal phase volumes, and polymerised low high internal phase emulsions, or polyLIPes, with less than 30 % volumes, do also exist (Wu et al., 2013), but are much less encountered in the literature and have not been explored in this work.

Cameron (2005) and Pulko et al. (2012) have both written succinct reports on the use of polyHIPE technology to achieve porous polymeric materials, whilst an up-to-date and highly detailed review on emulsion templating using HIPEs is given by Zhang et al. (2019). The production of polyHIPE materials was first patented in 1982 by researchers at Unilever,

who also coined the term ‘polyHIPE’ to refer to these new highly porous structures (Barby et al., 1982).

### 1.3.2 CHEMISTRY OF POLYHIPES

The structural characteristics of a polyHIPE are determined by the components of its precursor HIPE, including monomer type, crosslinker and surfactant, as well as the processing conditions in which the HIPE was generated. For monomers, styrene remains the most employed for the fabrication of polyHIPES, being inexpensive, readily available and sufficiently hydrophobic to form a stable emulsion, with its use extensively documented in the literature (Choudhury et al., 2016; Mercier et al., 2000; Yang et al., 2015; Xu et al., 2015). Other styrenic monomers frequently used include divinylbenzene — often in combination with styrene itself — typically as a crosslinker to covalently link the forming polymer chains and provided added strength (Jing et al., 2015; Woodward et al., 2017). Another, 4-vinylbenzyl chloride, has been used alongside divinylbenzene to form polyHIPES with reactive chloride moieties, allowing chemical modification of the resultant material, with amino and hydroxy functionalisations demonstrated (Barbetta et al., 2000; Krajnc et al., 2002). The post-fabrication functionalisation of polyHIPES is a popular area of research and will be discussed further in § 1.3.5.

Free radical polymerisation, often used as the mechanism for the fabrication of polyHIPES, are chain reactions involving initiation, propagation and termination steps. Initiator molecules are first degraded, through heat or radiation exposure, to generate free radicals (chemical species with an unpaired valence electron), which then ‘attack’ the pair of electrons found in double bonds, such as C=C groups within monomers. In doing so, a new chemical bond is formed between the initiator radical and one of the carbons of the double bonds, leaving a new radical on the other carbon. This is the initiation step, and is followed by propagation, where another monomer is attacked with the new radical on the first monomer, creating two units, and is repeatedly carried out, forming a polymer chain. The termination step describes the end of the polymer chain making process, where radicals on two growing chains eventual meet and join, with the polymerisation process then complete.

The degradation of initiators into radicals may be performed by thermal decomposition or photolysis, usually by UV radiation, amongst others. Despite their popularity, the use of styrene and its derivatives demand prolonged thermal decomposition for polymerisation to occur, often resulting in overnight oven use for polyHIPE fabrication. Whilst this may be deemed acceptable for HIPES poured into moulds for simple shapes such as discs and columns, i.e. monolithic structures, issues arise when more sophisticated formats are

required, such as microspheres or rods, where it may not be scalable, practical or even physically possible for such shapes to form during thermal polymerisation.

Acrylate, or acrylic, monomers are an attractive alternative to styrene-based monomers for polyHIPE manufacturing, with their advantages starting to be realised in research settings. In contrast to styrene, the double bonds found in acrylics are highly susceptible to breakage by free radicals, and thus acrylic-based HIPEs can polymerise within minutes, sometimes even seconds, when exposed to UV radiation at particular wavelengths. Such rapid photocuring opens up the possibility of fabricating more nuanced polyHIPE structures (see § 1.3.6), allows the creation of bespoke manufacturing set ups and even permits less stable HIPEs to be used.

Whilst styrene can theoretically be photocured, the inhibition effect of ambient oxygen on formed free radicals dramatically slows down the rate of polymerisation which, due to the relatively less reactive double bond, makes the curing process unfeasible. Strategies do exist to eliminate oxygen inhibition (Ligon et al., 2014), including the use of vacuum chambers for curing and oxygen radical suppression via certain gaseous molecules, but these have not been explored in this thesis and may add unnecessary complexity for investigators. Fortunately, this effect from oxygen can generally be ignored for the photocuring of small volume acrylics, such as those found in academic laboratories focusing on acrylic-based HIPEs.

To demonstrate the advantages of using acrylic monomers, Johnson et al. (2013) used a microchip laser of an appropriate wavelength to photopolymerise acrylic-based HIPEs into polyHIPE scaffolds with highly controlled formats, including grid arrays and hollow tubes. The same group further explored this UV stereolithography technique with the fabrication of polyHIPE ‘woodpile’ structures (Wang et al., 2016). For both reports, the acrylic monomers 2-ethylhexyl acrylate and isobornyl acrylate were used, and the technique would have been highly impractical with thermal polymerisation.

Acrylics comprise an incredibly diverse and versatile family of compounds, which can be exploited to tailor the properties of their resultant polymers. Methyl methacrylate and ethylene glycol dimethacrylate have been used to fabricate polyHIPEs with increased mechanical strength (Huš et al., 2014), and stearyl acrylate, isodecyl acrylate and isobornyl methacrylate were used for polyHIPEs with elastic and brittle characteristics (Tunc et al., 2012). In the last study, divinylbenzene was used as a crosslinker for all the HIPE materials, meaning the polymerisation process had to be thermally initiated, in this instance at 60 °C for 48 hr.

### I.3.3 POLYHIPES AS CELL CULTURE SCAFFOLDS

The practical advantages of using in-house polyHIPE technology include its simplicity, robustness and low cost, meaning laboratories possessing only basic equipment can still reproducibly fabricate highly porous materials with relative ease. These benefits may be pronounced when using photocurable acrylic-based HIPes, as the time required for manufacture is greatly reduced and allows serial material creation for testing and evaluation. The characteristic porous, interconnected nature of polyHIPE materials has resulted in them being employed for a range of applications, including as (i) filtration and separation media (Bhumgara, 1995; Chen et al., 2018; Schwab et al., 2009), (ii) solid phase chemistry supports and in catalysis (Koler et al., 2017; Krajnc et al., 2005), (iii) chromatography resins (Hughes et al., 2014; Pribyl et al., 2018) and (iv) sensors (Silverstein et al., 2005).

Relevant to the work reported here, however, is the use of PolyHIPes as materials for adherent cell culture. Their application as scaffolds in tissue engineering, particularly for bone replacement, is a recurring theme in the literature. Owen et al. (2016) cultured mesenchymal progenitor cells on acrylic polyHIPE ‘woodpile’ structures to demonstrate the potential for such materials to be used for bone engineering, whilst Akay et al. (2004) cultured osteoblasts on styrenic polyHIPE discs and Bokhari et al. (2005) did the same except used hydrogel-polyHIPE hybrid materials. Moglia et al. (2011) showed how HIPes generated using propylene fumarate dimethacrylate, a monomer capable of polymerisation at 37 C, could be injected into moulds and subsequently cured at physiological temperatures. The authors then successfully cultured 3T3 cells on the resulting polyHIPes and proposed such materials, which were also biodegradable, could be used as *in vivo* bone grafts. Other polyHIPes with similar properties have been explored; polycaprolactone, a biodegradable polymer, was chemically modified into polycaprolactone methacrylate — now an acrylic macromonomer — to allow photocuring into a polyHIPE (Dikici et al., 2019). These materials were cultured with human dermal fibroblasts for seven days. Polyester polyHIPes, fabricated using tetrakis-3-mercaptopropionate and divinyladipate, were cultured with human articular chondrocytes for cartilage engineering purposes, with the degradation of the materials demonstrated using simple PBS and NaOH solutions (Naranda et al., 2016).

Aside from tissue engineering, non-degradable polyHIPes have been widely explored as general cell culture materials, with reports often focusing on the newfound benefits of 3-D scaffolds. Hayman et al. (2005) cultured human stem cell-derived neurons on styrenic polyHIPE discs, themselves coated with polylysine and laminin substrates, to demonstrate the advantages of using porous materials. Sun et al. (2019) used styrenic polyHIPes as substrates for the culture of human lung adenocarcinoma cells to, intriguingly, study the ef-

fects of cigarette smoke cytotoxicity and compared the results to similar studies performed using 2-D culture. HepG2 liver cells were cultured on usual 2-D substrates and 3-D styrenic polyHIPE scaffolds (Bokhari et al., 2007b) with the authors reporting that albumin production, essential for hepatocyte activity, increased when polyHIPE materials were used. All the experiments in the reports listed were carried out using in-house fabricated polyHIPEs, with a variety of mammalian cells used, including primary cells, and demonstrate the accessibility and versatility of polyHIPE technology.

#### 1.3.4 COMMERCIAL POLYHIPE CASE STUDY: ALVETEX

*Alvetex*, a crosslinked polystyrene polyHIPE material (Knight et al., 2011), remains the only commercially available polyHIPE product range for cell culture applications. Beginning as a spin-out company, Reinnervate, from Durham University (which has a considerable output in polyHIPE research), UK, and now owned by Reprocell, *Alvetex* is available as 200  $\mu\text{m}$  thick disc-like structures in two formats, *Alvetex Scaffold* and *Alvetex Strata*, with the former possessing a larger average void size (42  $\mu\text{m}$  to 15  $\mu\text{m}$ ). Figure 1.3 shows electron scanning micrographs of both formats. Both are 90 % porous polyHIPEs, with the reduced void size of *Alvetex Strata* likely a result of different processing conditions during HIPE generation, e.g. greater mixing during HIPE formation to break up water droplets. The crosslinker employed for both is probably divinylbenzene, if the literature of the development of the products are reviewed (Bokhari et al., 2007a; Bokhari et al., 2007b), although this is not confirmed in current commercial documents.

Both *Alvetex Scaffold* and *Alvetex Strata* structures come installed within standard multiwell plates, either fixed to the bottom of wells or mounted within removable well inserts. Commercial sources advertise the products as substrate materials for adherent 3-D cell culture, and claim the biological relevance of cell research is enhanced when cells are cultured in environments similar to those found *in vivo* (Reprocell, 2019a). The specific application of *Alvetex Strata*, in comparison to *Alvetex Scaffold*, appears to be to allow epithelial-type cell lines or even tissue to grow on top of the material, rather than within, with nutrients then available from both above and below (Reprocell, 2019b).

Cell culture applications in the literature which have demonstrated the uses of *Alvetex* products include the growth of astrocytes for phenotypic studies (Ugbode et al., 2016), the use of transfected HEK cells as positive controls for *in situ* hybridisation techniques (MacDonald et al., 2014) and the characterisation of murine neurons in 3-D culture for comparison to usual 2-D culture (Smith et al., 2015), amongst many others. It is evident that, just like familiar polystyrene multiwell plates for 2-D culture, *Alvetex* materials for 3-D culture can be used as a substrate for virtually any adherent cell type. It can be proposed that usual

adherent culture methods would be repeated, such as the use of FBS within medium to enhance adhesion. Indeed, in all three reports listed earlier, 10 % FBS supplemented medium was used, with one even soaking the scaffolds overnight with FBS and another pre-coating with polyornithine, a cationic polymer. *Alvetex*, like plates and flasks, can thus be chemically treated before cell seeding with specific adhesion substrates. Official application protocols does advise users on the coating of *Alvetex* products with polylysine, fibronectin, collagen and Matrigel substrates, if they wish to enhance cell adherence to the material. This is relevant as the polyHIPEs fabricated for this work is also coated with substrates.

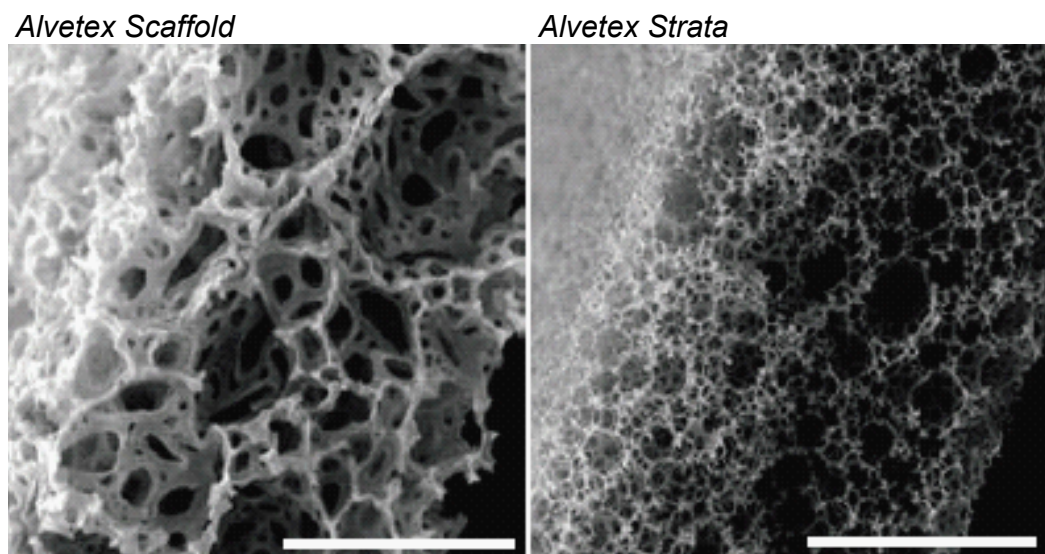


FIGURE I.3 Scanning electron micrographs showing the structure differences between *Alvetex Scaffold* and *Alvetex Strata*. Transverse sections of *Alvetex Scaffold* and *Alvetex Strata* obtained using electron scanning microscopy. The larger pore diameters in the former is apparent. Both materials show interconnectivity, with windows connecting surrounding pores. Scale bars = 100  $\mu\text{m}$ . Reproduced with kind permission from Reprocell (2019a).

Interestingly, *Perfusion Plate*, a 4-well polystyrene plate product for perfusion culture, is also available (Reprocell, 2019c). Well inserts, containing *Alvetex* structures, can be used with the plates so pairing 3-D culture with medium perfusion, and ensure cells can experience other *in vivo* conditions such as dynamic medium flow. Tubings, luer fittings, a pump and a medium vessel can be obtained by the user. With the set up suggested in commercial literature, cultured cells would experience perfusion of recycled medium, i.e. pseudo-continuous culture, where nutrient concentration would gradually diminish over time due to cell consumption. This contrasts with true continuous, or ‘normal’ perfusion as recognised in the biologics industry, where nutrients are kept sustained at defined concentrations by the continuous delivery of fresh medium. The product is clearly aimed at further mimicking *in vivo* dynamic flow environments, i.e. circulatory systems found in

mammals, rather than for intensified biologics processes, as is the case in this thesis. Nevertheless, the *Perfusion Plate*, with the use of *Alvetex*, is one example of continuous culture using cells adhered on polyHIPE materials.

The culturing of CHO-K1 cells, a parental adherent CHO cell line, with *Alvetex Scaffold* has been reported in a commercial protocol (Reprocell, 2019d), with evidence of cell penetration into the material. FBS, at 10 %, was used in the culture medium. No other examples of CHO cells being cultured using polyHIPE materials have been found.

### I.3.5 POLYHIPE FUNCTIONALISATION

An advantage of in-house polymeric material fabrication is the opportunity for investigators to tailor, and so enhance, the properties of the material to their specific application. A popular technique is the inclusion of comonomers with specific chemical species, such as functional groups, so that the resultant polymer now contains these groups. These can then either directly affect the characteristics of the material, or the groups can be used themselves as reactive species for further functionalisation by reacting with other compounds. Whilst all chemical species are capable of reacting with others, some are far more reactive than others and so are often highly sought after within comonomers, including amino and carboxyl moieties.

The comonomer approach has been utilised numerous times with polyHIPE technology. Hayward et al. (2013a) included the monomer pentafluorophenyl acrylate into their combined styrenic and acrylic HIPEs to give the polyHIPE material ester functionality. The authors used this species to chemically couple either glucose or galactose (both of which were aminated and thus reactive) onto the surface of the materials, yielding carbohydrate-functionalised polyHIPEs. To demonstrate the effect of galactose, which they note is known to bind hepatocytes and promote cell adhesion, they cultured primary rat hepatocytes on the new materials, including the non-functionalised original, and reported the highest albumin concentration on the galactose-functionalised polyHIPE in the first three hours.

Similarly, 4-vinylbenzylamine or 4-vinylbenzylphthalimide was included in the fabrication of styrenic polyHIPEs, with the incorporated amino groups then used to conjugate reactive polypeptides onto the materials (Audouin et al., 2012). The visual effect on the hydrophilicity of the materials was evident when a water droplet was dispensed onto the functionalised polyHIPEs. Langford et al. (2014) fabricated polyHIPEs using the monomers trimethylolpropane triacrylate, an acrylic, and trimethylolpropane tris(3-mercaptopropionate), a thiol. The generated HIPEs were stable and photopolymerised. The reactive S-H groups on the thiol, now incorporated into the polyHIPEs, were used in

both UV- and thermally-initiated “click” thiol-ene reactions, as well as Michael addition reactions, to conjugate the materials post-fabrication with various acrylics, including fluorescent compounds. The authors noted the mild reaction conditions required, suggesting sensitive, biological compounds could also be conjugated using these techniques.

As an alternative approach, Hayward et al. (2013b) included the comonomer acrylic acid into the internal phase, i.e. with the water, during the generation of a HIPE, due to acrylic acid’s hydrophilicity making it unsuitable for the external phase. The incorporated carboxyl groups were detected using toluidine blue, resulting in staining of the functionalised materials, and the familiar water droplet test was carried out.

Several considerations must be addressed when using the comonomer technique for poly-HIPEs. The effect of the comonomer on the stability of HIPE has to be determined, although this is less important when using photopolymerisable HIPEs. Whilst some comonomers may incorporate reactive functional groups in the final material, their presence in the HIPE, even if stable, will certainly affect the characteristics of the polymerised material. For both points, these effects may depend upon the amount of comonomer used and a trade-off may arise between functional group presence and any detrimental impact on final structural properties.

However, an advantage of post-fabrication conjugation, i.e. chemically coupling a new compound onto a reactive species present in the material, is that the structural characteristics of the polyHIPE, such as porosity and shape, are generally not affected, and instead only the chemical properties are modified.

### 1.3.6 POLYHIPE MICROSPHERES

The fabrication of spherical microparticles, or microspheres (sometimes referred to as beads or particles), has been reported using HIPEs. PolyHIPE microspheric materials are a highly specialised format, being considerably more challenging to fabricate than monolithic structures and often requiring bespoke set ups to reproducibly manufacture.

The use of syringe pumps within controlled fluidic systems is a technique widely demonstrated in the literature (Gokmen et al., 2009; Lapierre et al., 2015; Moglia et al., 2014; Paterson et al., 2018; Whitely et al., 2019). The principle being that a HIPE is controllably injected, via a syringe pump, into tubing containing a flowing carrier phase medium, consequently forming HIPE microspheres which are serially polymerised into spherical polyHIPEs. The injection flow rate of the HIPE, and the flow rate of the carrier phase, can be varied to control the size of the resulting microspheres. Because of the requirement of rapid curing, photopolymerisable HIPEs are the dominating type, and in all the reports listed acrylic

polyHIPE microspheres were fabricated using UV radiation. The carrier phase in the microfluid systems is sometimes called the continuous phase, though this should be not confused with the continuous phase, i.e. the external phase, of HIPEs as introduced earlier.

The composition of the carrier phase is a key decision in polyHIPE microsphere fabrication set ups and remains an active area of research, including in the work presented in this thesis. Polyvinyl alcohol, a synthetic, slightly viscous polymer, remains the most used (Moglia et al., 2014; Whitely et al., 2019), whilst Gokmen et al. (2009) also compared sodium dodecyl sulphate and glycerol solutions and Lapierre et al. (2015) used fluorinated oil Novec 7500 with an added surfactant. In all these reports, a co-flow orientation was used, with HIPE injected so as to follow the flow of the carrier phase. Paterson et al. (2018), interestingly, used only water as a carrier phase — described as a ‘water-in-oil-in-water’ technique due to the typical water-in-oil HIPE used — but instead relied on an alternative T-junction orientation, where the injection of the HIPE was perpendicular to the flow of the carrier phase. The authors also demonstrated a much simpler, albeit cruder, method where HIPE precursor was poured into a beaker of water agitated by an impeller; the shear of the water rapidly breaking up droplets into HIPE microspheres. The beaker was exposed to UV before sedimentation of the HIPE spheres could occur, but the diameters of the polymerised microspheres were hugely varied compared to the monodispersity seen with the T-junction lab-scale fluidic system.

Generally, the literature presented here reported polyHIPE microspheres with varying degrees of dispersity and porosity, and indeed material sphericalness, and confirmed these parameters to be dependent upon manufacturing conditions, including carrier phase composition and flow rate, HIPE injection flow rate and HIPE precursor fabrication. Where applications of polyHIPE microspheres were demonstrated, they included drug delivery carriers, protein delivery carriers within bone grafts and as scaffolds for the culture of human mesenchymal progenitor cells for angiogenesis. All examples showed low production rates.

Only one example documenting the fabrication of styrenic polyHIPE microspheres could be found. Desforges et al. (2002) prepared a styrene and divinylbenzene HIPE and used a syringe pump to dispense it into a vessel filled with a ‘suspension phase’ containing a solution of poly(diallyldimethyl) ammonium chloride. The vessel was stirred and heated to 80 °C. Stirring was continued for 15 min after all HIPE had been added, turned off, and heating continued for 6 hr to allow thermal polymerisation. This is similar to the beaker and water method reported by Paterson et al. (2018). The resulting microspheres were around 1000 µm in diameter and the single micrograph presented shows a slightly deformed spheri-

cal shape. It remains to be seen if it is possible for styrenic polyHIPE microspheres to be rapidly fabricated with a fluidic system using photopolymerisation. Eliminating oxygen inhibition, by use of a vacuum chamber, may be necessary in such a system. There could, in theory, be a set up using a syringe pump to generate spherical styrenic HIPE microspheres as before, with the system then fashioned so as the microspheres are subjected to a sufficiently long residence time within a heated chamber to polymerise, but this may be vastly impractical to carry out.

Due to the high relevance of the findings of these reports to major experiments described in this thesis, a study of the literature has been carried out later in § 5.1.2 alongside the results and discussion of that chapter. When employed as substrates for cell culture, microspheres are referred to as microcarriers, and have been used for many decades for anchorage-dependent cell lines. No commercial polyHIPE microcarriers have been found, although a patent relating to the fabrication of styrenic polyHIPE microspheres (using a similar heated beaker technique as described early) has been unearthed, but is now several decades old (Zhang et al., 2005).

A detailed review of the use of microfluidics to fabricate macroporous materials, including polyHIPE microspheres, has been given by Wang et al. (2017). Applications of these materials are also discussed.

### I.3.7 ALTERNATIVE METHODS OF MICROSPHERE FABRICATION

The use of HIPEs for the fabrication of porous microspheres has been discussed previously. Despite being an inexpensive and accessible method of production (when coupled with UV-initiated radical polymerisation), there remains other techniques to fabricate microspheres, both porous and solid, which may be of interest to readers. These techniques are usually described in terms of the actual polymerisation used, with three of them briefly explored here.

Suspension polymerisation relies upon the agitation of monomer(s) in a liquid phase, usually water, to keep forming particles suspended whilst they polymerise. Due to the agitation within the liquid phase, the monomers form spherical particles which subsequently cure to form polymerised microspheres. Hydrophobic monomer(s) may be needed, and surfactants added to stabilise the forming spheres and prevent aggregation. It is worth noting a variation on this technique was used by Paterson et al. (2018), as discussed previously, where HIPE was dispensed into a stirred beaker of water. Once HIPE spheres formed, the beaker was exposed to UV to initiate polymerisation. Singh et al. (2009) produced phenolic microspheres by mixing phenol and formaldehyde in water with an initiator, a stabilizer

and a crosslinker, whilst Abd El Mageed et al. (2021) produced magnetic polystyrene microspheres via continuous mixing and homogenisation, with both reports using suspension polymerisation.

Dispersion polymerisation describes a reaction where all reagents are first dissolved in a solvent to form a homogeneous system. It is crucial that the solvent used must be a nonsolvent for the anticipated polymer. Once the reaction begins the polymer forms and comes out of the system, with a heterologous system created. Jinhua et al. (2014) produced polystyrene microspheres using this technique, with ethanol or 2-methoxyethanol employed successfully as the solvent. Hong et al. (2007) likewise produced polystyrene microspheres using an aqueous alcoholic medium (ethanol, methanol and water) and added polyvinyl alcohol as a stabilizer.

Emulsion polymerisation utilises an emulsion, usually a hydrophobic monomer(s) within an aqueous solution containing a surfactant, to form microspheres. The monomer(s) form spherical particles within micelles (generated via the surfactant) which are polymerised to produce the microspheres. Feng et al. (2009) used emulsion polymerisation to fabricate poly(methyl methacrylate-co-butyl methacrylate) microspheres, with the authors reporting that the size of the particles was influenced by the amounts of surfactant and initiator used. Whilst this is an emulsion-based process, the technique is distinct from polyHIPE formation, where emulsion templating is used to generate a porous material.

### 1.3.8 COMMERCIAL MICROCARRIERS

Whilst the previous sections have explored the use of HIPEs as a means to generate porous microspheres, as well as alternative methods of microsphere fabrication, this section briefly describes commercially available microcarrier products. Microcarriers, which may be defined here as microspheres intended as a substrate for adherent cells, have been in use since the 1960s (van Wezel, 1967). The main benefit of using microcarriers is the application of suspension culture conditions for adherent cells, i.e. the use of agitated vessels such as bioreactors and shake flasks, which otherwise would not be possible for cells which are dependent upon adhesion to a surface. Another benefit is the ability to scale up adherent cells using a feasible amount of labware as, without the use of microcarriers, excessive numbers of flasks and plates would be needed to provide sufficient area. An in-depth guide discussing specific microcarrier products, general microcarrier culture and related processes is given by GE Healthcare Life Sciences (2013).

Table 1.4 lists all commercially available microcarrier products currently available (as far as could be identified), and includes their structural and adhesive properties. Products are

---

TABLE I.4 Commercial microcarrier products and their structural and adhesive properties, ordered by coating.

Microcarrier Product	Coating	Animal Origin?	Porosity	Diameter Size Distribution ( $\mu\text{m}$ )	Specific Surface Area ( $\text{cm}^2\text{-g}^{-1}$ )	Material	Manufacturer
Cytodex 1	Cationic charge	N	Micro	140–200	3000	Dextran	Cytiva (GE)
Cytopore 1	Cationic charge	N	Macro	200–280	1100	Cellulose	Cytiva (GE)
Cytopore 2	Cationic charge	N	Macro	200–280	1100	Cellulose	Cytiva (GE)
Hillex	Cationic charge	N	Solid	160–200	515	Polystyrene	Sartorius
Plastic Plus	Cationic charge	N	Solid	125–212	360	Polystyrene	Sartorius
Star-Plus	Cationic charge	N	Solid	125–212	360	Polystyrene	Sartorius
FACT III	Collagen/Cationic	Y	Solid	125–212	360	Polystyrene	Sartorius
Collagen	Collagen	Y	Solid	125–212	360	Polystyrene	Sartorius
Cytodex 3	Collagen	Y	Micro	120–180	2000	Dextran	Cytiva (GE)
Corning MC (Collagen)	Collagen	Y	Solid	125–212	360	Polystyrene	Corning
CultiSpher-G	Collagen	Y	Macro	130–380	(no data)	Gelatin	Percell Biolytica AB
CultiSpher-S	Collagen	Y	Macro	130–380	(no data)	Gelatin	Percell Biolytica AB
Corning MC (Synthemax II)	Synthetic peptides	N	Solid	125–212	360	Polystyrene	Corning
Corning MC (CellBIND)	Oxygen groups	N	Solid	125–212	360	Polystyrene	Corning
Plastic	None	N	Solid	125–212	360	Polystyrene	Sartorius
Corning MC (untreated)	None	N	Solid	125–212	360	Polystyrene	Corning

ordered according to their coating or rather, as related to the work here, their adhesion substrate(s). As will become evident in the data generated here, the coating used to encourage initial cell attachment and subsequent adherent growth is critical to the functioning of a microcarrier. As can be seen, cationic charge and collagen dominate. For the former, the materials are modified to include cationic amines to provide the positive charges needed to attract the negative membranes of mammalian cells and thus encourage adhesion. Cytodex 1, Cytopore 1 and Cytopore 2 employ diethylaminoethyl (DEAE) groups which, not surprisingly, also has widespread application as a component of resins in ion exchange chromatography (Qi et al., 2001). The difference between Cytopore 1 and Cytopore 2 relate to the charge density provided by these DEAE groups; Cytopore 1 has a lower charge, whilst Cytopore 2 has a greater charge, with the latter thus intended for cells which may be harder to attach to a surface (Cytiva, 2020a).

The popularity of collagen as a protein-based coating, as opposed to other commonly encountered extracellular matrix proteins, may be explained by its relatively low cost (as will be seen later in Chapter 3). Collagen is also the main structural protein in the connective tissues of mammals (Shoulders et al., 2009), so its adhesive effect will likely been felt by the most cell lines. The Plastic and Corning MC (untreated) microcarrier products do not possess any coating, which is likely so the user can coat the materials in an adhesion substrate of their choice, although it is expected a surfactant would need to be present before this occurs to discourage aggregation of uncoated particles.

The porosity of a microcarrier will affect the number of cells that can grow adherently upon the material and, along with the size diameter distribution and weight, determines the specific surface area. High surface areas, allowing plentiful space for adherent cells to grow, is a defining characteristic of microcarriers and relates to their use as a means to scale up adherent cell culture. Solid microcarriers are the most popular, with the surface acting as the only area upon which cells can attach and spread. Microporous microcarriers, such as Cytodex 1 and Cytodex 3, similarly only allow cells to grow upon their outer faces but instead have surfaces containing microporous grooves and ridges. This allows more physical area for cell adhesion as well as encourages adherent growth. It also means there may be nutrients available to the basolateral side of the cell, i.e. from within the structure, at least until full confluency is reached. Macroporous microcarriers, such as Cytopore 1 and Cytopore 2, as well as CultiSpher-G and CultiSpher-S, may be desirable if shear-sensitive cells are cultured or if increased surface areas are desired. These products contain pores large to allow cells entry to within the materials with physical area inside for adherence, and may be the most related to the polyHIPE microspheres previously discussed.

For the materials of these products, polystyrene is by far the most popular, likely a consequence of the wide experience of using styrenic monomers. Cytodex 1 and Cytodex 3 use dextran, whilst Cytopore 1 and Cytopore 2 use cellulose; both are polysaccharides. CultiSpher-G and CultiSpher-S use gelatin (a mixture of proteins derived from the hydrolysis of collagen). These polysaccharide- and gelatin-based microcarriers are biodegradable, which may be exploited with the use of enzymes to dissolve the microcarriers and thus force complete dissociation of adhered cells (Sart et al., 2009).

Microcarriers possessing a cationic charge, in contrast to a protein-based coating, benefit from being animal origin-free, provided their material is likewise not animal-derived (such as polystyrene). However, whilst this may be true for the product itself, the actual cell processes used with these microcarriers may still require animal-derived products. As previously discussed, FBS is a frequently added supplement in adherent cell culture, even for established cell lines such as CHO and HEK. The presence of adhesion-promoting proteins in FBS contributes to the attachment of cells to microcarriers, but it remains unclear if microcarriers can function without the addition of serum. Indeed, the information brochure for both Cytopore 1 and 2, despite having cationic charge as coatings, still advises the user to soak the microcarriers in serum (Cytiva, 2020b). Possessing a microcarrier that will work effectively in serum- and protein-free medium is a key aim of the work here.

This page intentionally left blank

---

# Chapter 2

---

## MATERIALS AND METHODS

---

### OVERVIEW

This chapter describes the materials and methods used for every experiment performed for the work presented in this thesis. The order in which experiments are listed generally follows the order in which their results are shown and discussed in the chapters that follow.

### 2.1 CELL CULTURE

All reagents were sourced from Sigma-Aldrich (Missouri, USA) unless otherwise stated.

#### 2.1.1 CHO CELL LINE ROUTINE MAINTENANCE

A suspension-adapted Chinese hamster ovary cell line (CHO-S IgG; donated by Cobra Biologics, Staffordshire, UK as 'Clone 38'), stably producing an anti-HER2 IgG1 antibody product, was seeded at  $0.2 \times 10^6$  cellmL<sup>-1</sup> in non-baffled, vented Erlenmeyer flasks (Corning, Surrey, UK) at 37 °C, 5 % (v/v) CO<sub>2</sub> and with 140 rpm orbital shaking on a 25 mm throw incubator (Infors HT, Bottmingen, Switzerland) for routine cell culture and passaged every 3–4 days. Cells were cultured using CD CHO medium (Thermo Fisher Scientific, Massachusetts, USA), supplemented with 8 mM L-glutamine and 12.5 µgmL<sup>-1</sup> puromycin (Thermo Fisher Scientific, Massachusetts, USA). A suspension-adapted Chinese hamster ovary cell line (CHO-S), not stably producing a product, was routinely maintained as above, except with CD CHO medium containing only 8 mM L-glutamine supplementation.

A Vi-Cell XR Cell Viability Analyzer (Beckman-Coulter, California, USA) employing a trypan blue exclusion method was used to determine viable cell density and viability for both cell lines. Both cell lines were routinely passaged in 125 mL Erlenmeyer flasks, but expanded into 250, 500 and 1000 mL Erlenmeyer flasks as needed for future experimentation where higher volumes of cells were required. Total working volume never exceeded 30 % (v/v) of the nominal volume of the flask to ensure sufficient headspace for gaseous exchange. Greater seeding densities, up to  $0.4 \times 10^6$  cellmL<sup>-1</sup>, were performed when higher cell numbers were required within 3–4 days. Cells were only used for experimentation after the fourth passage following revival from liquid nitrogen cryopreservation, and cells were discarded before the twentieth passage to prevent unwanted genetic effects.

To achieve the same mixing between an incubator with a 25 mm throw and that with a 50 mm throw, Equation 2.1 was used (Bates et al., 2011), where  $\text{rpm}_1$  and  $\text{rpm}_2$  refer to the revolutions per minute of the first and second incubator, respectively, and  $d_1$  and  $d_2$  refer to the throw (mm) of the first and second incubator, respectively.

$$( \text{EQU. 2.1} ) \quad \text{rpm}_2 = \sqrt{\text{rpm}_1^2 \times \left( \frac{d_1}{d_2} \right)}$$

### 2.1.2 HEK-293 CELL LINE ROUTINE MAINTENANCE

A suspension-adapted human embryonic kidney cell line (HEK-293), kindly given as a gift from Absolute Antibody (Redcar, UK), was routinely cultured using non-supplemented HEK 293 medium (Thermo Fisher Scientific, Massachusetts, USA). All other culturing methods, including determination of viability, remain as in § 2.1.1.

## 2.2 ADHESION SUBSTRATES

All reagents were sourced from Sigma-Aldrich (Missouri, USA) unless otherwise stated.

### 2.2.1 PRESTOBLUE CELL VIABILITY REAGENT FOR CELL ADHERENCE

PrestoBlue Cell Viability Reagent (Thermo Fisher Scientific, Massachusetts, USA), a fluorometric assay that utilises the intracellular conversion of resazurin to resorufin (Xu et al., 2015) to measure the metabolic activity, and hence viability, of cells, was adapted to determine the initial adherence and growth of adherent cells on multiwell plates. PrestoBlue (PB) was pre-warmed to room temperature, prepared as 10 % (v/v) with fresh CD CHO, itself pre-warmed to 37 °C, and mixed well immediately before use. Wells containing adhered cells were first aspirated of all culture medium and washed twice with pre-warmed PBS to ensure only adhered cells remained. A wash involved slowly dispensing PBS into the centre of a well, agitating gently by hand, then tilting the plate to fully aspirate from the side. The 10 % (v/v) PB-CD CHO mix was added, agitated gently by hand for 10 s and the plate left for 30 min in an incubator at 37 °C, 5 % (v/v) CO<sub>2</sub>. Wells containing only PB-CD CHO mix were included as a blank to account for fluorescence of medium. For specific wash and PB-CD CHO mix volume details, see the experimental methods that follow.

To quantify the metabolic activity after 30 min, plates were agitated gently by hand for 10 s, and 200 µL transferred from the incubated mix of each well to a fresh 96-well plate, making sure not to disturb the adhered cells. Fluorescence of the aliquoted samples was read using a SpectraMax iD5 (Molecular Devices, California, USA) with an excitation wavelength of 560 nm and an emission wavelength of 590 nm, with gain set to 'low'. Results were nor-

malised to the blank using Equation 2.2, with all raw fluorescence as RFU. Normalised fluorescence was unitless.

$$( \text{EQU. 2.2} ) \quad \text{Normalised Fluorescence} = \left( \frac{\text{Raw Fluorescence}}{\text{Raw Fluorescence of Blank}} \right) - 1$$

### 2.2.2 VALITATITER FOR IGG TITRE DETERMINATION

ValitaTITER (Valitacell, Dublin, Ireland) 96-well plates were used to determine the concentration of expressed IgG1 antibody product during CHO-S IgG cell culture. Briefly, ValitaTITER utilises the coupling of a fluorescently labelled Fc-binding protein to IgG antibodies, and subsequently relies on the fluorescence polarisation (Thompson et al., 2017) of the bound antibody as a measurement of IgG antibody concentration. Exciting the bound antibody with plane polarised light at the excitation wavelength of the Fc-binding protein will result in emitted light being more polarised than if the labelled was unbound. This is due to the slower rotation, in comparison to unbound protein, of bound antibodies in solution. The increase in polarisation is proportional to the amount of bound antibodies and serves as the principle of the assay.

Samples of cell culture, centrifuged at 1000 g for 5 min, were frozen at -80 °C and thawed together when required. A standard curve, i.e. a serial dilution (with a dilution factor of two) of IgG antibody concentration using medium starting from 100 and ending at 0.78125 mgL<sup>-1</sup>, was determined for each lot of valitaTITER plate and CD CHO medium. IgG1 kappa (of human myeloma plasma origin) was used as IgG standard for the standard curve. The specific concentration for each lot was stated by the supplier. Following manufacturer's instructions, supernatant samples were first diluted with the medium lot used in the experiments from which they were obtained. For the first generation of ValiaTITER, 60 µL buffer, supplied by the manufacturer, was dispensed into each of the ValitaTITER plate wells to desorb the Fc-binding protein, followed by 60 µL of each sample. In the subsequent generation, this buffer was removed and 60 µL medium was sufficient for Fc-binding protein desorption. This meant, in the second generation, the dilution factor of samples prior to reading did not have to be as high. At least three medium blanks were also used to account for background fluorescence polarisation. Once wells were filled, the contents of each was mixed by aspirating and dispensing three times, followed by 30 min incubation at room temperature in the dark. Fluorescence polarisation was then determined using a SpectraMax iD5. The mean of the blanks was deducted from these values, the appropriate dilution factor multiplied and the equation of the standard curve used to determine actual antibody titres. Suitable dilution was carried out so that, once the mean of the blank was deducted,

the raw values fell comfortably within the mid-range of the standard curve.

### 2.2.3 COATING AND SCREENING OF ADHESION SUBSTRATES

Three chemically defined polymers, poly-D-lysine hydrobromide (PDL), MW 70–150,000; poly-L-ornithine (PLO), 0.01 % (w/v) in water; and polyethylenimine (PEI), branched MW 10,000 (Polysciences, Pennsylvania, USA), were selected for testing as substrates for adhering suspension-adapted cells. PEI, sourced as a gel-like substance, was transferred to a glass bottle and dissolved in deionised water to give a 100 mgmL<sup>-1</sup> stock solution and stored at room temperature. PDL, sourced as a powder, was dissolved in 5 mL filter-sterilised borate-buffered saline (BBS), aliquoted and stored at -20 °C. PLO was aliquoted as sourced and stored at -20 °C.

Four animal origin proteins; collagen (CG), Bornstein and Traub type I, of calf skin-origin; fibronectin (FN), of bovine plasma-origin; laminin (LM), of murine sarcoma-origin and vitronectin (VN), of human plasma-origin, were also selected for testing as substrates for adhering suspension-adapted cells. CG was stored as sourced at 4 °C. FN was added to sterile-filtered deionised water, left to dissolve for 30 min at 37 °C and aliquoted. Both LM and VN were aliquoted from sourced material. FN, LM and VN were stored at -20 °C and thawed at 4 °C for several hours, when required, to eliminate possible degradation.

To determine the optimum coating concentration ( $\mu\text{gcm}^{-2}$ ) of each adhesion substrate when adsorbed on the well surfaces of multiwell plates, a range of coating concentrations ( $\mu\text{gmL}^{-1}$ ) were first prepared (see Equation 2.3). For PEI and PDL, 100, 10, 1, 0.1, 0.01 and 0.001  $\mu\text{gcm}^{-2}$ ; and for PLO, 10, 1, 0.1, 0.01, 0.001 and 0.0001  $\mu\text{gcm}^{-2}$  were tested. BBS was used to dilute coating concentrations for PEI, PDL and PLO. For FN, 50, 5, 0.5, 0.05 and 0.005  $\mu\text{gcm}^{-2}$ ; LM, 20, 2, 0.2, 0.02 and 0.002  $\mu\text{gcm}^{-2}$ ; for CG, 100, 10, 1, 0.1, 0.01 and 0.001  $\mu\text{gcm}^{-2}$ ; and for VN, 10, 1, 0.1, 0.01 and 0.001  $\mu\text{gcm}^{-2}$  were tested. Hank's Balanced Salt Solution (HBSS) was used to dilute coating concentrations for FN, LM and VN. For CG, sterile water was used.

$$\text{( EQU. 2.3 )} \quad \text{Coating} = \text{Desired Coating Concentration} \times \left( \frac{\text{Area to be Coated}}{\text{Coating Volume}} \right)$$

As an example; if a single well of a 24-well plate (2 cm<sup>2</sup>) was to be coated with 0.2 mL of an adhesion substrate at a desired coating concentration of 10  $\mu\text{gcm}^{-2}$ , a concentration of 100  $\mu\text{gmL}^{-1}$  of the adhesion substrate would be needed. This would need to be diluted from the stock solution using an appropriate coating buffer.

Tissue culture-treated Nunc 96-well plates were adsorbed with adhesion substrate in the concentrations given previously. For coating, 50  $\mu\text{L}$  of each coating concentration was pipetted in the centre of each well, and the plate agitated thoroughly by hand to ensure even spreading of coating liquid, before overnight incubation at 37 °C, 5 % (v/v)  $\text{CO}_2$ . The next day, all wells were fully aspirated. For wells adsorbed with PDL, PEI and PLO, 100  $\mu\text{L}$  PBS was dispensed, left briefly, then aspirated and discarded as a washing step. This was repeated once, and wells left to air dry for 15 min. For CG, FN, LM and VN, 100  $\mu\text{L}$  HBSS was dispensed, left briefly, then aspirated and discarded as a washing step. This was repeated once, then 50  $\mu\text{L}$  HBSS added to keep all wells hydrated. All multiwell plates were sealed with parafilm, stored upright at 4 °C and used within 12 hr. The 50  $\mu\text{L}$  HBSS was removed prior to cell seeding. Figure 2.1 shows the workflow of using adhesion substrates; multiwell plates are first coated with adhesion substrates overnight, followed by overnight seeding of CHO cells with subsequent analysis of cell adherent growth during the culture. This sequence of events was generally the same for all adhesion substrate work.

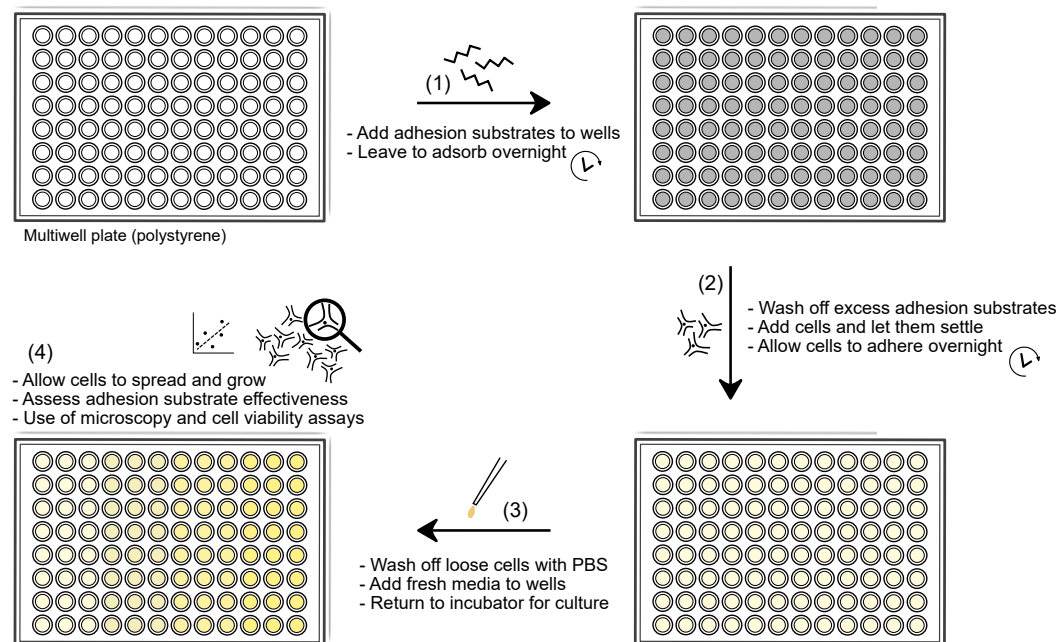


**FIGURE 2.1 Schematic detailing the workflow of using adhesion substrates on multiwell plates for CHO cell adhesion with subsequent analysis.** Adhesion substrates were adsorbed overnight onto the well surfaces of multiwell plates, followed by washing to remove any unbound substrate. CHO cells were prepared at a suitable concentration and seeded onto the surface of each well and allowed to adhere overnight in an incubator. Wells were briefly washed the next day to remove any loose cells and media added. The plates were returned to the incubator to allow cells to grow adherently, with the cultures assessed, e.g. microscopy and viability assays, to determine the effectiveness of the adhesion substrates.

To prepare coated multiwell plates for cell adherence, all plates were placed in an incuba-

tor at 37 °C, 5 % (v/v) CO<sub>2</sub> for several hours. On day 3 of a passage, CHO-S IgG cells were filtered twice using a 20 µm cell strainer (Pluriselect, Leipzig, Germany) to eliminate any clumped cellular material, and a  $0.5 \times 10^6$  cellmL<sup>-1</sup> suspension was prepared. 40 µL, i.e. 20,000 cells, was adherently seeded by slowly dispensing above the centre of each coated well. Plates were agitated gently by hand to ensure the entire surface of each coated well was covered with cell suspension, before being placed into an incubator at 37 °C, 5 % (v/v) CO<sub>2</sub> overnight. The next day, all media were aspirated, and two 150 µL PBS washes performed. 150 µL PB-media mix was added and incubated for 30 min. The fluorescence of incubated wells were determined directly using a SpectraMax iD5. For each adhesion substrate, normalised fluorescence values were further normalised as a percentage, with 100 % assigned to the coating concentration that gave the highest fluorescence value for each adhesion substrate.

#### 2.2.4 ADHERENT CULTURE IMAGING AND GROWTH TESTS

To determine which of the selected adhesion substrates could sustain the highest number of cells within an adherent culture period, coating concentrations from § 2.2.3 for each substrate were first chosen to give an excess coating of adhesion substrate. Tissue culture-treated and untreated Nunc 24-well plates were adsorbed with adhesion substrate in the chosen concentrations. For coating, 200 µL of each coating concentration was pipetted in the centre of each well, and the plate agitated thoroughly by hand to ensure even spreading of coating liquid, before overnight incubation at 37 °C, 5 % (v/v) CO<sub>2</sub>. The next day, all wells were fully aspirated. For wells adsorbed with PDL, PEI and PLO, 400 µL PBS was dispensed, left briefly, then aspirated and discarded as a washing step. This was repeated once, and wells left to air dry for 15 min. For CG, FN, LM and VN, 400 µL HBSS was dispensed, left briefly, then aspirated and discarded as a washing step. This was repeated once, then 200 µL HBSS added to keep all wells hydrated. The 200 µL HBSS was removed prior to cell seeding.

To prepare coated multiwell plates for cell adherence, all plates were placed in an incubator at 37 °C, 5 % (v/v) CO<sub>2</sub> for several hours. On day 3 of a passage, CHO-S IgG cells were filtered twice using a 20 µm cell strainer to eliminate any clumped cellular material, and a  $0.67 \times 10^6$  cellmL<sup>-1</sup> suspension was prepared. 150 µL, i.e. 100,500 cells, was adherently seeded by slowly dispensing above the centre of each coated well. Uncoated wells were also seeded. Plates were agitated gently by hand to ensure the entire surface of each coated well was covered with cell suspension, before being placed into an incubator at 37 °C, 5 % (v/v) CO<sub>2</sub> overnight. The next day, day 1, 350 µL medium was added and plates returned to the incubator, bringing the working volume to 450 µL.

On day 4, all media were aspirated, and two 400  $\mu\text{L}$  PBS washes performed. 450  $\mu\text{L}$  PB-media mix was added and incubated for 30 min. 200  $\mu\text{L}$  from each incubated well was transferred to a 96-well plate and the fluorescence determined using a SpectraMax iD5. The remainder of the PB-media mix in each well was aspirated, 400  $\mu\text{L}$  PBS added as a wash, before another full aspiration. Finally, fresh 450  $\mu\text{L}$  medium was added and plates returned to the incubator. On day 7, the PB assay was repeated and the plates discarded.

To determine how adhesion substrates perform on glass surfaces, untreated 8-well  $\mu$ -slide glass plates were adsorbed with substrates in the chosen concentrations. The next day, all wells were aspirated and washed with 200  $\mu\text{L}$  PBS or HBSS. Wells adsorbed with FN, LM, CG and VN were kept hydrated with 100  $\mu\text{L}$  HBSS before use. On day 3 of a passage, CHO-S IgG cells were filtered twice using a 20  $\mu\text{m}$  cell strainer to eliminate any clumped cellular material, and a  $0.25 \times 10^6$   $\text{cell mL}^{-1}$  suspension was prepared. 100  $\mu\text{L}$ , i.e. 25,000 cells, was adherently seeded by slowly dispensing above the centre of each coated well. Plates were agitated gently by hand to ensure the entire surface of each coated well was covered with cell suspension, before being placed into an incubator at 37  $^{\circ}\text{C}$ , 5 % (v/v)  $\text{CO}_2$  overnight. The next day, day 1, 150  $\mu\text{L}$  medium was added and plates returned to the incubator, bringing the working volume to 250  $\mu\text{L}$ . On day 4, all media were aspirated, and two 200  $\mu\text{L}$  PBS washes performed. 250  $\mu\text{L}$  PB-media mix was added and incubated for 30 min. 200  $\mu\text{L}$  from each incubated well was transferred to a 96-well plate and the fluorescence determined using a SpectraMax iD5.

To characterise morphologies of freshly adhered cells on polystyrene surfaces, untreated Nunc 24-well plates were coated as above and seeded with 100,500 cells overnight. The next day, medium was aspirated before two 400  $\mu\text{L}$  PBS washes. 200  $\mu\text{L}$  Image-iT Fixative Solution (Thermo Fisher Scientific, Massachusetts, USA), containing 4 % formaldehyde, was added and left at room temperature for 20 min to fix the adhered cells. It was then aspirated, washed once with 400  $\mu\text{L}$  PBS, before 200  $\mu\text{L}$  PBS was dispensed as a mounting medium. Adhered cells were imaged immediately using a DMI4000B inverted microscope (Leica, Wetzlar, Germany) with phase contrast at 10 $\times$  and 20 $\times$  magnifications. Micrographs were processed using ImageJ software and scale bars added.

### 2.2.5 ADHERENCE CAPABILITY FOR CELL LOADING

To determine how many cells can be adherently seeded within a short period of time, i.e. 'cell loading', PEI, PDL and FN were first adsorbed onto tissue culture-treated Nunc 24-well plates at concentrations as in § 2.2.4. On day 3 of a passage, CHO-S IgG, CHO-S and HEK-293 cells CHO-S IgG cells were centrifuged at 200 g for 5 min, and resuspended in a reduced volume to increase the viable cell density. All cell lines were filtered twice using a

20 µm cell strainer to eliminate any clumped cellular material, and a  $20 \times 10^6$  cellmL<sup>-1</sup> suspension for each was prepared. A serial dilution using medium, with a dilution factor of two, was prepared to give 10, 5, 2.5 and  $1.25 \times 10^6$  cellmL<sup>-1</sup> suspensions. 200 µL, i.e. 4, 2, 1, 0.5 and 0.25 million cells, of each concentration was adherently seeded by slowly dispensing above the centre of each coated well. Plates were agitated gently by hand to ensure the entire surface of each coated well was covered with cell suspension, before being placed into an incubator at 37 °C, 5 % (v/v) CO<sub>2</sub> for 1 hr. The cell suspension was then aspirated, and two 400 µL PBS washes performed. 450 µL PB-media mix was added and incubated for 30 min. 200 µL from each incubated well was transferred to a 96-well plate and the fluorescence determined using a SpectraMax iD5. Due to the large number of PB measurements, CHO-S IgG, CHO-S and HEK-293 plates were staggered in their cell loading.

### 2.2.6 ADHESION ASSAYS

A range of assays (PB, dissociation, crystal violet and neutral red) were compared for the adherence of CHO-S IgG cells on multiwell plates. To demonstrate the effectiveness of each assay, PEI was first adsorbed onto tissue culture-treated Nunc 24-well plates at  $10 \mu\text{gcm}^{-2}$  as in § 2.2.4. On day 3 of a passage, CHO-S IgG cells were centrifuged at 200 g for 5 min, and resuspended in a reduced volume of medium to increase the viable cell density. Cells were filtered twice using a 20 µm cell strainer to eliminate any clumped cellular material, and a  $10 \times 10^6$  cellmL<sup>-1</sup> suspension was prepared. A serial dilution using medium, with a dilution factor of two, was prepared to give 5, 2.5, 1.25, 0.625 and  $0.3125 \times 10^6$  cellmL<sup>-1</sup> suspensions. 200 µL, i.e. 2, 1, 0.5, 0.25, 0.125 and 0.0625 million cells, of each concentration was adherently seeded by slowly dispensing above the centre of each coated well. Plates were agitated gently by hand to ensure the entire surface of each coated well was covered with cell suspension, before being placed into an incubator at 37 °C, 5 % (v/v) CO<sub>2</sub> for 3 hr. Four plates were seeded, with each subsequently tested for adherence using either PB, dissociation by trypsinisation, crystal violet staining or neutral red staining assays.

For assaying cell adherence using PB, see § 2.2.1 for details. For the dissociation of cells by trypsinisation, cell suspension was aspirated, and two 400 µL Dulbecco's phosphate-buffered saline (DPBS) washes performed. 300 µL 0.25 % trypsin/EDTA (Thermo Fisher Scientific, Massachusetts, USA) was added to each well and the plate returned to the incubator for 10 min, with intermittent tapping on the sides of the plate to encourage dissociation. Complete cell dissociation was confirmed by microscopy, before the entire contents of each well was aspirated and centrifuged at 200 g for 5 min. The supernatant was discarded, and the cell pellet resuspended in 5 mL fresh medium. The viable cell density, i.e. the number of cells adhered to each well surface, was determined using a Vi-Cell XR Cell

Viability Analyzer. For further details regarding dissociation methods, see § 2.2.7.

For assaying cell adherence using crystal violet, a staining solution containing 1 mgmL<sup>-1</sup> crystal violet in 20 % (v/v) methanol was first prepared. A lysing solution, of 10 % (v/v) acetic acid, was also prepared. Cell suspension was aspirated, and two 400 µL PBS washes performed. 200 µL crystal violet staining solution was added to each well and the plate gently rocked at room temperature for 20 min. Staining solution was fully aspirated and the wells washed thoroughly by submerging the plate into a tub of tap water. This process was repeated with fresh water until the stained dye ceased to run off. The plate was dried for 30 min at 37 °C.

To lyse the cells and redissolve the crystal stain, 400 µL lysing solution was added to each well and the plate gently rocked at room temperature for 30 min. The newly dissolved crystal violet stains were diluted 1 in 25 with lysing solution. 2 µL from each diluted sample was transferred to a NanoDrop (Thermo Fisher Scientific, Massachusetts, USA) and the absorbance read at 590 nm.

For assaying cell adherence using neutral red, a staining solution containing 1 mgmL<sup>-1</sup> neutral red in 20 % (v/v) methanol was first prepared. A lysing solution, of 50 % (v/v) ethanol, 49 % (v/v) and 1 % (v/v) acetic acid, was also prepared. Cell suspension was aspirated, and two 400 µL PBS washes performed. 200 µL neutral red staining solution was added to each well and the plate placed in an incubator at 37 °C, 5 % (v/v) CO<sub>2</sub> for 2.5 hr. Staining solution was fully aspirated and the wells washed thoroughly by submerging the plate into a tub of tap water. This process was repeated with fresh water until the stained dye ceased to run off. The plate was dried for 30 min at 37 °C.

To lyse the cells and redissolve the crystal stain, 400 µL lysing solution was added to each well and the plate gently rocked at room temperature for 30 min. The newly dissolved neutral red stains were diluted 1 in 12 with lysing solution. 2 µL from each diluted sample was transferred to a NanoDrop and the absorbance read at 540 nm. Prior to lysing both crystal violet and neutral red stains, stained wells were first photographed and images digitally montaged together for visual comparison.

To demonstrate these assays in adherent cell cultures, PDL, PLO, PEI and FN were adsorbed onto tissue culture-treated Nunc 24-well plates at 10, 10, 10 and 5 µgcm<sup>-2</sup>, respectively, and seeded as in § 2.2.4. On day 4, all media were aspirated, and two 400 µL PBS (or DPBS) washes performed. Each of the proposed adhesion assays described was then tested on each of the wells.

---

### 2.2.7 DISSOCIATION AND REGROWTH FROM ADHESION SUBSTRATES

To demonstrate the dissociation of adhered cells and subsequent regrowth back into suspension culture, PDL, PEI and FN were adsorbed on tissue culture-treated Nunc 12-well plates using 400  $\mu\text{L}$  coating at concentrations 10, 10 and 5  $\mu\text{gcm}^{-2}$ , respectively, as in § 2.2.4. On day 3 of a passage, CHO-S IgG cells were filtered twice using a 20  $\mu\text{m}$  cell strainer to eliminate any clumped cellular material, and a  $0.33 \times 10^6 \text{ cellmL}^{-1}$  suspension was prepared. 300  $\mu\text{L}$ , i.e. 99,000 cells, was adherently seeded by slowly dispensing above the centre of each coated well. Uncoated wells were also seeded. Plates were agitated gently by hand to ensure the entire surface of each coated well was covered with cell suspension, before being placed into an incubator at 37 °C, 5 % (v/v) CO<sub>2</sub> overnight. The next day, day 1, 700  $\mu\text{L}$  medium was added and the plates returned to the incubator, bringing the working volume to 1 mL.

On day 4, all media were aspirated from every well, a single 400  $\mu\text{L}$  PBS wash performed, and 1 mL fresh medium added. On Day 7, all media were aspirated and two 400  $\mu\text{L}$  DPBS washes performed. 600  $\mu\text{L}$  0.25 % trypsin/EDTA (pre-warmed to 37 °C) was added and plates returned to the incubator for 5 min, with intermittent tapping on the sides of the plate to encourage dissociation. Repeated aspirating and dispensing after 5 min was performed to further dissociate cells. Complete cell dissociation was confirmed by microscopy. To neutralise the activity of trypsin on cells post-dissociation, soybean trypsin inhibitor (SBTI) was prepared by adding 0.05 mg to 20 ml DPBS, mixing well and filter-sterilising to give a 0.25 % (w/v) concentration. 600  $\mu\text{L}$  0.25 % SBTI, i.e. a 1:1 ratio with trypsin, was immediately added to the trypsin/EDTA-resuspended cell mix once complete dissociation was confirmed. Plates were agitated thoroughly by hand and allowed to incubate at room temperature for 2 min. The entire contents of every well was transferred each to 2 mL fresh medium and centrifuged at 200 g for 5 min. The supernatant was discarded, and the cell pellet resuspended in 5 mL fresh medium. The viable cell density, i.e. the number of cells adhered to each well surface, was then determined using a Vi-Cell XR Cell Viability Analyzer.

The newly dissociated cells were each seeded at  $0.1 \times 10^6 \text{ cellmL}^{-1}$  as 10 mL in TubeSpin Bioreactor 50 vessels (TPP, Trasadingen, Switzerland) and incubated at 37 °C, 5 % (v/v) CO<sub>2</sub> with 240 rpm orbital shaking on a 25 mm throw incubator. Viable cell density and viability were determined on days 0, 1, 3 and 5 using a Vi-Cell XR Cell Viability Analyzer.

To briefly investigate what effect trypsin had on the adhesion substrates themselves, fresh cells were seeded onto wells that had previously been exposed to trypsin. PEI and FN were first adsorbed on untreated Nunc 24-well plates at concentrations 10 and 5  $\mu\text{gcm}^{-2}$ ,

respectively, and cells seeded as in § 2.2.4. On day 7, all media were aspirated and the PB assay performed to quantify the number of adhered cells (cycle 1). After two PBS washes, 250  $\mu\text{L}$  0.25 % trypsin/EDTA was added to fully dissociate the cells, followed by two 400  $\mu\text{L}$  media washes. This process was then repeated twice using the same wells, but with fresh cells, to give PB readings at day 7 (corresponding to the adherent growth achieved) at cycles 2 and 3. Readings between cycles were compared to determine the loss of substrate effectiveness following repeated trypsin exposures.

To determine what effect trypsinisation had on cells dissociated from PEI substrates, exposure to 0.25 % trypsin/EDTA was tested at 2.5, 5 and 10 min. As above, PEI was adsorbed on tissue culture-treated Nunc 12-well plates using 400  $\mu\text{L}$  coating to give a  $10\ \mu\text{gcm}^{-2}$  concentration and seeded with 300  $\mu\text{L}$ , i.e.  $99,000$  cells, at  $0.33 \times 10^6\ \text{cellmL}^{-1}$ . Uncoated wells were also seeded. On day 4, all media were aspirated from every well, a single 400  $\mu\text{L}$  PBS wash performed, and 1 mL fresh medium added. Plates were returned to the incubator. On day 7, all medium was aspirated and two 400  $\mu\text{L}$  DPBS washes performed. 600  $\mu\text{L}$  0.25 % trypsin/EDTA (pre-warmed to  $37\ ^\circ\text{C}$ ) was added and plates returned to the incubator for either 2.5, 5 or 10 min, with intermittent tapping on the sides of the plate to encourage dissociation. Uncoated wells were exposed to trypsin/EDTA for 2.5 min only. Repeated aspirating and dispensing after 5 min was performed to further dissociate cells. Complete cell dissociation was confirmed by microscopy. 600  $\mu\text{L}$  0.25 % (w/v) SBTI was immediately added to the trypsin/EDTA-resuspended cell mix once complete dissociation was confirmed. Plates were agitated thoroughly by hand and allowed to incubate at room temperature for 2 min.

The entire contents of every well was transferred each to 2 mL fresh medium and centrifuged at 200 g for 5 min. The supernatant was discarded, and the cell pellet resuspended in 5 mL fresh medium. The viable cell density, i.e. the number of cells adhered to each well surface, was then determined using a Vi-Cell XR Cell Viability Analyzer. The newly dissociated cells were seeded at  $0.1 \times 10^6\ \text{cellmL}^{-1}$  as 10 mL in TubeSpin Bioreactor 50 vessels and incubated at  $37\ ^\circ\text{C}$ , 5 % (v/v)  $\text{CO}_2$  with 240 rpm orbital shaking. Viable cell density and viability were determined at day 0, 1, 3 and 5 using a Vi-Cell XR Cell Viability Analyzer. On day 5, cultures were passaged, again at  $0.1 \times 10^6\ \text{cellmL}^{-1}$  as 10 mL in fresh TubeSpin Bioreactor 50 vessels, and the viable cell density and viability determined again on days 0, 1, 3 and 5, to observe if resuspended cells could be subcultured a further time.

### 2.2.8 ANIMAL ORIGIN-FREE DISSOCIATION

TrypLE Express, Accutase and Cell Dissociation Buffer (Enzyme-Free), all sourced from Thermo Fisher Scientific (Massachusetts, USA) were selected as animal origin-free dis-

---

sociation reagents to test against trypsin (of porcine origin). PEI was adsorbed on tissue culture-treated Nunc 12-well plates and seeded and cultured as in § 2.2.7. On Day 7, all medium was aspirated and two 400  $\mu\text{L}$  DPBS washes performed. 600  $\mu\text{L}$  of either TrypLE Express, Accutase, Cell Dissociation Buffer or 0.25 % trypsin/EDTA was added to wells and incubated for 5 min, with intermittent tapping on the sides of the plate to encourage dissociation. To ensure only exposure to the particular dissociation reagent led to cell dissociation, the contents at four points of each well (top, bottom, left and right) were gently aspirated and dispensed once to encourage cell dissociation. This was also performed on wells without prior exposure to any dissociation reagent to compare dissociation via physical force only. Complete cell dissociation was not confirmed by microscopy in this instance. Accutase was thawed to room temperature only as advised by supplier instructions, whilst TrypLE Express, Accutase, Cell Dissociation Buffer and trypsin/EDTA were pre-warmed to 37 °C, before exposing to adherent cells. To neutralise the effects of the dissociative reagent, 600  $\mu\text{L}$  of SBTI was added for 0.25 % trypsin/EDTA, whilst excess media were sufficient for TrypLE Express and Cell Dissociation Buffer, and prolonged exposure to 37 °C sufficient for Accutase. The entire contents of every well was transferred each to 2 mL fresh medium and centrifuged at 200 g for 5 min. The supernatant was discarded, and the cell pellet resuspended in 5 mL fresh medium. The viable cell density, i.e. the number of cells adhered to each well surface, was then determined using a Vi-Cell XR Cell Viability Analyzer.

To determine what effect dissociation reagent had on subsequent regrowth, the newly dissociated cells were seeded at  $0.1 \times 10^6 \text{ cell mL}^{-1}$  as 10 mL in TubeSpin Bioreactor 50 vessels and incubated at 37 °C, 5 % (v/v)  $\text{CO}_2$  with 240 rpm orbital shaking. Viable cell density and viability were determined on days 0, 1, 3 and 5 using a Vi-Cell XR Cell Viability Analyzer.

### 2.2.9 SIMPLE GLUCOSE CONCENTRATION DETERMINATION

To rapidly determine the concentration of glucose within cell culture medium, a blood sugar monitoring device (Sinocare, China) with individual testing strips was acquired. To use, 2  $\mu\text{L}$  of culture medium was taken and (without any centrifugation) dispensed onto a clean gloved finger, mimicking that of a blood droplet. A test strip was inserted into the device immediately before use, and directed to the medium drop to allow wicking into the strip channel to occur. Readings displayed in  $\text{mmol L}^{-1}$  were converted to  $\text{g L}^{-1}$ . A fresh test strip was used for each reading.

To validate the device, CD CHO medium was serially diluted (with a dilution factor of two) using deionised water. Each concentration, beginning with an arbitrary '1' for undiluted media, '0.5' for the first dilution, '0.25' for the next and so on, was then tested for glucose

concentration. Technical triplicate readings were taken. The mean of these were plotted with a linear trendline and a  $R^2$  value calculated. To demonstrate the use of the device for measuring the concentration of glucose during actual cell culture, CHO-S IgG cells were seeded at  $0.2 \times 10^6$  cellmL<sup>-1</sup> as 10 mL in TubeSpin Bioreactor 50 vessels and incubated at 37 °C, 5 % (v/v) CO<sub>2</sub> with 240 rpm orbital shaking. Each day, starting from day 0, and ending on day 6, viable cell density and viability were determined using a Vi-Cell XR Cell Viability Analyzer. Glucose concentrations were determined using this blood sugar monitoring device as described.

For later experiments, a Cedex Bio Analyzer (Roche, Basel, Switzerland) was used to determine the concentration of glucose, as well L-glutamine, lactate and lactate dehydrogenase. For further details on the validation of the Cedex Bio Analyzer see § 2.6.1.

#### 2.2.IO ADHERENT CULTURE AND MILD HYPOTHERMIA

To determine the effect of hypothermic conditions on cells adhered to PEI substrates, PEI was first adsorbed on tissue culture-treated Nunc 12-well plates and seeded with CHO-S IgG as in § 2.2.7, but instead with cell densities of 0.25, 0.5 and  $1.0 \times 10^6$  cellmL<sup>-1</sup>, i.e. 0.075, 0.15 and 0.30 million cells. The next day, day 1, all liquid was aspirated and two 400 µL PBS washes performed. 1000 µL fresh medium was added, and each plate returned to an incubator either at 37, 32 or 30 °C, and 5 % (v/v) CO<sub>2</sub>. To determine the number of cells adhered overnight, a separate plate was washed as above and then exposed to 0.25 % trypsin/EDTA as in § 2.2.7 to dissociate adhered cells. These were quantified by using a Vi-Cell XR Cell Viability Analyzer and used as the actual adhered seeding cell concentration.

Each day, starting from day 1, and ending on day 6, 2 µL culture medium was aspirated and the concentration of glucose determined using a blood glucose monitoring device. Daily visualisation of adhered cells took place by the use of a microscope. On day 6, all plates were washed and exposed to 0.25 % trypsin/EDTA as in § 2.2.7 to dissociate adhered cells. These were quantified by using a Vi-Cell XR Cell Viability Analyzer and a fold change in adherent cells calculated.

#### 2.2.II CELL LOADING AND MILD HYPOTHERMIA

To determine the effect of hypothermic conditions on cell loads adhered to chemically defined and animal origin substrates, PEI and LM were first adsorbed onto tissue culture-treated Nunc T-25 flasks at 10 and 2 µgcm<sup>-2</sup>, respectively. 2.25 mL PEI or LM coating solution was dispensed into T-25 flasks, agitated thoroughly by hand to ensure even coverage and placed in an incubator at 37 °C, 5 % (v/v) CO<sub>2</sub> overnight. The next day, PEI coating solution was fully aspirated, two 2 mL PBS washes performed and the flasks allowed to

air dry for 15 min. For flasks adsorbed with LM, two 2 mL HBSS washes were performed and 1 mL HBSS dispensed to keep surface hydrated. The 1 mL HBSS was removed prior to cell loading.

To prepare coated flasks for cell adherence, all flasks were placed in an incubator at 37 °C, 5 % (v/v) CO<sub>2</sub> for several hours. On day 3 of a passage, CHO-S IgG cells were filtered twice using a 20 µm cell strainer to eliminate any clumped cellular material, and a 5.0 × 10<sup>6</sup> cellmL<sup>-1</sup> suspension was prepared. 2 mL, i.e. 10 million cells, was adherently seeded by dispensing into the centre of each coated flask. Flasks were agitated gently by hand to ensure the entire surface of each coated well was covered with cell suspension, before being placed into a humidified, static incubator at 37 °C, 5 % (v/v) CO<sub>2</sub> overnight. The next day, day 1, the entire contents of each flask was aspirated and a single 1 mL PBS wash performed to rid of unadhered cells. 5 mL medium (pre-warmed to either 37, 32 or 30 °C) was then added before flasks were returned to an incubator either at 37, 32 or 30 °C, and 5 % (v/v) CO<sub>2</sub>. To determine the number of cells adhered overnight, separate flasks were washed as above and then exposed to 2 mL 0.25 % trypsin/EDTA to dissociate adhered cells as in § 2.2.7. These were quantified by using a Vi-Cell XR Cell Viability Analyzer and used as the actual adhered seeding cell concentration.

Each day, starting from day 1, and ending on day 5, 200 µL culture medium was aspirated from each flask adsorbed with PEI, centrifuged at 1000 g for 5 min, and 180 µL supernatant retrieved and stored at -80 °C for later analysis. Culture media from flasks adsorbed with LM was not analysed daily. Daily visualisation of adhered cells took place by the use of a microscope. On day 5, all medium was aspirated, followed by a single 2 mL PBS wash. This was also aspirated, mixed with the removed medium and the viable cell density and viability percentage of suspended cells quantified by using a Vi-Cell XR Cell Viability Analyzer. 2 mL 0.25 % trypsin/EDTA was added to dissociate adhered cells as in § 2.2.7. After day 5, all samples from flasks adsorbed with PEI were thawed at once and daily glucose, L-glutamine, lactate and lactate dehydrogenase determined using a Cedex Bio Analyzer. Daily IgG titre was determined using ValitaTITER.

The cell-specific productivity,  $q_P$  (pgcell<sup>-1</sup>day<sup>-1</sup>), was determined using Equation 2.4, where  $T_1$  and  $T_2$  are the IgG titres (pgmL<sup>-1</sup>) at the first and second time points, respectively, and  $X_1$  and  $X_2$  are the viable cell densities (cellmL<sup>-1</sup>) at the first and second time points, respectively, and  $\Delta t$  is the change in days.

The cell-specific L-glutamine consumption rate,  $q_{GLT}$  (µmol 10<sup>6</sup> cell<sup>-1</sup>day<sup>-1</sup>), was determined using Equation 2.5, where  $GLT_1$  and  $GLT_2$  are the L-glutamine concentrations (µmolmL<sup>-1</sup>) at the first and second time points, respectively, and  $X_1$  and  $X_2$  are the viable

cell densities ( $\times 10^6$  cellmL<sup>-1</sup>) at the first and second time points, respectively, and  $\Delta t$  is the change in days.

$$( \text{EQU. 2.4} ) \quad qP = \frac{T_2 - T_1}{\left( \frac{X_2 + X_1}{2} \right) \times \Delta t}$$

$$( \text{EQU. 2.5} ) \quad qGLT = \frac{GLT_1 - GLT_2}{\left( \frac{X_2 + X_1}{2} \right) \times \Delta t}$$

To visualise how morphologies of cells adhered to PEI substrates change when cultured at hypothermic temperatures, flasks destined for imaging were also prepared as above. A single flask for day 1, i.e. showing cells adhered overnight at 37 °C, and single flasks at day 5 for 30, 32 and 37 °C were fully aspirated, a single 2 mL PBS wash performed and 1 mL Image-iT Fixative Solution added and left at room temperature for 20 min to fix the adhered cells. It was then aspirated, washed once with 2 mL PBS, before 2 mL PBS was dispensed as a mounting medium. Adhered cells were imaged immediately using a DMI4000B inverted microscope with phase contrast at 10 $\times$  magnification. Micrographs were processed using ImageJ software and scale bars added.

## 2.3 CELL PAUSING

All reagents were sourced from Sigma-Aldrich (Missouri, USA) unless otherwise stated.

### 2.3.1 TEMPERATURE CHECK FOR CELL PAUSING

The optimal temperature to pause CHO-S IgG cells in suspension was determined by observing what effect different temperatures had on cell viability after defined periods at that temperature without gaseous CO<sub>2</sub> exposure or vessel agitation. On day 3 of a passage, a  $1.0 \times 10^6$  cellmL<sup>-1</sup> CHO-S IgG suspension was prepared and seeded as 5 mL in TubeSpin Bioreactor 50 vessels and 15 mL centrifuge tubes. For cell pausing, cell suspensions within centrifuge tubes were placed upright and fully capped at either 4, 8 or 23 $\pm$ 1 (room temperature) and 37 °C. For non-paused cells, cell suspensions within TubeSpin Bioreactor 50 vessels were placed with vented caps in an incubator at 37 °C, 5 % (v/v) CO<sub>2</sub> and 240 rpm.

On days 2, 4 and 8 all paused cell suspensions were gently resuspended. The viability for all suspensions, including those from non-paused vessels, was then determined using a Vi-Cell XR Cell Viability Analyzer. Vessels were placed back to their temperatures immediately after a sample was taken. On day 8, the glucose concentration was determined for

all cell suspensions using a blood sugar monitoring device.

### 2.3.2 SUSPENSION PAUSING AND REGROWTH

To determine the possibility for CHO cells to be cultured back in suspension after periods of cell pausing, a  $1.0 \times 10^6$  cellmL<sup>-1</sup> CHO-S IgG suspension was prepared and seeded as 5 mL in 15 mL centrifuge tubes. These were paused at either 4, 8 or 23±1 (room temperature) °C. On days 2, 4 and 8 all paused cell suspensions were gently resuspended. The viable cell density and viability was determined using a Vi-Cell XR Cell Viability Analyzer. Paused cells were then seeded at  $0.2 \times 10^6$  cellmL<sup>-1</sup> as 10 mL in TubeSpin Bioreactor 50 vessels and incubated at 37 °C, 5 % (v/v) CO<sub>2</sub> with 240 rpm orbital shaking. Vessels were also seeded with non-paused cells taken from a routine passage on day 3 of the culture. Viable cell density and viability were determined on days 0, 1, 3 and 5 using a Vi-Cell XR Cell Viability Analyzer. On day 5, cultures were passaged, again at  $0.2 \times 10^6$  cellmL<sup>-1</sup> as 10 mL in fresh TubeSpin Bioreactor 50 vessels, and the viable cell density and viability determined on days 0, 1, 3 and 5.

To demonstrate regrowth in larger volumes, CHO-S IgG suspensions were prepared and paused as above at 4, 8 or 23±1 (room temperature) °C. On day 4, all paused cell were gently resuspended. The viable cell density and viability percentage was determined using a Vi-Cell XR Cell Viability Analyzer. Paused cells were then seeded at  $0.2 \times 10^6$  cellmL<sup>-1</sup> as 30 mL in 125 mL Erlenmeyer flasks and incubated at 37 °C, 5 % (v/v) CO<sub>2</sub> with 140 rpm orbital shaking. Flasks were also seeded with non-paused cells taken from a routine passage on day 3 of the culture. Viable cell density and viability were determined daily from day 0 until day 7 using a Vi-Cell XR Cell Viability Analyzer. 200 µL culture medium was aspirated from each flask daily, centrifuged at 1000 g for 5 min, and 180 µL supernatant retrieved for IgG titre determination using ValitaTITER.

The above was repeated and Erlenmeyer flasks seeded again with cells paused at the same temperatures. On day 3, flasks were passaged and viable cell density and viability determined daily from day 0 until day 7, with daily IgG titre also determined.

### 2.3.3 ADHERENT PAUSING IMAGING

To characterise morphologies of paused cells adhered to glass surfaces, untreated 8-well µ-slide glass plates were coated with PEI and FN at 10 and 5 µgcm<sup>-2</sup>, respectively, at 100 µL overnight. The next day, all wells were aspirated and washed with 200 µL PBS or HBSS. Wells adsorbed with FN were kept hydrated with HBSS before use.

On day 3 of a passage, CHO-S IgG cells were filtered twice using a 20 µm cell strainer to

eliminate any clumped cellular material, and a  $0.1 \times 10^6$  cellmL<sup>-1</sup> suspension was prepared. 50  $\mu$ L (i.e. 150,000 cells) was adherently seeded by slowly dispensing above the centre of each coated well. Plates were agitated gently by hand to ensure the entire surface of each coated well was covered with cell suspension, before being placed into a humidified, static incubator at 37 °C, 5 % (v/v) CO<sub>2</sub> overnight. The next day, day 0, the contents of each well was aspirated, two 200  $\mu$ L PBS washes performed and 250  $\mu$ L media added. Plates were immediately wrapped in parafilm and paused at either 4 or 8 °C. Non-paused plates were returned to the incubator at 37 °C, 5 % (v/v) CO<sub>2</sub>.

On day 4, paused and non-paused plates were fully aspirated, washed twice with 200  $\mu$ L PBS and incubated with 200  $\mu$ L Image-iT Fixative Solution for 20 min at room temperature. This was then aspirated, a single 200  $\mu$ L PBS wash performed and 50  $\mu$ L fresh PBS added as a mounting medium. Adhered cells were imaged immediately using a DMI4000B inverted microscope with phase contrast at 10 $\times$  and 20 $\times$  magnifications. Micrographs were processed using ImageJ software and scale bars added.

#### 2.3.4 ADHERENT PAUSING AND DISSOCIATION

To determine what effect pausing cells adhered to polystyrene surfaces had on possible dissociation over time, PEI and FN were first adsorbed onto tissue culture-treated Nunc 24-well plates as in § 2.2.4. On day 3 of a passage, CHO-S IgG cells were filtered twice using a 20  $\mu$ m cell strainer to eliminate any clumped cellular material, and a  $7.5 \times 10^6$  cellmL<sup>-1</sup> suspension was prepared. 200  $\mu$ L, i.e. 1.5 million cells, was adherently seeded by slowly dispensing above the centre of each coated well. Plates were agitated gently by hand to ensure the entire surface of each coated well was covered with cell suspension, before being placed into an incubator at 37 °C, 5 % (v/v) CO<sub>2</sub> overnight.

The next day, day 0, the contents of each well was aspirated, two 400  $\mu$ L PBS washes performed and 450  $\mu$ L media added. Plates were immediately wrapped in parafilm and paused at either 4 or 8 °C. Non-paused plates were returned to the incubator at 37 °C, 5 % (v/v) CO<sub>2</sub>. Other plate wells adsorbed with either PEI or FN were also aspirated, had two 400  $\mu$ L PBS washes performed but then were incubated with 450  $\mu$ L PB-media mix for 30 min at 37 °C, 5 % (v/v) CO<sub>2</sub>. 200  $\mu$ L from each incubated well was transferred to a 96-well plate and the fluorescence read using a SpectraMax iD5. This was to determine the quantity of cells adhered after overnight adherence and be used later for normalisation.

On days 2, 4 and 8, paused and non-paused plates were fully aspirated, washed twice with 200  $\mu$ L PBS and incubated with 450  $\mu$ L PB-media mix for 30 min at 37 °C, 5 % (v/v) CO<sub>2</sub>. 200  $\mu$ L from each incubated well was transferred to a 96-well plate and read on a SpectraMax

iD5. The plates were then discarded, i.e. separate plates were used for each of the three day intervals. Normalised fluorescence values were further normalised as a percentage, with 100 % assigned to the PB readings determined after initial overnight adherence concentration for both PEI and FN. The above was repeated, except only with plates adsorbed with PEI, to determine if dissociation and getting a direct cell count would be different to only using PB. On days 2, 4 and 8, paused and non-paused plates were fully aspirated, washed twice with 200  $\mu$ L DPBS and incubated with 300  $\mu$ L 0.25 % trypsin/EDTA for 5 min in an incubator. 300  $\mu$ L SBTI was then added and plates agitated thoroughly by hand and allowed to incubate at room temperature for 2 min. The entire contents of every well was transferred each to 2 mL fresh medium and centrifuged at 200 g for 5 min. The supernatant was discarded, and the cell pellet resuspended in 5 mL fresh medium. The viable cell density, i.e. the number of cells still adhered to each well surface after defined pausing periods, was then determined using a Vi-Cell XR Cell Viability Analyzer.

To briefly see what effect pre-warming had on paused cells, PEI was first adsorbed onto tissue culture-treated Nunc 24-well plates as in § 2.2.4. CHO-S IgG cells, at 1.0 million cells, were adherently seeded onto coated wells and plates paused at 8 °C as described above. On days 2 and 4, plates had their parafilm removed and were pre-warmed to 37 °C, 5 % (v/v) CO<sub>2</sub> for 3 hr, before being imaged. These same wells were imaged immediately prior to this pre-warming step and the morphologies of the cells compared.

## 2.4 POLYHIPE MATERIALS DEVELOPMENT

All reagents were sourced from Sigma-Aldrich (Missouri, USA) unless otherwise stated.

### 2.4.1 ROUTINE HIPES AND POLYHIPE FABRICATION

The fabrication of a polymerised high internal phase emulsion (polyHIPE) material starts with the generation of a high internal phase emulsion (HIPE), followed by a curing step, either via ultraviolet (UV) radiation or heat exposure, to polymerise the monomers within the emulsion. The physical process of generating a HIPE is generally independent of the specific components used (e.g. monomer(s), crosslinker, surfactant etc.). A HIPE can be thought of as an emulsion precursor for the corresponding polyHIPE.

All HIPes were prepared as a total mass of 3.33 g in a cleaned, heat-dried 100 mL glass beaker. To generate a HIPE, the monomers 2-ethylhexyl acrylate (EHA) and mono-2-(methacryloyloxy)ethyl succinate (MAES) and crosslinker trimethylolpropane triacrylate (TMPTA) were added together. Hypermer B246, a solidified mix of polyhydroxystearic acid and polyethylene glycol and sourced as a gift from Croda (Yorkshire, UK), was added as a surfactant and fully dissolved by exposure to heat for 30 s. Diphenyl(2,4,6-

trimethylbenzoyl)phosphine oxide and 2-hydroxy-2-methylpropiophenone, sourced as a pre-mixed blend, was added as a photoinitiator. Once all added, a motorised PTFE stirrer was placed into the beaker, operated at 300 rpm, and deionised water added dropwise using a pipette controller over 5 min. Figure 2.2 shows this process for generation of a water-in-oil HIPE and subsequent fabrication of a polyHIPE material via UV radiation.

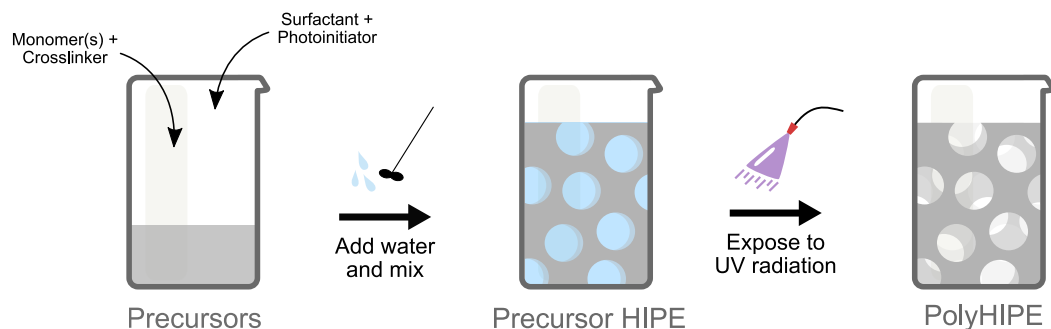


FIGURE 2.2 Schematic detailing the generation of an acrylic HIPE followed by the fabrication of a PolyHIPE via photopolymerisation. Precursors, including monomer(s), a crosslinker, a surfactant and a photoinitiator are first mixed together. Water is slowly added dropwise whilst these precursors are mixed to form the HIPE. Exposing this emulsion to UV radiation will polymerise the ‘oil’ phase, i.e. only the monomer(s) and crosslinker, leaving the water droplets. Upon drying, a highly porous material will be obtained.

After all the water was added the emulsion, now a HIPE, was left to mix for a further 2 min. All HIPEs were prepared as 90 % (v/v) internal phase, i.e. water added so as the final volume was 90 % (v/v) water volume, and 10 % (v/v) organic volume or external phase. Table 2.1 lists the densities of components used for all polyHIPEs fabricated; these were used to calculate the total organic volume for each HIPE formulation and from this, the volume of water needed to generate a 90 % (v/v) polyHIPE. The densities of the photoinitiator blend and surfactant were not included within the total organic volume.

TABLE 2.1 Densities of components employed for the fabrication of all polyHIPE materials.

Class	Component	Density (gmL <sup>-1</sup> )
Monomer	EHA	0.885
	MAES	1.190
Crosslinker	TMPTA	1.100
Misc.	Photoinitiator	n/a
	Hypermer B246	n/a

Once a HIPE was generated, the beaker was wrapped in aluminium foil to prevent gradual

polymerisation by ambient radiation. Monolithic polyHIPE materials were typically fabricated by either pouring HIPE into a glass petri dish or multiwell plate, or through the use of mould templates, before photopolymerisation with UV radiation for 2 min with an Omnicure spot lamp (Excelitas, Asslar, Germany). For polyHIPEs fabricated within petri dishes and plates, ‘cookie cutter’ punchers were used to obtain disc-shaped materials. For those fabricated with templates, PolyHIPEs were gently pushed out of moulds. Microspheric polyHIPE materials were fabricated using a bespoke fabrication system (see § 2.4.5).

Figure 2.3 shows skeletal formulae for EHA, MAES, IBOA and TMPTA, to allow an appreciation of the chemical structures of the monomers used. Whilst IBOA was not used to generate data for the work presented here, it was used in preliminary testing when techniques were being developed. The double C=C bonds can be seen in all four structures; for TMPTA, the three C=C bonds allow it to bond with multiple monomers, and thus act as a crosslinker between polymer chains. The carboxyl group can be seen at one end of the chain in the structure of MAES.

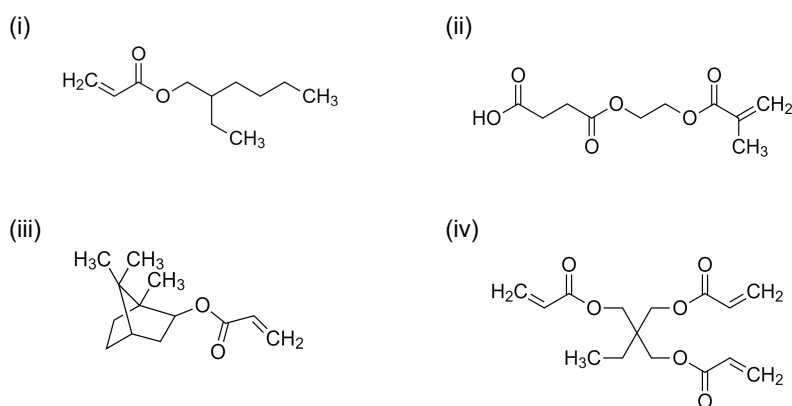


FIGURE 2.3 Skeletal formulae of the acrylate monomers employed for the fabrication of polyHIPE monoliths and microspheres. (i) 2-ethylhexyl acrylate (EHA); (ii) mono-2-(methacryloyloxy)ethyl succinate (MAES); (iii) isobornyl acrylate (IBOA) and (iv) trimethylolpropane triacrylate (TMPTA). The sole double C=C bond can be seen in the monomers EHA, MAES and IBOA. For TMPTA, the three C=C double bonds give the monomer its crosslinking nature, allowing it to link between polymer chains.

#### 2.4.2 SCANNING ELECTRON MICROSCOPY FOR POLYHIPES

Scanning electron microscopy (SEM) was employed to visualise the morphologies of both monolithic and microspheric polyHIPE materials at very high magnifications (> 50×), with both the total structure and local regions characterised. To prepare polyHIPE materials for SEM imaging, they were air dried overnight, mounted onto carbon tabs and sputtered with gold for 2 min whilst under vacuum using an Edwards S150B Sputter Coater (Edwards,

West Sussex, UK). Coated samples were imaged using a Tescan Vega3 (TESCAN, Brno, Czechia) with an acceleration voltage of 10 kV applied. Saved micrographs had a scale bar and info section. Images were later processed using ImageJ software and, where appropriate, this info section and scale bar removed and a custom scale bar added.

### 2.4.3 TOLUIDINE BLUE ASSAY DEVELOPMENT

Toluidine Blue (TBO), a cationic dye that binds reversibly to negative-charged chemical moieties, was selected as a coloured reagent for the presence of carboxyl groups. To determine which molarity to use, TBO was first dissolved in 50 % (v/v) acetic acid to give the following molar concentrations; 500, 400, 300, 200, 100, 50 and 25  $\mu\text{M}$ . Using a Nanodrop, full spectra data was obtained for each to observe areas of maximum absorbance for TBO. Starting from 50  $\mu\text{M}$ , a serial dilution using acetic acid (with a dilution factor of two) was also prepared down to 1.5626  $\mu\text{M}$ . The absorbance was determined at 626 nm and a standard curve obtained to test the suitability of TBO.

### 2.4.4 CARBOXYL FUNCTIONALITY ASSAY USING TOLUIDINE BLUE

To determine if the presence of MAES in the HIPE resulted in the subsequent polyHIPE possessing carboxyl functionality, HIPEs with decreasing EHA (100, 98, 96, 92 and 84) and increasing MAES (0, 2, 4, 8 and 16) weight percentages were generated, as shown in Table 2.2. The volumes of water needed to give a 90 % internal phase for each formulation are also shown here. The first formulation had 100 % EHA, 0 % MAES, the second had 98 % EHA, 2 % MAES, and so on.

TABLE 2.2 HIPE formulations for polyHIPEs containing varying weight percentages of EHA and MAES monomers.

Class	Component	Mass (g)	% (w/w)
Monomer	EHA	3.33, 3.26, 3.19, 3.06, 2.80	100, 98, 96, 92, 84
	MAES*	0.00, 0.06, 0.13, 0.27, 0.53	0, 2, 4, 8, 16
Crosslinker	TMPTA <sup>†</sup>	0.50	15
Misc.	Photoinitiator	0.19	5
	Hypermer B246	0.38	10

\* Volume of water needed for polyHIPEs with 0, 2, 4, 8 and 16 % MAES is 34, 35, 37, 37 and 37 mL.

<sup>†</sup> That is, as % (w/w) of monomer mass, rest % (w/w) of total organic mass (monomers and crosslinker).

300  $\mu\text{L}$  of each formulation was dispensed into wells of a 24-well Nunc plate, before curing with UV radiation for 2 min. A 'cookie cutter' puncher was used to cut cylindrical tablet-like shapes, or discs, of 3 mm diameter and 1 mm thickness. Care was taken to ensure each

tablet was exact in dimensions. These were washed in acetone for 12 hr. SEM images were obtained for each of the different polyHIPE tablets at 100× and 500× magnifications. Figure 2.4 shows the workflow of generating uniform polyHIPE discs, with increasing amounts of MAES, for the carboxyl functionality assay using TBO.

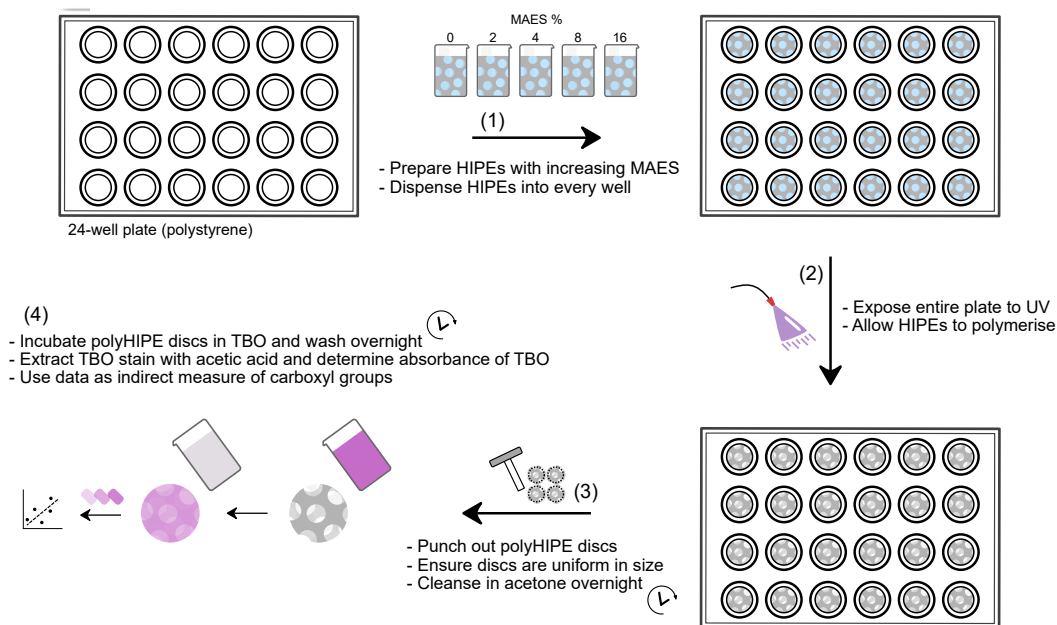


**FIGURE 2.4** Schematic detailing the workflow of generating uniform polyHIPE discs, with increasing amounts of MAES, for the carboxyl functionality assay using TBO. HIPEs with increasing amounts of MAES were prepared and equal volumes dispensed into the wells of a 24-well plate. The entire plate was exposed to UV to allow the HIPEs to polymerise. A 'cookie cutter' was used to cut out uniform polyHIPE discs. These were cleansed in acetone before being incubated in TBO to allow carboxyl identification via staining. Stains were extracted from the discs and the absorbance quantified to compare how the amount of MAES affected the amount of carboxyl groups in the materials.

A glycine-sodium hydroxide buffer, at pH 10, was prepared by mixing 50 mL 0.1 M glycine with 38.6 mL 0.1 M sodium hydroxide and then adding 111.4 mL water. 50 mL 50  $\mu$ M TBO working solution was prepared by adding 49  $\mu$ L 50 mM TBO master stock to 49.951 mL glycine-sodium hydroxide buffer and mixing well. Working solution was prepared fresh and used immediately. Each of the polyHIPE tablets were briefly washed in glycine-sodium hydroxide buffer to prime the materials. Using 15 mL centrifuge tubes, each tablet was added to 5 mL 50  $\mu$ M TBO working solution and incubated for 1 hr with end-to-end spinning at 20 rpm.

Tablets were removed, placed in fresh centrifuge tubes with 10 mL glycine-sodium hydroxide buffer and incubated for 24 hr at 30 rpm. Tablets were again removed and photographed

for visual comparison of TBO staining. To extract the bound TBO, tablets were placed in 5 mL 50 % (v/v) acetic acid and incubated for 1 hr at 20 rpm. 2  $\mu$ L of the supernatant, i.e. unbound TBO, was aspirated and the absorbance at 626 nm determined using a Nanodrop.

#### 2.4.5 FABRICATION OF POLYHIPE MICROSPHERES

A bespoke system, originally developed in part by Paterson et al. (2018), was adapted to fabricate polyHIPE microsphere materials containing EHA and MAES monomers. Figure 5.4 in § 5.1.2 shows a schematic detailing this bespoke system. A single-syringe pump (World Precision Instruments, Hertfordshire, UK) was loaded with a 20 mL syringe. To this, a dispensing needle (Intertronics, Oxfordshire, UK) was attached, and itself inserted into 6 mm internal diameter polyvinyl chloride (PVC) tubing, in either a co-flow or T-junction orientation.

The internal diameter of the dispensing needle was varied depending upon fabrication experiment. The tubing was fed through a Masterflex L/S peristaltic pump unit (Cole-Parmer, Cambridgeshire, UK), with an attached pump head (model: 7535-04). One open end of the tubing was submerged in a 1 L beaker, itself filled with a carrier phase containing either water, glycerol or polyvinyl alcohol (PVA) in varying amounts depending upon experiment.

The other open end of the tubing sat within a filter sock with 50  $\mu$ m porosity, placed above the beaker. A curing chamber, fashioned using cardboard and enclosing an in-house manufactured 'corkscrew' glass piece, was exposed to continual UV radiation from an Omnicure spot lamp. The curing chamber was lined on the inside with aluminium foil to reflect the radiation. The tubing was connected to the inlet and outlet of the glass piece via connectors with a barbed and a threaded end. When the peristaltic pump was in operation, carrier phase would circulate around the system at the defined pump rotational speed in a continuous, recycling loop.

The general method to fabricate polyHIPE microspheres involved first loading a syringe with a freshly generated HIPE. Any visible air bubbles within the HIPE were dispelled by covering the end of the syringe and pushing the plunger tightly to obtain a compact liquid. The peristaltic pump was switched on 10 min before fabrication to ensure the carrier phase was homogeneous within the system. A dispensing needle was attached to the syringe and then inserted into the tubing, with the syringe pump then turned on. The flow rate of the syringe pump, i.e. the rate at which HIPE would be injected into the circulating carrier phase, as well as the flow rate of the carrier phase, was dependent upon the experiment.

### 2.4.6 CO-FLOW FABRICATION OF MICROSPHERES

To investigate the fabrication of polyHIPE microspheres using the co-flow orientation, HIPEs were first generated using the formulation given in Table 2.3. A co-flow orientation was fashioned by attaching PharMed tubing (Cole-Parmer, Cambridgeshire, UK), with an internal diameter of 2.4 mm, to the end of the syringe containing the HIPE. This tubing was connected to a dispensing needle at the other end, which was directed to an angled section of the system tubing. The needle was inserted so as the flow of the injected HIPE would be in the same direction as the flow of the carrier phase, i.e. in co-flow.

To determine what effect carrier phase composition had on fabricated polyHIPE microspheres, four carrier phases were investigated; 10 % water, 50 and 80 % (v/v) glycerol, and 15 % (v/v) glycerol within 3 % (v/v) PVA. To prepare 3 % (w/v) PVA solution, 15 g PVA was added to 500 mL deionised water and stirred at 800 rpm whilst heated to 90 °C for 20 min to allow dissolution. The newly formed PVA solution was then allowed to cool to room temperature before use. To prepare 50 % (v/v) glycerol solution, 250 mL glycerol was added to 250 mL deionised water and mixed vigorously to achieve a homogenous solution. To prepare 80 % (v/v) glycerol solution, 400 mL glycerol was added to 100 mL deionised water. To prepare 15 % (v/v) glycerol within 3 % (w/v) PVA, 425 mL of 3 % (w/v) PVA was added to 75 mL of 15 % (v/v) glycerol and mixed vigorously. The system tubing and glass piece were cleaned extensively with deionised water when changing between different carrier phase compositions.

TABLE 2.3 HIPE formulation for polyHIPE microspheres containing 90 % EHA and 10 % MAES monomers.

Class	Component	Mass (g)	% (w/w)
Monomer	EHA	3.00	90
	MAES	0.33	10
Crosslinker	TMPTA*	0.50	15
Misc.	Photoinitiator	0.19	5
	Hypermer B246†	0.38	10

\* That is, as % (w/w) of monomer mass, rest % (w/w) of total organic mass (monomers and crosslinker).

† For Hypermer B246 at 1.25 % (w/w), 0.05 g was used.

In addition, to determine what effect surfactant percentage and water temperature had on resulting polyHIPE microspheres, surfactant percentage was decreased from 10 to 1.25 % (w/w) and the temperature of the water added was increased from ambient to 80 °C. For

100 % water and 50 % glycerol carrier phases, only a 'normal' HIPE was used for fabrication of microspheres, i.e. 10 % (w/w) surfactant and ambient temperature water. For 80 % glycerol and 15 % (v/v) glycerol within 3 % (w/v) PVA, a normal HIPE was used in addition to HIPEs generated with 1.25 % (w/w) surfactant and HIPEs generated with 1.25 % (w/w) surfactant and using 80 °C water.

Specific HIPEs generated were loaded into a 20 mL syringe with tubing attached to a 1.5 in dispensing needle with a blunted end 30 G (0.15 mm ID) PTFE tip (Intertronics, Oxfordshire, UK). The syringe flow rate was set initially at 12 mLhr<sup>-1</sup> to prime the dispensing needle and ensure a constant flow of HIPE from the tip. Once this was achieved, the needle was inserted into the system tubing and the syringe flow rate set to 0.3 mLhr<sup>-1</sup>. The carrier phase, either one of the four listed above, was pumped at 150 rpm. Only polyHIPE microspheres fabricated after 20 min of operation were collected for analysis.

Fabricated microspheres were spread as a monolayer onto glass microscope slides using a spatula, dried overnight and imaged using an inverted brightfield IX73 microscope (Olympus, Hamburg, Germany) at 10× magnification. Images were processed using ImageJ software, a scale bar set and the measure tool used to determine the diameter of 200 microspheres. These data were then used to produce diameter size distribution graphs. To attempt to quantify the surface porosity of microspheres, a 20× magnification lens was used, light turned up near maximum intensity and exposure time set to 200 ms to distinguish the surface pores. 50 microspheres were imaged with this method, with four of the largest pore sizes in the centre of each microsphere measured using ImageJ software and pore size distribution graphs produced. SEM images were obtained for each of the different polyHIPE microspheres at 100× and 500× magnifications.

#### 2.4.7 T-JUNCTION FABRICATION OF MICROSPHERES

To investigate the fabrication of polyHIPE microspheres using the T-junction orientation, HIPEs were first generated using the formulation given in Table 2.3 with the surfactant kept at 10 % (w/w). Parameters relating to the HIPE or its generation process, such as surfactant percentage or temperature of water added, were not altered. 80 % (v/v) glycerol was used as the sole carrier phase in this instance. A T-junction orientation was devised by attaching a dispensing needle to a syringe. The needle was inserted into the tubing to obtain a 'T' orientation, and hence the flow of HIPE was perpendicular to that of the carrier phase. No extra tubings were required.

Generated HIPEs were loaded into a 20 mL syringe with tubing attached to a 1.5 in dispensing needle with a blunted end 20 G (0.60 mm ID) PTFE tip. To investigate how carrier

phase flow rates and HIPE injection rates affect the diameter of fabricated polyHIPE microspheres, three condition pairs were attempted; 600 rpm and 6 mLhr<sup>-1</sup>, 400 rpm and 12 mLhr<sup>-1</sup> and 200 rpm and 18 mLhr<sup>-1</sup>. Due to the much faster dispensing rates used in these fabrications, the dispensing needle was not primed and instead inserted immediately into the tubing. Only polyHIPE microspheres fabricated after 20 min of operation were collected for analysis.

Microspheres were spread as a monolayer onto glass microscope slides using a spatula, dried overnight and imaged using an inverted brightfield IX73 microscope at 10× magnification. Images were processed using ImageJ software, a scale bar set and the measure tool used to determine the diameter of 200 microspheres. These data were then used to produce diameter size distribution graphs. Quantifying surface porosity for microspheres fabricated using these conditions was not attempted. SEM images were obtained for polyHIPE microspheres fabricated using each of the three condition pairs at 100× and 500× magnifications.

#### 2.4.8 T-JUNCTION FABRICATION OF 'SMALLER' MICROSPHERES

To attempt to fabricate polyHIPE microspheres with smaller average diameters than those fabricated using the conditions in § 2.4.7, four conditions were investigated; 400 rpm, 4 mLmin<sup>-1</sup>, 30 G needle; 400 rpm, 4 mLmin<sup>-1</sup>, 32 G needle; 400 rpm, 2 mLmin<sup>-1</sup>, 32 G needle, and 600 rpm, 2 mLmin<sup>-1</sup>, 32 G needle. The HIPE was generated using the formulation listed in Table 2.3 and 80 % (v/v) glycerol was kept as the carrier phase.

Microspheres were spread as a monolayer onto glass microscope slides using a spatula, dried overnight and imaged using an inverted brightfield IX73 microscope at 10× magnification. Images were processed using ImageJ software, a scale bar set and the measure tool used to determine the diameter of 200 microspheres. These data were then used to produce diameter size distribution graphs. Quantifying surface porosity for microspheres fabricated using these conditions was not attempted.

#### 2.4.9 PUMP SEED AND FLOW RATE OF CARRIER PHASE

For the experiments involving the fabrication of microspheres, the flow rate of the carrier phase is given, in both the methods here and in the data that follow, by the rpm of the pump head. There were four different pump speeds used in this work; 150, 200, 400 and 600 rpm. These corresponded, roughly, to carrier phase flow rates of 280, 370, 750 and 1120 mLmin<sup>-1</sup>, respectively. This was determined (after the experiments were completed) by reviewing the manufacturer's guide of the specific pump head, which listed flow rates at two pump speeds for a tubing with an internal diameter of 3.1 mm. Because the tubing

used here had an internal diameter of 6 mm, the two flow rates given were multiplied by 4 (as the area of a circle is proportional to the radius squared, and the flow rate within a tubing is proportional to the area) and a plot drawn of pump speed against these flow rates. The equation of the resulting trendline was used to determine the flow rates at the 4 pump speeds used in this work.

It must be stressed these calculations assume a Newtonian liquid was pumped, whilst the carrier phases actually used included varying amounts of glycerol and PVA. These viscous solutions mean the flow rates quoted above should be viewed only as an estimate and must be empirically confirmed if readers wish to exactly replicate fabrication conditions. In the work here, an experiment to determine the flow rates using the 6 mm internal diameter tubing and the specific pump head was not performed.

## 2.5 MICROSPHERE APPLICATIONS

All reagents were sourced from Sigma-Aldrich (Missouri, USA) unless otherwise stated.

### 2.5.1 MICROSPHERE WASHING, PEI ADSORPTION AND STERILISATION

To ensure easy handling of microspheres, 100  $\mu\text{m}$  cell strainer filters were employed. Decanting microspheres from a liquid was achieved by tipping microsphere suspensions through one of these strainers and allowing microspheres to be retained whilst 'supernatant' passed through. By turning the strainer upside down and positioning on top of a vessel, a new liquid could be flushed through, catching the microspheres and creating a new suspension. For aseptic handling within a laminar flow hood, sterile single-use strainers were used.

All fabricated polyHIPE microspheres destined for cell adherence were washed in acetone for 12 hr with end-to-end spinning. The microspheres were decanted, and fresh acetone added for a further 12 hr. Microspheres were once again added to fresh acetone and stored at room temperature until needed for experimentation. To adsorb PEI onto microspheres, a 10  $\text{mgmL}^{-1}$  PEI coating solution was prepared using deionised water. Microspheres were decanted from acetone and suspended in this coating solution using a 50 mL centrifuge tube. A maximum of 5 mL microspheres were suspended in 45 mL coating solution. Once added, centrifuge tubes were inverted several times by hand. This was followed by repeated aspirating and pipetting to ensure any microsphere aggregates were resuspended. Microspheres were incubated at room temperature overnight with end-to-end spinning to allow maximum adsorption of PEI. The next day, spinning was stopped and microspheres allowed to settle by gravity. The formation of a packed-bed of microspheres, with no aggregation, was regarded as evidence of successful PEI adsorption. All microspheres adsorbed

with PEI were used for experimentation within 24 hr.

To prepare for an aseptic environment, microspheres were decanted from the PEI coating solution and suspended into 70 % (v/v) ethanol and spun for 1 hr as a disinfectant step. After this, microspheres were treated as 'sterile' and decanted in a laminar flow hood and washed several times with autoclaved PBS to cleanse the ethanol. Alternatively, freshly adsorbed microspheres were suspended within PBS and autoclaved with steam at 121 °C for 20 min and then washed several times with autoclaved PBS in a laminar flow hood. The choice between ethanol exposure or autoclaving was dependent upon the experiment. For both options however, microspheres were ultimately suspended into pre-warmed medium before experimental use.

### 2.5.2 SYRINGE PUMP MICROSPHERE LOADING

It was proposed that pumping cells from in a syringe through a packed-bed of microspheres could be a technique to achieve cell adherence and subsequently rapidly load a defined volume of microspheres with cells. To investigate this, PEI-adsorbed polyHIPE microspheres (with an average diameter of approximately 470 µm) were first dispensed into 1 mL Mobicol columns (Mobitech, Lotzestrasse, Germany) and allowed to settle by gravity. Polypropylene frits, with 90 µm porosity, were inserted into these columns beforehand to retain the microspheres.

Three viable cell densities, 0.5, 1.0 and  $2.0 \times 10^6$  cellmL<sup>-1</sup>, and three flow rates, 1.0, 2.5 and 5.0 mLmin<sup>-1</sup>, were tested to determine what effect each had on the number of cells loaded onto the microspheres. The volume of microspheres was kept constant at 1 mL and the volume of each cell delivery kept at 50 mL. For each condition, microspheres settled within Mobicol columns were first briefly primed with buffered, pre-warmed medium. 55 mL of a particular viable cell density was then aspirated into a 60 mL syringe and attached to a syringe pump, set at a particular flow rate. To this syringe, a Mobicol column containing microspheres was attached via a luer connection, in a sideways orientation. The syringe pump was raised such that a 50 mL centrifuge tube could be positioned directly under the outlet of the Mobicol column.

When the syringe pump was in operation, effluent from the 1 mL column, i.e. cells that were not adhered as they passed through the microsphere bed, dripped into the centrifuge tube. Once 5 mL was collected, the tube was quickly replaced with an empty one. The 5 mL was subsequently agitated by hand and the viable cell density determined using a Vi-Cell XR Cell Viability Analyzer. This was repeated until 50 mL volume was delivered through the column. Due to only having two syringe pumps, measurements were limited to two per

condition. Breakthrough curves were calculated by deducting the number of cells present in each 5 mL effluent by the number present in 5 mL of the particular cell load used.

### 2.5.3 MICROSPHERE CELL GROWTH IN T-FLASKS

To demonstrate the growth of adherent cells on microspheres adsorbed with PEI, the syringe pump technique as described in § 2.5.2 was used to deliver 10 mL of cell suspension at a density of  $0.25 \times 10^6 \text{ cell mL}^{-1}$ , i.e. 2.5 million cells, at  $2.5 \text{ mL min}^{-1}$ . The number of cells adhered was calculated by deducting the amount of cells present in the effluent from the amount of cells present in the cell seed delivered. Immediately after seeding, microspheres were gently aspirated from the columns and dispensed into T-25 flasks. 10 mL medium was added and flasks placed in a static incubator at  $37^\circ\text{C}$ , 5 % (v/v)  $\text{CO}_2$ .

At day 4, microspheres were decanted and washed with 10 mL pre-warmed PBS into a 50 mL centrifuge tube to remove any weakly adhered cells. The presence of viable adhered cells on the microspheres was determined by using 10 mL PB-media mix, as described in § 2.2.1. The PB-media mix was used to flush microspheres back into a fresh 50 mL centrifuge tube before being placed in a T-25 flask for 30 min incubation. 200  $\mu\text{L}$  was transferred to a 96-well plate and the fluorescence determined using a SpectraMax iD5. Microspheres were washed once with 10 mL PBS to remove incubated PB-media mix, and returned to the incubator with fresh medium. The procedure was repeated to determine viability of adhered cells at day 7.

Fluorescent and brightfield micrographs were obtained on days 0 (immediately after seeding), 4 and 7. On these days, a small number of microspheres were sampled, decanted and incubated with ice cold methanol (as a crude fixative) for 10 min. The methanol was removed, the microspheres washed with PBS and incubated, whilst protected from light, for 30 min with 10 mL of  $5 \mu\text{g mL}^{-1}$  Hoechst solution. Microspheres were washed once with PBS and placed in fresh PBS for imaging using a DAPI filter.

For brightfield micrographs, only the above fixation step was performed and the microspheres imaged in fresh PBS. For both, microspheres were imaged immediately. Micrographs were processed using ImageJ software and scale bars added.

### 2.5.4 PERISTALTIC PUMP MICROSPHERE LOADING

The technique described in § 2.5.2 was developed upon to allow parallel volumes of microspheres, within columns, to be rapidly loaded with cells. 1 mL PEI-adsorbed polyHIPE microspheres (with an average diameter less than 300  $\mu\text{m}$ ) were dispensed into 2.5 mL columns (Mobitech, Lotzestrasse, Germany) and allowed to settle by gravity. Polypropy-

lene frits, with 90  $\mu\text{m}$  porosity, were inserted into these columns beforehand to retain the microspheres.

A bespoke 'perfusion plate', to hold up to six of these columns, was fashioned in-house. Briefly, a 5 mm thick transparent acrylic sheet was cut into three components with a HPC Laserscript laser cutter (HPC Laser, Halifax, UK) using models generated in SolidWorks. These components slotted in to place to give a free-standing structure. The plate was designed with clearance around each column point to allow for tubing, stopcocks and luer fittings to be attached and removed easily. Dr. Samand Pashneh-Tala, of the Department of Materials Science and Engineering, advised on, designed and fabricated the perfusion plate.

The general method to load three 1 mL microsphere volumes began with physically preparing the system. A 250 mL bottle, filled with cell suspension and a magnetic stirrer bar, was placed upon a stirrer plate. Cells were agitated at 200 rpm to ensure homogeneity. Three separate Masterflex tubings (Cole-Parmer, Cambridgeshire, UK), with 1/16 in (1.8 mm) ID, were submerged in the cell suspension, themselves attached to a 205U 12-channel peristaltic pump (Watson-Marlow, Falmouth, UK), and leading to a three-way stopcock attached to the top connection of each column. At the bottom of each column, a three-way stopcock was also attached, with tubing leading into a 50 mL centrifuge tube. Male and female luer fittings, with barbed ends suitable for 1.8 mm ID tubing, were used at connection points. The principle was that cells would be pumped from the bottle through the columns, captured by the microspheres, and any that were not would be collected in the effluent and subsequently quantified.

Once all microspheres were settled, the stopcock at the bottom of each column was positioned so no liquid could exit. 2 mL medium was added manually to each column to fill the column space. With the stopcock at the top positioned so that no liquid could enter, medium was pumped initially through the system to prime the tubings, exiting into waste line tubings. Once primed, these tubings were discarded, and the stopcocks positioned back so that liquid could now enter the columns. Once the stopcock at the bottom of each column was opened, medium was allowed to prime the cartridges until the volumes within each cartridge reached a steady state.

On day 3 of a passage, CHO-S IgG cells were centrifuged and resuspended in a reduced volume and either a  $10$  or  $20 \times 10^6$   $\text{cell mL}^{-1}$  suspension prepared as 200 mL in the 250 mL bottle. These suspensions were filtered twice using a 20  $\mu\text{m}$  cell strainer to eliminate any clumped cellular material. For the  $10 \times 10^6$   $\text{cell mL}^{-1}$  suspension, the pump flow rate was set to 1.0  $\text{mL min}^{-1}$  and 25 mL suspension delivered; for the  $20 \times 10^6$   $\text{cell mL}^{-1}$  suspension,

it was set to  $0.5 \text{ mLmin}^{-1}$  and 12.5 mL delivered. For both conditions, 250 million cells would be pumped through the columns after 25 min of operation. After this, 12.5 or 25 mL medium was flushed through at  $0.5$  or  $1.0 \text{ mLmin}^{-1}$ , respectively, and collected to ensure any weakly adhered cells were detached. The number of cells adhered was calculated by deducting the number of cells present in this effluent by the number present in the particular cell load used. For comparisons with a commercial product, Cytopore 2 microcarriers (GE Healthcare, Illinois, USA), hydrated and autoclaved following supplier instructions, were also tested alongside PEI-adsorbed microspheres.

#### 2.5.5 MICROSPHERE LOADING USING AMBR15 BIOREACTORS

The following work was performed at CPI in Darlington, UK. To demonstrate the use of polyHIPEs microspheres using a commercial system, ambr15 bioreactors were chosen as suitable vessels to investigate the rapid loading of microspheres with cells. On day 3 of a passage, CHO-S IgG cells were centrifuged and resuspended in reduced volumes and  $10$ ,  $20$  or  $40 \times 10^6 \text{ cellmL}^{-1}$  suspensions prepared. Suspensions were filtered twice using a  $20 \mu\text{m}$  cell strainer to eliminate any clumped cellular material. 10mL PBS containing 5 mL microspheres adsorbed with PEI were manually dispensed into ambr15 vessels and allowed to settle. 5mL was aspirated to leave only the microsphere bed. 7 mL pre-warmed medium was added to each vessel, the microspheres resuspended and settled, before 5 mL was aspirated. This was repeated twice to leave a 7 mL microsphere slurry within medium.

Ambr15 vessels were loaded into the system deck and the agitation rate set to 300 rpm. Once microspheres were resuspended, the liquid handler was allowed to dispense 5 mL of either  $10$ ,  $20$  or  $40 \times 10^6 \text{ cellmL}^{-1}$  suspensions, i.e. 50, 100 or 200 million cells. Once cells were added, a timer was set for 2 hr. Every 30 min, the liquid handler aspirated 1 mL (whilst the impeller was stirring to ensure homogeneity) and dispensed into a multiwell plate. This was manually aspirated and dispensed through a  $100 \mu\text{m}$  strainer to retrieve a cell suspension. The viable cell density of this suspension, i.e. cells that had not adhered onto microspheres, was determined using a Vi-Cell XR Cell Viability Analyzer. From this the number of cells adhered onto the microspheres could be calculated every 0.5 hr.

## 2.6 PSEUDO-CONTINUOUS SYSTEMS

All reagents were sourced from Sigma-Aldrich (Missouri, USA) unless otherwise stated.

### 2.6.1 VALIDATION OF CEDEX BIO ANALYZER

To demonstrate the use of a Cedex Bio Analyzer for the determination of metabolite and substrate concentrations within cell culture medium, glucose, L-glutamine, lactate and lac-

tate dehydrogenase assay reagent packs were first installed following supplier instructions. Three measurements (low, medium and high) were determined for control solutions supplied by Roche and compared to the stated values. To test the Cedex Bio Analyzer, standard curves were prepared for glucose and L-glutamine within fresh CD CHO medium, supplemented with 8 mM L-glutamine. Medium was serially diluted (with a dilution factor of two) using deionised water. Each glucose and L-glutamine concentration, beginning with an arbitrary '1' for undiluted media, '0.5' for the first dilution, '0.25' for the next and so on, was then determined using the Cedex. Technical triplicate readings were taken for glucose. A linear trendline was plotted and a  $R^2$  value calculated for both substrates.

To demonstrate the use of the Cedex during actual cell culture, CHO-S IgG cells were seeded at  $0.2 \times 10^6$  cellmL<sup>-1</sup> as 30 mL in a 125 mL Erlenmeyer flask and incubated at 37 °C, 5 % (v/v) CO<sub>2</sub> with 140 rpm orbital shaking. Each day, starting from day 0, and ending on day 9, viable cell density and viability were determined using a Vi-Cell XR Cell Viability Analyzer. 200 µL culture medium was aspirated daily from the flask, centrifuged at 1000 g for 5 min, and 180 µL supernatant retrieved and stored at -80 °C. All samples were thawed together and daily glucose, L-glutamine, lactate and lactate dehydrogenase concentrations determined using the Cedex.

### 2.6.2 SUSPENSION CELL CULTURE AND MILD HYPOTHERMIA

To investigate the effect of shifting to mild hypothermia conditions on CHO-S IgG culture, CHO-S IgG cells were seeded at  $0.2 \times 10^6$  cellmL<sup>-1</sup> as 30 mL in 125 mL Erlenmeyer flasks and incubated at 37 °C, 5 % (v/v) CO<sub>2</sub> with 140 rpm orbital shaking. On day 3, flasks were either moved to 32 or 30 °C culture, or kept at 37 °C.

Each day, starting from day 0, and ending on day 9, viable cell density and viability were determined using a Vi-Cell XR Cell Viability Analyzer. 200 µL culture medium was aspirated daily from flasks, centrifuged at 1000 g for 5 min, and 180 µL supernatant retrieved and stored at -80 °C. All samples were thawed together and daily glucose, L-glutamine, lactate and lactate dehydrogenase concentrations determined using a Cedex Bio Analyzer, with the cell-specific L-glutamine consumption rate determined for all temperatures between day 0 and 6 using Equation 2.5 as shown in § 2.2.11. Daily IgG titre was determined using ValitaTITER, with cell-specific productivity determined for all temperatures between day 0 and 6 using Equation 2.4 as shown in § 2.2.11.

### 2.6.3 PSEUDO-CONTINUOUS CULTURE USING ERLENMEYER FLASKS

To demonstrate pseudo-continuous culture, Erlenmeyer flasks were employed as vessels with polyHIPE microspheres as an internal cell retention device. Manually exchanging

medium was performed by tilting flasks to the side, allowing microspheres to settle and aspirating spent medium. An equal volume of fresh medium was added and microspheres resuspended. Loading of microspheres with CHO-S IgG cells was performed as in § 2.5.4, with microspheres retrieved from columns by first tilting columns sideways and then pumping fresh medium through the columns from the bottom to push the retrieved microspheres out of the top. Microspheres were collected in centrifuge tubes.

An initial experiment to investigate pseudo-continuous culture was performed using 1 mL microspheres within 20 mL medium in 125 mL Erlenmeyer flasks. Cell loading was performed using a cell load of 250 million cells at a flow rate of 0.5 mLmin<sup>-1</sup>. A Celltron (Infors HT, Bottmingen, Switzerland) shaker was used for agitation within a static incubator. Temperatures were set between 29 and 31 °C and agitation between 50 and 60 rpm. 100 % medium exchange was performed every 2, 3 or 5 days, depending upon time of experiment. Photographs of the conditions of Erlenmeyer flasks and microspheres throughout the experiment were taken. Each day, starting from day 1, and ending on day 25, viable cell density and viability of cells in suspension, i.e. cells that had dissociated from the microspheres, were determined using a Vi-Cell XR Cell Viability Analyzer.

200 µL culture medium was aspirated daily from flasks, centrifuged at 1000 g for 5 min, and 180 µL supernatant retrieved and stored at -80 °C. All samples were thawed together and daily glucose, L-glutamine, lactate and lactate dehydrogenase concentrations determined using a Cedex Bio Analyzer. Daily IgG titre was determined using ValitaTITER.

A second experiment was carried using 1 mL microspheres within 20 mL medium in 250 mL Erlenmeyer flasks. Cell loading was performed using a cell load of 300 million cells at a flow rate of 0.5 mLmin<sup>-1</sup>. Temperature was set at 30 °C for the first 4 days, and then turned down to 28 °C for the remainder of the culture. Agitation was kept at 45 rpm. 100 % medium exchange was performed after the first 4 days, and then every 3 days. Each day, starting from day 0, and ending on day 31, viable cell density and viability of cells in suspension, i.e. cells that had dissociated from the microspheres, were determined using a Vi-Cell XR Cell Viability Analyzer.

200 µL culture medium was aspirated daily from flasks, centrifuged at 1000 g for 5 min, and 180 µL supernatant retrieved and stored at -80 °C. All samples were thawed together and daily glucose, L-glutamine, lactate and lactate dehydrogenase concentrations determined using a Cedex Bio Analyzer. Daily IgG titre was determined using ValitaTITER. For both experiments, the medium removed during the media exchange days was sampled and used as the daily sample for that day. There was no second sample taken on media exchange days once the medium had been exchanged. The sample taken the next day was thus from

fresh medium that had been in culture for 24 hr.

## 2.7 PERFUSION SYSTEM DEVELOPMENT

All reagents were sourced from Sigma-Aldrich (Missouri, USA) unless otherwise stated.

### 2.7.1 PERFUSION SYSTEM IDEAS

For a discussion of the ideas which led to the development of the perfusion system, including a report of numerous unsuccessful attempts using columns containing microspheres as packed-beds, see § 6.2.1.

### 2.7.2 PERFUSION SYSTEM SET UP

An attempt at perfusion culture, using polyHIPE microspheres adsorbed with PEI as an internal cell retention device, was performed using an in-house developed perfusion system. Inspired in-part by a stirred tank reactor operating in chemostat mode, a spinner flask was acquired with an inlet tubing through one arm and an outlet tubing through the other. Medium was to be continually exchanged using these tubings, and with the flow rate in both tubings equal, a steady state system to be achieved. This was termed spinner flask-based perfusion. For a detailed discussion of the proposed process and an evaluation of specific materials selected, see § 6.2.2. A cleaned, heat-dried nominal 100 mL glass spinner flask (Bellco Glass, New Jersey, USA) with a magnetic PTFE impeller was filled with Sigma-Cote, a siliconising agent, to produce a hydrophobic inner coating on the inside walls. The flask was incubated for 2 min with gentle rotation to ensure sufficient exposure. The siliconising agent was removed and the flask allowed to air dry before washing. GL32 VapLock solvent delivery caps (Cole-Parmer, Cambridgeshire, UK), each with three female 1/4-28 UNF ports, were used to cap the two arms of the spinner flask. Male luer to male 1/4-28 UNF fittings were attached to connect a single-use 0.2 µm filter to each cap for gaseous exchange. Tubing adapters, with 1/8 in OD to male 1/4-28 UNF fittings and using a nut and ferrule system, were used to aseptically hold an inlet tubing through one cap and an outlet tubing through the other. Masterflex tubings with 1/16 in (1.8 mm) ID were used.

A frit holder, to house a frit and be attached to the end of the outlet tubing to retain the microspheres, was designed using SolidWorks and 3D printed in-house with a Form 2 3-D printer using Dental SG Resin (Formlabs, Massachusetts, USA). Following fabrication, structures were washed in propan-2-ol for 20 min in an ultrasonic bath and post-cured using a UV light box for 30 min at 60 °C. After curing, support structures were removed from the parts using side-cutters. Frit holders were designed with a tapered opening, allowing a 90 µm polypropylene frit to be inserted securely by hand, and with a barbed end suitable

for 1.8 mm tubing. The holder was later designed with a reduced diameter and a female luer ending, making it less intrusive and suitable for any tubing with a male luer fitting attached. Dr. Samand Pashneh-Tala, of the Department of Materials Science and Engineering, advised on, designed and fabricated all frit holders for this project.

The general method began with setting up the perfusion system. A refrigerator, set at 8 °C, was placed upon a non-humidified shaking incubator, which was not agitated in this instance. Within the refrigerator a 1 L bottle, filled with medium, was stored. Tubing ran from this feed bottle, out of the closed refrigerator door, and into the incubator. It passed through a 205U 12-channel peristaltic pump within the incubator and led into the inlet arm of the spinner flask, where medium was continually dispensed. The spinner flask was placed on a Micro-Stir magnetic stirrer plate (Wheaton, New Jersey, USA). Pump and stirrer power cables were able to fit safely through the incubator door when closed and plugged into a power supply. An outlet tubing, with frit attached, led out of the other arm of the spinner flask, passed through the pump and led to a 2 L waste bottle. Before it reached the waste bottle, it passed through a three-way stopcock. One end of this stopcock was attached to a single-use needle, which aseptically pierced a 10 mL bottle via a septum cap. This bottle, the sample tank, could be filled daily for a defined period with outlet medium by use of the stopcock mechanism to change the flow of liquid. To retrieve the sample, the needle could be carefully removed and inserted into a fresh sample tank, again via a septum cap.

### 2.7.3 PERFUSION SYSTEM OPERATION

The technique employed in § 2.5.5 to rapidly load microspheres within ambr15 vessels with cells was adapted for spinner flasks. 10 mL polyHIPE microspheres adsorbed with PEI were dispensed into a spinner flask within 20 mL medium. On day 3 of a passage, CHO-S IgG cells were centrifuged and resuspended in a reduced volume and a  $20 \times 10^6$  cellmL<sup>-1</sup> suspension prepared. This was filtered twice using a 20 µm cell strainer to eliminate any clumped cellular material. 20 mL, i.e. 400 million cells, was dispensed into the spinner flask and agitated gently by hand to mix cells and microspheres. The spinner flask was immediately placed upon a Micro-Stir plate and set to an intermittent agitation mode, whereby it would be operated at 25 rpm for 15 min, 0 rpm for 2 min and repeated. Every 30 min, i.e. after two start-stop cycles, the spinner flask was removed, agitated thoroughly by hand and a 1 mL sample taken. Microspheres were decanted and the viable cell density of the cell suspension, i.e. the cells that were not adhered, determined using a Vi-Cell XR Cell Viability Analyzer. This was carried out for 2 hr before microspheres were allowed to settle, and 20 mL medium aspirated. 20 mL fresh medium was added, the flask mixed and

---

the process repeated twice to dilute out cells that had not adhered to the microspheres. Finally, medium was added to a 100 mL total volume and modified caps, with inserted tubings, attached to the flask arms. Tubings were attached to the feed, sample and waste tanks within a laminar flow hood and all components set up within the incubator with tubings passed through the pump.

The pump was operated throughout at  $25 \mu\text{Lmin}^{-1}$ , the lowest flow rate possible, resulting in a dilution rate of approximately 0.38 vvd. Daily samples were taken, starting from the following day, day 1, until day 35. The incubator was set at 5 % (v/v)  $\text{CO}_2$ , and temperature varied between 30, 25 and 37 °C to demonstrate perfusion operation.

---

# Chapter 3

---

## ADHESION SUBSTRATES

---

### OVERVIEW

This chapter presents the results obtained at the beginning of the project, which generally centred around the search for an adsorbable 'sticky' substance, or adhesion substrate, to enable the reversible adherence of suspension-adapted CHO cells. It was expected an adhesion substrate would be a required and defining component of the in-house cell retention device, which itself would be used for the proposed continuous upstream system. The work here first identifies a range of adhesion substrates, and then discusses relevant testing on cell attachment, adherent growth and eventual dissociation using different commercial reagents. Finally, a surprisingly effective adhesion substrate, which is currently neglected in the literature, was selected to take forward. The effect of mild hypothermia, which would be employed later during continuous operation, was investigated for cells adhered to this substrate.

### 3.1 INTRODUCTION TO ADHESION SUBSTRATES

The overarching objective of the work presented here was the development and demonstration of a small-scale upstream continuous system for CHO cell line engineering. Such a set-up, essentially a cell culture rig operating in perfusion mode, first required an in-house cell retention device. It was decided from the beginning of the work to pursue cell adherence, i.e. attach cells to a surface, as a technically simple method of physical cell retention.

The first task was to identify, using literature sources, chemical reagents for use as adhesion substrates with suspension-adapted CHO cells. The requirement to continue to use cell lines normally cultured in suspension, as opposed to adherent cells, was to ensure suspension-adapted cell lines already in use in our laboratory could be used if any upstream system was indeed developed and successful. The ideal adhesion substrate would be; (i) capable of adhering suspension-adapted CHO cells, in this instance CHO-S and CHO-S IgG cell lines; (ii) effective at adhering these cell lines with continued use of CD CHO medium and without supplementation with animal-derived products such as FBS; (iii) able to allow adhered cells to dissociate, i.e. release cells back into suspension culture; (iv) itself chemically defined and animal origin-free; (v) inexpensive, and so scalable without significant cost, and (vi) adsorbable to common polymeric materials such as polystyrene. The capability of the adhesion substrate to rapidly adhere cells at a high

density, a concept termed as 'cell loading' in this work, was proposed later on.

Whilst initial work focused on adsorbing substrates to the wells of polystyrene multiwell plates for subsequent testing of CHO adhesion, the aim was for microspheres to be coated with the successful substrate, either by adsorption or covalent linkage, and be employed ultimately as the cell retention device. Due to the ill-defined nature of animal-derived products, as well as the associated high costs, it was decided not to use adhesion proteins, either within serum products or as isolated reagents, in the cell retention device. However, a selection of common animal-derived adhesion substrates have been tested alongside chemically defined substrates so as to compare their effectiveness.

The objectives of the work presented in this chapter were to; (i) identify a selection of adhesion substrates from the literature; (ii) test the effectiveness of these substrates at encouraging the initial attachment and subsequent adherent growth of suspension-adapted CHO cells; (iii) demonstrate the dissociation of CHO cells from these substrates with successful growth back in suspension culture, and (iv) begin to investigate the effects of mild hypothermia on CHO cells adhered to substrates.

### 3.1.1 IDENTIFICATION AND TESTING OF ADHESION SUBSTRATES

A selection of substances had to be identified, sourced and then screened to determine their effectiveness at adhering suspension-adapted CHO cells. It was known that dedicated substances, referred to here as adhesion substrates, are coated on to culture vessels prior to seeding to encourage initial cell attachment and subsequent spreading. Four animal-derived proteins; fibronectin, laminin, collagen and vitronectin, which are involved in the functioning of the extracellular matrix in *in vivo*, and three chemically defined cationic polymers; poly-D-lysine, poly-L-ornithine and polyethylenimine, were chosen as potential adhesion substrates. A range of coating concentrations were first tested for each substrate using 96-well plates, and from this, the optimal coating concentration taken forward for CHO growth comparisons. An optimal coating concentration was defined as one retaining the highest number of cells, when compared to the others. Micrographs were obtained to visualise the morphologies of adhered cells on the different substrates and finally, several substrates were used to evaluate their cell loading capabilities.

Figure 3.1 shows the percentage of cells adhered, or retained, in a coating concentration screen for each adhesion substrate. As PrestoBlue Cell Viability Reagent was adapted to quantify the amount of viable adherent cells, the relative fluorescence intensity data were normalised, and 100 % assigned to the highest fluorescence value to better show the adhesion effects of each concentration relative to the others. Each normalisation is specific

to the adhesion substrate, as comparing adherence capability between different substrates was not the aim of the experiment. Comparisons between substrates would be investigated after once optimal coating concentrations for each one were determined.

The adhesion effect of each of the substrates was apparent after overnight seeding, with a layer of cells visible on each well by eye when plates were held near a light source. It was surprising how easily suspension-adapted CHO cells could be made to adhere. The results obtained for each adhesion substrate shared a similar trend; the highest coating concentrations tested adhered the greatest number of cells, with a decrease seen as the concentrations were reduced. The highest two or three coating concentrations of all substrates retained similar cell numbers, suggesting a maximum coverage of substrate on wells may be occurring at these higher concentrations. An excess of substrate is likely dispensed upon the wells and is unable to be adsorbed due to surface 'saturation', and is later cleansed off during the washing step.

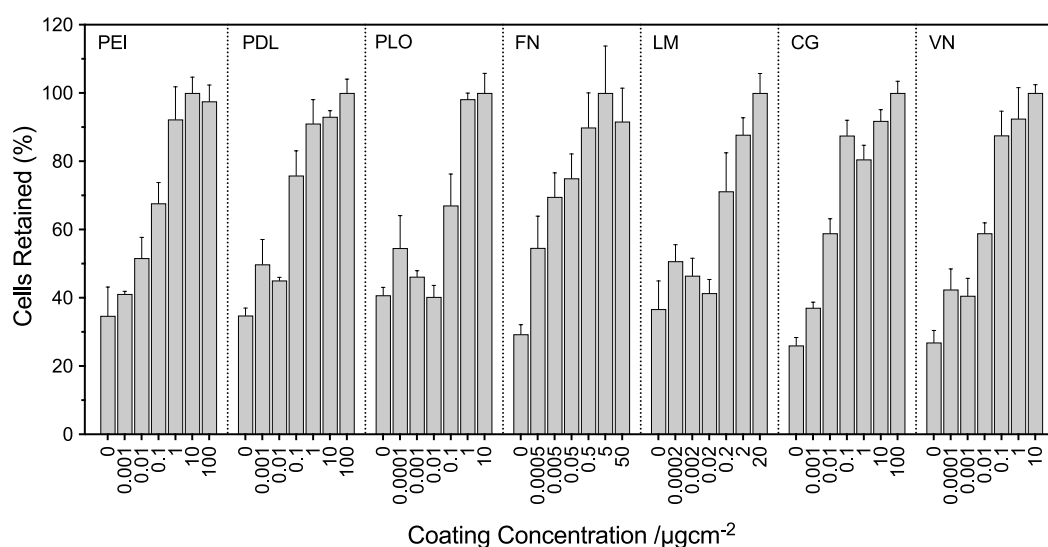


**FIGURE 3.1** Screen for optimal coating concentration for animal origin and chemically defined adhesion substrates. Adhesion substrates were adsorbed with a range of coating concentrations on Nunclon Delta 96-well plates, seeded with 20,000 CHO-S IgG cells and left to adhere overnight. The next day, unadhered and loosely adhered cells were washed off and a PrestoBlue assay performed to quantify the remaining adhered cells. All substrates revealed decreasing cell adherence as their coating concentrations were reduced. PEI, polyethylenimine; PDL, poly-D-lysine; PLO, poly-L-ornithine; FN, fibronectin; LM, laminin; CG, collagen; VN, vitronectin. Data represent mean  $\pm$  SD,  $n=3$  (biological triplicate).

At the lower concentrations tested, the cell adherence achieved when using polyethylenimine, poly-D-lysine, poly-L-ornithine and laminin was similar to that achieved by the uncoated wells, indicating an effective loss in their adhesion capability with these con-

centrations. This was most pronounced with poly-L-ornithine and laminin. Interestingly, fibronectin was the only substrate which did not have a dramatic reduction in cell adherence when its coating concentration was decreased, but gave a gradual downward trend in adherence capability. The effectiveness of fibronectin as an adhesion substrate was seen again in later experiments.

Uncoated wells, which were tissue culture-treated polystyrene surfaces (commercialised as Nunclon Delta polystyrene) without any adsorbed substrate, were also seeded with cells as negative controls. These uncoated wells repeatedly gave low, but still noticeable, fluorescence readings. It was thus clear that Nunclon Delta surfaces, despite not being enhanced with any substrate, was still capable of adhering suspension-adapted CHO cells even with the continued use of CD CHO medium. Nunclon Delta is a proprietary polystyrene material from Thermo Fisher Scientific, being treated so as to be more hydrophilic at its surface, and is available in both multiwell plates and T-flasks formats. The exact process by which Nunclon Delta is treated could be not found, though it is suspected plasma surface modification is performed on the polymerised materials post-fabrication. The technique of modifying the surfaces of polymers via plasma using numerous chemical species is well documented (Grace et al., 2003), and is discussed at the end of this section.

The adhesion substrates tested in this work can be divided into chemically defined (synthetic polymer) or animal origin (protein-based) substances. This categorisation also dictates their method of adhesion; all three chemically defined substrates rely upon electrostatic charge, provided by their amines upon protonation, to adhere cells. The four animal origin substrates rely upon ligand-receptor interaction to adhere cells. The former is crude adherence; the cells will adhere, at least initially, in any shape, whilst the latter is specific adherence, with cells forming particular morphologies as defined by these interactions.

The experiment presented here was performed to firstly ensure adsorption of these substances was possible on polystyrene and secondly to determine an effective coating concentration for each substrate to take forward for further investigations. The data were as expected; the adhering of CHO cells confirmed successful adsorption for all substrates, with the number adhering decreasing as the coating concentrations were reduced.

When the experiment was being planned, it was seen as important that only strongly adhered cells were counted in the assessment of each adhesion substrate, and so adherent cell layers were washed twice using PBS after overnight seeding and before every PB assay. This ensured both unadhered cells and loosely adhered cells were removed before quantification of the adherent layer was carried out. A successful substrate should be able to 'capture' cells and keep them retained over long periods, even when subjected to dynamic

environments, such as flowing medium in perfusion systems. The cells removed during washing were not quantified, as all culture medium was pooled and discarded, but it was evident from observation that cells were indeed physically removed by this step — particularly with substrates at the lower coating concentrations. An optical microscope was used to quickly observe the state of the adhered cells after seeding and again after this washing step. The uncoated wells and wells adsorbed with substrates at low concentrations did indeed show accumulated masses of suspended CHO cells after overnight seeding, which were subsequently removed by washing.

Substrates were themselves washed after adsorption due to their potential cytotoxicity, especially the cationic polymers. It was suggested any excess cationic polymer would simply be removed during this step, leaving only the adsorbed substrate, which appeared to be correct as no cell death was apparent when cells were visualised after seeding. Commercial protocols for poly-D-lysine and poly-L-ornithine confirmed coatings should be washed and air-dried after adsorption. The cytotoxicity from excess protein-based substrates could not be found in the literature, but it was seen as fair to also remove excess protein by washing, as was done for the cationic polymers. The extent of any cytotoxicity, either from unwashed or adsorbed substrate, was not explored in this work as it was always envisaged that the substrate eventually selected would be suitably washed prior to being used. However, reducing or even eliminating the number of washes performed on coated plate wells, before adding cells, could be a simple experiment to test any suspected cytotoxicity. The culture medium could be aspirated after a few days and a ViCell used to quantify any dead cells. Spiking cells in suspension culture with a concentrated dose of any of the substrates could also reveal any toxic effects.

The highest coating concentration used for each substrate was chosen partly after reviewing the literature, if available. The coating concentrations of all substrates did not need to match as the actual coating concentrations used were not being compared; rather, the optimal concentration specific to each substrate had to be determined. However, the coating concentrations employed were dictated by the initial concentration of the item supplied. For example, polyethylenimine was received as an undiluted gel, and was dissolved fully in water to give a master stock of  $100 \text{ mgmL}^{-1}$ , which was possible to then dilute to make the concentration needed to achieve  $100 \text{ } \mu\text{gcm}^{-2}$ . Poly-L-ornithine was supplied as a liquid at  $0.1 \text{ mgmL}^{-1}$  and so could only be prepared to coat at a maximum of  $10 \text{ } \mu\text{gcm}^{-2}$  and then diluted down.

The concentrations were serially diluted by a factor of 10 to ensure differences in cell adherence were observed. Early work performed with polyethylenimine, poly-D-lysine and

fibronectin used coatings with a much smaller concentration range, with the results showing little to no difference in their adherence capability (data not shown). It was suggested it was not possible to determine any consequential effects on cell adherence with such small ranges and the method was updated to reflect this. A total of six values for each substrate were chosen to simply obtain a satisfactory spread of data and to show an hypothesised gradual decrease in adhesion capability. It is proposed the only way to know the actual concentration of substrate adsorbed on a particular surface would be to save the washes and assay the substrates, i.e. determine the concentration of substrate in the wash not adsorbed, but this was not within the scope of the work here.

Once it was confirmed that all substrates were indeed capable of adhering cells, it was decided to further investigate cell retention at the following coating concentrations; polyethylenimine, 10; poly-D-lysine, 10; poly-L-ornithine, 10; fibronectin, 5; laminin, 2; collagen, 10 and vitronectin, 1  $\mu\text{gcm}^{-2}$ . These concentrations were chosen as they retained the highest number of cells for the particular substrate and appeared to coat wells with an excess of substrate, i.e. all wells were likely saturated. In addition, to explore the effect that the base material has on cell adherence, untreated polystyrene and untreated glass were also used alongside Nunclon Delta polystyrene surfaces.

Figure 3.2A shows the quantification of CHO-S IgG adherent cell growth on substrates adsorbed to both Nunclon Delta and untreated polystyrene 24-well plates. Untreated in this instance refers to polystyrene that has not been modified by the manufacture to increase the hydrophilicity of the surface. Days 4 and 7 were selected as time points to wash the cells and perform viability readings using PrestoBlue. In this instance, and in all subsequent PrestoBlue data presented in this work, raw fluorescence values were normalised to the medium blank as described in equation 2.2.

For untreated polystyrene plates, the cell growth achieved on days 4 and 7 was similar for all animal origin substrates. Comparing the chemically defined substrates, cell growth on polyethylenimine was higher than both poly-D-lysine and poly-L-ornithine at both time points. These findings were similar for the Nunclon Delta plates, in relation to how the substrates compared with each other. However, there was a marked difference in adherent growth between the two plate types when using poly-D-lysine and poly-L-ornithine. For these two substrates, growth achieved was higher on Nunclon Delta plates by day 7, suggesting the base material does indeed have an effect on adherence, but is specific to the substrate. Intriguingly, with poly-L-ornithine on both base materials there was little cell growth between days 4 and 7, and the adherent cell density achieved by day 7 was even lower than the uncoated wells. As expected, the cell growth with uncoated wells was

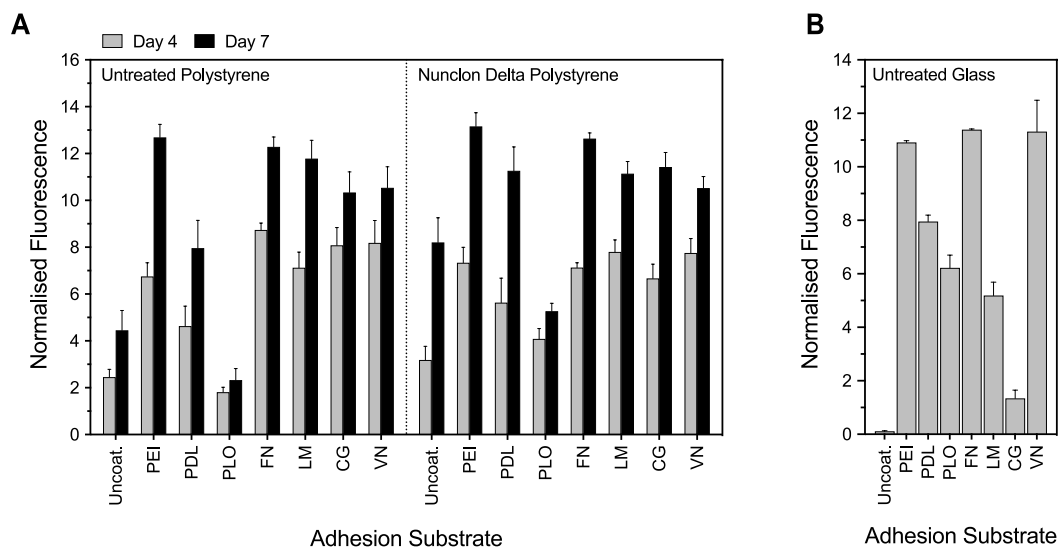


**FIGURE 3.2** Comparisons of adherent CHO cell growth using animal origin and chemically defined adhesion substrates on three base material types. Adhesion substrates were adsorbed on untreated 24-well plates, Nunclon Delta 24-well plates and untreated 8-well glass plates. 24-well plates were seeded with 100,500 CHO-S IgG cells, allowed to adhere overnight and (A) adherent growth quantified on days 4 and 7 using PrestoBlue. 8-well glass plates were seeded with 25,000 CHO-S IgG cells, allowed to adhere overnight and (B) adherent growth quantified on day 4. Uncoat., uncoated; PEI, polyethylenimine; PDL, poly-D-lysine; PLO, poly-L-ornithine; FN, fibronectin; LM, laminin; CG, collagen; VN, vitronectin. Data represent mean  $\pm$  SD,  $n=3$  (biological triplicate).

higher on day 7 when using Nunclon Delta plates rather than untreated plates. For both plate types on day 7, polyethylenimine substrates achieved comparable adherent densities to the four animal origin substrates and surpassed the two other cationic polymers.

Figure 3.2B shows the quantification of CHO-S IgG adherent cell growth on untreated glass plates, again using all adhesion substrates previously described. Day 4 was selected as the only time point to wash the cells and perform viability readings using PrestoBlue Cell Viability Reagent. The uncoated wells did not achieve any adherent cell growth, whilst polyethylenimine, along with fibronectin and vitronectin, achieved the highest adherent cell growth. Interestingly, collagen achieved the lowest cell growth out of all substrates.

This experiment differed to the initial coating screen in that adherent cell growth, and not just initial cell attachment, was investigated. This was to confirm if adhesion substrates could promote adherent cell spreading on the surfaces as cells grew, and thus achieve monolayer confluency. It must be remembered a suspension-adapted CHO cell line was used here, but it grew remarkably well in adherent culture. Despite PrestoBlue being primarily intended for plate-based suspension culture, its adaption in this work for the quantification of adherent cells proved successful. The technique of aspirating mid-culture

medium, giving the adherent cells two washes and then dispensing the PrestoBlue-media mix was sufficient to assay adherent cell density, with a wash after ensuring no reacted mix was left for the remainder of the culture. This showed the benefit of effective cell retention is indeed the ability to replenish medium without cell loss, provided effective adhesion substrates are used.

The choice of days 4 and 7 as assay points was partly based on the observation that, in early validation work, cells reached near total confluency around day 4 (data not shown), and a medium change at this time seemed appropriate. It was also to observe if substrates kept cells adhered or if they desorbed off the well surfaces after extended periods. On untreated and Nunclon Delta polystyrene plates, all substrates except poly-L-ornithine yielded confluent cell layers around day 4, with cells either beginning to peel off by day 7 or growing in clumped masses upon the monolayers. It was unclear if cell peeling was due to an accumulation of toxic metabolites or if adhesion substrates were beginning to fail. The clumped masses observed was especially prominent with polyethylenimine and poly-D-lysine, where 'bunched up' cells scattered about the adherent layer were visible towards the end of the experiment. When viewed under a microscope, gently agitating the plates would cause these masses to wobble, yet they remained attached to the monolayer beneath, presumably by linkages with a few adhered cells. It appears these cells, despite being suspension-adapted, acted adherently and grew alongside each other if the environment was suitable. This persistent growth, even when 100 % confluency was achieved, is likely attributed to the immortalised nature of CHO cells, which perhaps do not experience contact inhibition and cease further growth when 100 % confluency is reached. It was suggested that cell peeling can, in some cases, actually be caused by rapid growth. This would lead to full confluency being reached with subsequent cell detachment. However, this was not the case here as cells were visibly inspected using a microscope each day during the culture. There was no indication of rapid growth for cells seeded on any of the substrates that were eventually determined to be the least effective.

Visual evidence of the adhesion effect of these substrates was also apparent if, prior to cell seeding, cells were not filtered using a 20 µm cell strainer, as any cell clumps in the prepared seed would eventually adhere and move, partially attached to the well surface, when the plate was agitated. Whilst intriguing to observe, this was not what was desired and cell straining was found to be crucial for every experiment if a monolayer was needed. Unwanted cell detachment, which was seen mainly with the uncoated surfaces and those adsorbed with poly-L-ornithine, resulted in accumulated cell suspension near the centre of the wells. This effect of cells accumulating at the centre was also noticeable immediately after seeding, which was why agitating the plates thoroughly by hand was essential to

ensuring cells were evenly spread before settling and adhering.

The weak performance of poly-L-ornithine with the untreated plates was surprising, especially as it did not occur to the same extent when using untreated glass wells. For the untreated plates, it may be due to the coating buffer employed. BBS, at around pH 8.5, is frequently used for adsorbing polylysine substrates (Kam et al., 2001; Kojima et al., 2016), and so was repeated here and for the two other cationic polymers. This was to make the final coating solutions have a pH at or close to the isoelectric points, which for polylysine is around pH 9 (Chheda et al., 2015), and is assumed to be similar for polyethylenimine and poly-L-ornithine. At their specific isoelectric points, these cationic polymers will have a net charge, and so will adsorb via hydrophobic interactions, and not by charge, to polystyrene surfaces. At neutral pH, i.e. below the isoelectric point, they will gain a positive charge (due to their amines) and consequently attract and adhere cells.

However, poly-L-ornithine was supplied in water and the coating concentration used for this experiment did not require considerable dilution with borate buffer, meaning its pH was likely closer to neutral. It is not known whether poly-L-ornithine subsequently failed to adsorb sufficiently, desorbed during the experiment, or if cells dissociated from the substrate due to weak adherence. It may be a combination of all three. It is likely, however, that both the coated substrate and the base material contributed to the overall adherence capability of the wells, but this was only observed for weaker substrates, such as poly-D-lysine and poly-L-ornithine.

Even though glass microspheres as a cell retention device was never proposed, a decision was made to also investigate the coating of substrates onto untreated glass plates. A successful adhesion substrate should be capable of adsorbing to any material, polymeric or otherwise, and consequently encourage the adherent growth of cells to that material. Uncoated glass wells yielding no adherent cell growth was expected; the extreme hydrophobicity of these surfaces meant seeding cell suspension resulted in a droplet forming with a high contact angle, which was then difficult to spread via agitating by hand. The cells did not seed, and were removed during the wash step. For glass wells that were adsorbed with substrate, droplet formation did not occur, with the coated wells ensuring some degree of hydrophilicity and encouraging adherent seeding and cell spreading. The use of glass wells demonstrated the effect substrates can have on the surface properties of a base material.

A similar study on the adhesion effects of extracellular matrix proteins and cationic polymers has been carried out (Chen et al., 2008). The authors cultured adherent rat islet cells on polystyrene plates adsorbed with laminin, fibronectin, vitronectin, three types of colla-

gen, poly-L-lysine and interestingly, polyallylamine, using both serum-free medium and medium supplemented with FBS. Results obtained, in this instance, revealed laminin to be the best performer in terms of adhesion after 4 hr without serum. It was seen that successful cell adhesion did not necessarily result in successful cell spreading, with certain substrates and conditions causing adherent cells to aggregate as they grew. Quantification of adhered cells was determined using a metabolic assay similar to PrestoBlue, though the authors did not appear to wash adhered cells before assaying.

The success of polyethylenimine as an adhesion substrate, as demonstrated in this work, should not be understated, with its effectiveness being a very positive outcome which influenced the remainder of the project. First demonstrated in the mid 1990s as an inexpensive method to introduce DNA into cells (Boussif et al., 1995), polyethylenimine is now known within the biopharmaceutical industry primarily as an inexpensive transfection reagent, with its beneficial effects on cell adhesion not generally known or widely reported. Polyethylenimine performed as well as all animal origin substrates, despite being a fraction of their cost, both in terms of bulk price and price per plate coating (see Table 3.1, which lists the costs of the adhesion substrates used).

TABLE 3.1 Cost comparison of all adhesion substrates used.

Adhesion Substrate	Cost (£) /mg <sup>*</sup>	Cost (£) /96-well plate <sup>†</sup>
Polyethylenimine	0.0012008	0.00037
Poly-D-lysine	15.12	1.48
Poly-L-ornithine	9.34	2.70
Fibronectin	160	23.04
Laminin	195	11.23
Collagen	7.15	2.06
Vitronectin	1320	38.02

<sup>\*</sup> Calculated using online prices from the suppliers used, July 2020.

<sup>†</sup> If all wells of a 96-well plate were adsorbed using optimal coating concentrations.

Polyethylenimine was also comparable to, if not surpassed, poly-D-lysine and poly-L-ornithine substrates, but again was considerably cheaper. Polyethylenimine is chemically defined, industrially produced, animal origin-free and readily available to purchase from multiple suppliers. Its exceptionally low cost means its application as a substrate is scalable — coating microspheres in animal origin substrates, or even chemically defined poly-D-lysine, would not be feasible if performed repeatedly and in large volume. Polyethylenimine is also more practical for the user; every other substrate had to

be aliquoted and frozen, as advised by supplier instructions. For the entire four year period of the work presented here, polyethylenimine was stored in a glass bottle at room temperature and exposed to ambient light, and suffered no noticeable reduction in its effectiveness to encourage cell adhesion. This meant it was available to coat materials rapidly on demand; in contrast, the protein-based substrates had to be thawed at 4 °C for several hours to ensure no loss in their activity.

Only two reports of polyethylenimine employed as an adhesion substrate could be found in the literature. Vancha et al. (2004) adsorbed polyethylenimine onto polystyrene plates to compare with polylysine and collagen, and used them as substrates for the culture of adherent HEK-293, PC-12 and MYS cells. They observed, as is the case here, the favourable adhesion seen with polyethylenimine coatings. However, the authors continued to supplement their media with FBS, and for PC-12 cells, horse serum was also used, both of which may contribute to the observed adherence due to the presence of extracellular matrix proteins. Whilst the topic of the article was indeed the beneficial effects of polyethylenimine in facilitating adhesion, the authors did not appear to appreciate the advantages gained when using this polymer, especially in regards to its low cost and scalability. Its effectiveness without serum was also not explored. A second study tested a range of adhesion substrates, including polyethylenimine, with primary human Schwann cells (Vleggeert-Lankamp et al., 2004). Although all substrates gave similar results with respect to initial attachment, the authors observed low proliferation rates and even eventual death of cells adhered to polyethylenimine. The paper was concluded with the authors saying they would not recommend polyethylenimine as an adhesion substrate for Schwann cells. Once again sera was added to the medium.

Figure 3.3 shows the morphologies of adhered CHO cells after overnight seeding onto untreated polystyrene plates adsorbed with all substrates. The cell adhesion seen with polyethylenimine, poly-D-lysine and poly-L-ornithine substrates revealed 'splattered' cells upon the surfaces, i.e. cells appeared to adhere in the exact shape in which they made contact and were 'captured' by the positive charge of the substrates. Evidence of cells being stretched at different contact points, or interactions, can also be seen (marked by the white arrows). For fibronectin, laminin, collagen and vitronectin, adhered cells formed 'classic', neat adherent morphologies. This was most pronounced with fibronectin and vitronectin, with cells elongating in an orderly fashion to form the beginning of a monolayer. For the uncoated wells, the cells that did adhere formed spherical shapes, with some interaction seen between cells and the surfaces.

Untreated polystyrene was selected to ensure only the substrate would dictate the mor-

---

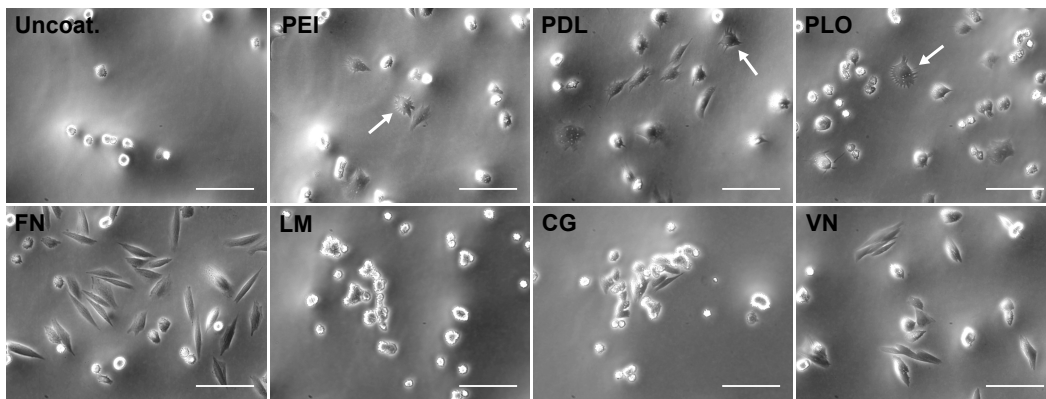


**FIGURE 3.3** Micrographs of adhered CHO cells after overnight seeding using animal origin and chemically defined adhesion substrates. Adhesion substrates were adsorbed on untreated 24-well plates, seeded with 100,500 CHO-S IgG cells and left to adhere overnight in an incubator. The next day, wells were washed and adhered cells fixed, before imaging with a phase contrast microscope at 20× magnification. Cationic polymers showed crude adherence, with cells showing stretched morphologies at locations where membranes are attracted to the substrate (white arrows). FN, CG and VN showed elongated morphologies, typical of adherent cells, whilst LM showed multiple contact points. Uncoat., uncoated; PEI, polyethylenimine; PDL, poly-D-lysine; PLO, poly-L-ornithine; FN, fibronectin; LM, laminin; CG, collagen; VN, vitronectin. Scale bars = 100  $\mu\text{m}$ .

phologies of the adhered cells, although similar morphologies were also seen when using Nunclon Delta plates. The defining difference observed between chemically defined and animal origin substrates was the time taken for cells to acquire the adherent morphologies observed. For the cationic polymers, it was upon contact during seeding, i.e. less than a minute after the cell suspension was dispensed onto the surfaces of the wells.

This rapid adhesion contrasted with the protein-based substrates which, despite appearing to adhere within an hour, did not take the typical morphologies as seen in Fig. 3.3 until several hours had passed. It was not known if, during the time before the elongated morphologies formed, the adherence of the cells on protein-based substrates was weaker than those cells adhered on the cationic polymer substrates. However, the crude adhesion seen with the chemically defined polymers was regarded as highly beneficial for the bespoke cell retention device, where rapid cell retention, or indeed cell capture, was required.

Xue et al. (1997) have performed experiments relevant to the work here; human cancer cells were adhered to coverslips, adsorbed with poly-L-lysine, fibronectin, laminin and vitronectin substrates, for the study of integrin interactions. The authors imaged the adherent cells and stained for various integrins, observing elongated morphologies of cells attached to the animal origin substrates, as is the case here, with the presence of integrin interactions observed. Cells adhered to poly-L-lysine, which was employed as a negative control in their work, formed spherical shapes and had no obvious stained integrin patterns.

To explore the maximum adherence capability of the substrates tested here, polyethylenimine, poly-D-lysine and fibronectin were adsorbed onto Nunclon Delta plates and seeded with suspensions of increasing cell density. CHO-S, a non-producing suspension-adapted CHO cell line and HEK-293, a suspension-adapted HEK cell line, were investigated alongside CHO-S IgG cells.

Figure 3.4 shows the normalised fluorescence obtained for each substrate at each of the cell suspensions seeded. The trends seen for the three substrates were similar for both CHO-S and CHO-S IgG cells, with each substrate retaining a higher number of cells with every increase in cell density. However, fibronectin was the weakest performer and from 0.5 million cells onwards did not retain as many cells as either polyethylenimine or poly-D-lysine.

Compared to wells coated with substrates, uncoated wells adhered far fewer cells, with much smaller increases in cell retainment observed despite the increase in cell loads. However, these findings were not shared with the adherence of HEK-293 cells. Uncoated wells did retain HEK-293 cells, at similar cell numbers to that seen with all other substrates until

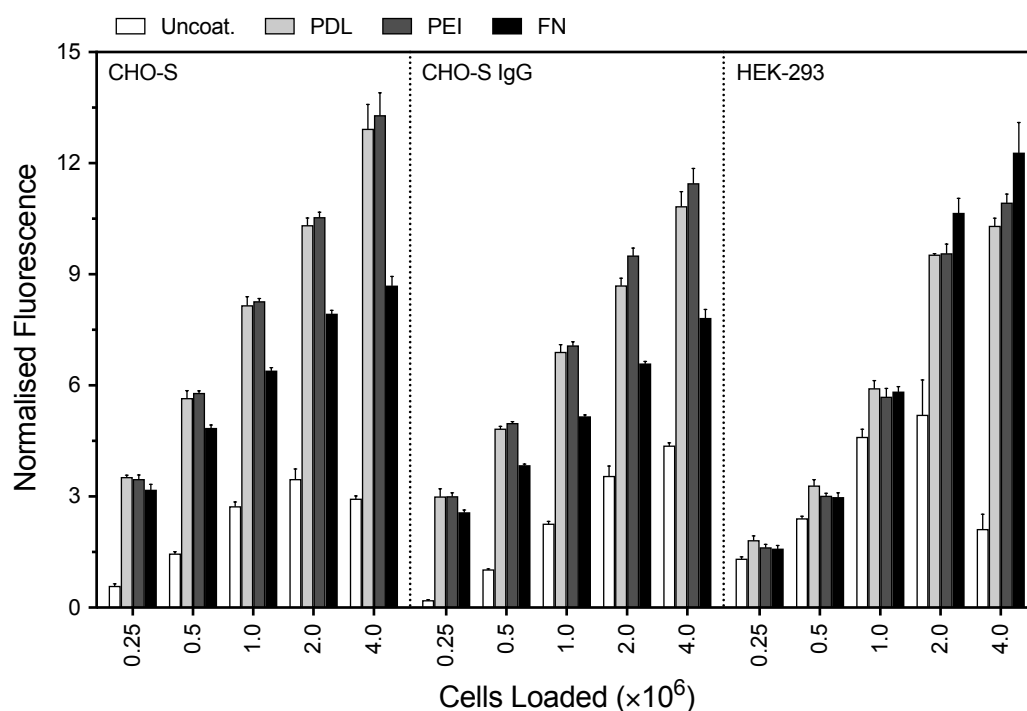


FIGURE 3.4 Comparisons of cell loading capability, for CHO and HEK cell lines, using polyethylenimine, poly-D-lysine and fibronectin substrates. Adhesion substrates were adsorbed on Nunclon Delta 24-well plates, seeded with either CHO-S, CHO-S IgG or HEK-293 cells at 0.25, 0.5, 1, 2 and 4 million cells, and left to adhere for 1 hr in an incubator. Wells were washed and PrestoBlue used to quantify the remaining adhered cells. Uncoat., uncoated; PDL, poly-D-lysine; PEI, polyethylenimine; FN, fibronectin. Data represent mean  $\pm$  SD,  $n=3$  (biological triplicate).

1 million cells were seeded, and then experienced a drop in cell retention with 4 million cells. Interestingly, fibronectin performed as well as the two cationic polymers at all loading densities.

The experiment performed was an initial test into the loading of cells onto substrates, i.e. seeding cells at a high density and retaining them rapidly on a substrate. The rationale behind this was the bespoke cell retention device would likewise be rapidly loaded with cells for immediate use within a continuous upstream process. The use of a second CHO cell line was to test if other suspension-adapted CHO cells would also adhere to polyethylenimine. The poor performance of the uncoated wells was expected, with most cells not seeding after 1 hr and instead removed during the wash step. The best performers for both cell lines, polyethylenimine or poly-D-lysine, was again as expected. Their crude adherence ensured cells were captured upon contact. With loading densities above 1 million cells, it was apparent how rapid cell adherence was a few seconds after dispensing the cell loads onto the wells, with a hazy layer of adherent cells immediately visible by eye. Tilting the plates slightly, so as to move medium aside, would reveal these cell layers.

An hour seeding time was suitable for these cationic polymers, but not for fibronectin. It is suggested, as was noted earlier, that adherence is indeed weak for fibronectin before cells have had sufficient time to interact with the protein and form their elongated morphologies. The results may have been different if the seeding time was increased beyond 3 hr, although overnight seeding was not considered here due to the possibility of cell growth and would not be suitable for the ultimate purpose of the cell retention device.

The HEK cells used were suspension-adapted, and are routinely employed in suspension using shaking roller bottles; however, their behaviour in adherent culture was markedly different to that of CHO cells. They rapidly adhered to all substrates, including uncoated wells, with the 'spidery' morphologies typically seen with adherent HEK cultures. The decrease in fluorescence with uncoated wells, seen when 4 million cells were loaded, was due to a significant layer of HEK cells peeling off together during the wash step; cells appeared to interact with both themselves and the substrate, causing an accumulated loss when a section of the cell layer detached.

The improved performance of fibronectin observed with HEK may be due to quicker interaction with the protein-based substrate, or these HEK cells may simply be less adapted to suspension than the two CHO cell lines and more capable of 'returning' to an adherent state. It was also suggested any difference in specific integrins between the two CHO cell lines and the HEK cells may have also contributed to the differences observed in these data.

*Substrates & Base Materials*

It must be stressed only CD CHO media, i.e. chemically defined, animal origin-free and without serum supplementation, was used for these experiments. These data thus show the capability of each substrate to adhere and retain suspension-adapted CHO cells independently of any undefined sera products. This contrasts with typically reported adherent culture experiments, where FBS is almost always supplemented into the medium, mainly due to the extensive — but poorly understood — benefits on cell culture, but also in part due to the presence of adhesion-promoting proteins.

For the biologics industry, chemically defined processes are becoming the presumed standard. Whilst the protein-based substrates employed here were isolated products, and not contained within serum, they nevertheless are animal-derived and as a consequence remain undefined, prone to variability and are expensive. The range of polylysines available has been an option to those wishing to employ chemically defined adhesion, but the high cost may prohibit their use when the coating of increased surface areas, such as with microcarriers, is required. Table 3.2 shows the cost (£) /mg for polyethylenimine products, whilst Table 3.3 shows the cost of polylysine products, both using prices from two online suppliers. The difference in price is immediately apparent, regardless of the specific product type, and whilst this information may seem excessive, it further illustrates the importance of the key finding presented here; namely, the effectiveness, yet considerable low cost, of polyethylenimine substrates.

These two tables also reveal the chemical differences between product types of the same substrate. Polyethylenimine is available as either a linear or branched polymer; the former having a single straight chain, and the latter having multiple branched chains. Polylysine, being derived from lysine, a chiral compound, is available as either D or L enantiomers. Polyethylenimine and polylysine are sold in varying molecular weight ranges; the molecular weight of a polymer defines the average length of the chains, with higher molecular weight indicating larger polymers. The differences in cost between the two polymers arise due to their different production processes. For polylysines, L-Lysine is first produced from microbial fermentation (Shukla et al., 2012), with the D enantiomorph subsequently made using this L form via an enzymatic process (Wang et al., 2016). Both enantiomers are subsequently polymerised to form the particular polylysine. In contrast, no bio-based processes are employed for the production of polyethylenimines. Instead, the polymerisation of aziridine (itself produced from aminoethanol) gives rise to the branched and linear forms of the polymer (Gleede et al., 2019), depending upon specific reaction conditions. This total chemical synthesis may explain the low cost of polyethylenimines.

TABLE 3.2 Costs of available polyethylenimines from Polysciences US, with their structures, molecular weights and compositions listed. Ordered by increasing molecular weight.

Structure*	Molecular Weight	Composition	Cost (£) <sup>†</sup> /mg
Branched	600	Gel	0.00070
Branched	1,200	Gel	0.00092
Branched	2,000	Gel	0.00051
Linear	2,500	Solid	0.050
Linear	4,000	Solid	0.039
Branched	10,000	Gel	0.0012
Branched	10,000	Solution, 30 %	0.0042
Branched	70,000	Solution, 30 %	0.0046
Branched	70,000	Solution, 50 %	0.0022
Linear	100,000	Solid	0.022
Linear	160,000	Solid	0.019
Linear	250,000	Solid	0.048
Branched	750,000	Solution, 33 %	0.0016

\* 'Transfection grade' polyethylenimine products were not included.

<sup>†</sup> Calculated using prices found online, July 2020. \$1 = £0.79 conversion used.

In this work, poly-D-lysine, and not the L enantiomorph, was selected for testing as concern was raised with the possibility that enzymes could digest the naturally occurring L enantiomorph, causing the substrate to potentially fail mid-culture. However, poly-L-lysine has been employed successful as a substrate in cell culture elsewhere (Khademhosseini et al., 2004). Polyethylenimine is not chiral, and the branched, molecular weight 10,000 type was chosen as it was the largest, branched version available as a bulk gel, and not already dissolved in water. This meant it could be diluted down to a desired coating concentration. The extent to which linear or branched and average molecular weight affects adherence capability was not explored in this work, but it was generally assumed that higher molecular weight, branched cationic polymers provided more attachment sites for cells than smaller, linear ones. It is proposed this is simply due to the increased presence of amines. Interestingly, all commercial polylysines that could be found were linear polymer types, but the synthesis of a branched version of poly-L-lysine has been reported (Rodríguez-Hernández et al., 2003).

The four protein-based substrates were investigated to provide benchmarks for comparison with the three cationic polymers. It was predicted each of these proteins would be

effective at adhering CHO cells and this was indeed the case, at least when adsorbing to polystyrene base materials. However, their animal origins and high cost meant they were not suitable in the development of the bespoke cell retention device. Recombinant versions of fibronectin, laminin, collagen and vitronectin do exist — and so satisfy the animal origin-free criterion — but are even more expensive and so cannot be considered in this work.

TABLE 3.3 Costs of available polylysines from Sigma-Aldrich UK, with their structures, molecular weights and compositions listed. Ordered by increasing molecular weight.

Enantiomorph	Molecular Weight	Composition	Cost (£)* /mg
Poly-D-lysine	30,000–70,000	Powder	15
Poly-L-lysine	30,000–70,000	Powder	12
Poly-L-lysine	70,000–150,000	Solution	21
Poly-D-lysine	70,000–150,000	Powder	15
Poly-L-lysine	70,000–150,000	Powder	15
Poly-L-lysine	150,000–300,000	Solution	19
Poly-L-lysine	≥300,000	Powder	14
Poly-D-lysine	>300,000	Powder	15

\* Calculated using prices found online, July 2020. \$1 = £0.79 conversion used.

Finally, the choice of base material, such as polystyrene, glass or indeed some specially-modified version, is an important consideration for the culture of adherent cell in this work. This is because of the added effects of adhesion caused by the underlying material upon which any substrate is coated. Observing the cell growth achieved on the uncoated wells of untreated polystyrene, Nunclon Delta polystyrene and untreated glass materials demonstrated these effects in the work here. Many suppliers have online guides showcasing a range of surface types for their multiwell plates. These detail the unique chemistries available, with each often tailored to specific applications. A study of different polystyrene culture surfaces has been carried out (Zeiger et al., 2013) using seven commercial surface types, including Nunclon Delta, and assessed surface topography, wettability, protein adsorption and adherent cell behaviour. Protein adsorption, tested using albumin and collagen, did not vary between types suggesting protein-based substrates could be adsorbed to any polystyrene material with ease. Surface roughness varied between each surface, with faster population doubling for those surfaces with greater roughness. This finding, which the authors note is widely shared in the literature, highlights how the base material, regardless of coating, may itself affect cell adherence growth.

The base material ultimately employed for an adherence-based cell retention device in a continuous system would likewise, as stated above, be important. If this device was made up of high surface area structures, such as microspheres, and the base material of these structures was hydrophobic, then aggregation of the materials may eventually occur in aqueous solution. The base material is thus important, along with the coating used to encourage adherence. The choice of base material is discussed in greater depth in Chapter 5.

Lerman et al. (2018) provides a history of polystyrene as a cell culture material, and discusses the methods employed to overcome the hydrophobic surfaces of untreated polystyrene surfaces which, as mentioned earlier, primarily involves plasma modification. As discussed, Nunclon Delta materials are a commercial type of surface-modified polystyrene, which is likely fabricated via the creation of oxygen species, such as carbonyl, carboxylic and lone oxygen groups, on the polystyrene surface using plasma treatment. These altered chemistries consequently increase the wettability of the surface and promote cell adhesion and spreading; indeed, plasma modification has even been used to render polystyrene microspheres hydrophilic for cell culture purposes (Arifin et al., 2016). The choice of gas used in plasma treatment dictates the specific chemical species created, although ambient air, with its oxygen content, can be used.

Lerman et al. (2018) also mentions the possible effects on the adsorption of substrates on treated surfaces. Adsorption occurs via hydrophobic or ionic interactions; untreated polystyrene should thus readily adsorb substances via hydrophobic interaction, provided a suitable coating buffer is used, and treated polystyrene should adsorb via both hydrophobic and ionic interactions — if compatible ionic groups are present. The top performers presented here, polyethylenimine and the four protein-based substrates, showed no observable difference between the two polystyrene types, suggesting either their high effectiveness at adsorption or at cell adhesion, or both.

### 3.1.2 ADHESION ASSAYS

Once polyethylenimine was demonstrated to be an effective adhesion substrate with rapid cell loading capability, it was decided to investigate and compare four cell adhesion assays. Dissociation by trypsin exposure is a direct measure to assay cell adhesion, with the unadhered cells quantified using the familiar trypan blue exclusion method. PrestoBlue, already employed in previous experiments, was adapted for adherent culture and exploits the metabolism of cells as an indirect measure of cell adhesion. Finally, crystal violet and neutral red dyes were employed as cell stains, with the removal of the stains quantified to give, once again, indirect measures of adhered cells.

Cells, at either 0.0625, 0.125, 0.25, 0.5, 1.0, 2.0 or 4.0 million, were loaded onto polyethylenimine substrates within 24-well plates. Figure 3.5A shows the four adhesion assays performed on these cells after 3 hr. For dissociation, as direct cell counts were taken, the number of cells adhered could be directly compared to the cells loaded. As can be observed for the lowest five seeding densities, the relationship between the two gave a straight line, with actual cells adhered being slightly lower for the 0.5 and  $1.0 \times 10^6$  loads. The number of cells adhered is considerable lower for the higher 2.0 and  $4.0 \times 10^6$  loads, with a plateauing observed, indicating a maximum coverage of cells was eventually met.

The values from the actual cells adhered, as determined from the dissociation experiment, were used on the  $x$ -axis for PrestoBlue, crystal violet and neutral red as the cells actually adhered. Their results were plotted against them, using simple linear regression, to yield standard curves. From this, it could be seen how suitable each of the assays were in measuring adherent cells. All three indirect measures gave  $R^2$  values above 0.90, indicating a good fit, and all correctly gave close readings for the final two seeding densities, i.e. the 2.0 and  $4.0 \times 10^6$  loads, where substrate coverage was similar. However, the error bars calculated for crystal violet and neutral red were larger than PrestoBlue, and the third highest seeding density was similar to the highest two when using neutral red.

To demonstrate the use of these assays, an adherent cell culture was carried out using polyethylenimine, poly-D-lysine, poly-L-ornithine and fibronectin substrates. Figure 3.5B shows the results from each of these assays on day 4 of the culture. Dissociation, which gives an accurate measure of cell adhesion, gave similar results to those shown in Fig. 3.2, i.e. the uncoated wells achieved similar adherent growth to poly-L-ornithine, with polyethylenimine and fibronectin giving the highest growth. The pattern in these results, in respect to how each of substrates relate to one other, was similar for the three other assays.

The reasoning behind testing dissociation initially, before the creation of these adhesion assay standard curves, was to acquire data of actual cell adherence for each of the seeding densities. As noted, the use of trypsin to enzymatically remove the cells remains the only direct measure of cells adhered — provided, of course, cells are washed beforehand to remove unbound cells or loosely adhered cells. Using these data, standard curves can then be generated using the assay data for each of the other assays.

The plateauing of the curve, observed with dissociation, was interesting and showed the limits to cell loading on particular surfaces, such as multiwell plates. The seeding time was limited to 3 hr, but it was visually apparent the entire surface was adhered with cells after this period, and so was regarded as a sufficient time for attachment to polyethylenimine substrates. This was the first experiment in which the dissociation of cells adhered

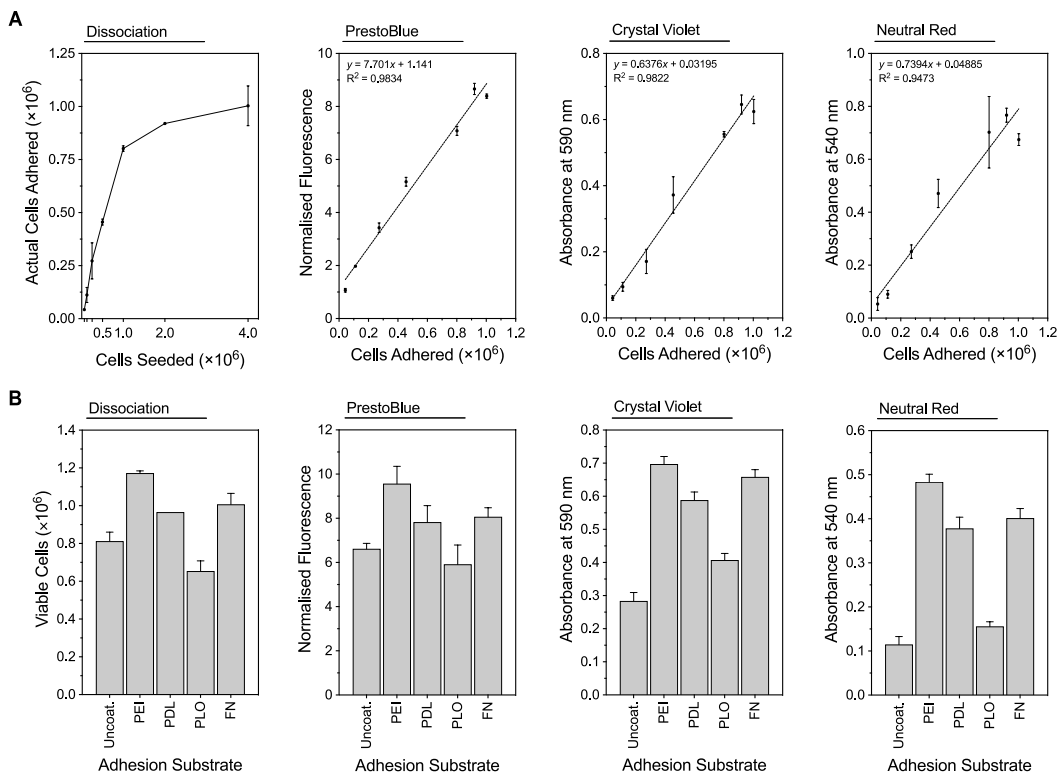


**FIGURE 3.5** Standard curves for CHO cells adhered to polyethylenimine substrates using dissociation, PrestoBlue, crystal violet and neutral red assays. PEI was adsorbed on Nunclon Delta 24-well plates, seeded with 0.0625, 0.125, 0.25, 0.5, 1.0, 2.0 and 4.0 million CHO-S IgG cells, and left to adhere for 3 hr in an incubator. Wells were washed and adhered cells quantified by either (A) dissociation by trypsin exposure, PrestoBlue, crystal violet or neutral red assays. In a subsequent experiment (B), cells seeded adherently to FN, PDL, PLO or PEI substrates were quantified on day 4 post-seed using these same four adhesion assays. PrestoBlue, crystal violet and neutral red standard curves were plotted using the actual cells adhered, as determined from the trypsinisation assay. Uncoat., uncoated; PEI, polyethylenimine; PDL, poly-D-lysine; PLO, poly-L-ornithine; FN, fibronectin. Data represent mean  $\pm$  SD,  $n=3$  (biological triplicate).

to polyethylenimine was attempted, and the next section of results presented here will discuss this in further detail.

The standard curve for PrestoBlue gave the smallest error bars for each reading, and the highest  $R^2$  value out of the three assays tested.  $R^2$ , denoting the coefficient of determination, describes the proportion of the variance in the dependent variable, in this case normalised fluorescence, that is predictable from the independent variable, in this case cells adhered. Or more simply, it measures how well the standard curve, or regression line, fits the data points. A high  $R^2$  indicates a good fit, and predictions in data can be confidently made. This was expected; PrestoBlue is a commercial reagent and its adaption to adherent cell culture was not too far removed from its original application, with viability still being measured via the metabolic activity of cells. The standard curve here demonstrated that

lower fluorescence data does correlate with low cell viability, and higher data with higher cell viability.

The practicality of PrestoBlue is apparent when recognising, for adherent cultures, it is effectively a mid-point assay, i.e. it is not destructive on the cells and can be easily washed off after a measurement, with the culture then resumed, as was the case in the earlier experiments. Commercial literature advertises PrestoBlue as non-cytotoxic, and this was found to be the case here as far as could be seen. Crystal violet and neutral red staining are, of course, end-point assays; the methods are destructive on the cells and the experiment effectively terminates at the point of measurement. However, both are inexpensive and can be performed without the need for aseptic technique.

Crystal violet was chosen as a potential assay after earlier work carried out used it for cell visualisation purposes. It was later realised the stain could be resolubilised from fixed cells and quantified. Crystal violet is more widely known as the primary dye used in the classification of bacteria as either Gram-negative or Gram-positive, depending upon the composition of their cell wall (Beveridge, 2001). Gram-positive bacteria have a thick layer of peptidoglycan in their cell walls, thus retaining crystal violet stains, whilst Gram-negative have a thinner layer and so easily lose the stain upon washing. The process makes the two types easier to visualise when using an optical microscope. Crystal violet has also been used to stain the nuclei of mammalian cells, including CHO cultures; this being the principle behind the popular nuclei counting method for determining the number of cells adhered to microcarriers (Tharmalingam et al., 2011). In the work presented here, however, crystal violet was used as a crude, general stain; the intention was that any dye taken up, regardless of specific location within the cells, would later be extracted via a lysing solution and quantified spectrophotometrically. The more dye ultimately retrieved, the more adhered cells present in the culture.

The crystal violet solution was prepared using methanol, which acted as both a fixative and a permeabilisation agent, and so ensured cells would take up crystal violet dye and not be washed away afterwards. Cells indeed did readily stain when incubated with crystal violet, with staining saturation appearing to occur after 10 min. The wash step afterwards was found to be critical in ensuring excess dye was removed, and submerging rigorously and repeatedly into a large beaker of fresh water did not seem to affect either the cell stains or the adherence of the stained cells themselves. The  $R^2$  value almost matched that of PrestoBlue, but the error bars were larger, which was not surprising considering the technique relies upon the quantification of an extracted stain, and involves more experimental steps until a measurement is eventually made.

Figure 3.6 shows the stains of the standard curves for both the crystal violet and neutral red assays. For the 2.0 and 4.0  $\times 10^6$  cell loads, it can be seen a maximum coverage of cells has occurred on the wells, with both loads giving near 100 % stained surfaces.

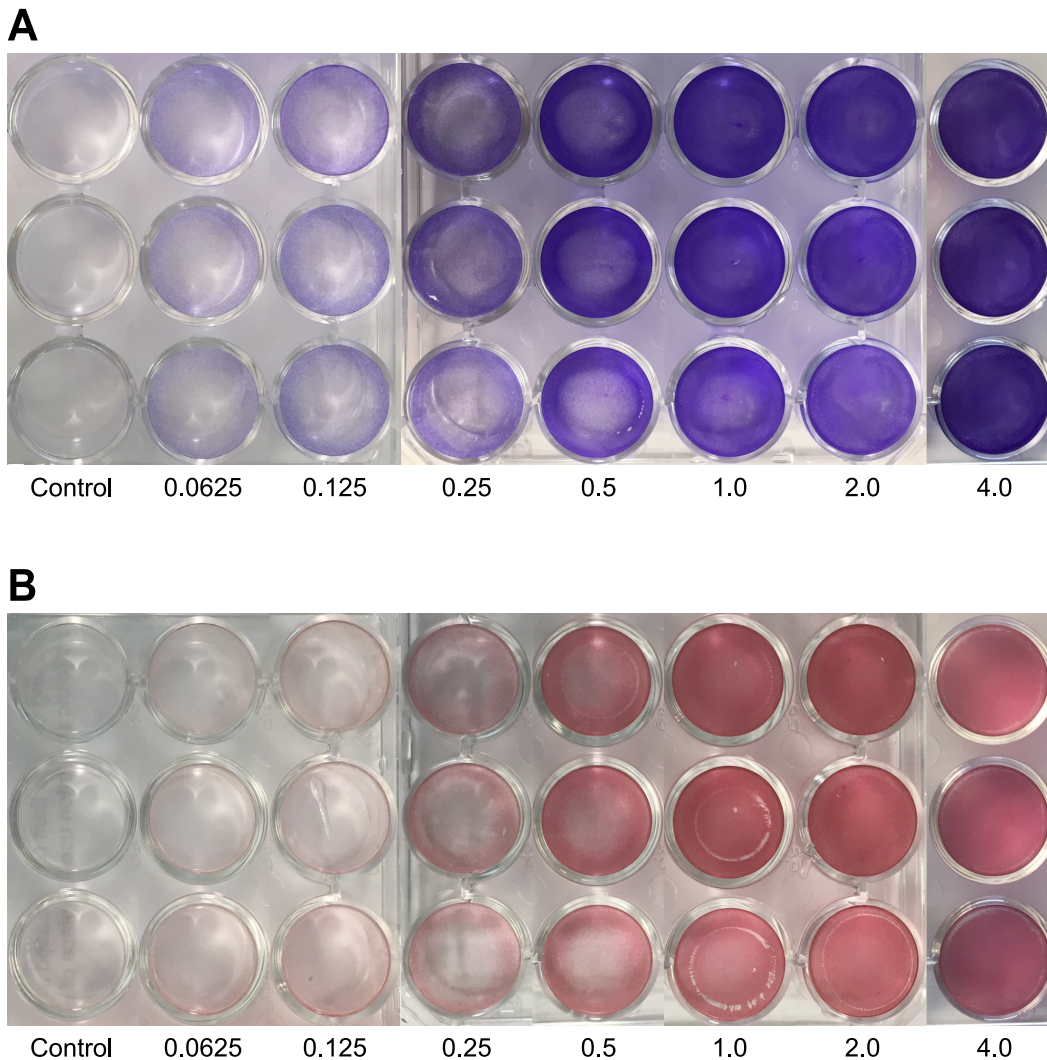


**FIGURE 3.6** Photographs of crystal violet and neutral red stains for CHO cells adhered to polyethyleneimine substrates. CHO-S IgG cells were adhered to PEI substrates and exposed to (A) crystal violet or (B) neutral red staining solutions, before being washed and dried, with wells photographed and digitally montaged together for visual comparison. The stains represented the location of adhered cells, showing more complete cell coverage of the wells as the cell load was increased. The numbers shown are the amount of cells (in millions) loaded onto each set of wells. Control wells were uncoated and not seeded, but were still exposed to the same staining solutions. Data represent n=3 (biological triplicate).

Stains were imaged after drying, with early validation work showing a decrease in intensity of the colour after a few days. This also meant solubilisation had to be performed immediately after drying. The clear circle in the bottom two wells of the 1.0  $\times 10^6$  load of the neutral red assay may be an artefact of the staining and washing method, where a portion

of cells peeled off, as cells certainly did not adhere avoiding those particular areas during cell loading. The two stains revealed the location of loaded cells; at the lower loading densities cells were retained more around the edges of the wells, with the centres relatively clear. This may be due to the meniscus of the cell load liquid distributing the cells more towards the outside whilst, at larger cell loads, this effect is less prominent with cells settling more evenly. The 'Control' wells confirmed uncoated polystyrene did not stain when exposed to either of crystal violet or neutral red.

The neutral red assay was essentially a replica of the crystal violet method. Like crystal violet, neutral red has widespread application in histological staining as both a general stain and as a specific stain for lysosomes. The uptake of neutral red is dependent upon the ability of cells to keep a suitable pH gradient; thus only viable cells will readily allow neutral red to pass through their membranes and accumulate in their lysosomes (Repetto et al., 2008). The dye can then be extracted and quantified. This affinity to be retained within the lysosomes of live cells has meant it has been employed as a viability assay, with this use demonstrated in experiments where quantification of cell death after exposure to a toxicity agent is required (Fields et al., 2017).

The intention here, however, was to use it as a general rapid stain, similar to that of crystal violet. Whilst it did easily stain, the uptake did not appear as marked as it was for crystal violet, with the relatively low  $R^2$  value demonstrating this. Neutral red has been used before with CHO cells as a crude stain to help visualisation, with a commercial document using neutral red to stain CHO-K1 cells, adhered in Alvetex materials, to easily visualise adhered cells within a 3D scaffold (Reprocell 2019e).

The demonstration for each of the four assays on day 4 of an adherent cell culture (Fig. 3.5B) revealed several different points concerning these techniques. The first observation that the relative growth between each substrate is generally the same for all assays is encouraging and can be considered the first step towards validating these assays. Taking PrestoBlue, the uncoated wells gave a normalised fluorescence of around 6.5 which, if the standard curve is consulted, should correlate to a number between  $0.7$  to  $0.8 \times 10^6$  cells. This indeed matches with the data obtained for the uncoated wells when dissociation was carried out. Similar values were matched up between the other substrates; however, polyethylenimine, which gave a fluorescence approaching 10, is out of the range of the standard curve. This indicates that by day 4 cells had either covered the surface and were beginning to clump, meaning more cells were present than the cell loading could initially achieve, or the metabolic activity of these cells is higher than those during the creation of the standard curve. It was likely the former, as the growing of cells as clumps once a monolayer had formed was observed

---

here and in earlier experiments. The actual cell number adhered may be difficult to assess using PrestoBlue for multiwell plates, although it may be possible to use suspension cell culture instead during the creation of a standard curve, as this would allow much higher densities to be measured.

The data between the crystal violet and neutral red assays with dissociation is not as comparative. The uncoated well data is around 0.3 and around 0.1 absorbance for crystal violet and neutral red, respectively. If their standard curves are consulted, this should give 0.4 and  $0.2 \times 10^6$  cells adhered; however, the dissociation for uncoated wells is stated to be  $0.8 \times 10^6$  cells. The rest of the absorbance values for each of the substrates using neutral red likewise does not correlate with dissociation values, suggesting cell numbers are not accurately being quantified. Despite this, the relative values of each substrate still agreed with the other assays, meaning neutral red could be employed if only relative comparisons between adherent cell growth were required. For crystal violet, ignoring the uncoated well, the cell growth on the poly-D-lysine, poly-L-ornithine and fibronectin matched with dissociated values and polyethylenimine was, as before, outside the range obtained for the standard curve. Whilst techniques such as crystal violet or neutral red staining are unlikely to actually be used for assessing cell adherence on multiwell plates — except to enhance cell visualisation — they could be employed for quantifying cells within specialised materials such as microspheres.

The use of multiple assays to quantify adhered cells is not new. Chiba et al. (1998), frustrated with the disadvantages posed by individual viability assays, combined neutral red, crystal violet and MTT assays to produce a composite method for cell proliferation and xenobiotic cytotoxicity studies. Using adherent HeLa cells, the authors consecutively applied each of the three reagents; after each incubation the product (or stain) was removed and quantified spectrophotometrically before the next assay began. The results from each of the three assays within the composite method compared in agreement when the particular assay was instead applied independently. Whilst the aim of the paper is not strictly relevant to the work presented here, it does however highlight the number of techniques that can be employed to determine the viability of adherent cells.

### 3.1.3 DISSOCIATION FROM PEI SUBSTRATES

The successful dissociation of adhered cells was a criterion that had to be met for an adhesion substrate to be considered suitable for the cell retention device. Trypsinisation, where the enzyme trypsin is employed to detach adhered cells from vessel surfaces, is a ubiquitous method for the dissociation of adherent cells. It was attempted here on cells adhered to polyethylenimine, poly-D-lysine and fibronectin substrates. Alongside this, growth of

these dissociated cells back into suspension culture was performed, with growth comparisons made between cells previously adhered to different substrates.

Figure 3.7A shows the viable cell density of resuspended CHO-S IgG cells after trypsinisation for 2.5 min. As previously indicated, the uncoated wells gave the least cells compared with the three substrates tested here. Seeds were taken from these new suspended cells and cultured for 5 days in shaking culture. Figure 3.7B shows the viable cell densities and viabilities at days 0, 1, 3 and 5 for the growth of resuspended cultures. All previously adhered cells achieved successful growth back in suspension, but after day 1, the growth of all was surpassed by the suspension-origin cultures. These cultures, which belonged to the same CHO-S IgG cell line, were not previously adhered to any substrate and were instead obtained from a routinely passaged suspension flask. From day 3, the density of the cells previously adhered to uncoated wells, interestingly, began surpassing those previously adhered to the three substrates. There was no considerable difference in growth of cells between any of the substrates.

The viabilities reflect the growth curves observed; the measurement at day 0 gave viabilities under 98 % for all four previously adhered cells, which dropped to 95 % or less on day 1, but then recovered by day 3. The viabilities of cells previously adhered to uncoated wells dropped the least on day 1. Viabilities were back to expected levels by day 5 for all cultures. The suspension-origin cultures were consistently at high viabilities throughout the culture, as expected.

Trypsin, a serine protease, functions by cleaving peptides on the C-terminal side of L-lysine or L-arginine amino acid residues and is believed to detach cells by acting on the proteins that enable cell adhesion. EDTA, frequently included with trypsin to make a combined dissociation solution, acts as a chelator of magnesium and calcium ions; these ions encourage cell-to-cell and cell-to-substrate adhesion (Ueda et al., 1976) and the presence of EDTA, as well as the DPBS wash prior to trypsinisation, thus ensures their removal.

Dissociation with trypsin/EDTA was technically simple and quick to perform. Plates were tapped numerous times during trypsin exposure to encourage resuspension. It was observed that forceful tapping was required to get all cells to dissociate and if trypsin exposure was used, without any physical help, then only a small portion of cells would resuspend. This was especially true for polyethylenimine and poly-D-lysine substrates, where cells remained strongly adhered even after incubation with trypsin. Gently aspirating and dispensing culture medium, so as to provide extra force, was likewise seen to be an essential technique for full dissociation. Visual progress was monitored using a microscope, with cells clumping together as they detached from the well surface. General observation from

numerous dissociation experiments found that cells with 100 % confluency were harder to detach, likely due to trypsin being physically unable to access attachment proteins. This phenomenon is widely recognised within adherent cell culture.

As the measurements were taken at days 0, 1, 3 and 5, the growth curves shown for each of the resuspended cultures do not show curves typically seen within batch experiments, i.e. lag, exponential and stationary phases cannot be distinguished. However, they do show the effects of being adhered to a substrate on subsequent growth back in suspension. The suspension-origin cells, independent of any previous adherence, were included as a bench-

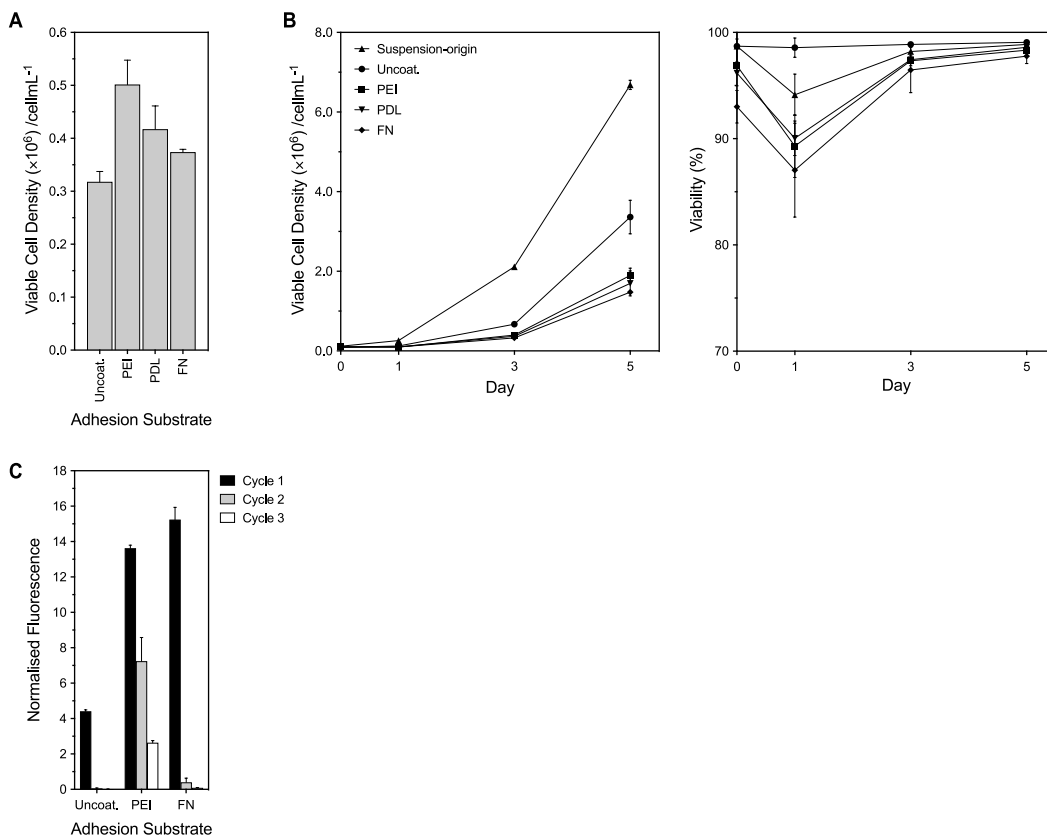


**FIGURE 3.7** Trypsinisation of CHO cells adhered to polyethylenimine, poly-D-lysine and fibronectin substrates, followed by growth back in suspension culture. CHO-S IgG cells adhered to PEI, PDL and FN substrates and grown for 4 days on 12-well plates were exposed to 0.25 % trypsin/EDTA and dissociated. Dissociated cells were (A) quantified using a ViCell and (B) grown in suspension culture using shaking TubeSpin vessels for 5 days with viable cell densities and viabilities determined. In a separate experiment (C), fresh cells were reseeded onto PEI- and FN- adsorbed wells, and uncoated wells, that had previously undergone trypsinisation steps. The growth achieved by day 7 was quantified to determine if any loss in adhesion effectiveness was occurring from these exposures to trypsin. The cycles refer to the number of trypsinisation steps the wells had undergone; with cycle 1 being wells freshly adsorbed with PEI and FN, cycle 2 being these same wells but with one trypsinisation step, and cycle 3 being two trypsinisation steps. Fresh cells, from suspension culture, were seeded for each cycle. Uncoat., uncoated; PEI, polyethylenimine; PDL, poly-D-lysine; FN, fibronectin. Data represent mean  $\pm$  SD,  $n=3$  (biological triplicate).

mark to test the adhered cells against healthy suspended cells, and illustrated the effect of adherence on resuspended growth. In routine suspension culture with this cell line, viabilities are typically in excess of 95 % until death phase, where it drops dramatically.

The slow growth is likely to be caused, partly at least, by the loss of viability seen on day 1; it is suggested cells were not in an optimal state after trypsinisation, some die, with the remainder then having an extended lag period until the growth rate reached usual levels. This viability loss was not evident upon seeding, i.e. in the day 0 viability reading, suggesting cells take at most one day to experience this viability drop. However, the cause of this loss in viability was unknown. The effect of trypsinisation on the health of cells could be a factor (which is explored later in this section), or the cellular stress, if any, experienced by cells on being physically unadhered. Cytotoxic effects from liberated substrates may help explain the viability drops, which is possible with polyethylenimine and poly-D-lysine, but less so with fibronectin, where cytotoxicity is not expected. Due to poly-D-lysine being the D enantiomorph, the substrate should be resistant to the action of trypsin (which is specific to L-forms), although fibronectin may be getting hydrolysed. Extracellular matrix proteins on polystyrene, from the use of FBS supplements, have been reported to be degraded by trypsinisation (Canavan et al., 2005).

Figure 3.7C shows the growth achieved by day 7 by cells grown on PEI and FN-adsorbed wells that had previously undergone trypsinisation steps. Cycle 1 refers to cells grown on wells freshly adsorbed with PEI and FN; cycle 2 to fresh cells reseeded on these same wells after a single trypsinisation step, and cycle 3 to fresh cells reseeded again to these wells after a second trypsinisation step. The exposure of trypsin to wells adsorbed with either PEI or FN affected the effectiveness of these coated wells to enable adherent cell growth, with growth decreasing on cycles 2 and 3. However, this loss of effectiveness was more apparent with wells adsorbed with FN, with almost no adherent cell growth achieved by the second cycle. This contrasted with PEI, where evidence of some growth was still seen by the third cycle.

The loss in effectiveness was likely due to the action of trypsin on the adhesion substrates themselves. It was suggested FN, being an ECM protein, was prone to degradation by enzymatic action. This compared with PEI which, as a cationic polymer, may be more stable when subjected to dissociation reagents. Wells were washed in between cycles to ensure no residue cells were left behind; this was not investigated further but repeated washes of wells may have also contributed to the loss of adhesion effectiveness. Uncoated wells were also tested as a control and, intriguingly, suffered the same loss in adherent cell growth when exposed to trypsin, with no growth achieved by the second cycle. This suggested

a detrimental effect on the base material itself may likewise have occurred. These data came from a relatively simple experiment but could be investigated further, especially as an adherence-based cell retention device with the capability of being used repeatedly — without gradual loss in adherence — would be both useful to the operator and cost effective.

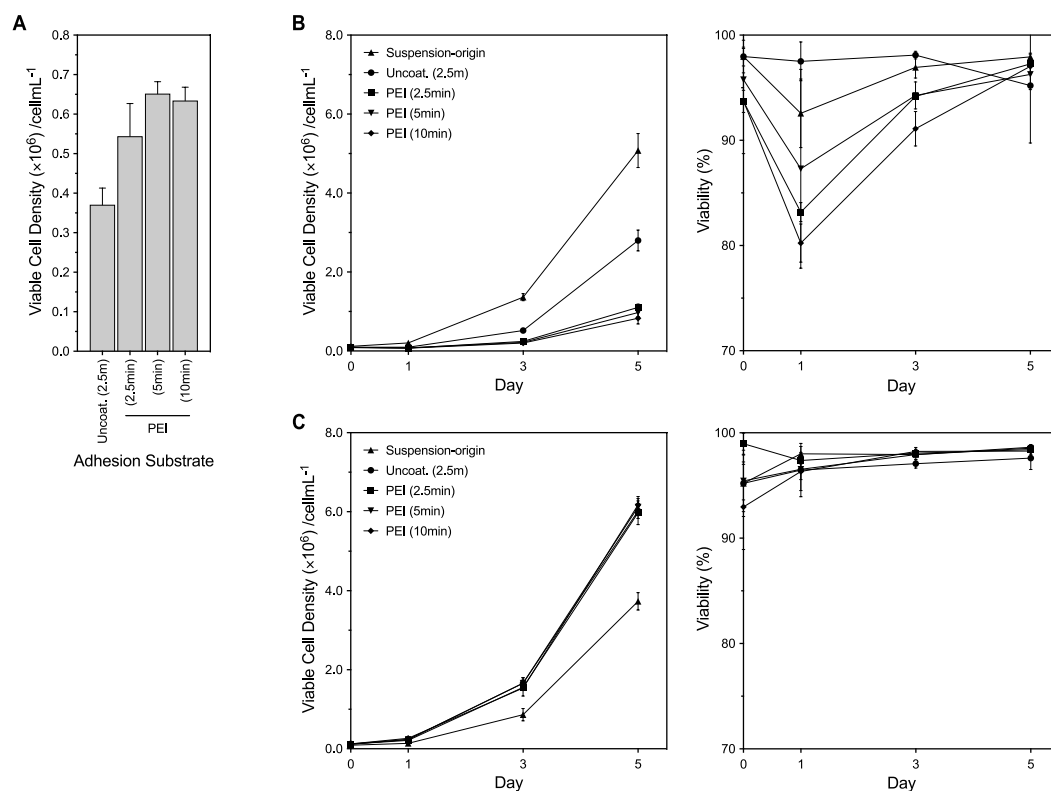
To determine if trypsinisation time had an effect on subsequent growth of dissociated cells back in suspension culture, trypsin exposure times of 2.5, 5 and 10 min were investigated. Polyethylenimine substrates, which were of more interest, were only employed in this experiment. Subculturing newly resuspended cultures into a new vessel with fresh media was also attempted.

Figure 3.8A shows the viable cell density of resuspended cells previously adhered to polyethylenimine substrates and exposed to trypsin for either 2.5, 5 or 10 min. Cells adhered to uncoated wells were exposed for only 2.5 min for comparison. There was no considerable difference in the number of cells dissociated between the trypsinisation times. Figure 3.8B shows the growth of resuspended cells in shaking culture, as well as the viabilities, and is similar to that seen in Fig. 3.7B, i.e. cells taken from routine suspension cultures reached higher cell densities than previously adhered cells from day 3 onwards. Cells from uncoated wells, once again, grew at a faster rate than cells adhered previously to polyethylenimine substrates. The exposure time to trypsin had no effect on regrowth in suspension, which was again stunted during the 5 day culture. Cell viabilities show a drop on day 1, but there is considerable overlap between error bars, with a similar gain from day 3 onwards.

Figure 3.8C shows the growth curves and viabilities for the subculture of all cells, i.e. the subsequent passage, previously adhered to uncoated wells and polyethylenimine substrates, as well as the suspension-origin cells. The difference in cell growth from the previous passage was evident; all cultures surpassed the suspension-origin cells from day 3 and reached similar densities as the suspension-origin cells in the first passage. The viabilities were much more uniform, with a return made to expected levels by day 1.

It is widely known that excessive trypsin exposure time can have a detrimental effect on cell viability, which explains why protocols from commercial suppliers recommend keeping the incubation time to a minimum. Trypsin requires an inhibitor to cease its enzymatic function; soybean inhibitor was chosen here as an animal origin-free inhibitor, although serum products are typically used due to the presence of undefined protease inhibitors. The differences in the amount of cells dissociated from polyethylenimine substrates was expected to be the same, regardless of trypsinisation time, as it was ensured all cells were

---



**FIGURE 3.8** Differing trypsinisation exposure times on CHO cells adhered to polyethylenimine substrates, followed by growth in suspension culture and one subsequent subculture. CHO-S IgG cells adhered to PEI substrates and grown for 4 days on 12-well plates were exposed to 0.25 % trypsin/EDTA for either 2.5, 5 or 10 min and dissociated. Dissociated cells were (A) quantified using a ViCell and (B) grown in suspension culture using shaking TubeSpin vessels for 5 days with viable cell densities and viabilities determined, followed by (C) a single subculture into new Tubespin vessels. Uncoat., uncoated; PEI, polyethylenimine. Data represent mean  $\pm$  SD,  $n=3$  (biological triplicate).

fully dissociated by gentle pipetting and plate tapping. This was confirmed again by microscopy. Thus, cells were exposed to trypsin for different times before it was made sure that complete dissociation was achieved. The growth curves demonstrated that the range of exposure times tested here had little impact on suspended growth, and a time of 5 min or under is sufficient for cells adhered to polyethylenimine. The observation that cells previously adhered to uncoated polystyrene once again grew faster than the cells adsorbed to polyethylenimine suggests the presence of a substrate is contributing to the reduced growth seen. Whether the polyethylenimine is causing changes in the cell, due to its adhesion functionality, or whether the polyethylenimine is desorbed during trypsinisation (as potentially shown previously in Fig 3.7) and harming cells, remained unknown.

The subculture was performed to see if there would be a return to normal growth in the resuspended cells in fresh medium and with a new seed. It was not entirely surprising that this was the case; it was suggested that the possibility of an extended lag phase in the first

passage meant cultures on day 5 were actually at the start of exponential phase and so, when seeded in fresh medium, grew rapidly in the new passage. This also explained the reduced growth of the suspension-origin cultures in this new passage, with the seed taken from the stationary phase of the previous passage. The observation that the day the seed is derived from in the previous passage dictates the growth in the next is well known.

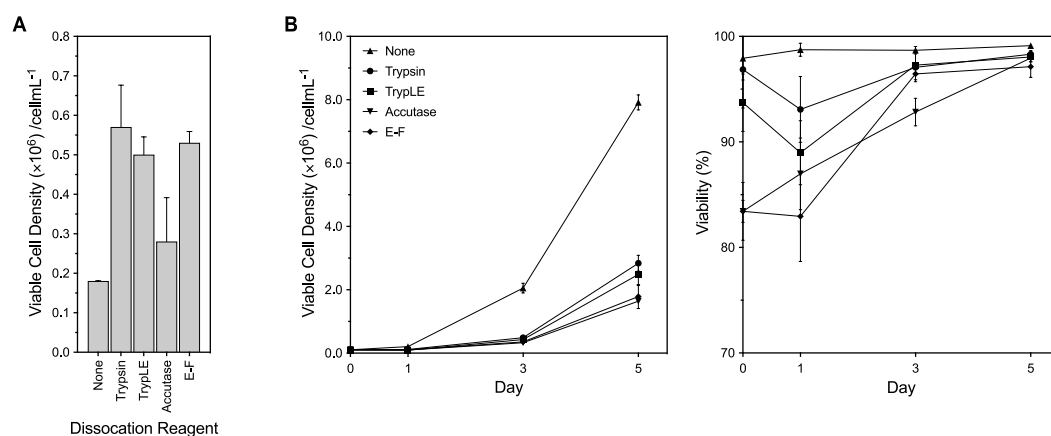
The trypsin/EDTA product used in these dissociation experiments contained trypsin of porcine-origin. Other animal origin trypsin formulations can be purchased, including bovine-origin forms. For similar reasons given for the adhesion substrates, an animal origin-free dissociation reagent was desirable. TrypLE, a recombinant trypsin alternative, Accutase, a mixture of proteolytic and collagenolytic enzymes of marine-origin (not to be confused with murine), and Cell Dissociation Buffer (Enzyme-Free), a non-enzyme solution of salts and chelating agents, were selected for investigation. To compare the action of these reagents with cell dissociation by physical force, the use of pipetting action alone to detach cells was also performed.

Figure 3.9A shows the viable cell density of resuspended cells previously adhered to polyethylenimine substrates and exposed to either trypsin, TrypLE, Accutase, Cell Dissociation Buffer (Enzyme-Free) or solely physically dissociated ('None'). Cells were not fully dissociated in this experiment; rather, all samples were incubated for 5 min and then liquid in four opposite locations of each well was aspirated and dispensed once to encourage detachment. The cells not exposed to any dissociation reagent thus were only unadhered by physical force. Trypsin, TrypLE and Enzyme-Free reagents dissociated the highest cell densities, followed by Accutase. Physical force via pipetting action detached the least cells.

Figure 3.9B shows the growth curves of resuspended cultures in shaking culture. By day 3, the viable cell density of cells dissociated by physical force alone surpassed all other cells, with the viability not decreasing on day 1. For cells exposed to trypsin, TrypLE and Accutase, the viability, once again, dropped by day 1 and then recovered by day 3. For cells exposed to Enzyme-Free, the viability was below 85 % on day 0 but again recovered. Subculture was not performed for this experiment.

The data here immediately showed the effect of dissociation reagent on cell growth and viability in resuspended cultures. Despite only resuspending a relatively small percentage of cells, using physical force alone resulted in cells achieving typical suspension growth with no drop in viability. The usual trend, an extended lag phase and reduced viability, continued with all cells dissociated using dedicated reagents. This indicated that the action of these reagents were indeed having an effect on the health of cells as they dissociate,

---



**FIGURE 3.9** Dissociation, using animal origin-free reagents, of CHO cells adhered to polyethylenimine substrates, followed by growth in suspension culture. CHO-S IgG cells adhered to PEI substrates and grown for 4 days on 12-well plates were exposed to either trypsin/EDTA, TrypLE Express, Accutase or Cell Dissociation Buffer (E-F) for 5 min. Dissociated cells were (A) quantified using a ViCell and (B) grown in suspension culture using shaking TubeSpin vessels for 5 days with viable cell densities and viabilities determined. Data represent mean  $\pm$  SD,  $n=3$  (biological triplicate).

rather than any detrimental effect arising from physical force. Care was taken to ensure this physical force was ‘even’ across all cultures, although this force was performed by hand. The success of Enzyme-Free in comparison to trypsin and TrypLE was surprising, given it relies on non-enzymatic action for dissociation.

An advantage of using an animal origin-free dissociation reagent is that the user is no longer required to meet the demands of trypsin. Unlike trypsin, TrypLE, Accutase and Enzyme-Free do not require inhibitors to neutralise their effects, with TrypLE and Enzyme-Free deactivated by excess medium and Accutase by prolonged incubation at 37 °C. TrypLE and Enzyme-Free can also be stored at room temperature and thus used rapidly.

### 3.1.4 PEI ADHERENCE AND MILD HYPOTHERMIA

Perfusion operations are typically carried out at a physiological relevant temperature, i.e. 37 °C, for a defined period to allow seeded cells to grow and then, once a sufficient biomass has been achieved, further growth is either limited or arrested. For the former, a ‘cell bleed’ is performed, describing a scenario whereby cells are physically allowed to leave the system at periodic intervals to enable the average cell number to remain constant over time. For the latter, newly added supplements in the medium can arrest growth or, far more commonly, the culture temperature can be lowered to arrest cells within their cell cycles. Cell bleeding is dependent on the accessibility of the retention device and in some set ups cells may be unable to be reached, whereas reduced temperatures can be applied for

virtually any cell retention configuration. The use of mild hypothermia, typically around 32 °C, to stunt the growth of CHO cells is widely reported with a range of phenotypic responses known, a lot of which are beneficial to biopharmaceutical production. Such an approach is not limited to perfusion, but also to fed-batch processes where operators wish to extend the length of the culture. The literature on mild hypothermia within CHO culture is explored throughout this section and again in § 6.1.1.

Mild hypothermia was the method chosen in this work to stop the overgrowth of retained cells within the continuous upstream system. However, the use of lower temperatures to growth arrest adherent cell cultures has not been widely demonstrated. The bulk of this section is dedicated to exploring the effect of cold temperature on the growth, adherence and productivity of CHO cells attached to polyethylenimine substrates. However, it first introduces the rapid measurement of glucose concentration using an inexpensive blood sugar monitoring device. Such a device was seen as helpful in the planned experiments that followed and for general usage within the laboratory.

Figure 3.10A shows a 'standard curve', prepared using a blood sugar monitoring device, for the concentration of glucose within diluted CD CHO medium solutions. The high  $R^2$  value, 0.9977, demonstrated the capability of the device to measure, at least in relative terms, a known range of glucose concentrations within cell culture medium. Figure 3.10B shows the viable cell density of CHO-S IgG cells during routine suspension culture, along with the daily glucose concentration of medium used. The concentration was high at the beginning, days 1 and 2, but decreased rapidly as cells entered exponential phase, with the increase in biomass related to this drop. By day 6, glucose was almost entirely consumed, with cells now toward the end of stationary phase. The culture was ended at day 6, but a drastic drop in viability on day 7 was expected given the depletion of glucose.

The blood sugar monitoring device was acquired so glucose concentration determination could be performed on-demand, with a reading given within a few seconds. This product is marketed for people with diabetes who wish to measure their blood sugar levels throughout the day, but can be easily employed for glucose measurement within other aqueous solutions, including cell culture medium.

One of the most accurate ways to measure glucose concentration is by the use of a Cedex Bio Analyzer — which was indeed used later in this work — but this requires training and greater expense. Whilst technically simpler glucose assay kits are available for life sciences work, these are often high throughput, plate-based tests, and so are unsuitable if rapid measurement of glucose is needed for a small number of samples. For kits which are not high throughput, the ease and low cost of a blood sugar monitoring device still remains an

appealing option for the rapid determination of glucose. The ‘standard curve’ presented here, which is not a genuine calibration graph, was created so as to confirm the monitoring device, along with the testing strips, would indeed reveal the relative differences between diluted solutions of medium. The use of the monitoring device for actual cell culture confirmed it could be trusted for the measurement of glucose in real experiments, with the data here as expected for a standard suspension culture.

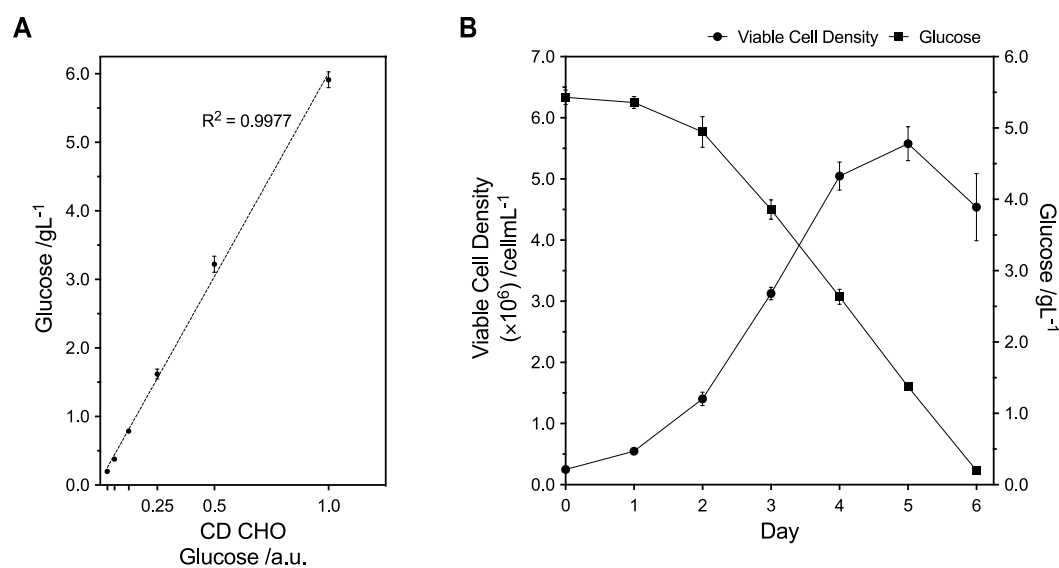
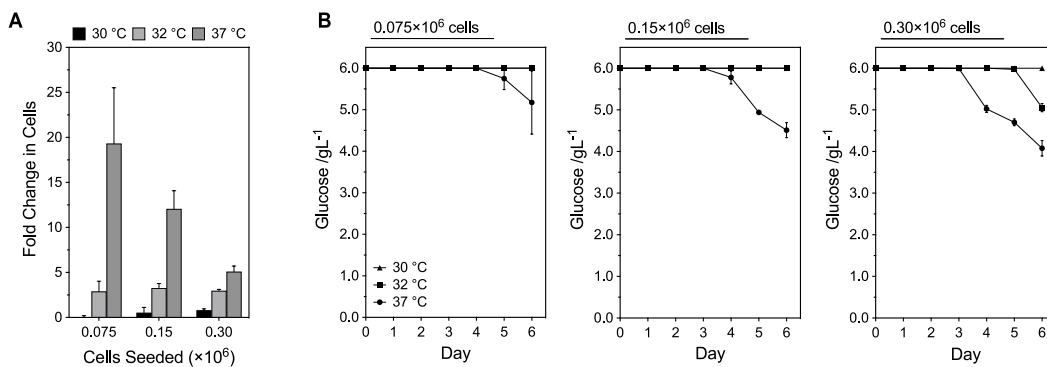


FIGURE 3.10 ‘Standard curve’ to assess suitability of a blood sugar monitoring device for determination of glucose concentration in CD CHO medium, and demonstration of its use in actual cell culture. Medium was serially diluted with water and its (A) glucose concentration determined using a blood sugar monitoring device. The  $x$ -axis has arbitrary units, with 1 being undiluted medium, 0.5 the first dilution and so on. For the demonstration, CHO-S IgG cells were seeded in TubeSpin vessels and grown in suspension for 6 days, with (B) viable cell density and glucose concentration determined daily. For (A), data represent mean  $\pm$  SD,  $n=3$  (technical triplicate); for (B), data represent mean  $\pm$  SD,  $n=3$  (biological triplicate).

It is generally known that the glucose concentration of fresh CD CHO medium is around  $6 \text{ gL}^{-1}$ . Determining the concentration of glucose in different lots of CD CHO, however, returned slightly varied glucose concentrations, with an average of  $6 \text{ gL}^{-1}$ . Subtle differences in media composition are expected and past experience confirmed that cell growth does vary slightly between medium lots, which may be partly due to different glucose concentrations. Interestingly, it was found that there was variability between different lots of the glucose testing strips, with each lot giving different readings of glucose concentration when performed on the same sample (data not shown). This was likely down to the manufacturer and the fact an inexpensive method of glucose determination was chosen. To counter this, only one lot was used for each experiment to ensure results could be fairly compared.

An initial experiment investigated the effects of temperature on the growth of cells adhered to polyethylenimine substrates. Cells at three different seeds, 0.075, 0.15 and 0.30 million, were adhered overnight on 12-well plates, washed the next day and then placed in incubators at either 30, 32 or 37 °C. Glucose concentrations were determined daily and, on the sixth and final day, adhered cells were dissociated using trypsin and the fold change in cell number calculated.

Figure 3.11A shows the fold change in cell number after 6 days of culture at each of the three temperatures used for each of the three seeding densities. For 30 °C, the fold change was 2 or under for all three seeds, whilst for 32 °C, it was fairly consistent around 4. For 37 °C, the fold change was considerably higher and was affected by the seeding density; for 0.075 million cells, a change of 20 was achieved, for 0.15 million around 15 and for 0.30 million, around 5. The difference in fold change between temperatures of the same seeding density decreased as the seeds were increased.



**FIGURE 3.11 Effect of mild hypothermia on the growth and glucose consumption of CHO cells adhered to polyethylenimine substrates.** PEI was adsorbed on 12-well plates, seeded with 0.075, 0.15 or 0.30 million CHO-S IgG cells and left to adhere overnight in an incubator. The next day, wells were washed, fresh media added and plates incubated at either 30, 32 or 37 °C for 6 days, with dissociation performed on the final day to determine (A) fold change in growth, with (B) glucose concentration also determined daily. Data represent mean  $\pm$  SD,  $n=3$  (biological triplicate).

Figure 3.11B shows the glucose concentrations on each of the 6 days. Both the temperature of culture and the seeding density affected the decrease in glucose concentration observed. For 0.075 million cells, the glucose concentration remained at 6 gL<sup>-1</sup>, for both 30 and 32 °C, for the entire duration of the experiment with a decrease, i.e. glucose consumption, occurring only from day 5. For 0.15 million cells, similar data are seen, except the consumption of glucose was seen with 37 °C from day 4. Finally, for 0.30 million cells, cultures at 37 °C saw a greater decrease in glucose concentration from day 4, and those at 32 °C saw a decrease at day 6. Cells adhered at 30 °C did not appear to consume glucose at any of the

seeding densities.

The experiment here was performed to assess the effect of temperature on growth. It is widely known that mild hypothermic temperatures arrest cell growth and this was indeed confirmed in the data presented, with a reduction in fold change as temperature was decreased, although there was still growth observed in all samples. Daily observation of cells was carried out using a microscope. For cultures incubated at 30 and 32 °C, it was noted that cells began detaching from the surfaces of the wells. This was particularly evident by the third day of the culture. This did not appear to be newly divided cells not adhering, but rather adhered cells dissociating into suspension, and thus it was most prevalent with the highest seed. Detached cells visually appeared healthy. This was a surprise, and did not occur with cultures at 37 °C, except in cases where cells had clumped from overgrowth and detached, as was seen in previous experiments. During the dissociation step, unadhered cells from all cultures were washed off before cell counting, so the fold changes given may be somewhat lower than the true values if detached cells are also considered.

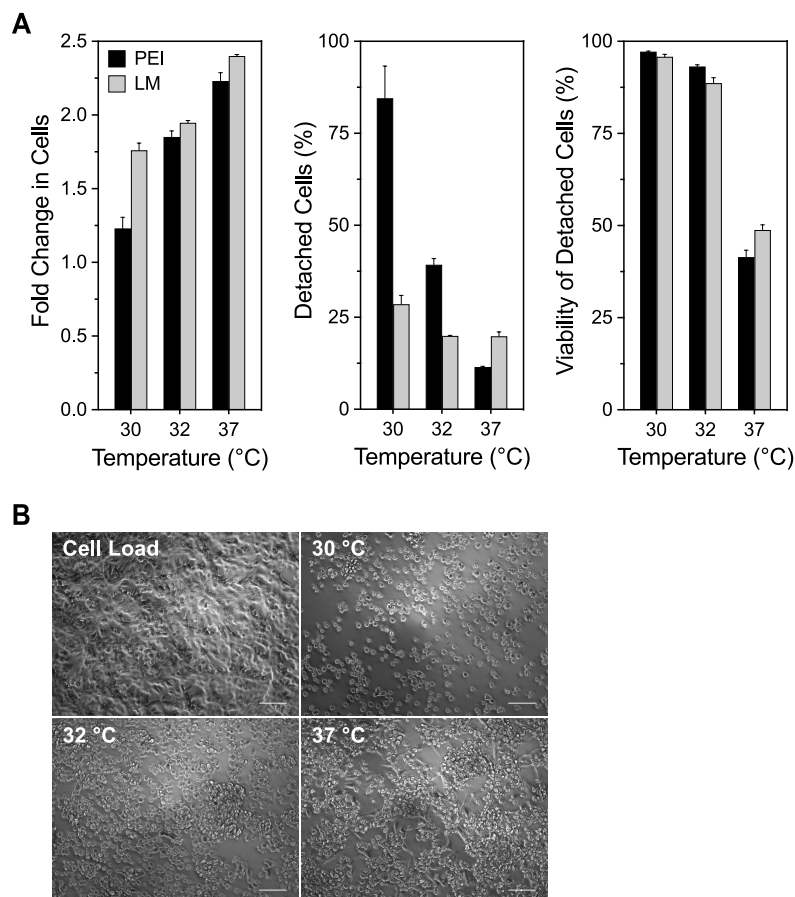
To investigate this detachment effect from mild hypothermia, T-25 flasks were loaded with 10 million CHO-S IgG cells overnight and, as before, placed into incubators at either 30, 32 or 37 °C. On day 5, flasks were washed and the number of detached cells determined. Polyethylenimine and laminin, as coatings providing crude and specific adherence, respectively, were both used as substrates. Whilst biphasic cultures — where a process starts at 37 °C and is later cooled to 32 °C or under — are encountered (Yoon et al., 2006), this experiment aimed to eliminate the initial growth phase and instead loaded cells at a high density overnight with immediate cooling to mild hypothermia the next day.

Figure 3.12A shows the fold change in cell number for cells adhered to polyethylenimine and laminin substrates, over 5 days, for all three temperatures, as well as the percentage and viability of cells that had detached. For cells adhered to polyethylenimine, reducing the temperature to 32 °C and under decreased the fold change, i.e. the growth rate was reduced, with 30 °C yielding the lowest fold change. For cells adhered to laminin, the relative values in fold change between temperatures was not as marked, with 30 and 32 °C giving similar fold changes. Interestingly, whilst the fold change between the two substrates was similar for 32 and 37 °C, there is considerable difference for 30 °C. Unlike previous data, the fold change here included detached cells.

The percentage of cells that had detached by day 5 was over 75 % for cells adhered to polyethylenimine substrates at 30 °C and decreased considerable for cells cultured at 32 °C and 37 °C. For cells adhered to laminin, the detachment was considerably less at both 30 and 32 °C, whilst being slighter higher at 37 °C. The viability of cells that detached was

similar for both substrates, with unadhered cells at 30 and 32 °C having viabilities above 80 %, whilst for those at 37 °C, it was under 50 %.

Figure 3.12B shows the morphologies of cells adhered to polyethylenimine substrates after overnight seeding and then at 30, 32 and 37 °C on day 5. Cells possessed typical elongated morphology when loaded at high density, as can be seen, which was unlike the stretched shapes observed when seeding with usual low cell densities, as seen previously in Fig. 3.3. By day 5, adhered cells at 30 °C were rounded, with most having detached; the same was observed at 32 °C but detachment was less prominent. For cells at 37 °C, cells had grown as clumps, with some segments still retaining the elongated shapes. The morphologies of



**FIGURE 3.12** Effect of mild hypothermia on the growth, viability and adherence of CHO cells adhered to polyethylenimine and laminin substrates. PEI and LM were adsorbed on T-25 flasks, seeded with 10 million CHO-S IgG cells and left to adhere overnight in an incubator. The next days, flasks were washed, fresh media added and vessels incubated at either 30, 32 or 37 °C for 5 days, with dissociation performed on day 5 to determine (A) fold change in growth and percentage of dissociation for each temperature, with (B) the morphologies of the cells adhered to PEI substrates on day 5 imaged using a phase contrast microscope at 10× magnification. PEI, polyethylenimine; LM, laminin. Data represent mean  $\pm$  SD,  $n=3$  (biological triplicate). Scale bars = 100  $\mu\text{m}$ .

cells adhered to laminin were not imaged.

The data confirmed the effect of mild hypothermia on cell detachment and began to explore how this relationship was dependent upon the adhesion substrate used. As a high cell density load was now used, the detachment was more apparent. For cells adhered to polyethylenimine, the temperature shift to 30 °C had a dramatic effect, with cells beginning to round up from the second day with eventual dissociation, which continued until the end of the experiment when the majority of cells were back in suspension. This effect was not as noticeable with cells at 32 °C, but still did occur. The high viability of detached cells at both 30 and 32 °C confirmed dissociation was likely due to the temperature shift and not because of any substrate limitation or toxic metabolite accumulation. This was backed up by the lower viability for detached cells at 37 °C, where it was proposed that a non-optimal medium environment, along with cell clumping, caused some non-viable cell detachment, as would be expected from a highly confluent adherent culture.

Laminin was used to investigate if animal origin adhesion substrates, i.e. those which rely on specific interaction to encourage attachment, were also prone to detachment from mild hypothermia. This was done in a separate experiment with laminin the only animal origin substrate available to test. Its ability to keep a majority of cells adhered, even at 30 and 32 °C, was surprising, with cells not losing their distinct morphologies like those adhered to polyethylenimine. It is suggested the specific, protein-based interactions between cells and substrate are not as prone to change by mild hypothermia, whilst non-specific electrostatic adhesion to cell membranes, as with polyethylenimine, is highly dependent upon temperature. It is expected other animal origin substrates, such as fibronectin, are similarly capable of retaining cells at <37 °C temperatures, but this was not tested.

The difference in relative fold changes between both substrates may be due to detachment. For laminin, where detachment was at a minimum, the fold change at 30 and 32 °C was similar, whereas for polyethylenimine, there was considerable difference. It is proposed, as this was a static adherent culture with cells loaded at a high density, the actual temperature at the cell monolayer may indeed be higher than the culture temperature, which may explain the small difference in growth. For polyethylenimine, as cells detached and were resuspended, culture medium surrounded the entire cell, and the effects of temperature on growth may be more apparent. The CHO-S IgG cell line, in suspension culture, is indeed prone to growth arrest by reducing the temperature, with this demonstrated later in the work here in § 6.1.1.

Whilst sudden temperature decreases have been utilised to detach adherent cells from surfaces, e.g. by adhering cells to poly-N-isopropylacrylamide, a thermosensitive substrate

that becomes hydrophobic below 32 °C (Yang et al., 2010), no literature could be found replicating this detachment effect of mild hypothermia on adherent cultures. It is expected that anecdotal evidence does likely exist where operators have turned down the culture temperature — perhaps in error — and observed cell detachment some days later in their cultures, however this may be dependent upon the substrates used, if any, and perhaps even the cell line. This finding was important as the use of microspheres for cell retention, at reduced temperatures, was anticipated later on in the work.

It is widely known that reducing the temperature of a culture has a wide range of phenotypic effects on CHO cells. These have been well reviewed by Masterton et al. (2014), and include changes to cell growth (reduced), viability (increased) and metabolism (numerous changes to metabolite production and substrate consumption), which in turn affect culture duration (increased) and medium composition (related to changes in cell metabolism). For the biologics industry, however, the effect on recombinant protein production may be considered the greatest advantage of mild hypothermia. Whilst it must be remembered this effect is both product- and cell line-specific and has to be proved experimentally, it has been documented using available literature that reducing the temperature for CHO cultures typically increases the cell-specific productivity of recombinant proteins (Becerra et al., 2012).

A Cedex Bio Analyzer was used to determine the daily concentrations of glucose, L-glutamine, lactate and lactate dehydrogenase using samples taken each day for this experiment. Very briefly, glucose and L-glutamine are required for energy creation amongst others and are consumed by CHO cells, whilst lactate is an unfavourable by-product of metabolism. Lactate dehydrogenase is an enzyme found in high amounts in cells, including in CHO cells, and its presence indicates cell necrosis and thus can be used as a marker of cell death. An in-depth discussion of these analytes, as well as a description of the validation steps performed for the Cedex Bio Analyzer, can be found in § 6.1.1.

The effect on IgG titre and metabolism was investigated for cells loaded onto polyethylenimine substrates using T-25 flasks at different temperatures, in the same experiment as previously discussed. Figure 3.13A shows the daily IgG titre and L-glutamine concentrations for cultures at 30, 32 and 37 °C, with cell-specific productivity and the cell-specific L-glutamine consumption rate between day 0 and day 5 also shown. The titre increased each day for cultures at every temperature from day 1 onwards; 37 °C gave the highest titre, followed by 32 °C and then 30 °C. There was no considerable difference in cell-specific productivity between the three temperatures, with all three achieving approximately 15 pgcell<sup>-1</sup>day<sup>-1</sup>. For L-glutamine, cells adhered at 32 and 37 °C consumed the

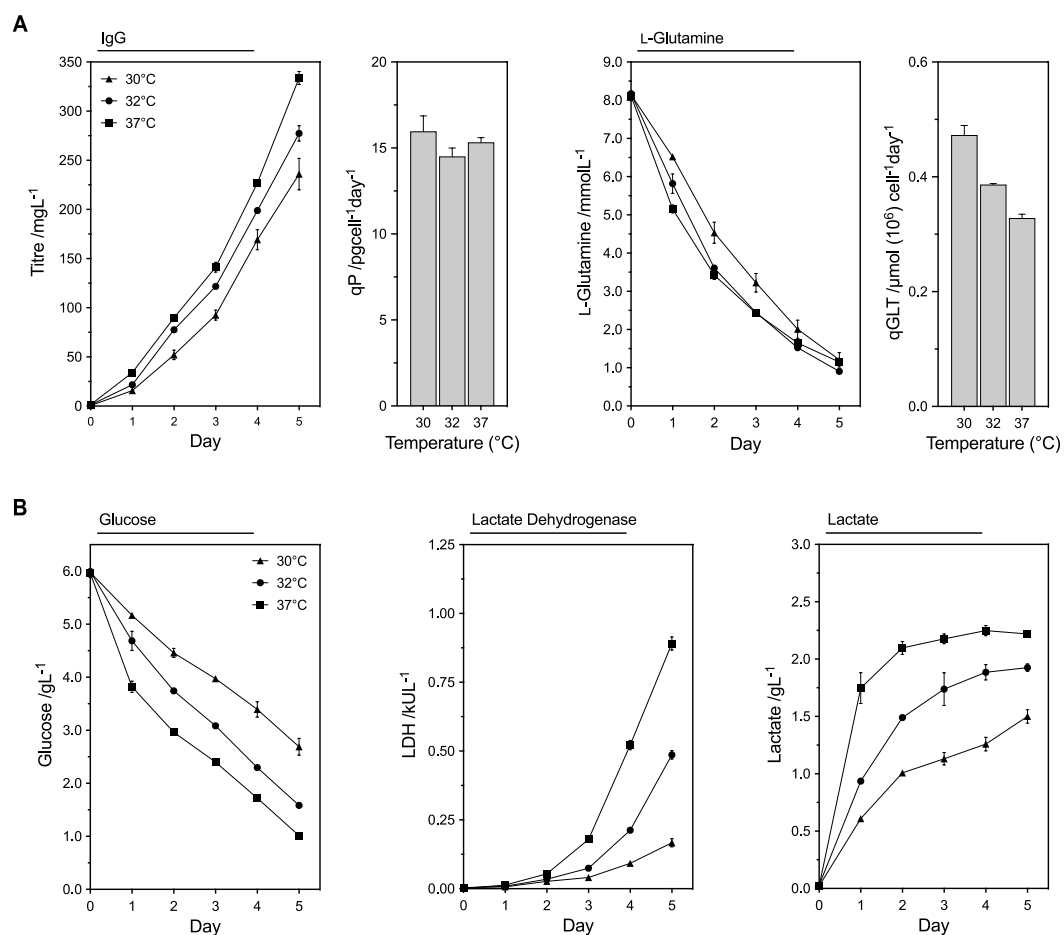


**FIGURE 3.13** Effect of temperature on daily metabolite and substrate concentrations and IgG titre of CHO cells adhered to polyethylenimine substrates. In the same experiment as presented in Fig. 3.12, CHO-S IgG cells were adhered to PEI substrates in T-25 flasks and incubated at 30, 32 or 37 °C for 5 days, with (A) IgG titre and L-glutamine concentration determined daily, as well as cell-specific productivity (qP) and cell-specific L-glutamine consumption rate (qGLT) calculated, and (B) glucose, lactate dehydrogenase and lactate determined daily. Data represent mean  $\pm$  SD, n=3 (biological triplicate).

most L-glutamine each day, i.e. the concentration decreased the most until day 5, when all three temperatures matched their L-glutamine concentrations. The specific L-glutamine consumption rate, interestingly, was dependent upon the temperature, with 30 °C giving the highest with almost 0.5  $\mu\text{mol (10}^6\text{) cell}^{-1}\text{day}^{-1}$  reached, followed by 32 and 37 °C, indicating a change in cell metabolism arising from mild hypothermia.

Figure 3.13B shows the daily glucose, lactate dehydrogenase and lactate concentrations for cells cultured at each of the three temperatures. For glucose, the concentration decreased the least at 30 °C, whilst for lactate, the concentration increased the least at 30 °C. The release of lactate dehydrogenase, a marker of cell death, was almost uniform for the first two days, before increasing rapidly for cells at 37 °C, with much smaller increases for those

at 32 and 30 °C.

As previously shown in Fig. 3.12, reducing the temperature for cells adhered to polyethylenimine dramatically arrested cell growth. As can now be observed, this had an effect on metabolite production and substrate consumption; the concentration of glucose decreased at a reduced rate each day with lower temperature cultures. Interestingly, the change in L-glutamine each day did not differ as much between temperatures, with all three cultures sharing similar L-glutamine concentrations on the final day. This translates into an increased cell-specific L-glutamine consumption rate for 32 and 30 °C, indicating the shift to mild hypothermia increased the utilisation of L-glutamine. This is observed again in § 6.1.1 and is discussed further there. The reduced lactate concentrations observed for mild hypothermic cultures was expected. Lactate is a product of anaerobic glucose metabolism, produced rapidly as cells proliferate in the exponential phase of cell culture. With reduced temperatures, there is an arrest in cell growth, meaning less lactate is produced.

Lactate dehydrogenase is an enzyme involved in the production of lactate from pyruvate; as cells die, they burst and release their contents. As lactate dehydrogenase is ubiquitous in CHO cells (and almost every living cell), it may be assayed and used as an indirect marker of cell death. The sudden increase observed for cultures at 37 °C after day 3 was expected. Due to the high cell load, cells rapidly consumed both glucose and L-glutamine substrates; once these become scarce, medium environments were no longer optimal for growth and cells died. The much lower production of lactate dehydrogenase for 32 and 30 °C cultures is related, once again, to the reduced growth rates.

The most surprising data here were the lack of increase in cell-specific productivity seen with cultures at 32 and 30 °C. This may be explained by the majority of cells detaching by day 5 and not being agitated, which perhaps had a detrimental effect on their productivities.

### 3.1.5 CONCLUSIONS

The work in this chapter focused upon the testing and evaluation of a range of chemically defined and animal origin adhesion substrates for the attachment, and thus retainment, of suspension-adapted CHO cells. It was expected a substrate would be employed ultimately within the in-house cell retention device. The aim from the very start was to continue using CD CHO medium during cell culture and not have to rely on animal-derived supplements, such as serum products, for the prolonged adhesion of cells. Because of this demand, a chemically defined, animal origin-free adhesion substrate had to be found.

Using literature sources, three cationic polymers and four animal origin proteins were first identified and subsequently investigated via their adsorption onto polystyrene and glass surfaces. The optimal coating concentration was determined for each, followed by adherent cell culture tests where growth of adherent cells was tested at two time points using an adapted viability assay. It was observed that polyethylenimine was an extremely effective adhesion substrate for both cell attachment and subsequent cell spreading during adherent growth. This substrate, which is chemically defined, performed as well as the four animal origin proteins and the other two cationic polymers, despite being the least expensive. Polyethylenimine was consequently selected early in the work as the substrate of choice for effective cell retention.

Cell loading, which was explored as a process technique to rapidly retain a high density of cells, was attempted with polyethylenimine, poly-D-lysine and fibronectin substrates using two suspension-adapted CHO cells lines and one suspension-adapted HEK cell line. For both CHO cell lines, polyethylenimine and poly-D-lysine adhered an increasing number of cells as the load was increased, and even surpassed the cells captured by fibronectin at the highest loads. For HEK cells, fibronectin gave similar readings to polyethylenimine and poly-D-lysine, suggesting particular interaction between this human cell line and fibronectin was more favourable than that seen with CHO cells. The idea of rapidly loading a high number of cells, in this instance to the surfaces of simple polystyrene vessels, has not been widely demonstrated before in the literature.

To characterise and better understand the adhesion of suspension-adapted CHO cells, four potential adhesion assays were attempted. These included dissociation by trypsin exposure, PrestoBlue reagent to assess adherent cell viability and finally, crystal violet and neutral solutions as crude staining techniques. For the latter two assays, letting the stained cells dry before resolubilising the dyes allows quantification and acts as a measure of adherent cell number. All assays performed well, during both the generation of standard curves and within actual cell culture, with the two stains providing visual data on where within wells cells adhered.

Dissociation, a key aspect at the beginning of this work, was performed again using trypsin as well as animal origin-free reagents. Newly dissociated cells from various substrates were successfully grown back in suspension culture, but with a reduced growth rate when compared to suspension-origin cultures. Subculturing these previously adhered cells returned cell growth to normal suspension levels. It appeared using a dissociation reagent had a detrimental effect on the growth of resuspended cells.

Finally, cell loading on polyethylenimine substrates was again demonstrated, but in this

---

instance was followed by culture at two mild hypothermic temperatures, 32 and 30 °C, with the effects on cell growth, detachment, titre and metabolism observed. For cells at 30 °C, the majority of cells detached after five days, yet remained viable with the growth rate arrested. This detachment was concerning, but it did not occur with cells adhered to laminin substrates. Metabolite and substrate analysis also revealed changes in L-glutamine consumption, as well as showing the reduced production of lactate and lactate dehydrogenase at these lower temperatures.

To conclude, polyethylenimine is severely neglected as an adhesion substrate in the literature, yet its effectiveness for adhering suspension-adapted CHO cells was repeatedly demonstrated here in a variety of experiments. The data in this chapter suggest the use of polyethylenimine to adhere CHO cells, without high cost, needs to be more widely recognised, with even the possibility of commercial usage. The observation that polyethylenimine performed well ensured it was taken forward to the next stage of the work and used alongside the in-house fabricated microspheres. The dramatic cell detachment of cells from polyethylenimine substrates at 30 °C — which did not occur with laminin substrates — was immediately acknowledged as a potential issue, as the cell retention device proposed was expected to operate effectively within processes carried out at reduced temperatures. However, later work proved this was not entirely the case when porous microcarriers, adsorbed with polyethylenimine, were tested in mild hypothermic cultures.

---

# Chapter 4

---

## CELL PAUSING

---

### OVERVIEW

This chapter presents the results obtained whilst investigating cell ‘pausing’, a novel technique where severe hypothermic temperatures are employed to halt the metabolism and growth of CHO cells. Such methods could enable prolonged storage without cryopreservation and may be beneficial within research and development scenarios, e.g. for the storage of different cell cultures with on-demand culturing then possible. The work here first determines the optimum pausing temperature for a range of pausing periods, before exploring the pausing of both suspended and adhered CHO cells.

### 4.1 INTRODUCTION TO CELL PAUSING

Cell pausing, a surprisingly neglected area of research within bioprocessing, was investigated as a side project after inspiration from a piece of work published some years ago. This work, by Hunt et al. (2005), described several techniques where a range of severe hypothermic temperatures (24 °C and under) were employed to stop the growth of — or ‘pause’ — adhered and suspended CHO cells. The authors found that their technically simple methods, which did not involve any cryogenic materials, could be used to store cells for several weeks at a reduced metabolite state and with no growth — yet the cells remained viable. Upon returning to usual physiological conditions, cells resumed growth and continued largely as before. The only other reports found demonstrating hypothermia to ‘pause’ biological material concerned cell therapies, where the refrigerated storage and transportation of stem cells, cellular masses or even whole tissues would be clinically beneficial (Correia et al., 2016; Robinson, 2017; Petrenko et al., 2019). For applications like these, where the recipient is ultimately a patient, cryopreservation is not always suitable, and instead simple refrigeration becomes appealing. A review, focusing on pausing for cell therapy, has been provided by Robinson et al. (2014) and gives a comparison between cryopreservation and refrigeration for cell storage.

Returning to the pausing of immortalised cell lines, it is recommended that Hunt et al. (2005) is reviewed if readers are interested in the concept of cell pausing. However, the main findings of the paper will be compared and discussed alongside the data obtained for this chapter. For the sake of clarity, cell ‘pausing’ is defined in this work as the storage of cells

within a severe hypothermic environment (below average room temperature) and without any external buffering system (such as exogenous CO<sub>2</sub>) or agitation, so as to ensure growth is arrested and cells kept within a low metabolic state. Pausing must occur without the use of liquid nitrogen or other cryopreservation materials and cells must be able to return — or ‘awaken’ — to typical metabolic function once physiological temperature and buffering systems are resumed. There should be no considerable drop in viability from cell pausing. As an example of a condition that would break this definition, the storage of cells using temperatures at or below 0 °C, without the use of cryoprotectants, would not be considered pausing due to the complete loss of viability anticipated by the formation of ice crystals. Likewise, culturing cells at mild hypothermic temperatures, e.g. 32 °C with agitation and CO<sub>2</sub> exposure, would not be pausing, even if growth was successfully arrested.

Cell pausing already brings tremendous benefit, albeit outside of upstream processing. The refrigeration of food and drink dramatically slows down the metabolism, and consequently the growth of, potentially harmful bacteria and fungi. This in turn helps to prevent the spoilage of perishable items, such as food and drink. Whilst such items are able to be stored for prolonged periods using these cooler temperatures, microorganisms are likewise kept stored. Items which are brought out of refrigeration will soon show evidence of microorganisms as cells are awakened and growth resumed. Cell pausing does hold some relevance to the overarching aim of the work presented here. For cells that are retained using external cell retention devices, i.e. devices that can be physically handled by operators outside of a bioreactor, ‘pausing’ them on-demand at any time during a continuous process could be highly advantageous. Whilst this may seem somewhat lacking in application, such a technique could allow multiple sets of retention devices, loaded with CHO cells, to be ‘paused’ and then ‘awakened’ as required. It can be argued this would be especially beneficial to research and development laboratories, where an array of CHO cell clones could be serially loaded, paused and then rapidly employed within continuous processes.

The objectives of the work presented in this chapter were to; (i) determine the optimal temperature(s) for the pausing of CHO-S IgG cells; (ii) demonstrate these temperature(s) for the pausing of CHO-S IgG cells in suspension culture for a range of time periods, including awakening to resume normal culture; (iii) demonstrate the pausing of CHO-S IgG cells adhered to adhesion substrates, and (iv) determine what effects, e.g. dissociation and morphology, severe hypothermia have on adhered cells that are paused.

#### 4.1.1 SUSPENSION CELL PAUSING

The temperature at which cells are paused was the first parameter that needed to be determined before pausing could be employed in real scenarios, so it was decided first to test

---

a range of temperatures with CHO-S IgG cells for a range of time periods. The definition of cell pausing previously given did not allow agitation, i.e. the storage of cells had to be technically easy to achieve, so suspended cells were first paused within upright 15 mL centrifuge tubes, with caps tightly sealed. Cell viability was determined for each time period using the trypan blue exclusion method. An optimal temperature would be one where cell viability remained high, even after prolonged periods of storage.

Figure 4.1A shows the viability of cells paused at 4, 8, 23±1 (room temperature) and 37 °C after 0, 2, 4 and 8 days. The cells paused at 37 °C were sealed, with no buffering system, whilst non-paused cultures at 37 °C, with usual CO<sub>2</sub> exposure and agitation, were included as a control. For cells paused at 4 and 8 °C, viabilities of cells remained high for each of the days tested, remaining above 95 % by day 8. There was no considerable difference between the two. The viability of cells paused at room temperature began to drop on day 2, to less than 90 %, and by day 8 had dropped further to 70 %. For cells paused at 37 °C (which, technically, was not pausing), viabilities dropped dramatically from day 2 onwards. The control, which simply measured the viability of cells within a normal 37 °C, 5 % (v/v) CO<sub>2</sub> incubator with agitation, had viabilities which remained high on days 2 and 4 until a dramatic drop, to under 40 %, on day 8.

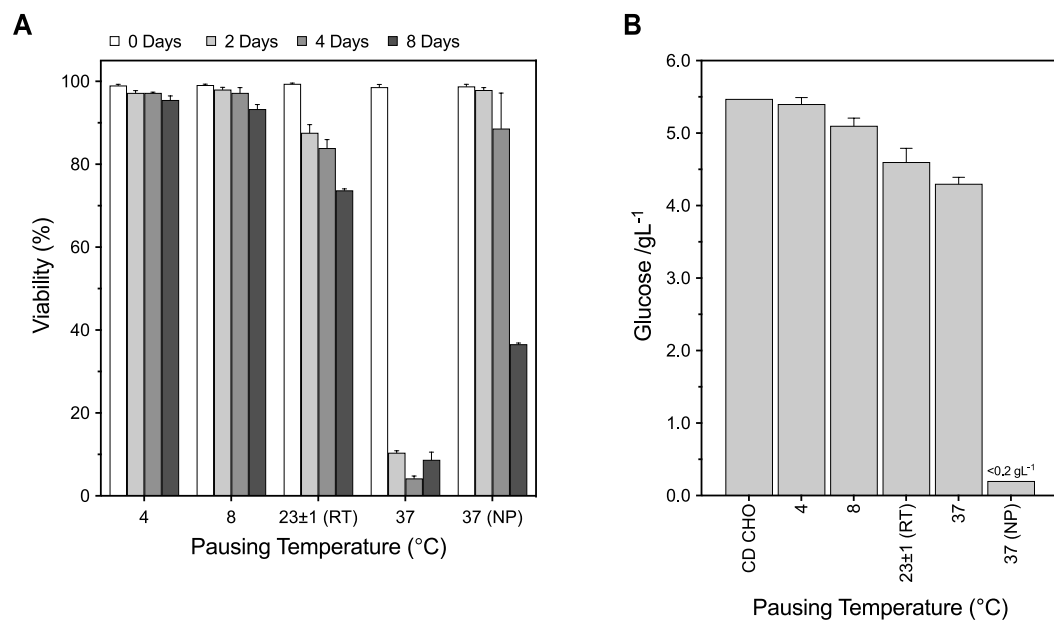


**FIGURE 4.1** Effect of temperature, during cell pausing, on CHO cell viability and glucose consumption. 5 mL CHO-S IgG cells, at  $1.0 \times 10^6$  cellmL<sup>-1</sup>, were seeded in centrifuge tubes and ‘paused’ at either 4, 8, 23±1 (RT) or 37 °C for 2, 4 and 8 days. On each of these days, cells were gently resuspended and (A) viability determined, with (B) glucose concentration determined on day 8. RT, room temperature; NP, non-paused. Data represent mean ± SD, n=3 (biological triplicate).

Figure 4.1B shows the glucose concentrations of cell culture medium of paused cells on day 8 for each of the pausing temperatures tested. The concentration of glucose steadily decreased as the pausing temperature increased, i.e. cells appeared to consume less glucose at the lower pausing temperatures. For the non-paused cultures, glucose was totally consumed with the concentration below the sensitivity of the blood sugar monitoring device. The concentration of glucose within unspent CD CHO, which was from the same lot of medium as used for pausing, was also tested for comparison.

The aim of the experiment here, which was simple to carry out, was to find a temperature where cell viability would remain high during pausing, despite vessels being unagitated, buffered or warmed. The number of cells paused, 5 million within 5 mL, was chosen to ensure enough samples could be taken for viability determination on each of the days.

During pausing, all cultures quickly formed cell pellets at the bottom of the centrifuge tubes. For days 2, 4 and 8, these pellets were gently aspirated and dispensed using a pipette and the viability of the resuspended cells determined. Immediately afterwards, cells were placed back into their pausing environments to ensure temperature shifts were kept to a minimum. It was not known if this brief resuspension affected cell viability, but it did not appear to. The highest number of viable cells for each of the days tested were those paused at 4 and 8 °C; amazingly, by day 8, cells paused at these temperatures still kept over 90 % viability, despite not being agitated or buffered. The 4 °C environment used was the cold room in our laboratory, which was highly accurate in keeping temperature, whilst the 8 °C environment was a small refrigerator containing two independent thermometers. The decision to attempt pausing using room temperature (which was recorded over several days as around 23 °C in the laboratory ) was to observe if cells could instead be placed within a secure cupboard, and thus would eliminate the need for refrigeration altogether. It was considered remarkable that cells kept within a cupboard at ambient temperature remained around 80 % viable, even by day 4, but not surprising that viability dropped further by day 8. For cells paused at 37 °C, the sudden drop in viability by day 2 was always expected; tubes were not agitated and caps sealed, but the physiological relevant temperature remained and so cells were not subjected to any cold shock. The pH likely increased rapidly as cells attempted to grow, but no buffering was possible.

The optimal pausing temperatures reported by Hunt et al. (2005) were actually 6, 17 and 22 °C. This was determined by pausing an adherent CHO cell line in microcentrifuge tubes for 4 days without agitation. In their case, cells paused at 4 °C had viabilities below 30 %, whilst those at 6, 17 and 22 °C were at least 60 % viable, with cells at 17 °C remaining the most viable. The difference in the work here to that seen by Hunt et al. is likely down to

the specific cell line used, as well as it being an adherent cell line paused in suspension. Just like here, a  $1.0 \times 10^6$  cell $\text{mL}^{-1}$  cell density was used. Later experiments by Hunt et al. paused cells again at 6 °C for 2, 6 and 20 days, with the viability decreasing to 60 % by day 6, and to 40 % by day 20. From this and the data presented here, it is suggested that the optimal temperature is likely cell type- and cell line-specific and should be empirically determined every time for new cells.

Exposing mammalian cells, including CHO cells, to hypothermic temperatures results in cold shock, which is a form of thermal stress. Whilst prolonged cold shock will almost certainly kill whole mammals (with the exception of those that hibernate), cells that have been isolated from these mammals can often 'survive'. The wide array of cellular responses to this, which are essentially stress responses, has been discussed in the literature, albeit with more emphasis on mild hypothermia (for the purposes of biopharmaceutical production in culture), as demonstrated with data previously in § 3.1.4 and later in § 6.1.1. These responses to cold shock have been reviewed by Al-Fageeh et al. (2006) and include, but are not limited to; (i) a substantial reduction in metabolism, including a decrease in glucose and L-glutamine consumption; (ii) inhibition of metabolic waste release; (iii) arrest of the cell cycle (primarily in the  $G_1$  phase); (iv) disassembly of the cell cytoskeleton; (v) inhibition of translation, and (vi) a slowdown in ATP expenditure. The severity of these changes is likely related to the extent of the temperature drop, e.g. whilst cells may still grow, albeit very slowly, at mild hypothermia, total cell growth arrest may be observed at severe hypothermia, as was the case here. It must be remembered cells are sealed during pausing, so severe hypothermia and even hypoxia has to be considered, although at lower temperatures the amount of oxygen that can dissolve actually increases.

The data obtained for CHO-S IgG pausing were very promising, with cells able to be stored with minimum effort, at 4 and 8 °C, for up to 8 days with viabilities remaining above 90 %. The health of cells upon awakening, i.e. when returned to 37 °C, CO<sub>2</sub> exposure and agitation, was the next consideration. It was decided cell growth and IgG titre within shaking culture were two parameters that could be measured after pausing to determine what effect hypothermic storage had on cells once they had awakened. The above pausing techniques described were repeated, with cells paused once again for 2, 4 and 8 days. At these time-points, cells were resuspended and seeded into TubeSpin vessels for subsequent growth studies. A subculture was attempted on day 5 of these cultures.

Figure 4.2A shows the viable cell densities during the first suspension culture (P1) of cells previously paused at 4, 8 and  $23 \pm 1$  (RT) °C for 2, 4 and 8 days. A non-paused culture was included as a benchmark for comparison. Pausing, for any of the time periods tested,

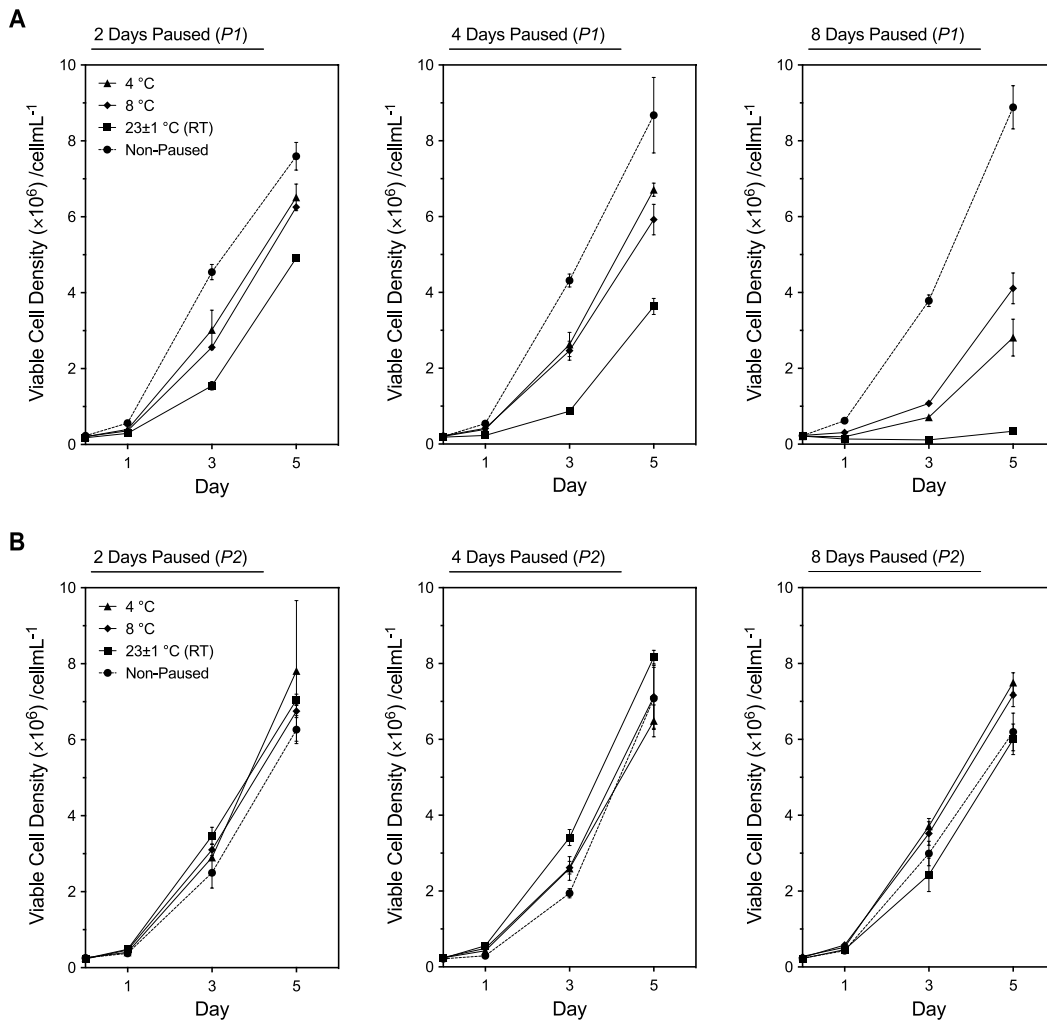


**FIGURE 4.2** Effect of temperature and pausing duration on subsequent regrowth of CHO cells in suspension culture using TubeSpin vessels. 5 mL CHO-S IgG cells, at  $1.0 \times 10^6$  cellmL<sup>-1</sup>, were seeded in centrifuge tubes and ‘paused’ at either 4, 8 or  $23 \pm 1$  (RT) °C for 2, 4 and 8 days. On these days, cells were gently resuspended and seeded into TubeSpin vessels for (A) suspension culture at 37 °C for 5 days (*P1*), before (B) subculturing for a further 5 days (*P2*), with viable cell density determined on days 0, 1, 3 and 5 for both. RT, room temperature. Data represent mean  $\pm$  SD,  $n=3$  (biological triplicate).

caused a reduced growth rate for subsequent cultures upon awakening, with differences in growth observed at days 3 and 5 of the suspension cultures. For cells paused at room temperature for 2 days, growth was stunted the most when compared with cells paused at 4 and 8 °C. This trend continued for cells paused for 4 and 8 days, with those paused at room temperature having decreasing growth rates; cells paused at room temperature for 8 days subsequently achieved very low cell densities, with an extremely stunted growth rate. Cells paused at 4 and 8 °C shared similar growth patterns when paused for 2 and 4 days, achieving around  $6.0 \times 10^6$  cellmL<sup>-1</sup> by day 5. However, for cells paused for 8 days a reduction in growth rate became apparent for both temperatures and a difference in growth

between them was now observed. Cell densities achieved by day 5 were between  $2$  to  $4 \times 10^6$  cellmL<sup>-1</sup>, with cells paused at 8 °C now reaching a higher cell density than those paused at 4 °C.

Figure 4.2B shows the viable cell densities during the second suspension culture (P2) of cells previously paused at 4, 8 and 23±1 (RT) °C for 2, 4 and 8 days. These cultures were seeded using cells from day 5 of the first suspension culture (P1). The cell growth achieved for each culture was now more uniform, regardless of the amount of days cells were previously paused, with no considerable difference by day 5 between any of the cultures.

For each of the time points in this experiment, cells were not returned to pausing once viabilities were taken, but instead seeded into shaking culture. The aim was to determine if normal or near-normal cell growth could be resumed, despite hypothermic storage. The viabilities of these cells after pausing matched those found in Fig. 4.1 (data not shown), indicating the reproducibility of these conditions. The most immediate observation from the awakening data were that the pausing of cells caused an extended lag phase once cells were back in routine culture. This lag phase increased depending upon both the temperature used to pause cells and the period of time that cells were paused. As expected, this was most apparent with cells paused at room temperature; the small growth achieved by these cells after 8 days paused indicated simply storing cells in the cupboard was not optimal for ensuring normal or near-normal growth once back in culture. The observation that, for cells paused at 4 and 8 °C for 2 and 4 days, the growth once awakened was not too dissimilar to non-paused cells was encouraging. This demonstrated for the first time the feasibility of using these two temperatures for hypothermia storage. Hunt et al. (2005) likewise resumed culturing after pausing at 6 °C for 2, 6 and 20 days, but relied on the heterologous expression of GFP as an indirect measurement of cell growth, so direct comparisons cannot be made here. However, the authors found similarly that the length of pausing had an effect on subsequent GFP expression, with cells paused for 20 days having an extended 'lag phase'. Interestingly, by day 5 cells paused for 2 and 6 days eventually reached similar GFP expression levels, whilst those paused for 20 days approached similar expression before day 6. Of course, this technique measured the productivity of the cells rather than their actual growth.

The subculture, or the second passage, carried out in this work gave data as expected; the results were similar to that seen during the passaging of previously dissociated cells in § 3.1.3. If an extended lag phase was indeed happening, it was suggested taking a seed on day 5 on the first passage would effectively mean seeding the second passage with cells actually at early exponential stage. On the other hand, subculturing the non-paused cultures on day

5 meant seeding the next passage with cells at mid-stationary phase, which would explain its slight drop in growth in the second passage. However, the first theory does not exactly hold true; the cells paused at room temperature for 8 days achieved very little growth after 5 days, yet they showed a rebound during the culture of the second passage, as was the case with the other pausing periods. There was possibly some recovery process going on, as cells 'awakened', and it was proposed to simply passage at an earlier time point to attempt to return the cells to normal function more rapidly. Hunt et al. (2005) did not attempt subculturing in their experiments.

As was the case in Chapter 3, the measurements of viable cell density were only taken on days 0, 1, 3 and 5 and so no complete growth curve can be seen. A similar experiment was attempted, except Erlenmeyer flasks were used as vessels for awakened cells; the increased volumes meant daily samples could now be taken, and antibody titres also determined. Figure 4.3A shows the viable cell densities during the first suspension culture of cells previously paused at 4, 8 and  $23\pm 1$  (RT) °C for 4 days. The non-paused culture was, once again, included as a benchmark for comparison. With the growth each day now visible, the previously paused cells do not have an extended lag phase as previously thought; rather, the growth achieved during the lag phase is lower before a stationary phase occurred. The cells paused at 4 and 8 °C shared almost matching viable cell densities, with cells paused at room temperature showing the lowest. Interestingly, all three previously paused cultures appeared to 'jump' in their viable cell densities after day 6, resulting in what appeared to be a transient stationary phase. Because of this, the cultures previously paused at 4 and 8 °C actually reached the same viable cell densities as the non-paused cultures by day 7.

The IgG titre was determined daily, with a reduction in titre seen between days 4 and 5 for all previously paused cells. However, by day 7 cells previously paused at 4 and 8 °C achieved the same titre as the non-paused cultures, agreeing with that seen by Hunt et al. (2005). The cell-specific productivity,  $q_P$ , was determined for all cultures at two different time periods, between 0 to 5 days, and between 0 to 6 days. For the former, the non-paused cultures had the higher  $q_P$ , approaching  $6 \text{ pgcell}^{-1}\text{day}^{-1}$ , whilst for the latter, interestingly, all cultures had similar productivities between  $7\text{--}8 \text{ pgcell}^{-1}\text{day}^{-1}$ . This may be caused by a general lag in cellular function for all cells that were paused.

Figure 4.3B shows the suspension culture of cells previously paused at 4, 8 and  $23\pm 1$  (RT) °C for 4 days, except in this instance they were subcultured to a second passage on day 3. For the first passage (P1), the pattern in growth was as previously; yet for the second (P2), all previously paused cultures now grew at similar rates, with these cells actually achieving

higher growth from day 2 until day 6, when compared to the non-paused cultures. The IgG titres were also determined daily, and now showed a similar pattern between all cultures.

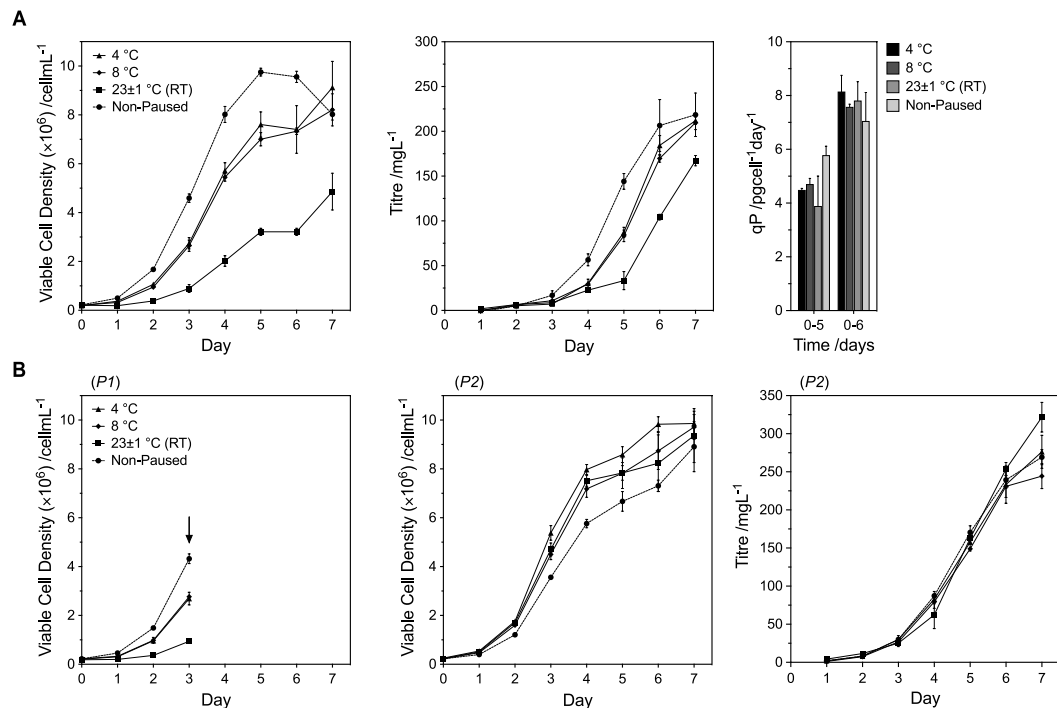


**FIGURE 4.3** Effect of temperature and pausing duration on subsequent regrowth of CHO cells in suspension culture using Erlenmeyer flasks. 5 mL CHO-S IgG cells, at  $1.0 \times 10^6$  cellmL<sup>-1</sup>, were seeded in centrifuge tubes and ‘paused’ at either 4, 8, 23±1 (RT) or 37 °C for 4 days. On this day, cells were gently resuspended and seeded into 125 mL Erlenmeyer flasks for (A) suspension culture at 37 °C for 7 days, with IgG titre determined daily. This was repeated except (B) at day 3 (black arrow), cultures were subcultured for a further 7 days. RT, room temperature. Data represent mean ± SD, n=3 (biological triplicate).

The data here matched the regrowth experiment previously carried out using TubeSpin vessels. The jump in viable cell density after day 6 was intriguing; it did not occur with the non-paused cultures and so could be the consequence of some cellular function eventually resuming after the pausing period. For cells paused at 4 and 8 °C, there is, however, overlap between the error bars of the data points on days 6 and 7. Repeating this experiment would be helpful to see if this sudden increase in viable cell density occurs again. Hunt et al. (2005) could not report a similar finding due the use of GFP expression as an indirect measurement of cell growth. However, in a separate experiment which measured cell number directly, the regrowth of CHO and HEK cell lines previously paused at 4 °C revealed there was a slight boost towards the end of the culture, with cultures eventually reaching similar viable cell densities as the non-paused cells. The qP, when determined between days 0 and 6, demonstrated an apparent switch from cell growth and the accumulation of biomass to IgG production — in much the same way as usually occurs when mammalian cells are

subcultured at mild hypothermic temperatures. For instance, the cells paused at room temperature achieved similar qP to the non-paused cells, despite not achieving a similar cell density and despite being previously sealed in a cupboard for 4 days.

The return to normal growth, as demonstrated when paused cultures were subcultured on day 3 within Erlenmeyer flasks, offers a technique to speed up the awakening process for previously paused cells. It must be remembered that subculturing, by its very nature, effectively takes the most viable cells from the current passage into the new one, and so this could simply be a case of carrying over the cells least affected by cold shock. The time and materials needed to perform an initial subculture several days after awakening may be a tolerated requirement for cell pausing, especially when compared to cell storage via cryopreservation.

#### 4.1.2 ADHERENT CELL PAUSING

The pausing of adherent CHO cells was of greater interest due to its potential use in any cell retention device developed in this work. The ability to simply and easily store cells, themselves adhered onto a structure (be it microsphere or otherwise), could prove extremely beneficial for research and development purposes. The biggest issue posed by the use of severe hypothermia was any possibility of cell detachment during the pausing period. Mild hypothermia had already been shown, in § 3.1.4, to cause considerable detachment of CHO-S IgG cells adhered to polyethylenimine substrates. Hunt et al. (2005) confirmed cool temperatures used for pausing did indeed cause dissociation of cells from vessels, with both CHO and HEK cells detaching from uncoated polystyrene surfaces, when stored at 4 °C for 9 days. This occurred even in the presence of serum.

It was decided a visual analysis of the morphologies of cells, adhered to adhesion substrates, after pausing via severe hypothermia would be interesting. Figure 4.4A and 4.4B, on the next page, shows the morphology of CHO cells paused whilst adhered to fibronectin and polyethylenimine substrates, respectively. Cells were adhered to glass plates overnight and paused the following morning at either 4 or 8 °C for 4 days. The 37 °C (non-paused) micrographs show the morphologies of cells immediately before pausing. These observations match those seen previously in Chapter 3; cells adhered to fibronectin took on elongated shapes, with ‘classic’ adherent cell morphologies seen. Cells adhered to polyethylenimine remain rounded, yet multiple contact points, which appeared as ‘stretched’ areas of the membrane, can be seen between each cell and the plate surface.

Pausing revealed obvious visual effects on cells adhered to fibronectin and polyethylenimine substrates; however, the apparentness of these effects depended upon the temper-

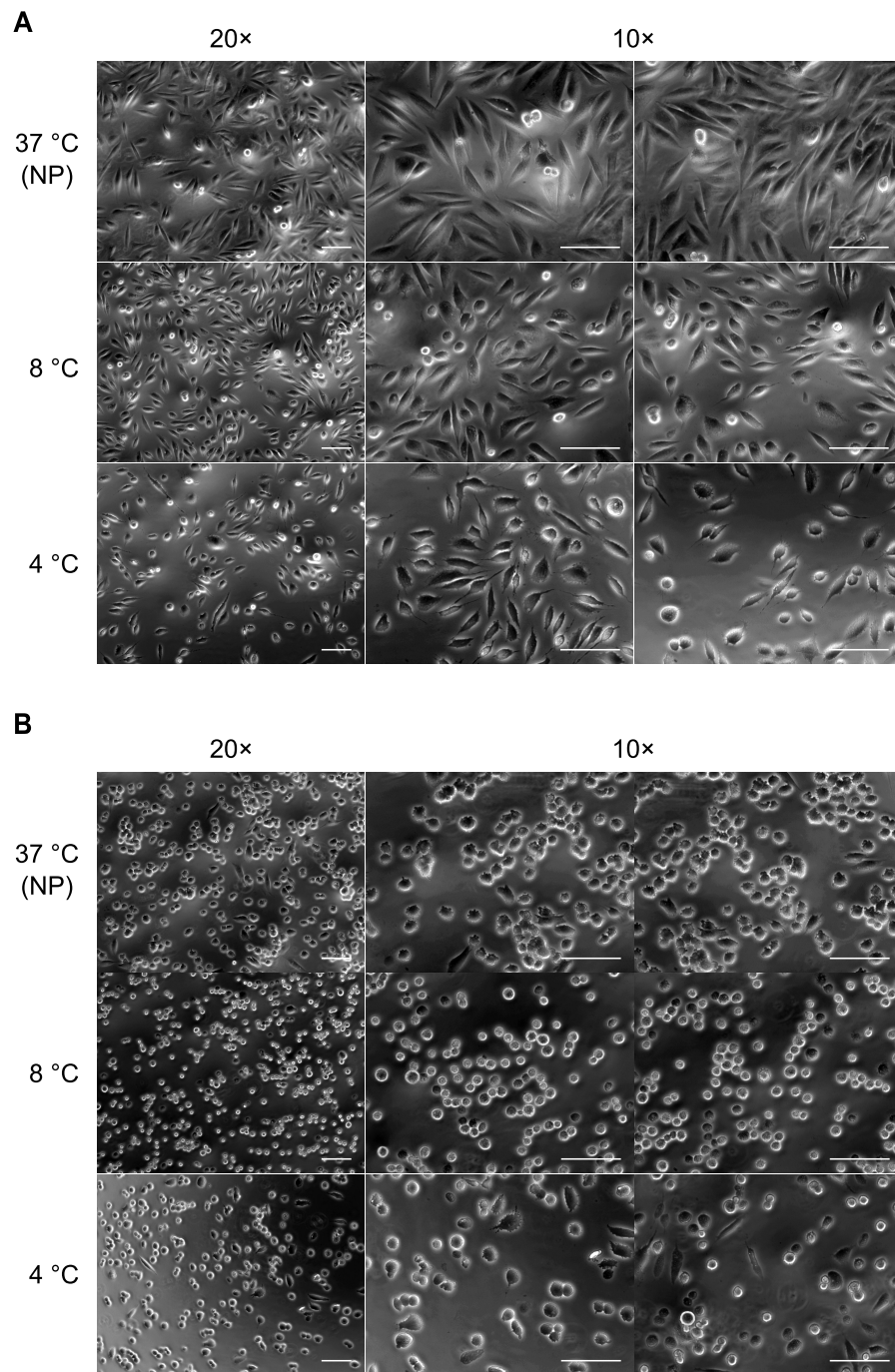


**FIGURE 4.4** Effect of temperature, for cell pausing purposes, on the morphology of CHO cells adhered to polyethylenimine and fibronectin substrates. 150,000 CHO-S IgG cells adhered to PEI and FN substrates on untreated 8-well glass plates were ‘paused’ for 4 days at either 4 or 8 °C. After washing, adhered cells were fixed, and (A) cells on fibronectin and (B) cells on polyethylenimine imaged using a phase contrast microscope at 10× and 20× magnifications. NP, non-paused. Scale bars = 100 μm.

ature employed. For all temperatures and substrates, pausing for 4 days caused cells to slightly shrink and appear rounded. Cells adhered to fibronectin and paused at 8 °C ap-

peared less elongated, with cells seeming to separate from one another. This effect was amplified for those paused at 4 °C, with cells now appearing 'shrivelled' with spider-like contact points visible between cells and the vessel. Cells adhered to polyethylenimine revealed similar observations when paused, with those at 8 °C becoming much more rounded in shape, with less contact, or 'stretched' areas, visible on the vessel surface. Once again, this was exaggerated for cells paused at 4 °C. For the smaller number of cells which had taken elongated shapes prior to pausing, storing them at 4 °C also caused them to show spider-like contact points with 'wrinkled' appearances.

The use of severe hypothermia had a striking effect on the appearance of adhered cells, with these changes likely a result of cold shock on the cell cytoskeleton. Changes to cytoskeletal components, including the membrane, have been demonstrated with cells placed in low temperature environments. The culturing of CHO-K1 cells by Roobol et al. (2009) at 4 °C for just 6 hr caused cells to become rounded and less well spread, whilst those at 27 °C did not show these same observations and appeared similar to cells kept at 37 °C. Any change in cellular appearance is likely to be cell line-specific and highly likely to be cell type-specific. Neutelings et al. (2013) cultured adherent human lung fibroblasts for 5 days, at just 25 °C, and reported detachment and morphological alterations, with cells now rounded and 'apoptotic-like'. These new appearances persisted even after 37 °C had been restored for 24 hr.

Glass was chosen for this experiment due to the optical properties, with clearer micrographs capable. Whilst far outside the scope of this work, the selective staining of individual cytoskeleton components may be useful here. With the potential application of cell pausing, the effect of severe hypothermia on detachment and cellular function is important. In the above experiment, the viability of cells was not determined and cells were washed twice before imaging, so any detachment, if present, was not observed or measured. The pausing of adherent cells was attempted again with polystyrene plates, but PrestoBlue and trypsinisation was now employed to determine if cells were indeed being detached.

Figure 4.5A shows the number of cells present after CHO cells, adhered to fibronectin or polyethylenimine substrates, were paused for 2, 4 and 8 days at either 4 or 8 °C. PrestoBlue was used in this instance, with the fluorescence observed with cells prior to pausing being assigned 100 % (dashed lined), and all fluorescence values thereafter normalised to this. A non-paused culture at 37 °C was included as a control. Paused cells were washed twice before incubation with PrestoBlue to determine fluorescence values. Cells adhered to both fibronectin or polyethylenimine substrates, at either of the two temperatures, experienced similar reductions in fluorescence when paused at 2 or 4 days. Cells paused at 4 °C for 8

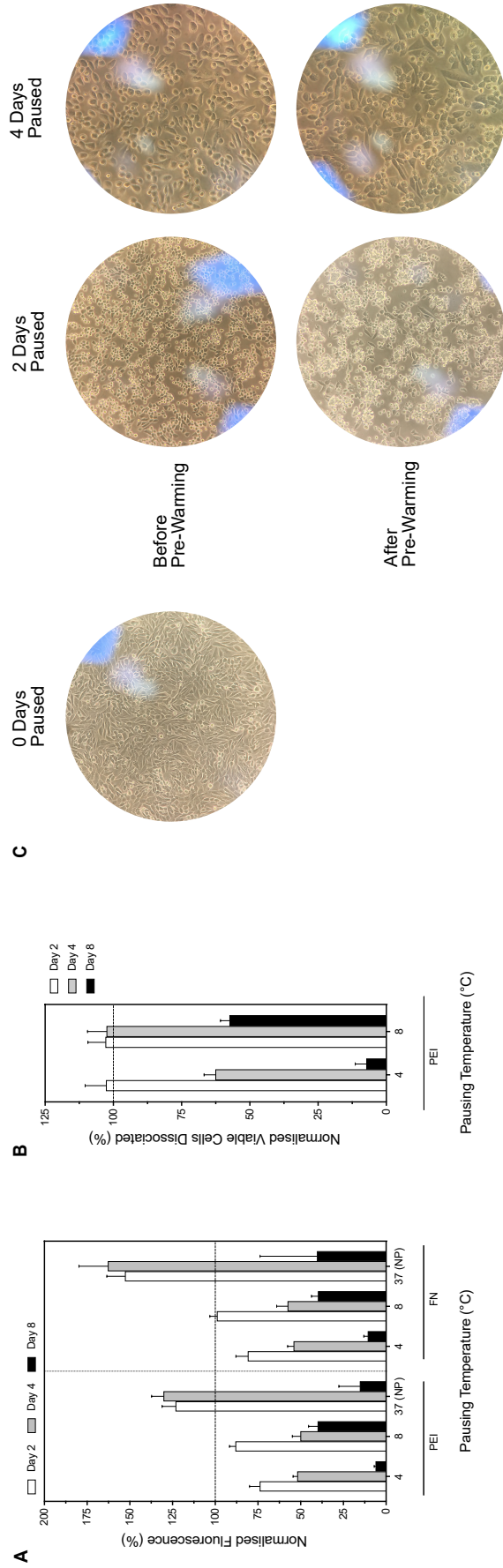


**FIGURE 4.5** Effect of temperature, for cell pausing, on dissociation of CHO cells adhered to polyethylenimine and fibronectin substrates, and the effect of pre-warming on paused adherent cells. 1.5 million CHO-S IgG cells adhered to PEI and FN substrates on Nunclon Delta 24-well plates were ‘paused’ for 2, 4 or 8 days at either 4 or 8 °C. After washing, adhered cells were quantified by either (A) PrestoBlue or (B) dissociation by 0.25 % trypsin/EDTA. For (A) and (B) data were normalised to the cell load on day 0, i.e. before pausing began, with 100 % being the concentration of those cells. In a separate experiment (C), 1.0 million CHO-S IgG cells were adhered to PEI substrates in 24-well plates and paused at 8 °C for 4 days. On days 2 and 4, plates were immediately imaged (before pre-warming) before being placed in a 37 °C incubator, with 5 % CO<sub>2</sub> exposure, for 3 hr and imaged again (after pre-warming). 0 Days Paused refers to the cells after they were loaded and immediately before being paused. PEI, polyethylenimine; FN, fibronectin; NP, non-paused. Data represent mean ± SD, n=3 (biological triplicate).

days showed a greater reduction in fluorescence than those paused at 8 °C. This was similar for both adhesion substrates. As expected, the non-paused cultures grew on days 2 and 4 before experiencing a dramatic drop in cell number by day 8. These data were surprising and disappointing, but it did not match what was observed. Whilst some detachment of cells was evident upon washing, it did not correlate with the severe reductions in fluorescence seen after incubation with PrestoBlue. Indeed, the data suggested that around 50 % of cells were detached by day 4, for both substrates, but over half the surface area of the wells still visually retained cells on this day, particularly for cells paused at 8 °C. It was quickly suggested that, remembering PrestoBlue is essentially a measure of cell metabolism, the use of this assay was not suitable on cells which had been subjected to severe hypothermia — which affects metabolism — for extended periods. Repeating the experiment, but instead dissociating the cells with trypsin on each of the days and using direct cell counting was attempted.

Figure 4.5B shows a repeat of the experiment just described, except using dissociation via trypsinisation to observe any detachment from cell pausing. Only polyethylenimine was employed as an adhesion substrate in this instance. For this experiment, the number of cells directly counted by the trypan blue exclusion method after trypsinisation was assigned 100 %, with all cell counts thereafter normalised to this. The difference when compared to Fig. 4.5A is apparent; pausing cells for 2 days at either 4 or 8 °C did not cause any cell detachment, despite cells being washed prior to trypsinisation. Cells paused at 8 °C for 4 days continued to experience no detachment, yet those stored at 4 °C for this same period did, with cell numbers falling below 70 %. For cells paused for 8 days, the correlation between detachment and temperature continued; cells at 4 °C dropped below 15 % of their initial number, whilst those at 8 °C dropped to less than 60 %.

The use of 8 °C as a pausing temperature was favourable over 4 °C, with less detachment observed from cells adhered to polyethylenimine substrates. The ultimate aim would be to load a cell retention device to full capacity before placing it within a severe hypothermic environment for pausing. Because of this a suspension of 1.5 million cells was chosen here to load onto 24-well plates as this was found, in earlier work, to cover the entire area of each well. However, the data here did not show what effect pausing had on adhered cells, in respect to their growth or productivity, and if it differed to that seen with cells paused in suspension. This remains an area of future work.

Figure 4.5C shows images obtained before and after the pre-warming of paused cells adhered to PEI-adsorbed wells. Cells were paused for 2 and 4 days, with separate plates used for each time point to ensure cells were not placed back into pausing conditions after day

2. The effect of pre-warming (placing plates in an incubator at 37 °C, 5 % (v/v) CO<sub>2</sub> for 3 hr, was immediately apparent on the morphology of the cells. As first shown in Fig. 4.4, paused cells took on a rounded appearance (similar in shape to yeast) with a reduced size. These changes appeared to reverse after the pre-warming step, with visible evidence of cells regaining attachment points to the well surface and losing their rounded appearance. This was most apparent with cells paused for 4 days, with most cells rounded by that time.

'0 Days Paused', in this instance, shows the cells immediately before they were paused at 8 °C. The visual differences between day 0 and days 2 and 4 (before pre-warming) showed that pausing caused cells to shrink and lose their confluency. After pre-warming, cells appeared somewhat aggregated as they took on reattached morphologies but remained in their 'new' locations on the well surface. Whilst not attempted here, it was suggested pre-warming could be utilised as a method to reduce the loss of adhered cells during pausing. With some evidence of cell detachment observed in Fig. 4.5B, heating plates for several hours could enable the reattachment of cells that had previously detached during the pausing process.

#### 4.1.3 CONCLUSIONS

The work in this chapter began to explore the use of severe hypothermia to store, or 'pause', CHO cells for prolonged periods without the need for cryopreservation. It was expected these techniques could eventually be employed for the pausing of CHO cells within external cell retention devices, such as the one developed here. This could enable rapid and on-demand pausing and awakening of different cell cultures. The use of hypothermia to store CHO cells has been neglected in the literature, with only Hunt et al. (2005) investigating this potential application with dedicated experiments. The aim here was to determine a temperature suitable to pause a specific cell line, CHO-S IgG, both in suspended and adhered cultures.

A selection of temperatures were first tested, for a range of days, using CHO-S IgG cells in suspension culture. Cells paused at 4 or 8 °C kept the highest viabilities and seeding these previously paused cells back into shaking culture at 37 °C revealed they could indeed be re-grown, albeit with lower cell densities achieved. Subculturing cells once appeared to return cell growth and IgG titre to normal levels. The findings were interesting, as the optimum pausing temperatures did not entirely agree with Hunt et al. (2005), which instead chose 6 °C, and found 4 °C unsuitable.

It was known prior to these experiments that temperatures below 37 °C affected the ability of cells to remain adhered to vessel surfaces. Detachment from T-25 flasks was previously

demonstrated when CHO-S IgG cells, adhered to polyethylenimine substrates, were cultured at 30 °C. The appearance of adhered cells, when paused at low temperatures, was determined. Micrographs were acquired for cells adhered to fibronectin and polyethylenimine substrates and paused at either 4 or 8 °C for 4 days. Visual observation revealed changes in cell morphology, with the majority of cells now displaying a rounded, shrunken appearance. For those paused at 4 °C, these observations were more striking. Literature on the effects of hypothermia on adherent cell lines agreed with this data, and confirmed the cytoskeleton is strongly affected by cooler temperatures. Finally, the extent of cell detachment from pausing was briefly investigated, with 8 °C, as opposed to 4 °C, found to keep cells adhered for longer periods.

This chapter was a side project, and indeed was a tangent to the main aim of the work presented here. However, as with most of the experiments in this thesis, it has acquired data which may prove useful for the development of future techniques. Whilst the pausing of immortalised cell lines is largely an academic exercise at present, the use of hypothermic storage could become more widespread if it can be shown the effects on cells are kept to a minimum.

---

# Chapter 5

---

## POLYHIPE MICROSPHERE TECHNOLOGY

---

### OVERVIEW

This chapter presents the results obtained in the middle of the project, which focused upon the development of acrylic polyHIPE microspheres and their possible use as the physical component of the cell retention device. It is divided into two parts; (i) the development of polyHIPE microspheres, including a focus on the conditions required to fabricate highly monodisperse, macroporous microspheres, and (ii) the initial uses of these fabricated microspheres, including functionalisation with polyethylenimine and subsequent seeding with cells at high density within novel cell loading systems. The majority of the work presented in this chapter is materials science-related and discusses the challenges that needed to be overcome for the adaptation of polyHIPE microspheres, and their fabrication, for use in this project.

### 5.1 INTRODUCTION TO POLYHIPE MATERIALS DEVELOPMENT

Polyethylenimine had previously been identified as an inexpensive, animal origin-free adhesion substrate. It was found to be as effective as animal-derived proteins and other commonly used animal origin-free substrates, and so was taken forward as the chemical component of the cell retention device. The next task was to develop a fabrication process for the physical component of this proposed retention technology. One of the major benefits from employing continuous culture is intensification, or the ability to sustain very high cell densities at smaller volumes — however, this is only possible if the cell retention device can itself hold a large number of cells.

Microspheres were suggested as the physical component of the cell retention device due to their potentially high surface-area-to-volume ratios. Such an attribute means simply that a relatively small volume of microspheres can adhere and retain a large number of cells. It was reasoned macroporous microspheres, i.e. spherical structures containing pores large enough to permit cells entry to internal surfaces, would present even greater surface areas for cells to attach. Microspheres are also versatile and scalable; they can be utilised within virtually any vessel and, potentially, at any volume. Microspheres, or microcarriers, are currently available commercially in either solid, microporous and macroporous formats. However, they frequently demand coating with serum — to encourage the adsorption of attachment proteins — before cells can be attached. They are also generally expensive and

so any plan for scaling up or out needs to take this into consideration. Many cell retention devices have been demonstrated and indeed employed industrially, with some available to purchase. But the lack of versatility (many retention devices need to be paired with corresponding systems) and the relatively large scales (there are no easily adaptable, bench-scale retention devices) meant these off-the-shelf products were, again, not compatible with the main aim of the project. Polymerised high internal phase emulsions, or polyHIPEs, were an attractive material type to explore for the purposes of retaining cells at high density. By their very definition, polyHIPE materials are at least 74 % porous; such materials, if obtained in microspheric formats and if paired with polyethylenimine substrates, could prove to be an extremely effective cell retention device. PolyHIPEs can be fabricated rapidly without high cost or advanced equipment, being particularly suitable for the in-house manufacture of specialised materials. They are usually fabricated using monomers industrially produced using synthetic sources, keeping with the animal origin-free requirement of the proposed cell retention device.

The Department of Materials Science and Engineering had prior experience of fabricating polyHIPEs, mainly in monolithic formats, for use as cell scaffolds and supports in tissue engineering applications. The fabrication of polyHIPE microspheres had also been reported by a group in the laboratory (Paterson et al., 2018), where the acrylic monomers 2-ethylhexyl acrylate (EHA) and isobornyl acrylate (IBOA) were used within a bespoke lab-scale fluidic system. This system, which was available to use for the work here, could be readily modified as required by the operator. The very nature of HIPE generation meant the properties of the resultant polyHIPE could likewise be easily changed to meet the demands of the application. This prior experience in a neighbouring department made polyHIPEs an attractive option to explore for the physical component of the cell retention device.

The main objective of the work presented in this chapter was to adapt current in-house polyHIPE materials for use with polyethylenimine substrates. The chemical and physical components would combine to become the in-house cell retention device. The specific objectives for the first part of this chapter were to; (i) ensure the monomers used for polyHIPE fabrication are suitable for microsphere handling, and (ii) rapidly and reproducibly fabricate < 300  $\mu\text{m}$  macroporous polyHIPE microspheres, ensuring a high degree of monodispersity. The second part of this chapter looks at the initial applications of the polyHIPE microspheres that were ultimately developed.

### 5.1.1 BUILDING IN CARBOXYL FUNCTIONALITY

It is widely known that polymeric materials fabricated using hydrocarbons, such as styrenic or acrylic monomers, are hydrophobic. As demonstrated in Chapter 3, treated

(hydrophilic) polystyrene was more effective at attaching and allowing the adherent growth of CHO cells than untreated (hydrophobic) polystyrene. Whilst it has been shown previously in this work that the attachment of CHO cells can be vastly improved by the prior adsorption of adhesion substrates, other issues may arise when the polymeric material is not a plate or a vessel, but rather a suspension of microspheres. For instance, untreated polystyrene microspheres will rapidly aggregate when placed in aqueous solutions, including cell culture medium. It is correct to suggest that adsorbing adhesion substrates to polystyrene microspheres would increase their wettability and prevent this; however, the aggregation within the coating solution itself may actually hinder adsorption. Solutions do exist to overcome this. Polystyrene microspheres are often fabricated with a surfactant to ensure proper stability in solution. Some manufacturers suggest the addition of a surfactant post-fabrication, such as Tween 20, to help break up clumps when they occur. However, there is still the issue presented to the operator of ensuring sufficient adsorption of substrate, with questions asked as to whether there is any competition occurring between the surfactant already present and the substrate added.

These issues were particularly important in the work presented here; microspheres were to be fabricated in-house, washed and sterilised and then adsorbed with polyethylenimine. It had to be guaranteed that microspheres would not aggregate upon fabrication, or during the coating process, or even later in medium during culture. Whilst this may appear trivial to readers, the aggregation of microspheres in the early stages of the project proved to be extremely troublesome — and frequently delayed the next section of planned work. It was proposed that a monomer, containing a reactive functional group, could serve to stabilise fabricated polyHIPE microspheres. Such a group could be ionic in nature and thus cause electrostatic repulsion between neighbouring microspheres when in aqueous solutions, such as coating buffers or culture medium. These localised repulsions, if strong enough, would eliminate aggregation and allow a stable suspension of microspheres.

Previous polyHIPE work carried out by the Department of Materials Science and Engineering employed numerous acrylic monomers, such as EHA and IBOA as monomers and trimethylolpropane trimethacrylate (TMPTA) as a crosslinker — a cross linker being a monomer employed to join adjacent polymer chains. Whilst compatible with the generation of a HIPE, none of these three monomers contained any functional groups of interest. This posed no issue when monolithic polyHIPEs were desired, as the materials could be easily coated with serum, or any dedicated adhesion substrate, prior to cell culture without the risk of aggregation. However, for microspheres, the lack of any reactive groups may cause handling issues post-fabrication, including clumping, and indeed this did occur. With respect to their chemical structures, the acrylic family is diverse with

---

countless monomers available to purchase from multiple suppliers. This diversity means acrylic monomers exist that indeed contain reactive functional groups. Theoretically, these monomers could be included in a HIPE, rapidly cured upon exposure to UV radiation and the resultant polyHIPE then presumed to possess these same functional groups within its structure. In practice, and particularly for the generation of high volume emulsions like HIPEs, it is not so simple. The presence of one or more functional groups may impact the formation of the emulsion (particularly if the monomer is not sufficiently hydrophobic) or, if successfully formed at first, the emulsion may eventually become unstable and the phases separate before polymerisation can be performed.

A literature search revealed several acrylic monomers with potentially useful functional groups. The first, trimethylolpropane tris(3-mercaptopropionate), possessed three thiol ( $-SH$ ) moieties and had been demonstrated as compatible for the fabrication of stable polyHIPEs by Langford et al. (2014). In this instance, the authors were mostly concerned in the potential to use monolithic polyHIPEs for thiol-ene 'click' chemistry reactions, rather than to overcome aggregation or improve material handling. The second, 2-aminoethyl methacrylate hydrochloride, contained a primary amine ( $-NH_2$ ) group. This had already been investigated as a potential monomer in the laboratory, but it was supplied as a coarse powder and could not be easily dissolved in either water or any other solvent tested. It was regarded as not compatible for HIPE generation, but further investigation into this could prove worthwhile. For instance, if polyHIPE microspheres were fabricated entirely using this monomer, and if the primary amines were indeed exposed on the surfaces of each structure, coating with a substrate such as polyethylenimine (which, of course, encourages adhesion via its amines) may not be strictly needed. Essentially, this could enable the fabrication of a ready-to-use cationic microsphere.

The third and fourth monomers identified both contained a single carboxyl ( $-COOH$ ) group; mono-2-(methacryloyloxy)ethyl maleate and mono-2-(methacryloyloxy)ethyl succinate (later assigned the initialism 'MAES' in this work). The covalent linking of an amine to a carboxyl, to form an amide bond, was a well-established reaction and so could potentially be used to chemically link fabricated microspheres with polyethylenimine substrates. It was also known that carboxyls will cause repulsion between structures in aqueous solutions due to their charged, ionic forms in pH 7 environments. No reports in the literature could be found regarding the use of these two monomers in polyHIPE synthesis, although MAES had been employed previously within a polyelectrolyte brush (a type of responsive polymer, or smart surface) due to its carboxyl functionality (Xu et al., 2011). It was decided MAES would be purchased as the chemical structure appeared, from a glance, more suitable for polymerisation; a carboxyl group was present at one end

---

of the main hydrocarbon chain, with an acrylate double bond at the other end. It was expected this carboxyl group would be easily exposed within any polymerised material. Mono-2-(methacryloyloxy)ethyl maleate, in comparison, contained another C=C bond within its main chain and any reaction relating to this was not desirable. Fortunately, as with EHA and other acrylic monomers used in the laboratory, MAES was supplied as a viscous liquid and no dissolution testing was necessary. It was also inexpensive.

Before an attempt was made to fabricate a polyHIPE using this newfound monomer, a method to detect carboxyl groups within a porous, polymeric material was required. Critically, these carboxyl groups had to be exposed on the surface to give the material both hydrophilicity and the potential to covalently link with the amines present in polyethylenimine. Hayward et al. (2013b) employed the stain toluidine blue O (TBO) to visually detect carboxyl groups within polyHIPEs fabricated using acrylic acid. In this instance, the authors had simply added acrylic acid into the aqueous phase. These polyHIPEs did successfully incorporate carboxyl groups at their surface and as a result were stained after exposure to TBO. This mechanism of detection is based upon charge; TBO is a cationic compound (by virtue of its single tertiary amine) and will bind to negatively-charged chemical moieties (such as deprotonated carboxyl groups) within materials when incubated in basic ( $\text{pH} > 7$ ) solutions. Structures containing no negatively-charged groups will not readily stain and can be cleansed of the reagent upon prolonged washing. Hayward et al. (2013b) only provided visual data of TBO uptake (a sample alongside a control, which did not stain), but quantitative data would be beneficial to see if adding a greater volume of acrylic acid (or rather MAES, as for the work here) would consequently cause an increase in TBO uptake. This would then confirm a relationship between an increase in monomer and an increase in the concentration of carboxyl groups eventually present in the material.

A technique to determine the concentration of TBO — bound to carboxyl groups within a material — would be to extract, or release, TBO from the material and subsequently measure its concentration. TBO in solution is a brilliant purple and so its absorbance can be determined using a spectrometer. A method to extract TBO would rely on reversing the ionic interactions between the tertiary amine and any negatively-charged moiety within the material. Acetic acid had previously been used to extract bound TBO from carboxylic acid-containing structures (Jackson et al., 2014a). Due to its protic nature, the addition of acetic acid to a material bound with TBO would interrupt the ionic attraction and release TBO back into solution. Before this assay could be attempted, typical wavelengths of maximum absorbance of TBO would first have to be determined.

TBO was supplied as a fine, dark-purple powder. As acetic acid would ultimately be used

---

to extract TBO from any polyHIPE material, a range of solutions using 50 % acetic acid were first prepared. The absorbance of these could subsequently be measured, with spectra produced for each used to confirm that any wavelengths of maximum absorbance agreed with values reported in the literature. In this instance a NanoDrop spectrophotometer, which only required 2  $\mu\text{L}$  sample, was used. Figure 5.1A shows the full absorbance spectra, from 250 to 750 nm, for TBO dissolved in 50 % acetic acid at solutions of 25, 50, 100, 200, 300, 400, and 500  $\mu\text{M}$ . The spectra showed two peaks, or wavelengths of maximum absorbance; the first around 280 nm and the second around 625 nm. These two peaks gave greater absorbance values as the concentration of TBO was increased, as expected. The inset shows the spectra of 25  $\mu\text{M}$  TBO in greater detail, which gave absorbance values under 3. Figure 5.1B shows the full absorbance spectra for TBO, but this time dissolved in 50 % acetic acid at 50, 25, 12.5, 6.25, 3.125 and 1.5625  $\mu\text{M}$ , i.e. a serial dilution beginning at 50  $\mu\text{M}$ . The standard curve shows the absorbance at these concentrations, at 626 nm only (the primary maximum absorbance of TBO), with a regression line added. The  $R^2$  value was determined as 0.9998.

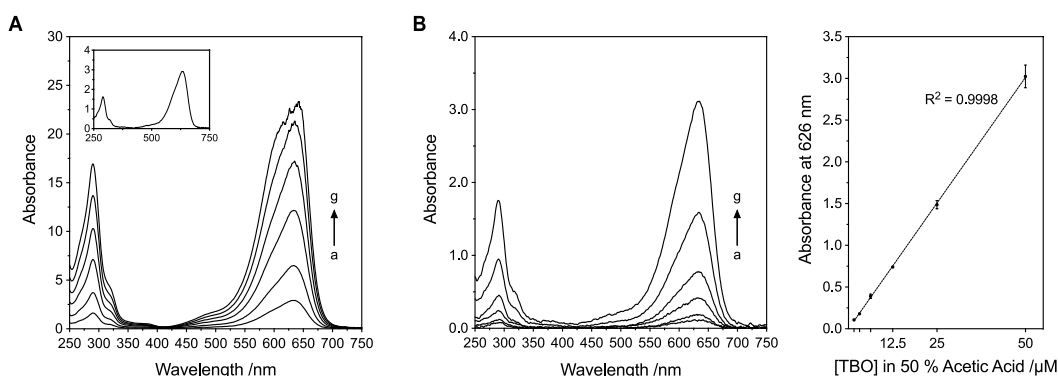


**FIGURE 5.1 Absorbance spectra of TBO at a range of molarities.** TBO was dissolved in 50 % acetic acid to give a range of molar concentrations, whose (A) absorbance spectra were determined (a, 25; b, 50; c, 100; d, 200; e, 300; f, 400; g, 500  $\mu\text{M}$ ); top left inset shows absorbance for TBO at 25  $\mu\text{M}$ , showing wavelengths of maximum absorbance at more suitable values, i.e. approaching 1.0. Starting from 50  $\mu\text{M}$ , a serial dilution was prepared whose (B) absorbance spectrum was determined (a, 1.5625; b, 3.125; c, 6.25; d, 12.5; e, 25; f, 50  $\mu\text{M}$ ) and a standard curve with absorbance at 626 nm also prepared. For the absorbance spectra in (A) and (B), only one technical reading was carried out. For the standard curve in (B), data represent mean  $\pm$  SD,  $n=3$  (biological triplicate).

TBO readily dissolved in 50 % acetic acid at all the molarities tested to give bright purple solutions, with 50 % acetic acid used as a blank before each absorbance measurement was performed. The highest molarities tested gave intensely coloured solutions. The two wavelengths of maximum absorbance observed, 280 nm and 625 nm, agreed with literature reports (Jebaramya et al., 2009; Jackson et al., 2014b), indicating the methods applied here

were correct to take forward as an assay for carboxyl group detection. High molarities of TBO were initially tested as a crude validation experiment, simply to see if any repeatable absorbance could be identified. For actual experimentation, these molarities were far too concentrated for absorbance testing and it was decided to use lower molarities, to ensure absorbance values of 1.0 or under, for eventual use in material analysis. The standard curve was determined using serial dilutions beginning at 50  $\mu$ M to see if this was indeed possible. These data, produced using absorbance values at 626 nm, confirmed the absorbance at this wavelength could be employed as a metric. This value could be later used for the accurate detection of carboxyl groups within any materials previously bound by TBO.

The generation of HIPEs, using increasing concentrations of MAES, was attempted. Due to its familiarity within the laboratory, EHA was paired with MAES in varying combinations to see what effect this may have, if any, on the formation of the emulsion. As with all polyHIPE work in the laboratory, TMPTA was used as a crosslinker and a surfactant, Hypermer B246, was added at 10 %. If an emulsion was successfully generated and a polyHIPE then fabricated, the materials could be exposed to TBO to determine if carboxyl groups, as present on MAES, were incorporated into the cured structure. The first test was to see if carboxyl groups would indeed be present in a polyHIPE, regardless of the specific material format. Because of this, the creation of monolithic structures was initially performed due to ease and speed of fabrication. Figure 2.2, shown previously in § 2.4.1, is a schematic detailing the tasks taken to generate the HIPEs described here, and indeed every HIPE, in this work.

The generation of HIPEs, containing EHA and MAES (as monomers) and TMPTA (as a crosslinker) was a success. MAES was added to a beaker at either 0, 2, 4, 8 or 16 % of the total monomer weight, after a corresponding amount of EHA had been added. Whilst agitating this monomer mix (which also contained the crosslinker and the dissolved surfactant) at 300 rpm, water was added dropwise over 5 min to make a 90 % HIPE. For all weights of MAES attempted, an emulsion began to form 20 s after the start of the water addition. The monomer mix, initially a clear sticky liquid, began to turn a milky white after this point. Continuing to add water increased the viscosity of the emulsion, as expected, until an opaque, white HIPE had formed. The final viscosity of the HIPE did not, at least by eye, appear to be as high as that seen with other HIPEs, particularly those generated using EHA and IBOA monomers. For HIPEs generated using IBOA, the emulsion eventually generated was a thick paste which could be ‘spooned’ out using a laboratory spatula. Interestingly, HIPEs generated with higher concentrations of MAES appeared to have reduced viscosities, relative to HIPEs generated using lower concentrations of MAES. Indeed, for those with 8 or 16 % MAES, the final HIPE could be easily poured or shaken by hand. How-

ever, the emulsion remained stable and did not separate, even if the beaker was removed from the stirrer and left undisturbed. These low viscosities would later prove to be highly beneficial in the fabrication of polyHIPE microspheres, as discussed in § 5.1.3.

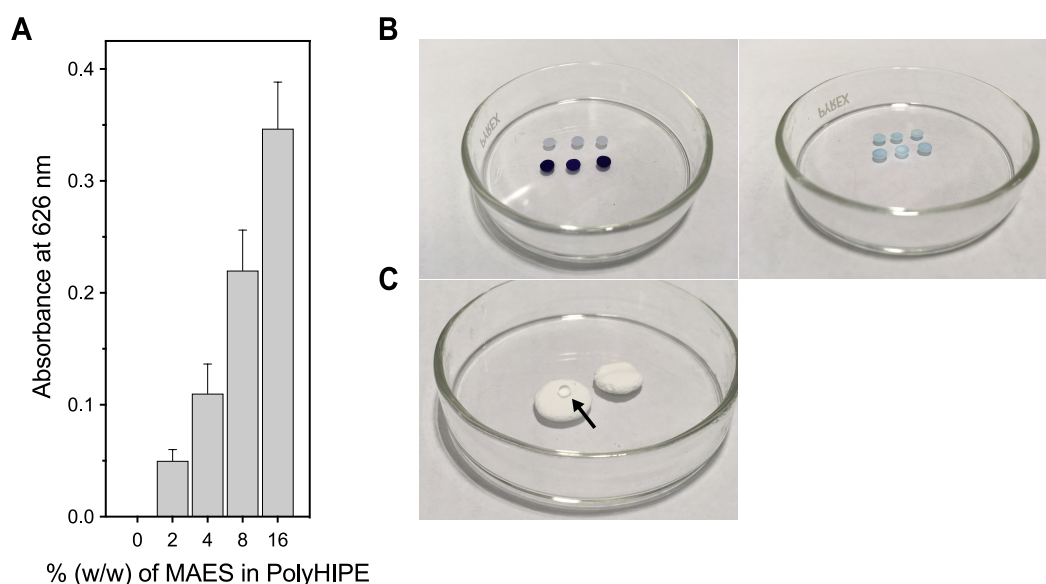
PolyHIPE monoliths containing MAES were fabricated by dispensing 300  $\mu\text{L}$  of each HIPE into wells of a 24-well plate, curing until polymerisation had occurred, and then cutting out disc-like shapes using a metallic cutter. Care was taken so as to ensure all discs were identical in dimension. Discs were washed in acetone before TBO exposure to cleanse the surfactant and any monomer remnants not cured during polymerisation. This acetone wash was performed for all polyHIPE materials, regardless of their monomer content, immediately after fabrication and so was continued here. Operators in the laboratory previously employed methanol for this wash, but it was found that methanol did not actually dissolve the surfactant, yet acetone did. Discs were later primed in glycine-sodium hydroxide buffer, at pH 10, to ensure full deprotonation of any exposed carboxylic groups, before incubation with 50  $\mu\text{M}$  TBO within a fresh solution of the same buffer. After incubation, all discs were washed for 24 hr, again with fresh glycine-sodium hydroxide buffer, before extraction with acetic acid and determination of absorbance at 626 nm.

Figure 5.2A shows the absorbance of TBO, at 626 nm, extracted from polyHIPE discs fabricated with increasing concentrations of MAES. As MAES was increased, the amount of TBO taken up, i.e. the amount bound to the carboxyl groups, also increased. This increase was confirmed by measuring the absorbance of the extracted TBO, with 2 % MAES giving an absorbance of 0.5, 4 % MAES over 0.1, 8 % over 0.2 and 16 % around 0.35. Thus, the concentration of MAES used in the HIPE dictated the concentration of carboxyl groups present in the resultant polymer material. PolyHIPEs fabricated using only EHA did not associate with TBO and did not give any extracted TBO upon acetic acid exposure. The acetic acid for these samples thus gave no absorbance when measured at 626 nm.

Figure 5.2B and 5.2C show visual evidence of TBO uptake and a difference in hydrophilicity between the 0 and 16 % MAES polyHIPEs; these materials were photographed after overnight washing following incubation with TBO, and again after TBO extraction. The 16 % MAES discs heavily associated with TBO, with the materials staining a deep purple. The 0 % MAES also did stain, however, the difference became apparent during the washing step. The 0 % MAES discs returned to their usual white colour, whilst the 16 % MAES remained stained. The TBO within the 16 % MAES discs was readily extracted upon acetic acid exposure, returning the polyHIPE to their white colour. In a separate experiment, crudely shaped discs of 0 and 16 % MAES were fabricated and water droplets dispensed upon both. The 16 % MAES materials were wettable, and rapidly absorbed the

droplet, whilst the 0 % MAES discs did not, with the droplet remaining upon the surface (shown by the black arrow). This experiment was done to simply demonstrate the striking effect of MAES on the hydrophilicity of the materials.

The 24 hr washing step, post-TBO incubation, was found to be critical to ensure non-specific TBO staining was cleansed out of the materials. All polyHIPE discs, including 100 % EHA materials, were initially stained by TBO. Indeed, TBO appeared to stain any material it contacted. It was after a washing step that only materials with specific TBO interactions remained stained. This appeared to be especially true for polyHIPEs, where their intense porosities and large surface areas appearing to encourage non-specific, widespread staining.



**FIGURE 5.2 TBO uptake for polyHIPE materials fabricated using MAES monomer.** MAES monomer was included in precursor HIPEs at 0, 2, 4, 8 and 16 % (w/w) concentrations. The polyHIPEs were exposed to TBO, washed overnight, the bound dye extracted and the (A) absorbance at 626 nm determined, with (B) photographs of 0 and 16 % materials taken. As MAES was increased in the precursor HIPE, the amount of extracted TBO also increased, indicating the presence of carboxyl groups. The relative hydrophilicities of (C) 0 and 16 % MAES materials was demonstrated, with water droplets dispensed onto both. 0 % MAES showed greater hydrophobic properties, i.e. poor wettability, with the water droplet remaining at a high contact angle (black arrow). The 16 % MAES material was readily wetted by the water droplet. Data represent mean  $\pm$  SD,  $n=3$  (biological triplicate).

To determine the effect of MAES on the morphologies of the polyHIPE monoliths, the generation of MAES HIPEs was repeated and new discs fabricated. These were washed in acetone as before, dried by air overnight and then imaged using a scanning electron microscope. Figure 5.3 shows scanning electron micrographs for polyHIPE discs fabricated from

HIPes containing 0, 2, 4, 8 or 16 % MAES. The top surface of each disc was imaged. The 0 % MAES material, i.e. fabricated using 100 % EHA, showed a typical polyHIPE structure, with clearly defined pores and windows, and evidence of interconnectivity. Those fabricated using 2, 4 and 8 % MAES, again, showed expected scaffold-like structures; however, the sizes of the surface pores appeared to decrease.

The 16 % MAES polyHIPE showed a shrunken structure, with pores not clearly seen; however, viewing the micrographs closely revealed pores were indeed present, but had collapsed into the material. Areas where an interface seemed to appear, as seen in the 100 $\times$  micrographs, suggested that the mixing time was not long enough and the emulsion not totally homogeneous. Mixing was initially allowed to continue for 2 min, though this was increased by at least 30 s after seeing these data. HIPes can be left to stir for extended durations once the aqueous phase been added, but this only serves to further break up the water droplets and increase the viscosity of the emulsion. This in turn would create polyHIPes with smaller pore diameters.

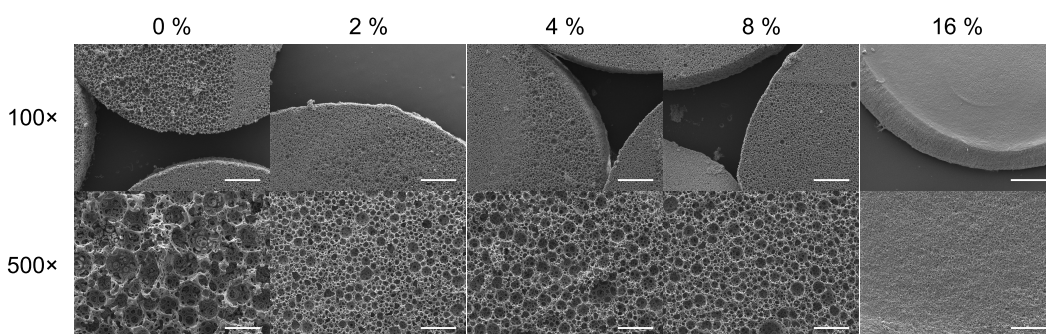


FIGURE 5.3 Scanning electron micrographs for polyHIPE materials fabricated using MAES monomer. MAES was included in precursor HIPes at 0, 2, 4, 8 and 16 % (w/w) concentrations. The polyHIPes were air-dried overnight, sputtered with gold and imaged using SEM at 100 $\times$  and 500 $\times$  magnifications. Scale bars for 100 $\times$  = 500  $\mu$ m; for 500 $\times$  = 100  $\mu$ m.

The images confirmed, for HIPes generated using MAES, typical polyHIPE structures were indeed being fabricated post-polymerisation. The shrunken morphology of the 16 % MAES polyHIPes was expected, as the discs were observed to have collapsed overnight after washing with acetone and were physically smaller. Before washing, it was noticed 16 % MAES discs were delicate and could easily tear when handled. This washing step was performed prior to imaging as it would ultimately have to be carried out every time for all materials eventually used for the work. Thus the effect of all steps within the fabrication process on the tested polyHIPes had to be known. The relatively high concentration of MAES in the 16 % condition had likely resulted in the collapse of the resulting polyHIPE

materials, with the material appearing weak once fabricated. The effect of acetone, which tends to swell polymeric materials, contributed to the collapse. Adding more crosslinker, TMPTA, to the HIPE could rectify this issue by increasing the linkages between adjacent polymer chains. This was not attempted here but could be an area of future work, particularly if higher amounts of MAES within the final polyHIPE materials are desired.

The fabrication of 90 % polyHIPEs, with confirmation of exposed carboxyl groups as a result of the addition of the MAES co-monomer within the oil phase, had been demonstrated here. It is important not to underestimate this; the inclusion of functional groups, whose specific chemistries enable post-fabrication functionalisation, is an active area of polyHIPE research. No other examples of carboxyl functionality could be found in the literature, except the report by Hayward et al. (2013b), which relied upon acrylic acid in the aqueous phase rather than the co-monomer approach. Acrylic acid is by itself hazardous and the alternative use of a relatively benign co-monomer may be more suitable in the laboratory. In this work it has also been shown that increasing the MAES amount subsequently increased the amount of carboxyl groups present in the polymerised material. This finding could allow operators to specifically tailor the surface chemistries of the final material.

### 5.1.2 CO-FLOW FABRICATION OF MICROSPHERES

The fabrication of polyHIPE monoliths, i.e. block-like structures such as discs and columns, is technically simple to perform and requires little expertise or training. The process is not particularly sensitive, often involving the pouring of a HIPE into a mould or labware vessel, allowing it to polymerise for a few minutes and then gently removing the newly formed polyHIPE. This ease of fabrication is part of the reason why polyHIPEs are so desirable for the development and use of in-house materials, with operators quickly mastering the simple techniques and adapting them to their specific applications. However, the fabrication of more specialised structures, such as microspheres, is far more experimentally challenging and frequently requires unique manufacturing systems to be successfully performed. Changes in the parameters of these systems, in contrast, can highly affect the resulting polyHIPE structure.

The Department of Materials Science and Engineering had previously constructed a bespoke system for the fabrication of polyHIPE microspheres. This was developed for a doctoral project that explored the use of injectable polyHIPE microspheres for bone tissue engineering (Paterson, 2017), with the main findings later reported in the literature by Paterson et al. (2018).

Figure 5.4 shows a schematic detailing the operation of this microsphere fabrication system.

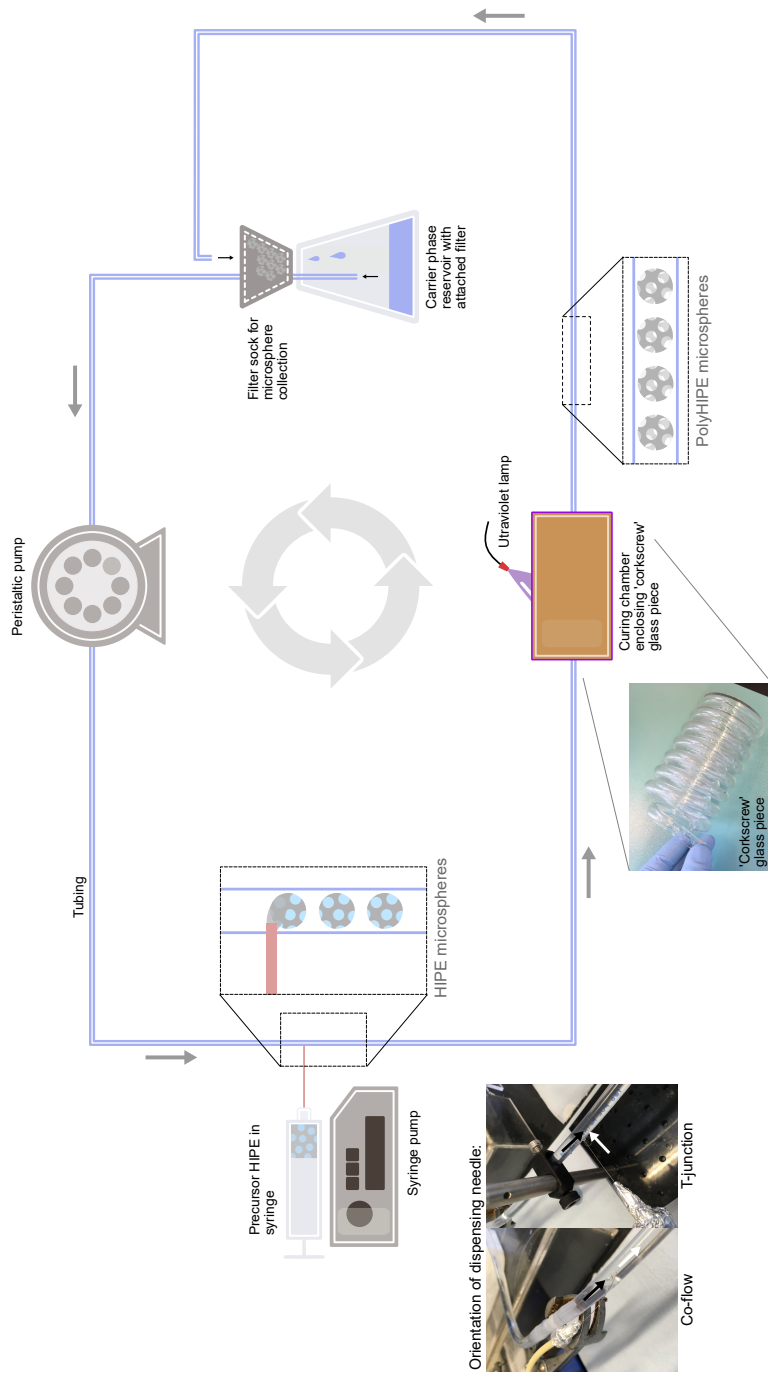


**FIGURE 5.4 Schematic detailing the bespoke system employed for the fabrication of polyHIPE microspheres.** A piece of tubing, with one open end in a flask and the other placed above a filter sock, forms a continuous loop around the system. The flask contains a carrier phase, which is continually pumped around the system via a peristaltic pump. At one section of the system, a syringe pump delivers HIPE into the carrier phase via a needle. This HIPE, upon contact with the carrier phase, forms individual HIPE microspheres which are carried by the carrier phase into a 'corkscrew' glass piece (photograph shown). This piece, housed within a curing chamber, is continually exposed to UV radiation. Upon entering the curing chamber, HIPE microspheres are polymerised into polyHIPE microspheres. Microspheres then collect in the filter sock above the flask, with the carrier phase dripping down to continue the process. The T-junction orientation is shown here within the schematic, where HIPE is injected perpendicular to the flow of the carrier phase, although a co-flow orientation (where HIPE is injected in the same direction as the flow of the carrier phase) is also possible. The photographs show the physical differences between these two orientations, with the black arrows representing carrier phase flow, and the white arrows representing HIPE flow. Originally designed by Paterson et al. (2018).

The process relies on the continuous flow of a liquid, termed a carrier phase in this work (but sometimes called a continuous phase in the literature), around the system. A piece of tubing containing this carrier phase forms a connecting loop. A peristaltic pump delivers the carrier phase around the system. The tubing has two open ends; one submerged within a flask (containing an exchanging volume of the carrier phase) and the other placed within a filter stock, itself placed on top of the flask. A syringe pump, with an attached syringe containing a generated HIPE, is positioned near a dedicated area of the tubing. A needle, attached to the syringe, is used to puncture the tubing and form a path for the HIPE to enter. This entry point can either be a T-junction orientation (where the flow of HIPE is perpendicular to that of the carrier phase) or a co-flow orientation (where the flow of HIPE is in the same direction to that of the carrier phase). The schematic shows side-by-side photographs of these co-flow and T-junction orientations. For the T-junction, the stream of HIPE (indicated by the white arrow) followed the direction of the carrier phase (indicated by the black arrow). With the syringe pump operating, HIPE is injected into the carrier phase at a controlled rate to form microspheres. These new structures, which are still emulsions, are carried by the liquid (hence carrier phase) into a curing chamber — a cardboard box whose inside walls are covered in aluminium foil — where they enter a ‘corkscrew’ glass piece exposed to UV radiation (shown in a photograph in Fig. 5.4). Because of the extended residence time within this glass piece, the microspheres are exposed to UV for approximately 20–30 s (depending upon the flow rate of the carrier phase) during which time they are polymerised into polyHIPE microspheres. After exiting the curing chamber they are carried to the filter stock, where they are captured and stored until the end of the process. The system can be operated without any interaction from the operator for many hours, or until the syringe has injected all of the HIPE.

The shape of the HIPE microsphere as it enters the curing chamber becomes the shape of the polymerised microsphere that forms. If a HIPE, shaped as a perfectly spherical particle, enters the chamber, a perfectly spherical polyHIPE will exit. On the other hand, if a HIPE, shaped as a disfigured oval-like particle enters, then a disfigured oval-like particle polyHIPE will be produced. In contrast to monolithic polyHIPE fabrication, there were many parameters that needed to be understood and controlled in order to produce microspheres of sufficient quality. The quality of a polyHIPE microsphere can be judged with regards to average diameter, monodispersity and porosity. For the work here, a high quality batch of polyHIPE microspheres was defined as <300  $\mu\text{m}$  in average diameter, highly monodisperse (all microspheres a similar diameter) and with macroporous structures. The parameters that required controlling included the injection rate of the HIPE, the flow rate of the carrier phase (as dictated by the rotational speed of the pump), the internal diam-

eter of the needle, the composition of the carrier phase and the contents (e.g. monomers, surfactant etc.) of the HIPE itself, including the conditions in which it was formed. The orientation of the injection point was later discovered to also play a role.

The principles behind this process were not new. Indeed, all reports in the literature demonstrating the fabrication of polyHIPE microspheres used one or more syringe drivers to controllably deliver a HIPE into a carrier phase liquid for subsequent exposure to UV radiation (Gokmen et al., 2009; Lapierre et al., 2015; Moglia et al., 2014; Whitely et al., 2019). The theory was that the interaction between HIPE and carrier phase will force a spherical particle, or microsphere, to form out of the emulsion. All reporting authors fabricated polyHIPE microspheres using acrylic monomers; indeed, the requirement for rapid polymerisation demands reactive acrylic HIPEs are used, although the fabrication of polystyrene polyHIPE microspheres has been demonstrated (Desforges et al., 2002). A key benefit of the system presented here, however, is its ability to continuously produce microspheres; the looped tubing ensures the carrier phase is recycled around the system, with the volume of the carrier phase liquid remaining constant as a steady state within the flask. With the exception of Paterson et al. (2018), who indeed developed the system described here, all other reports instead relied upon non-looped tubing. In these instances, the carrier phase was not recycled but instead pumped from a finite source, meaning the system would have to be eventually stopped and the carrier phase replenished.

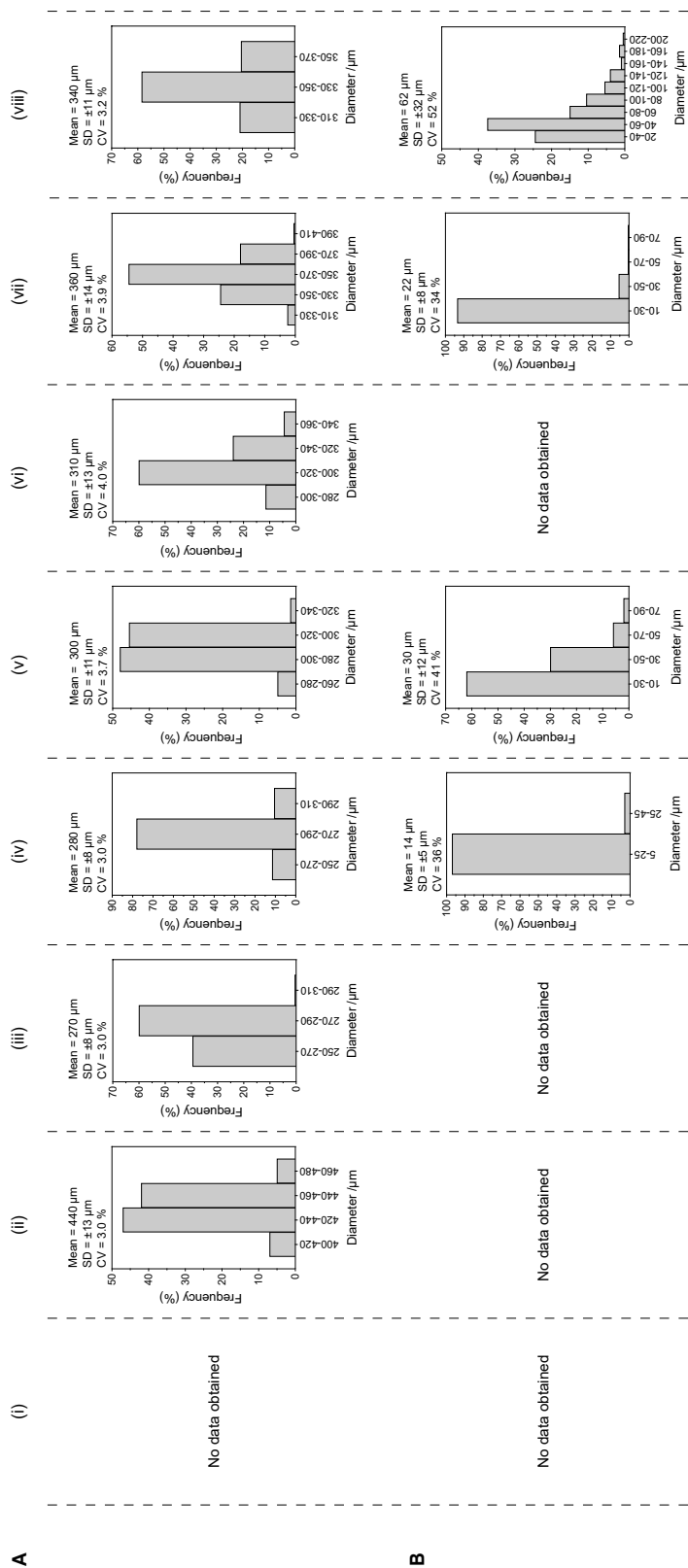
The previous operator of this system in the laboratory had used HIPEs generated from EHA and IBOA (Paterson, 2017; Paterson et al., 2018). The carrier phase employed was 100 % water, being unique within the literature where others had instead employed surfactants, oils and other viscous liquids to ensure the formation of spherical particles. Due to the high viscosity of HIPEs containing IBOA, injecting these thick emulsions into water does indeed create spherical particles. This technique, termed ‘water-in-oil-in-water’, was not regarded as suitable here due to the relatively low viscosities of HIPEs containing MAES. These low viscosities were mentioned previously, having first been noted during the initial generation of HIPEs using MAES. However, other operators in the laboratory who had experimented with the microsphere fabrication system had discovered that employing 80 % glycerol as a carrier phase appeared to achieve spherical particles with relative ease, regardless of the specific HIPE composition used. With MAES confirmed as a compatible monomer for the generation of stable HIPEs, and with the resulting polyHIPE demonstrated to have exposed carboxyl groups, the next step was to attempt to fabricate MAES polyHIPE microspheres using this very system. Each parameter had to be understood and optimised in order to create high quality microspheres (as defined earlier), with a routine process then developed so as to allow the rapid production of materials for the cell retention device.

Early validation work was performed using the system as it was first presented in the laboratory. It was soon clear the quality of the microspheres was highly dependent upon the composition of the carrier phase. Despite the system being originally designed to operate using a T-junction orientation, an attempt at co-flow was carried out. This orientation was thought to enable a more precise method of creating microspheres, arising from its fluidic characteristics, i.e. the emulsion will be acted upon in the direction in which it flowed into the system. It was decided that 10 % MAES would be used within all HIPEs for the fabrication of the microspheres here, allowing a sufficient amount of carboxyl groups to be present within the final material. It was hoped this concentration would also prevent any risk from structural collapse as seen previously with polyHIPEs made using 16 % MAES. The needle employed for all testing had an internal diameter of 0.15 mm (30 G), a relatively narrow gauge not used previously in this system. It was suggested a needle with a smaller diameter would simply yield smaller microspheres.

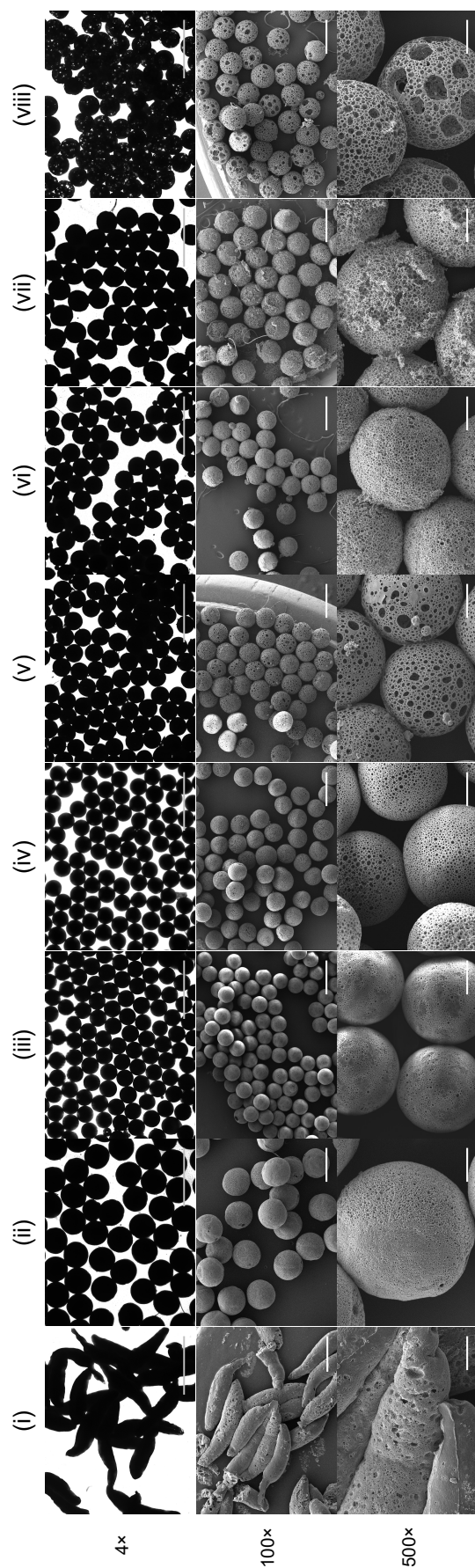
A co-flow orientation was created via dedicated tubing (which was opaque to ensure no polymerisation of HIPE could occur via ambient light) to direct the HIPE into the system at the desired position. This tubing was connected to the syringe, with the other end attached to a needle. To make this orientation, the part of the system where the carrier phase tubing was bent would be punctured to gain entry. Injected HIPE would thus flow in the direction of the carrier phase. Figure 5.4 shows side-by-side photographs of the co-flow and T-junction orientations and should be viewed to ensure the differences between the two are understood. To demonstrate the effect of carrier phase on the polyHIPE microspheres, four compositions were prepared; 100 % water, 50 and 80 % glycerol, and a solution of 15 % glycerol within 3 % polyvinyl alcohol (PVA). The injection rate of the HIPE was set at 0.3 mLhr<sup>-1</sup> and the carrier phase pumped at 150 rpm for all carrier phase compositions.

Figure 5.5 shows a spread of data relating to the diameter and surface porosity of the MAES polyHIPE microspheres fabricated using the co-flow orientation. Figure 5.6 shows visual data relating to the morphology of these same microspheres. The small case Roman numerals above each data column or image, in both Fig. 5.5 and 5.6, denote the specific conditions employed; (i) no HIPE modifications, 100 % water; (ii) no HIPE modifications, 50 % glycerol; (iii) no HIPE modifications, 80 % glycerol; (iv) surfactant reduced to 1.25 %, 80 % glycerol; (v) surfactant reduced to 1.25 % and water heated to 80 °C, 80 % glycerol; (vi) no HIPE modifications, 3 % PVA; (vii) surfactant reduced to 1.25 %, 3 % PVA, and (viii) surfactant reduced to 1.25 % and water heated to 80 °C, 3 % PVA. The 3 % PVA is used in place of the '15 % glycerol within 3 % PVA' for brevity. These denotations will be used in the text that follows to ensure clarity is maintained. 'No HIPE modifications' refers to the instances where the surfactant was kept at 10 % and water at ambient temperature was

---



**FIGURE 5.5 Diameter and surface porosity analysis of MAES polyHIPE microspheres fabricated using co-flow orientation and four different carrier phase compositions. 10 % MAES microspheres were fabricated using either water, glycerol or PVA carrier phases with some precursor HIPE modifications. (A) 200 microspheres were measured to determine average diameter with (B) surface porosities also determined. The labelling at the top of the figure denotes the carrier phase used and any HIPE modifications. (i) No HIPE modifications, 100 % water; (ii) no HIPE modifications, 50 % glycerol; (iii) no HIPE modifications, 80 % glycerol; (iv) surfactant reduced to 1.25 %, 80 % glycerol; (v) surfactant reduced to 1.25 % and water heated to 80 °C, 80 % glycerol; (vi) no HIPE modifications, 3 % PVA; (vii) surfactant reduced to 1.25 %, 3 % PVA and (viii) surfactant reduced to 1.25 % and water heated to 80 °C, 3 % PVA. For all conditions, the HIPE injection rate was 0.3 mL/hr and the pump speed set at 150 rpm. For (A), data represent mean ± SD, n=200 discreet microspheres; for (B), data represent mean ± SD, n=50 discreet microspheres.**



**FIGURE 5.6 Morphology analysis of MAES polyHIPE microspheres fabricated using co-flow orientation and four different carrier phase compositions.** 10 % MAES microspheres were fabricated using either water, glycerol or PVA carrier phases with some precursor HIPE modifications. Scanning electron micrographs, at 100 $\times$  and 500 $\times$  magnifications, and brightfield micrographs, at 4 $\times$  magnification, obtained to visualise monodispersity and surface porosity. The labelling at the top of the figure denotes the carrier phase used and any HIPE modifications. (i) No HIPE modifications, 100 % water; (ii) no HIPE modifications, 50 % glycerol; (iii) no HIPE modifications, 80 % glycerol; (iv) surfactant reduced to 1.25 %, 80 % glycerol; (v) surfactant reduced to 1.25 % and water heated to 80  $^{\circ}$ C, 80 % glycerol; (vi) no HIPE modifications, 3 % PVA; (vii) surfactant reduced to 1.25 %, 3 % PVA and (viii) surfactant reduced to 1.25 % and water heated to 80  $^{\circ}$ C, 3 % PVA. For all conditions, the HIPE injection rate was 0.3 mL/hr and the pump speed set at 150 rpm. Scale bars for 4 $\times$  = 1000  $\mu$ m; for 100 $\times$  = 500  $\mu$ m; for 500 $\times$  = 100  $\mu$ m.

added to generate the HIPE. These conditions were used previously for the demonstration of the presence of carboxyl groups, as discussed in § 5.1.1, and were now considered a control.

Figure 5.5A shows the diameter size distributions of the fabricated microspheres, as determined by measuring 200 individual particles, for each of the conditions tested. These plots were frequency distributions and showed the percentage of measured microspheres that fell within a particular diameter range. These ranges were divided into 20  $\mu\text{m}$  groups. The data above each plot tells the mean diameter, the standard deviation and the coefficient of variance for that particular condition. Figure 5.5B shows the surface pore size distributions of the fabricated microspheres, as determined by measuring the 4 largest pores visible on the surface of 50 microspheres from an optical micrograph, for each of the conditions tested. The data above each plot, once again, tells the mean diameter, the standard deviation and the coefficient of variance for that particular condition. Figure 5.6 shows brightfield and scanning electron micrographs and has been presented here to complement the quantitative data given in Fig. 5.5. The brightfield micrographs helped show, by eye, the relative dispersities of microspheres for each condition, whilst the highly magnified scanning electron micrographs revealed the exact structural nature for each of the materials.

Condition (i) yielded crude rod and flake-like structures. Using 100 % water as a carrier phase proved to be futile, with the emulsion continually ‘dribbling’ into the liquid as string-like structures. The turbulence of the carrier phase broke these emulsions into separate structures before the curing chamber was reached. No spherical particles were obtained and so none of the materials were measured, but it was noted that many of the longer rods approached 1000  $\mu\text{m}$  in length. The surface pore size distribution was likewise not measured for this condition, but there were some pores visible at the surface. However, there was also signs of collapse or ‘cave-in’, as seen previously with the 16 % MAES materials in § 5.1.1.

The use of 50 % glycerol in condition (ii) immediately caused spherical particles to form, with the increased viscosity starting to cause the HIPE to ‘bud off’ from the needle tip as it entered the flowing stream. Gokmen et al. (2009) likewise commented on the need for a viscous carrier phase, in combination with a relatively less viscous HIPE, for reproducible spherical particles to form. For this condition, a mean diameter of 440  $\mu\text{m}$  was measured. The micrographs revealed no obvious areas of ‘cave-in’, but the surfaces produced showed a roughened texture but with no visible pores or obvious areas of entry into the material. Because no pores could be easily distinguished, the surface pore size distribution was not determined.

Condition (iii) yielded highly monodisperse microspheres, with the vast majority of the microspheres in the 250–290  $\mu\text{m}$  range, with a mean diameter of 270  $\mu\text{m}$  determined. The increase to 80 % glycerol dramatically improved the fabrication process, agreeing with the anecdotal evidence provided by other operators in the laboratory. Due to the further increase in viscosity of the carrier phase, the budding of spherical particles was observed to occur instantaneously as the emulsion emerged into the carrier phase. This resulted in microspheres being smaller in diameter than those produced in the previous condition. Despite this success, these micrographs revealed something peculiar regarding their surface morphologies; once again, there was no evidence of collapse or ‘cave-in’, yet the pores observed were extremely small (even when viewed under a scanning electron microscope) and could not be accurately measured. In effect smoothed microspheres, with microporous surfaces, had been fabricated.

Condition (iv) was the first to modify the conditions of the HIPE by reducing the surfactant from 10 to 1.25 %. The carrier phase was kept at 80 % glycerol. Highly monodisperse microspheres were achieved once more, with a mean diameter of 280  $\mu\text{m}$  determined. This confirmed the capability of 80 % glycerol to reproducibly fabricate spherical particles. The reduction of surfactant from 10 to 1.25 % was performed in an effort to increase the average surface pore size of the materials, whilst keeping the newfound benefits of the 80 % glycerol carrier phase. Because of this, pores were now visible and able to be measured, with a mean of 14  $\mu\text{m}$  determined.

Condition (v) continued to employ 80 % glycerol and kept the surfactant at 1.25 %. To further increase the potential porosity, the water added to the monomers (to generate the HIPE) was first heated to 80 °C. These two modifications appeared to push the HIPE to the limits of its stability. Tilting the beaker containing the HIPE to one side and back to draw the emulsion in specific directions would reveal large droplets of water contained within. The colour of the emulsion, usually an opaque white, was now a pale grey with areas of transparency. The viscosity was also considerably reduced with the HIPE now feeling like thickened water rather than a relatively more viscous emulsion. A larger mean diameter of 300  $\mu\text{m}$  was determined, with this reduced viscosity seeming to have an effect on the size of the microspheres. However, the pores were indeed larger and could be easily distinguished; a mean of 30  $\mu\text{m}$  was determined.

Glycerol, as an 80 % solution, proved to be an excellent carrier phase — but it came at a cost. Microspheres readily formed from the tip of the needle, with little intervention from the operator needed. The process was robust, with the exact location of the needle within the tubing not seeming to make much difference to the correct and repeated budding of

the HIPE. However, glycerol clearly had an effect on the surface porosity of the fabricated materials. Despite the reduction of surfactant and the dramatic increase in the temperature of the water added, the surface pores remained small — and certainly did not look like a typical polyHIPE. Speaking to those in the laboratory with more experience of polyHIPEs, modifying the HIPE, as was attempted here, should result in vastly greater porosities. This, of course, seemed to only hold true for monolithic polyHIPEs.

Glycerol is hygroscopic; its three hydroxyl groups will attract water from their nearby environment. This includes a spherical emulsion, which in the case here was 90 % water. It was suggested that upon entering the carrier phase, the HIPE progressively lost its water content as it got carried through the system. Once polymerised in the curing chamber, it was too late, so to speak, with the resulting polyHIPE having lost a portion of its water — at least near to the surface — to the glycerol. Despite the attempted modifications of the HIPE, glycerol still had this effect, yet some evidence of macroporosity arising from these modifications was apparent. Using 80 % glycerol presented a compromise; fabricated polyHIPE microspheres were highly monodisperse and under 300  $\mu\text{m}$  in average diameter, yet they did not possess macroporous characteristics typical of a polyHIPE. Glycerol ultimately had two effects; its high viscosity resulted in neat sphericalness, yet its hygroscopic nature resulted in microporous surfaces.

It was decided to test another carrier phase composition. PVA had been demonstrated in the literature as a carrier phase capable of producing spherical particles. Its polymer chain possessed a single, yet repeating, hydroxyl group. Because of this, it was believed any hygroscopic effect would not as pronounced as that seen with glycerol; however, this would also mean its viscosity would not be as high. A 3 % PVA solution was prepared, as reported in the literature, but it was immediately noted that the viscosity indeed was not as high as that seen with 80 % glycerol. An initial validation test confirmed that 3 % PVA achieved oval, rather than spherical, particles (data not shown) and so 15 % glycerol was later added to the solution. This relatively small supplementation had the effect of ensuring fabricated particles were once again spherical.

Condition (vi) was the first to use this glycerol-supplemented 3 % PVA carrier phase with no HIPE modifications carried out. Spherical particles continued to bud off the needle, but the microspheres were larger on average than those fabricated using glycerol, with a mean of 310  $\mu\text{m}$  determined. The surface porosity of the microspheres was again smaller than anticipated, yet larger than those seen in condition (iii). This porosity, however, was still too small to be accurately measured. As predicted, it was likely a hygroscopic effect was again being seen with PVA, but the effect was not as apparent as that seen with 80 %

glycerol.

Condition (vii) continued using 3 % PVA but reduced the surfactant to 1.25 %, as attempted before. The reduction in viscosity increased the average diameter of the resulting microspheres, with a mean of 360  $\mu\text{m}$  determined. The porosity, however, was now considerable more obvious with a mean pore size of 22  $\mu\text{m}$  achieved. Whilst smaller than that seen in condition (v), the morphology of these particular materials appeared to look like 'typical' polyHIPEs, i.e. they possessed a network or mesh of interconnecting voids. Indeed, microspheres fabricated using this condition were the first to demonstrate the potential of polyHIPE microspheres; that of materials with very high surface-area-to-volume ratios.

Condition (viii) kept PVA, the reduced surfactant and in addition increased the temperature of the water to 80 °C. As before, the viscosity of the modified HIPE was considerably reduced, with microspheres fabricated now having an average diameter of 340  $\mu\text{m}$ . The pore sizes dramatically increased, however, with an average pore size of 62  $\mu\text{m}$  reached. Micrographs revealed considerable voids at the surface of every particle, with some having clear pathways through the entire structure. Critically, there appeared to be some surface area within these semi-hollow materials. Such characteristics may allow cells entry to populate the area within. Because of these open structures, light was able to fully pass through for some microspheres, enabling pores to be seen even on brightfield micrographs.

Conditions (vii) and (viii) were a small success. Despite not achieving an average diameter of 300  $\mu\text{m}$  or less, the materials fabricated were indeed porous; condition (vii) gave structures typical of polyHIPEs, whilst (viii) gave macroporosity with most microspheres having vast openings leading to interconnected areas. Using 3 % PVA as a carrier phase appeared to keep the characteristics of glycerol, i.e. a high viscosity (when compared to the relatively lower viscosity of the HIPE), but without the severe hygroscopicity. But it was not so simple. It was soon realised that a majority of microspheres fabricated using conditions (vii) and (viii) began to collapse. This was described as catastrophic, with the materials turning to a mushy, soft substance upon drying. This occurred before any acetone washing and so, unlike the 16 % MAES materials previously discussed, was not the result of any harsh solvent exposure. Some of the microspheres, particularly those fabricated at the beginning of the process, managed to stay structurally intact and it was these that were eventually imaged and analysed here. Figure 5.7 shows an electron scanning micrograph of microspheres that had collapsed, fabricated using condition (viii). The spherical shapes are still distinguishable, but each material had an 'exploded' appearance with vast openings where the structure had given way. The layers of polyHIPE debris around the microspheres are from the scraping of the collapsed materials upon the stub prior to imaging.

Whilst these images were fascinating to look at — and show the highly interconnectedness of a polyHIPE — it proved the particular macroporous structures produced from the final two conditions could not be sustained.

The aim of the testing discussed here was to determine optimal conditions for the fabrication of MAES polyHIPE microspheres. Any MAES polyHIPEs eventually fabricated would be later coated with polyethylenimine to complete the cell retention device. As anticipated, the fabrication of polyHIPE microspheres proved considerable more difficult than polyHIPE monoliths, but some parts of the data were reassuring. Spherical particles could indeed be fabricated and the monodispersities of these — ignoring those made using condition (i) — were surprisingly good, with a coefficient of variance of 4.0 or under consistently achieved. The composition of the carrier phase, however, clearly had a definite effect on the quality of the materials.

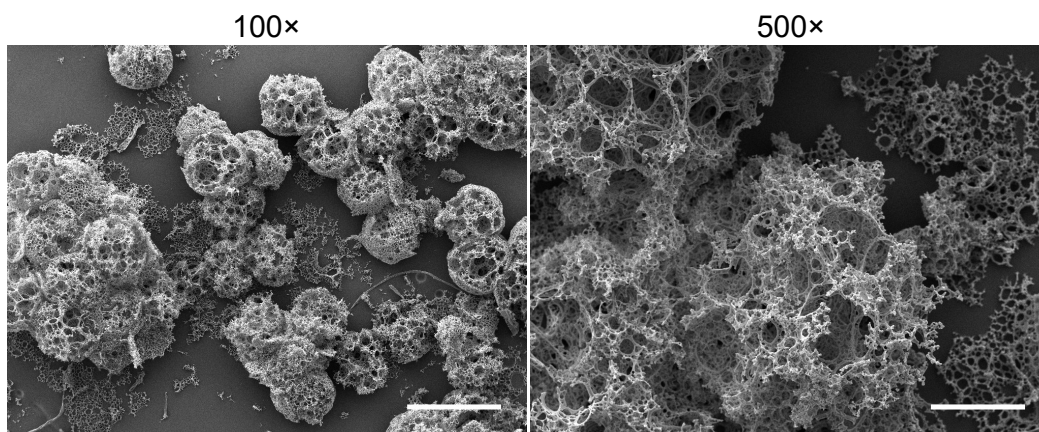


FIGURE 5.7 Scanning electron micrographs showing the physical collapse eventually experienced by MAES polyHIPE microspheres fabricated using 3 % PVA carrier phase. 10 % MAES HIPEs were prepared using 80 °C water and 1.25 % surfactant, before being used to fabricate microspheres with 3 % PVA carrier phase (condition viii, as denoted in Fig. 5.5 and 5.6). Materials were left at room temperature and imaged using SEM at 100× and 500× magnifications. Scale bars for 100× = 500 μm; for 500× = 100 μm.

The use of 100 % water in condition (i) immediately demonstrated a more advanced carrier phase was required, with no evidence of spherical particle formation. Interestingly, the images revealed some ‘caved-in’ areas at the surface, similarly to that seen in Fig 5.3 with the 16 % MAES polyHIPE. It was likely the case that the use of 10 % MAES, and not less, was not optimal, with this concentration of MAES perhaps being too high once again and leading to a weakened polyHIPE prone to this type of collapse. Switching to 50 % glycerol achieved spherical particles, with the vastly increased viscosity of the carrier phase now forcing the emulsion into spheres as they were dispensed from the needle. However, the

initial use of glycerol in condition (ii) appeared to resolve the issue of 'caved-in' areas. Due to the hygroscopic effect of glycerol, the specific properties of the HIPE immediately before the initiation of polymerisation may have been vastly different to the properties of the HIPE when using just water. The result being that no areas of 'cave-in' could be identified in condition (ii), with open pores, albeit small ones, still visible at the surface. This hygroscopic effect was not immediately noted during condition (ii); it was not until 80 % glycerol was attempted that a connection was made regarding the potential interaction between emulsion and carrier phase. The microspheres fabricated in condition (iii) were indeed unique. Whilst produced from a HIPE, the microspheres were not typical polyHIPEs. Their microporous, smooth surface led them to be termed 'deformed' polyHIPEs. This deformation, it was thought, was a direct result of the hygroscopicity of the glycerol acting upon the HIPEs as they were carried to the curing chamber.

The composition of the carrier phase is important; Gokmen et al. (2009), Moglia et al. (2014) and Whitely et al. (2019) had used 3 % PVA (without any glycerol supplementation), Lapierre et al. (2015) had used fluorinated oil with a 2 % 'Picosurf' surfactant supplement and Paterson et al. (2018) had used 100 % water. Due to the popularity of PVA, it was attempted here with HIPEs generated using MAES. The 15 % glycerol supplement appeared necessary to return materials to a more spherical shape, although this was only performed after seeing the high degree of sphericalness that could be achieved when using 80 % glycerol. The hygroscopic effect of PVA was not as marked as that seen from glycerol, with microspheres produced possessing a more typical polyHIPE morphology. When paired with the HIPE modifications, microspheres were produced that effectively achieved what was originally envisaged, namely macroporous materials with clear voids for cells to enter and attach within the structures. The dramatic collapsing seen with these microspheres, however, may in part be due to the high concentration of MAES used. Any future work could potentially explore reducing this concentration of MAES and increasing that of the crosslinker, TMPTA. It may be the case that increased linkage between polymer chains could prevent the collapsing of these highly porous microspheres.

The injection rate of the HIPE was kept low, at  $0.3 \text{ mLhr}^{-1}$ , to ensure no bulging of the emulsion once it had emerged into the carrier phase. The original T-junction orientation was initially explored at the beginning of the project by injecting HIPEs, generated using EHA and IBOA, into a glycerol carrier phase. Whilst it did achieve microspheres, there was an issue of 'blobbing', which is described here as HIPE accumulating around the side of the needle tip as it entered the carrier phase. The HIPE would appear to wick onto the side of the needle tip. Once this had occurred, HIPE microspheres would subsequently form from this blobbing area, rather than from the needle tip itself. This had no effect on the spher-

icalness of the resulting particles — they remained highly spherical — but it did make them considerably larger than if the blobbing had not occurred. Frustratingly, this blobbing effect did not always happen. Stopping the system and replacing the needle tended to resolve the issue. The idea of using a co-flow orientation was to avoid any blobbing or wicking around the needle; with the syringe now positioned so as to inject HIPE in the same direction as the carrier phase, it was anticipated blobbing would less likely occur. An aim was to create a process where distinctly separate microspheres would be formed and thus ensure both reproducibility and monodispersity. The co-flow orientation, when using 80 % glycerol and with HIPES generated using MAES, did indeed achieve this. Very early work crudely attempted different injection rates and carrier phase flow rates and observed, by eye, the ability of each to produce separate microspheres. It was found an injection rate of  $0.3 \text{ mLhr}^{-1}$  was required to ensure single microsphere fabrication. The flow rate of the carrier phase, as dictated by the rotational speed of the pump, was kept at 150 rpm. This was to ensure the carrier phase liquid flow at the entry point was gentle (which was considered laminar flow, though the Reynolds number was not calculated), so as not to disturb the formation of the spherical particle, but still be enough to force it off the tip of the needle.

Unlike PVA, which had to be dissolved at a high temperature and then cooled down for several hours before use, glycerol was supplied ready to use. It was also inexpensive and relatively safe to handle. A common suggestion posed numerous times throughout the project was to simply increase the injection rate of the HIPE when the co-flow orientation was used. This could enable a rapid production process. However, this was not the case, with bulging and larger microspheres occurring for the co-flow orientation, when the injection rates were increased, and even if 80 % glycerol was used. A decision was eventually made to continue using 80 % glycerol as a carrier phase with 10 % MAES polyHIPES, but revert back to the T-junction orientation the system originally used. It was suggested a more rapid production may occur when using this orientation.

The data here were empirical and obtained using the one factor at a time approach, i.e. they were acquired through the testing of individual variables and recording the observations that followed. To the enhance the collection of data here, it was suggested any further investigation into the fabrication of microspheres using this co-flow orientation should instead use a design of experiments approach. Whilst designed experiments were not utilised in any of the work presented here, using this method may better enable operators to better evaluate the variables that determine the properties of the microspheres. As was done previously, variables to test could be the flow rate of the carrier phase, injection speed of the HIPE, diameter of the injection needle, as well as the fabrication conditions of the HIPE itself. An explanation of the differences between one factor at a time and designed experi-

ments, as well as the advantages given by the latter, is given by Czitrom (1999).

### 5.1.3 T-JUNCTION FABRICATION OF MICROSPHERES USING GLYCEROL

Using the co-flow orientation to fabricate MAES polyHIPE microspheres unintentionally gave an insight into the effect of glycerol, when used as a carrier phase, on the final materials. Glycerol is both viscous and hygroscopic; the former ensured the fabricated microspheres were monodisperse, whilst the latter appeared to extract water from the emulsion immediately before it cured. This resulted in 'microporous polyHIPEs' forming — perhaps an oxymoron — and thus the materials were termed 'deformed' polyHIPEs due to the unconventional microporous topographies seen at their surfaces. A realisation was also happening at this point in the project where microporous microspheres might have to be tolerated, and indeed could be accepted, if the fabrication process was rapid and reproducible. Because the co-flow orientation had to be operated at low injection rates, it was not feasible for the routine and rapid fabrication of microspheres, as envisaged later on in the project. As an example, with condition (iii) as denoted in Fig. 5.5 and 5.6, i.e. employing 80 % glycerol, the injection rate of  $0.3 \text{ mLhr}^{-1}$  would lead to the fabrication of under 2 mL of settled microspheres every hour. Whilst suitable for an academic exercise, such as the study of carrier phase conditions as demonstrated earlier, a much quicker production process would eventually be needed. It was decided to switch back to the T-junction orientation, i.e. inject the HIPE into the tubing at a 'T' so as to allow the flow to be perpendicular to the flow of the carrier phase. With the new knowledge that glycerol greatly encouraged spherical particle formation, it was hypothesised that increasing both the injection rate and the carrier phase flow rate could result in a vastly increased yield of material. As mentioned, this was not possible with the co-flow orientation, where low injection rates and slow carrier phase flow rates had to be employed.

Paterson et al. (2018) had demonstrated the fabrication of microspheres using a T-junction orientation with 100 % water as a carrier phase, but not with glycerol. The authors concluded that the diameter of the microspheres was dependent upon both the injection rate of the HIPE and the flow rate of the carrier phase. For microspheres with small diameters, a decreased injection rate and an increased carrier phase flow rate was needed. This simultaneously ensured a smaller volume of HIPE was injected and carried away quickly before a larger spherical particle could form. For large microspheres, the reverse was true, with a quick injection rate and a lower carrier phase flow rate ensuring a larger sphere was generated before being carried away. Three conditions were selected to test these findings from the report; small, with an injection rate of  $6 \text{ mLhr}^{-1}$  and a carrier phase flow rate at 600 rpm; medium, with an injection rate of  $12 \text{ mLhr}^{-1}$  and a carrier phase flow rate at 400

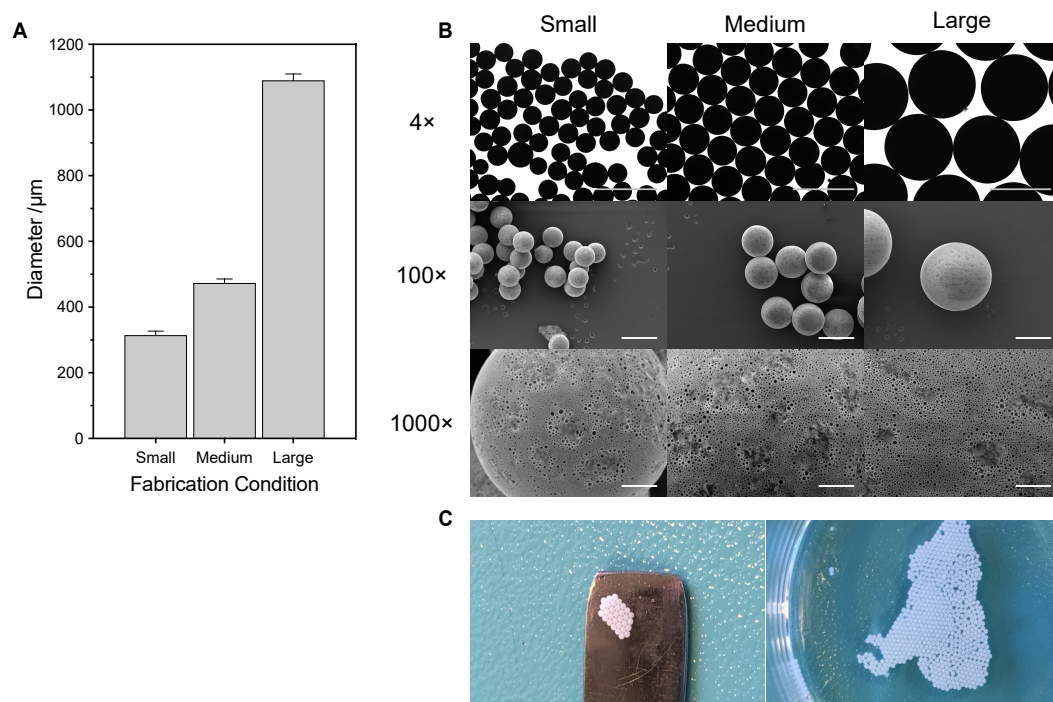
rpm, and large, with an injection rate of  $18 \text{ mLhr}^{-1}$  and a carrier phase flow rate at 200 rpm. The 'small', 'medium' and 'large' names came from the expectation that these conditions would yield microspheres with increasing average diameters. A needle with an internal diameter of 0.60 mm (20 G), larger than that used for the co-flow study, was employed for these tests. Unlike the 30 G used previously, it was expected this needle would allow a faster production rate of microspheres due to its increased size.

Figure 5.8A shows the average diameter, from the measurement of 200 microspheres, for each of the three conditions. The prediction that these parameters would give increasingly large microspheres was indeed correct, with 'small' achieving an average diameter of approximately  $315 \mu\text{m}$ , 'medium' achieving  $470 \mu\text{m}$  and 'large' achieving  $1090 \mu\text{m}$ . The T-junction orientation, with the use of the 80 % glycerol carrier phase, enabled the rapid fabrication of microspheres, but the actual process of spherical particle creation was different to that seen during co-flow. Because of the increased injection rates, no priming was necessary, with the needle inserted into the tubing immediately after the syringe pump was started. Upon initially exiting from the needle, the HIPE appeared unstable and 'flicky' as it adjusted to the new dynamic environment. It was determined that approximately 20 min was needed to ensure the system had equilibrated. After this time, the diameters of the fabricated microspheres appeared to remain consistent. It was only these microspheres that were eventually retrieved for analysis.

The creation of microspheres no longer occurred from the 'budding' of emulsion into the glycerol, as with the co-flow orientation; rather, a steady stream of HIPE would continually exit and get pushed along with the flow of the carrier phase. Upon closer inspection, it was clear that microspheres were being serially formed within this stream and not at the exit point of the needle. Due to the faster injection rates, the frequency of single microsphere creation was considerably faster, with the filter sock filling up within a matter of minutes after the system had started. For the 'small' and 'medium' conditions, the actual fabrication of microsphere was not distinguishable by eye; instead, an emulsion stream could be seen with microspheres only starting to appear further along the tubing. For the 'large' condition, this particle creation was clearly visible. Due to the slower carrier phase flow rate, the process appeared more like the typical budding seen with the co-flow. In this instance, the larger microspheres could clearly be observed flowing out of the needle before being forced off by the carrier phase.

For all conditions, a repeating set of events seemed to occur, with each microsphere forming at the exact same moment and place as the last and then following the same path along the system. To ensure this happened, however, the system had to always act within a steady

state. The carrier phase flow rate and the injection rate had to remain constant. If there was any issue within the process, e.g. the carrier phase was blocked within the filter sock and the tubing consequently ran dry, the fabrication system would be disrupted and the microspheres would change shape and size. Any air bubbles within the syringe would eventually make it through the needle, causing a change in the flow and likewise causing a change in the state of the system. To counter this, the syringe was always knocked and gently pushed to dispel any air prior to attaching to the system. Unlike that frequently observed when using HIPES generated using IBOA, there were no instances of ‘blobbing’ or ‘wicking’ for HIPES made using MAES. This was related to the relatively low viscosities that occurred when MAES was included in the emulsions. This was beneficial, as it ensured the process would not have to be periodically stopped to resolve these issues.



**FIGURE 5.8** Diameter and morphology analysis of MAES polyHIPE microspheres fabricated using the T-junction orientation and 80 % glycerol carrier phase. 10 % MAES microspheres were fabricated at three different conditions (‘small’; 600 rpm, 6 mLhr<sup>-1</sup>, 20G, ‘medium’; 400 rpm, 12 mLhr<sup>-1</sup>, 20G and ‘large’; 200 rpm, 18 mLhr<sup>-1</sup> and 20G — corresponding to carrier phase flow rate, HIPE injection rate and dispensing needle gauge respectively) to demonstrate contrasting diameters. (A) 200 microspheres were measured to determine average diameter and (B) scanning electron micrographs, at 100 $\times$  and 1000 $\times$  magnifications, and brightfield micrographs, at 4 $\times$  magnification, obtained to visualise monodispersity and surface porosity. (C) shows the self-assembling nature of ‘medium’ microspheres due to their very narrow size distribution and sphericalness. Data represent mean  $\pm$  SD, n=200 discreet microspheres. Scale bars for 4 $\times$  = 1000  $\mu\text{m}$ ; for 100 $\times$  = 500  $\mu\text{m}$ ; for 1000 $\times$  = 50  $\mu\text{m}$ .

Figure 5.8B shows brightfield and scanning electron micrographs for the microspheres fab-

ricated using the three conditions described. It was immediately apparent that all three gave microspheres with a high monodispersity. As expected, the hygroscopic effect of the glycerol continued to be felt upon the materials, with each condition giving smooth, microporous surfaces. The 1000× magnification, in particular, shows the effect of glycerol upon the emulsion prior to polymerisation. Figure 5.8C shows photographic evidence of the self-assembly of microspheres fabricated using the ‘medium’ condition. It was soon observed that, when microspheres reached a certain degree of monodispersity, they began to self-assemble. This appeared to be especially true for ‘medium’ microspheres. This self-assembly initially occurred within the filter sock during fabrication; upon entering the sock microspheres floated around for several seconds before accumulating on top of the recycling glycerol.

Due to each microsphere having identical physical dimensions — or at least very similar dimensions — the materials started to neatly gather around each other as they experienced the dynamic environment in similar ways. This was not aggregation — the microspheres could be easily suspended by simply tapping the sock. Once this tapping was stopped, however, they would continue once again to assemble themselves. This also happened when microspheres were decanted and spread out onto slides and plates for microscopy, enabling photographs to be obtained. Readers are encouraged to look close (or zoom in) to appreciate the self-assembling nature of these microspheres.

These data were promising. It was demonstrated that the T-junction orientation, along with the 80 % glycerol carrier phase, could be employed for the fabrication of MAES polyHIPES. Despite being ‘deformed’, i.e. smooth and microporous, the resulting microspheres were highly monodisperse and structurally sound. Crucially, the rate of production for each of the conditions was rapid. HIPE was always aspirated to a final volume of 20 mL into a syringe; the maximum time required to deliver this was over 3 hr (when using the ‘small’ condition injection rate of 6 mLhr<sup>-1</sup>). This would give a packed bed of at least 25 mL microspheres, which was regarded as enough for later experimentation. Despite these successes, the smallest microsphere fabricated was, of course, from the ‘small’ condition, with an average diameter of 315 µm achieved. Having microspheres larger than 300 µm posed handling issues, with respect to the aspirating of microspheres when suspended in liquid with a pipette. It was found that microspheres larger than 300 µm tended to jam in the tip. This could be overcome by simply diluting the microspheres and so eliminating any chance of accumulation before the point of entry, but this was not feasible for later use when exact volumes containing a high number of microspheres would be employed.

Large bore pipette tips were available and these were indeed used later in the project for

---

those microspheres larger than 300  $\mu\text{m}$ . However, it was decided to determine the conditions in which microspheres would be fabricated with an average diameter of 300  $\mu\text{m}$  or under. This would allow 'normal' pipette tips to be eventually used and increase compatibility of the cell retention device with standard laboratory equipment. It was now known that the injection rate and the carrier phase flow rate could be modified to adjust the diameters of the fabricated particles. It was also known from the co-flow experiments that the internal diameter, or the gauge, of the needle also played a part.

Figure 5.9A shows the diameter size distributions of microspheres produced from 4 new conditions, as determined by measuring 200 individual particles. The small case Roman numerals above each data column denote the specific fabrication conditions employed; (i) an injection rate of 4  $\text{mLhr}^{-1}$ , a carrier phase flow rate at 400 rpm and a needle gauge of 30 G; (ii) an injection rate of 2  $\text{mLhr}^{-1}$ , a carrier phase flow rate of 400 rpm and a needle gauge of 32 G; (iii) an injection rate of 2  $\text{mLhr}^{-1}$ , a carrier phase flow rate of 600 rpm and a needle gauge of 32 G, and (iv) an injection rate of 6  $\text{mLhr}^{-1}$ , a carrier phase flow rate of 600 rpm and a needle gauge of 32 G. Needles with a gauge of 32 G had an internal diameter of 0.11 mm and were the thinnest attempted in this work. The HIPE was the same as that used in the first attempt with the T-junction, i.e. 90 % emulsion, 10 % MAES and with no further modifications.

Condition (i) was tested after reviewing the data from the first T-junction demonstration. It was decided to reduce the injection rate from 6 to 4  $\text{mLhr}^{-1}$ , whilst reducing the carrier phase flow rate from 600 to 400 rpm. The needle was switched back from 20 G to the smaller 30 G. The reduction in the injection rate was obvious; it was known that a slower volume of HIPE emerging from the needle would result in physically smaller microspheres. The reduction in the carrier phase flow rate (as dictated by the rotational speed of the pump) went against what was previously observed. Increasing the flow rate should decrease the size of the microspheres; however, one important aspect of microsphere quality was monodispersity. It was actually found during validation testing for these data that when using 80 % glycerol the turbulence of the carrier phase began to have a considerable effect on the resulting dispersion of diameters, i.e. at high carrier phase flow rates the emulsion would actually be broken up vigorously into multiple-sized particles. This only seemed true for slower injection rates, as was now being tested. If the carrier phase flow rate was too high, it would force the emulsion out of the needle tip and break it up before a steady stream was formed. The resulting particles may be spherical, but they would be made up of a range of different diameters.

The average diameter of the microspheres fabricated using condition (i) was determined

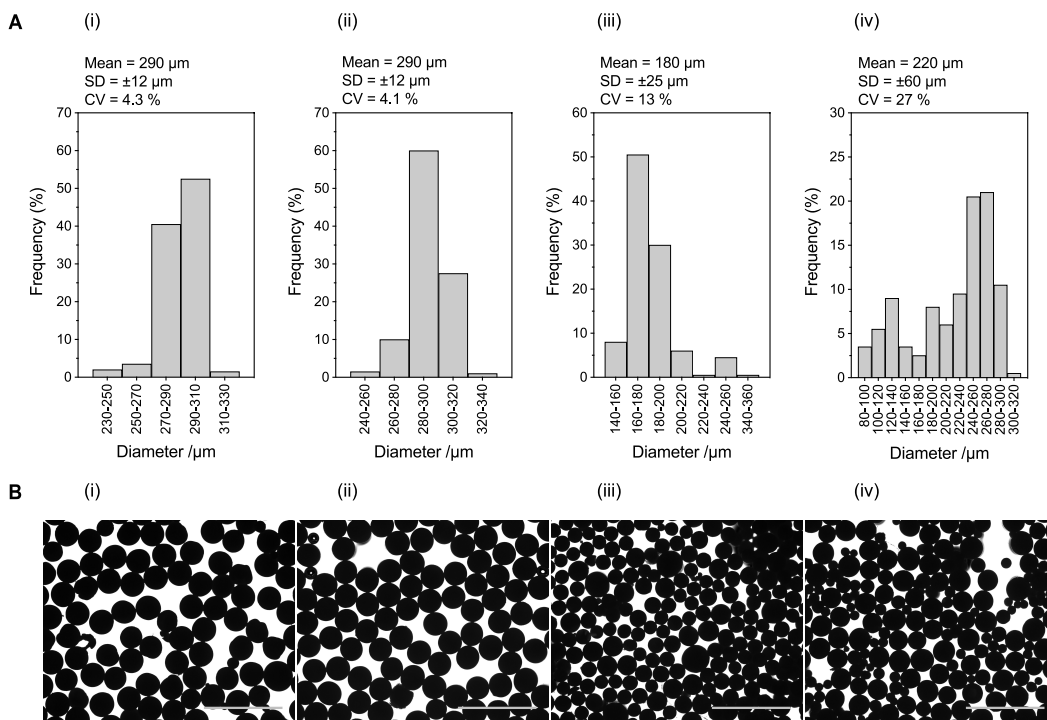


FIGURE 5.9 Diameter and morphology analysis of MAES polyHIPE microspheres fabricated using the T-junction orientation and 80 % glycerol carrier phase at four different process conditions. 10 % MAES microspheres were fabricated at four different conditions (carrier phase flow rate, rpm / HIPE flow rate, mLhr<sup>-1</sup> / needle gauge, G); (i) 400/4/30; (ii) 400/2/32; (iii) 600/2/32 and (iv) 600/6/32, with (A) 200 microspheres measured to determine average diameter and (B) bright-field micrographs, at 4 $\times$  magnification, obtained to visualise monodispersity. Data represent mean  $\pm$  SD, n=200 discreet microspheres. Scale bars = 1000  $\mu\text{m}$ .

to be 290  $\mu\text{m}$ , with a coefficient of variance of 4.3 %. These data were satisfactory. To test if the microspheres could further be reduced in size, condition (ii) switched to a 32 G needle, kept the carrier phase flow rate at 400 rpm and reduced the injection rate further from 4 to 2 mLhr<sup>-1</sup>. The average diameter in this instance was determined, again, to be 290  $\mu\text{m}$ , with a coefficient of variance of 4.1 %. Interestingly, there was no considerable difference between microspheres fabricated using conditions (i) or (ii), although for (ii), the particles appeared, by eye, slightly more spherical.

Condition (iii) kept the 32 G needle and the 2 mLhr<sup>-1</sup> injection rate, whilst increasing the carrier phase flow rate from 400 to 600 rpm. This demonstrated what was introduced earlier; namely, the effect of turbulence on HIPEs that were slowly injected. The average diameter was determined to be 180  $\mu\text{m}$ , yet the coefficient of variance was 13 %, a relatively high value at this point in the work. Indeed, the spread of sizes can be seen in the frequency distribution, with a range from 140 to 360  $\mu\text{m}$  observed. To try to counter this, condition (iv) kept the 32 G needle but returned to the conditions attempted previously with the 'small' condition, i.e. an injection rate of 6 mLhr<sup>-1</sup> and a carrier phase flow rate at 600 rpm. Inter-

estingly, despite the success of the ‘small’ condition, the coefficient of variance remained high at 27 %, with a mean diameter of 220  $\mu\text{m}$  determined. It was proposed that the smaller needle in this instance, 32 G compared to 20 G, was causing the HIPE to be considerable smaller at the injection point. As discussed, this in turn resulted in more break up via the turbulence of the carrier phase.

Figure 5.9B shows brightfield micrographs for all 4 conditions tested. The polydispersity of sizes can be noticed with those fabricated using conditions (iii) and (iv). Scanning electron micrographs were not obtained for the microspheres fabricated in these conditions, but ‘deformed’ structures were confirmed using optical microscopy. Conditions (i) and (ii) were the ‘sweet spot’, so to speak, and both gave microspheres with mean diameters under 300  $\mu\text{m}$  and a relatively low coefficient of variance. Condition (i) was regarded as more suitable for the aims of the work due to the faster injection rate; using these parameters would result in a larger volume of microspheres produced in a shorter time. It was thus decided to employ condition (i) for the routine fabrication of 10 % MAES ‘deformed’ polyHIPEs.

By this time in the project, it was realised the microsphere fabrication system was incredibly sensitive, in regards to the microspheres produced, and also highly empirical. What worked for a 10 % MAES HIPE would not necessarily work for other formulations and whilst certain conditions proved successful, there were still times where the system appeared to behave differently to what was previously shown. To present the way in which the system sometimes ‘misbehaved’, Figure 5.10A shows the diameter size distributions of three sets of microspheres retrieved using condition (i), i.e. the newly designated condition for the routine fabrication of microspheres. The system sometimes produced a ‘by-product’, or rather another set of smaller microspheres with a fairly narrow range of diameters, alongside the expected set of larger microspheres. This can be seen with the two separate peaks in Fig. 5.10A(i).

In Fig. 5.10, (i) refers to all microspheres as they were retrieved from the filter sock, whilst (ii) refers to the smaller by-product and (iii) to the expected ‘normal’ microspheres. Microspheres were separated by flushing microsphere suspension into a 200  $\mu\text{m}$  cell strainer; the smaller by-product passed through and the larger microspheres were retained. For the unfiltered microspheres, i.e. those collected from the filter sock and not filtered, a mean diameter of 189  $\mu\text{m}$  was determined with a coefficient of variance of 47 %. For the microspheres that passed through the filter, a mean diameter of 101  $\mu\text{m}$  was determined with a coefficient of variance of 8.7 %, and for the retained microspheres, a mean diameter of 276  $\mu\text{m}$  was determined with a coefficient of variance of 2.9 %. As discussed previously, this appeared to be related to the turbulence of the glycerol carrier phase, with two de-

finer sets of microspheres forming independently and continually within the same stream of emulsion. These sets accumulated within the filter sock and, upon collection, resulted in a mixed batch of two differently sized materials. The smaller microspheres were referred to as a by-product as, strictly speaking, only the larger microspheres were desired. These larger microspheres were similar in diameter to those initially produced using condition (i) in Fig. 5.9, which first demonstrated this condition. As this was the intended outcome of the condition, the by-product was tolerated.

Bizarrely, the fabrication of a by-product did not always happen. This seemed related to the fact, first mentioned at beginning of this section, that the system used was essentially crude

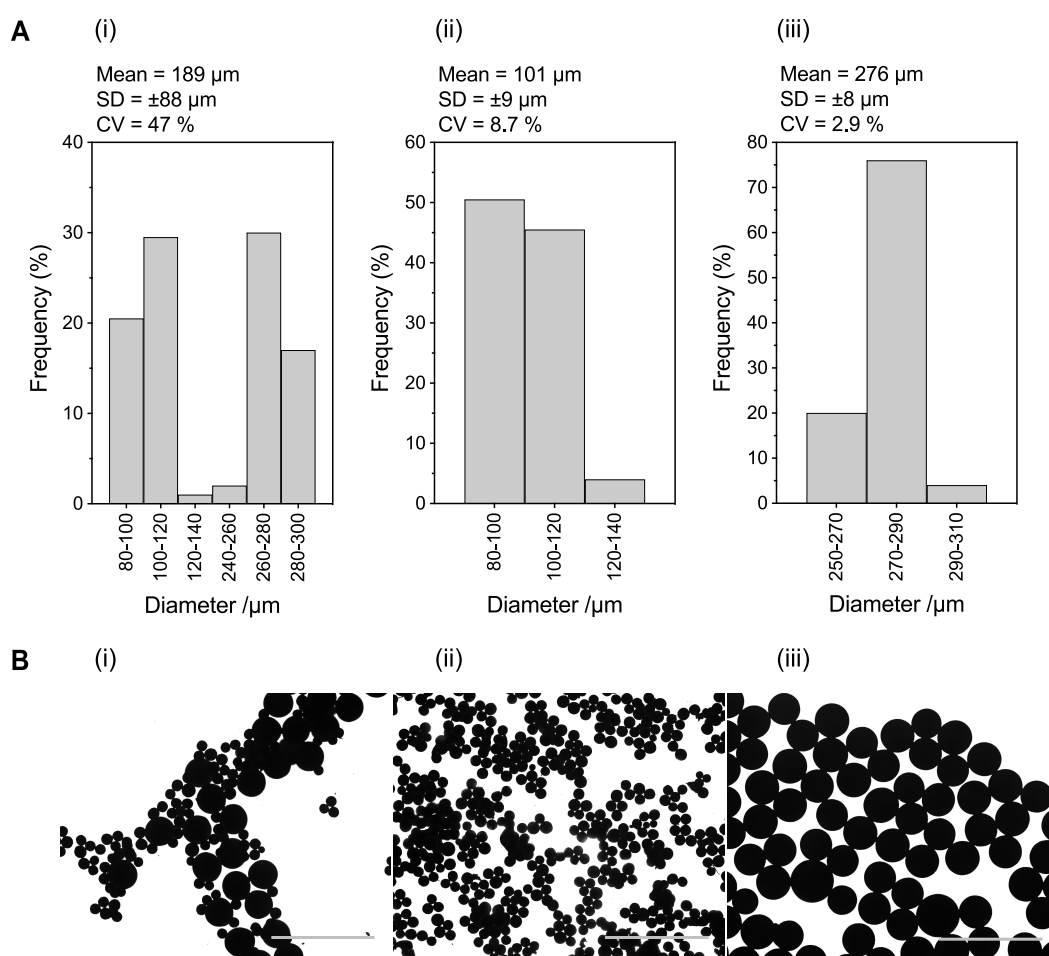


**FIGURE 5.10** Evidence of by-product when fabricating MAES polyHIPE microspheres using the T-junction orientation and 80 % glycerol carrier phase. 10 % MAES microspheres were fabricated at 400 rpm / 4 mLhr<sup>-1</sup> / 30 G (the routine fabrication condition). Collected microspheres, which were unfiltered (i) were analysed, before being filtered with a 200  $\mu\text{m}$  strainer. The smaller by-product (ii) and larger retained (iii) microspheres were subsequently analysed. (A) 200 microspheres were measured to determine average diameter and (B) brightfield micrographs, at 4 $\times$  magnification, obtained to visualise monodispersity. Data represent mean  $\pm$  SD, n=200 discrete microspheres. Scale bars = 1000  $\mu\text{m}$ .

and not entirely understood. Liquid manipulations were performed by simply inserting a needle into a flowing stream of liquid, contained within a piece of tubing. Because of this, any seemingly small changes, either related to the relative viscosities of the HIPE or the carrier phase, appeared to have an effect on what the size of the fabricated microspheres would be. In contrast to the larger microspheres (as first demonstrated in Fig. 5.8), when fabricating smaller microspheres the position of the needle within the T-junction orientation did indeed now seem to have an effect. Tweaking the distance of the needle, as it was inserted into the tubing, could sometimes eliminate by-product formation. With this in mind, the task at this particular part of the project was always to use the current technology that was available and as it was presented. Whilst it was tempting to imagine or indeed plan a microfluidic system (and so enable greater manipulation of liquids), the development of any such system was far beyond the scope of the project and would have taken considerably more time to achieve.

#### 5.1.4 CONCLUSIONS

The work in the first part of the chapter explored the use of polyHIPEs, a type of porous material, as the physical component of the cell retention device. Due to the planned use of polyHIPE materials as microspheres, any handling issues had to first be addressed. This included the aggregation typically seen when hydrocarbon-based spherical particles were placed in aqueous solutions, such as culture medium.

PolyHIPE fabrication technology available to use currently employed acrylic monomers without any functional groups. It was proposed monomers with such 'reactive' moieties could be used to both prevent aggregation and covalently link the materials to polyethylenimine substrates. However, any new monomer would have to be inexpensive, readily available and compatible with the HIPE generation process. The acrylic monomer mono-2-(methacryloyloxy)ethyl succinate, termed MAES here, was identified as a compound containing both an acrylic C=C group and a carboxylic acid group. It was suspected including this within a HIPE would result in these carboxyl groups being exposed on the surface of the subsequent material upon polymerisation. These groups would ensure repulsion between neighbouring microspheres once in solution, by virtue of their ionic behaviour.

MAES was successfully incorporated into fabricated polyHIPE monoliths, alongside the monomer EHA, at increasing concentrations. The presence of MAES appeared to reduce the viscosity of the generated HIPE, although the emulsion remained stable at all concentrations used. TBO, a reagent employed as a cationic stain, was adapted so as to detect any exposed carboxyl groups within the fabricated polyHIPEs. This assay demonstrated, quantitatively, that increasing the concentration of MAES within the HIPE increased the

amount of carboxyl groups within the polymerised materials. Images were provided to show the extent of staining on MAES polyHIPEs and the absence of staining on materials fabricated solely using EHA.

The use of the microsphere fabrication system was demonstrated, with both co-flow and T-junction orientations attempted using HIPEs containing 10 % MAES. For co-flow, different carrier phase compositions were explored, including water, glycerol and PVA. Only with glycerol or PVA did spherical particles form. For glycerol, signs of water loss within the HIPEs were observed, with microspheres possessing microporous, rather than macroporous, structures. This was not as pronounced when using PVA. For the T-junction orientation, 80 % glycerol was employed with a range of microspheres fabricated. Unlike co-flow, the rate of production was considerably faster and was decided to be ultimately used for the routine fabrication of polyHIPE microspheres, with an injection rate of 4 mLhr<sup>-1</sup>, a carrier phase rate at 400 rpm and a 30 G needle deemed to be sufficient. These data contrasted with that observed by Paterson et al. (2018), who used 100 % water as a carrier phase to produce macroporous polyHIPE microspheres. Readers should review this paper if they wish to see what 'typical' polyHIPE microspheres look like. This, however, was achieved with HIPEs containing IBOA, which were considerably more viscous than those containing MAES. The relative viscosities of the HIPE and the carrier phase were observed here to be extremely important in determining the degree to which spherical particles formed within the system.

This first part of the chapter revealed the effect of glycerol on the fabricated polyHIPE microspheres. All microspheres fabricated were highly monodisperse, yet their morphologies were smooth and microporous. These materials were 'deformed', having been modified by the hygroscopic effects of the glycerol immediately prior to polymerisation. This led to a compromise within the project. PolyHIPE microspheres with carboxyl groups could be fabricated, routinely and rapidly, and with an average diameter of less than 300 µm. However, these materials were not macroporous and instead of the vast surface areas originally anticipated with these materials, only microporous structures could be obtained. It was thus certain that cells would attach only upon these surfaces and not within the structures as initially hoped. It was decided to keep these microporous polyHIPEs and continue with the overarching objective of the project, namely the in-house development of a continuous upstream system.

The work presented here was the result of many months of work. It took several discussions to realise glycerol was having an effect on the morphologies of the fabricated polyHIPEs. Despite this setback, the fabrication of MAES polyHIPE microspheres was achieved by the

use of both the co-flow and T-junction orientations. Whilst the co-flow proved not suitable for actual production purposes, its ability to fabricate microspheres ‘one by one’ in a recurring fashion could enable it to be employed for future work on HIPE formulation and carrier phase composition. It was also the first time it was attempted in the laboratory. It is argued here that co-flow, by its ability to produce microspheres in a distinctly separate fashion, is the only way to truly ensure monodisperse materials. The T-junction, by comparison, presented a working alternative, but had some drawbacks that were eventually accepted. It was suggested a designed experiments approach may be more appropriate for any future investigation into the fabrication of polyHIPE microspheres.

## 5.2 INTRODUCTION TO MICROSPHERE APPLICATIONS

The first part of this chapter investigated the capability to rapidly fabricate polyHIPE microspheres in-house. The inclusion of a novel acrylic monomer, MAES, containing a carboxylic group into the HIPE ensured the cured polyHIPE likewise contained these groups. The TBO reagent confirmed their exposure on the surfaces of the materials and hydrophilic properties, resulting from these groups, were apparent. Whilst macroporous microspheres were not ultimately possible, the use of glycerol as a carrier phase in combination with the T-junction orientation gave highly monodisperse microspheres, with average diameters of 300  $\mu\text{m}$  or less achievable — although these microspheres lacked typical polyHIPE macroporosity, but instead had microporous structures. Such microspheres, which have been termed ‘deformed’ polyHIPEs here, likely occurred as a result of the hygroscopic nature of the glycerol. These data collectively ended in a compromise; macroporous polyHIPE microspheres could not be obtained reliably and without eventual material collapse, yet microporous microspheres could and the process was generally reproducible. It was accepted that cells would likely only attach upon the surface of each microspheres and not within.

The fabrication of the polyHIPE microspheres (the physical component of the cell retention device) was now complete for the purposes of the work presented here. Microporous polyHIPEs, with average diameters between 270–300  $\mu\text{m}$  would be employed for the main objectives of the project. The next stage was to bring the materials back to a cell culture setting for initial testing, first with microsphere handling and then with cell attachment. Cell loading, which was first demonstrated in § 3.1.1 with multiwell plates and flasks, describes a method where microspheres, or indeed any surface capable of adhering cells, are exposed to a very high cell density suspension. This ensures microspheres, as the cell retention device in this instance, are rapidly seeded with their entire available surface area saturated with cells. If performed successfully, it also opens up the possibility of immedi-

ately initiating an intensified continuous culture after cell loading.

The specific objectives for the second part of this chapter were to; (i) attempt to wash, sterilise, and coat the 'deformed' polyHIPE microspheres with polyethylenimine substrates, and (ii) further explore the idea of cell loading first introduced in Chapter 3, using a technique where coated microspheres are retained themselves within columns and exposed to CHO cells at very high cell densities.

### 5.2.1 PEI ADSORPTION TO MICROSPHERES

Early validation work had fabricated polyHIPE microspheres using EHA and IBOA. As previously discussed, these possessed no reactive functional groups and so were prone to hydrophobic aggregation when placed in aqueous solution. The adsorption of polyethylenimine onto EHA/IBOA polyHIPEs was successfully performed (data not shown), although it was incredibly cumbersome. Microspheres had to be added in small batches — scooped in using a spatula — to a polyethylenimine coating solution and agitated gently to encourage adsorption. If microspheres were shaken suddenly by hand, or agitated using end-to-end spinning (via a motorised 'carousel' device), they would instantly clump. Resuspending aggregated microspheres was practically impossible, unless acetone was used, which returned all clumps to single particles. Acetone was a useful solvent for microsphere handling. All microspheres, including those made using MAES, were washed twice with acetone post-fabrication and then stored in fresh acetone to ensure no aggregation overtime. All microspheres could be shaken, stirred and handled with no stability issues when stored in acetone. Figure 5.11A shows MAES polyHIPE microspheres stored in acetone, with their self-assembly behaviour seen once again. Observations throughout the project revealed no identifiable changes to the structure of the materials if this was done; indeed, a benefit of acrylic polymers (in contrast to styrenic polymers) is their resistance to chemical attack from acetone.

The first indication that carboxyl groups had successfully incorporated into the fabricated MAES polyHIPE microspheres was, of course, related to the behaviour of the materials in suspension. Unlike those produced using solely EHA and IBOA, the MAES polyHIPE microspheres did not aggregate as readily when placed in any aqueous solutions. Indeed, they could be added to PBS with gentle agitation without any clumping; this, of course, being due to the ionic behaviour of the carboxyls in a pH 7 environment. The benefits of having these carboxyl groups was only truly realised when adsorption of polyethylenimine was attempted. In contrast to EHA/IBOA microspheres, MAES polyHIPEs could be directly and rapidly exposed to polyethylenimine coating solution without them suffering any major aggregation. The small clumps which did arise could be resuspended,

and seemingly were then adsorbed with polyethylenimine, by simply pipetting the microspheres up and down several times. Microspheres could then be mixed overnight using end-to-end spinning to ensure sufficient coverage of the materials. Following adsorption with polyethylenimine, MAES polyHIPE microspheres could be placed into PBS, culture medium or any other aqueous solution with no handling or stability issues whatsoever.

Because of this ease of adsorption, which proved to be incredibly robust and technically simple, the coating of polyHIPE microspheres by overnight incubation with polyethylenimine became a standard protocol. The extremely low cost of polyethylenimine meant no study was performed, or indeed needed, relating to the precise adsorption limits of the materials. Instead, 5 mL of polyethylenimine stock solution was added to 45 mL water to prepare a 10 mgmL<sup>-1</sup> coating solution. 45 mL of this was then added to 5 mL microspheres and mixed overnight. These values were arbitrary. However, it was assumed due to the rapid resuspension seen with the materials that this was sufficient to coat the surface of each microsphere. Figure 5.11B shows MAES polyHIPEs, in PBS, after overnight adsorption with polyethylenimine. The quick settling of microspheres, once in aqueous liquids, was regarded as a marker of successful polyethylenimine coating, with the amines now guaranteeing repulsion between neighbouring microspheres. All experimental work relating to the use of MAES polyHIPE microspheres used this technique to adsorb polyethylenimine. For experiments that required more than 5 mL microspheres, batch incubations, where each 5 mL volume of microspheres was exposed to separate 45 mL polyethylenimine solutions, were carried out.

Sterilisation was performed by two techniques, either by a 70 % ethanol wash for 1 hr immediately before use or an autoclave cycle at 121 °C. The former was used for the vast majority of the work presented in this project. Strictly speaking, ethanol is a disinfectant, not a sterilant, but was regarded as sufficient for the purposes of the work. The disinfecting of polyHIPE monolithic materials using ethanol, for aseptic cell culture use, has been reported in the literature (Owen et al., 2016). However, a small risk of contamination, largely from fungal spores, was always present with this method. Exposing polyethylenimine-adsorbed microspheres to ethanol had no noticeable effect on the adhesion properties of the coated materials. Indeed, after it was coated, polyethylenimine continued to stay 'active', e.g. after incubating with ethanol, microspheres would still readily resuspend in PBS or culture medium, as before. Immediately prior to cell culture use, microspheres were washed first in sterile PBS and then incubated briefly in medium. Uncoated microspheres did not aggregate once placed into medium due to the carboxyl groups, but vigorous agitation had to be avoided. The ease of overnight adsorption with polyethylenimine, followed by a 1 hr ethanol disinfecting schedule, was regarded as a key reason why these microspheres were

a technically simple cell retention device.

### 5.2.2 CELL LOADING AND MICROSPHERE CELL GROWTH

The principle behind cell loading was introduced previously in the work presented here. In § 3.1.4, T-25 flasks adsorbed with polyethylenimine were ‘loaded’ with 10 million cells overnight. This cell amount was vastly greater than any typical seed used for routine batch passaging — thus the term ‘loading’ — but it ensured the entire surface of each vessel was saturated with cells. Cell loading was first suggested at the beginning of the project when novel ideas were being explored. A small-scale perfusion device, utilising microspheres within micro-scale columns, was an early concept. Before the continuous process is started, microspheres would not be seeded, but instead rapidly ‘loaded’ by perfusing a high cell density suspension through the columns. In effect, this would actively saturate the cell retention device by forcing the cells to interact with the microspheres. Once loaded, the columns could be connected, via tubings, to a simple perfusion system and medium exchange could begin. As polyethylenimine was found to be an effective adhesion substrate,

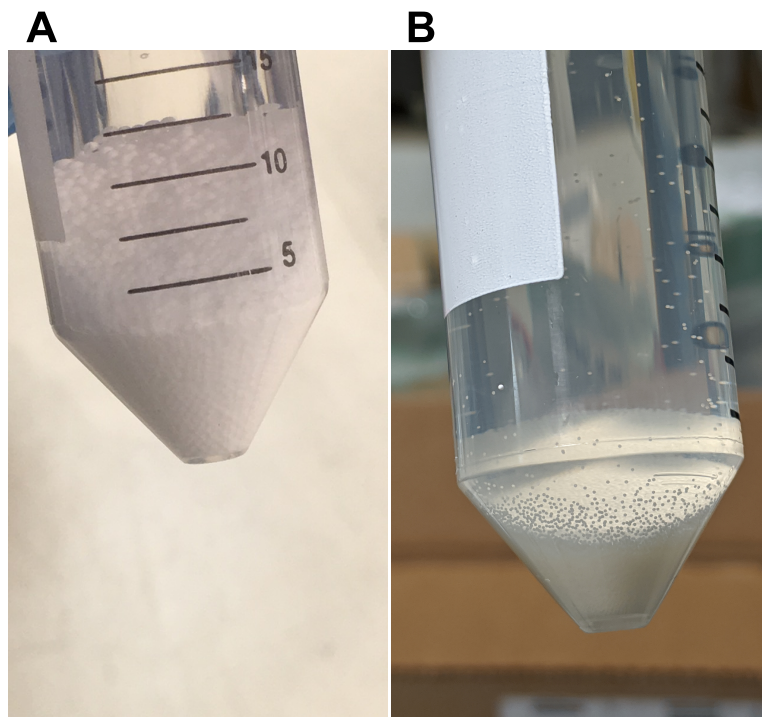


**FIGURE 5.II** Photographs of MAES polyHIPE microspheres in storage using acetone and after adsorption with polyethylenimine. (A) shows ‘medium’ sized MAES polyHIPE microspheres stored in acetone. All polyHIPE microspheres were washed in acetone and then stored in fresh acetone until required. Acetone ensured microspheres did not aggregate overtime, and it did not appear to have any effect on the structure of the materials. (B) shows MAES polyHIPEs, as fabricated using routine conditions, in PBS after adsorption with polyethylenimine.

and one which cells rapidly adhered to, the idea of cell loading was regarded as feasible.

Using columns, with microspheres retained within as packed-beds, was partly inspired by column chromatography operations within downstream processing of biopharmaceuticals. Using rudimentary terminology, in chromatography a mobile phase containing a compound of interest is passed through a stationary phase or matrix — usually microspheres or some form of resin — with the compound of interest captured, or retained, as it interacts with this matrix. In a similar way, the question was asked whether CHO cells could be passed through a matrix, or polyethylenimine-adsorbed microspheres as was the case here, and thus forced to interact and be retained. If the number of cells entering the column was known, and the number of cells in the effluent of the column determined, then the number of cells retained upon the microspheres could be easily calculated.

Autoclavable 1.0 mL polypropylene columns, intended for chromatography, were obtained. These were supplied empty with frits included so operators could fill the columns with a resin of their choice. For the work here, these columns were filled with 1 mL MAES polyHIPE microspheres and attached, via a luer connection, to a syringe. The microspheres employed were those fabricated using the 'medium' condition, as defined in Fig. 5.8 previously, with an average diameter of approximately 470  $\mu\text{m}$ . This syringe could be filled with CHO cell suspension and operated with a syringe pump, delivering the suspension at a controlled flow rate through the column and onto the microspheres. It was decided to test three flow rates (1.0, 2.5 and 5.0  $\text{mLmin}^{-1}$ ) and three increasing CHO cell loads (25, 50 and 100 million cells), using 50 mL suspension, for the loading of both uncoated microspheres and microspheres adsorbed with polyethylenimine. The number of cells were measured in each 5 mL of effluent, i.e. the cells that had not attached to the microspheres and exited the column. The breakthrough percentage (the percentage of cells that had not been retained) for every 5 mL delivered was then determined by deducting the cells in the particular effluent sample from the number of cells initially present within 5 mL of the cell load. A breakthrough of 100 % would indicate all of the cells within a 5 mL volume were being passed through into the effluent, i.e. no cells were retained as they passed through the column. For a breakthrough of 0 %, all the cells within 5 mL of the load would be retained, with none passing through into the effluent.

Figure 5.12A shows the breakthrough of cells, as a percentage, for the loading of uncoated microspheres. The three different flow rates were tested for each cell load. Uncoated microspheres did not readily retain cells, with the majority of cells breaking through in the very first 5 mL effluent sample, regardless of the cell load. For the 2.5 and 5  $\text{mLmin}^{-1}$  flow rates, by the 10 mL effluent sample 100 % of the cells were breaking through, i.e. none of

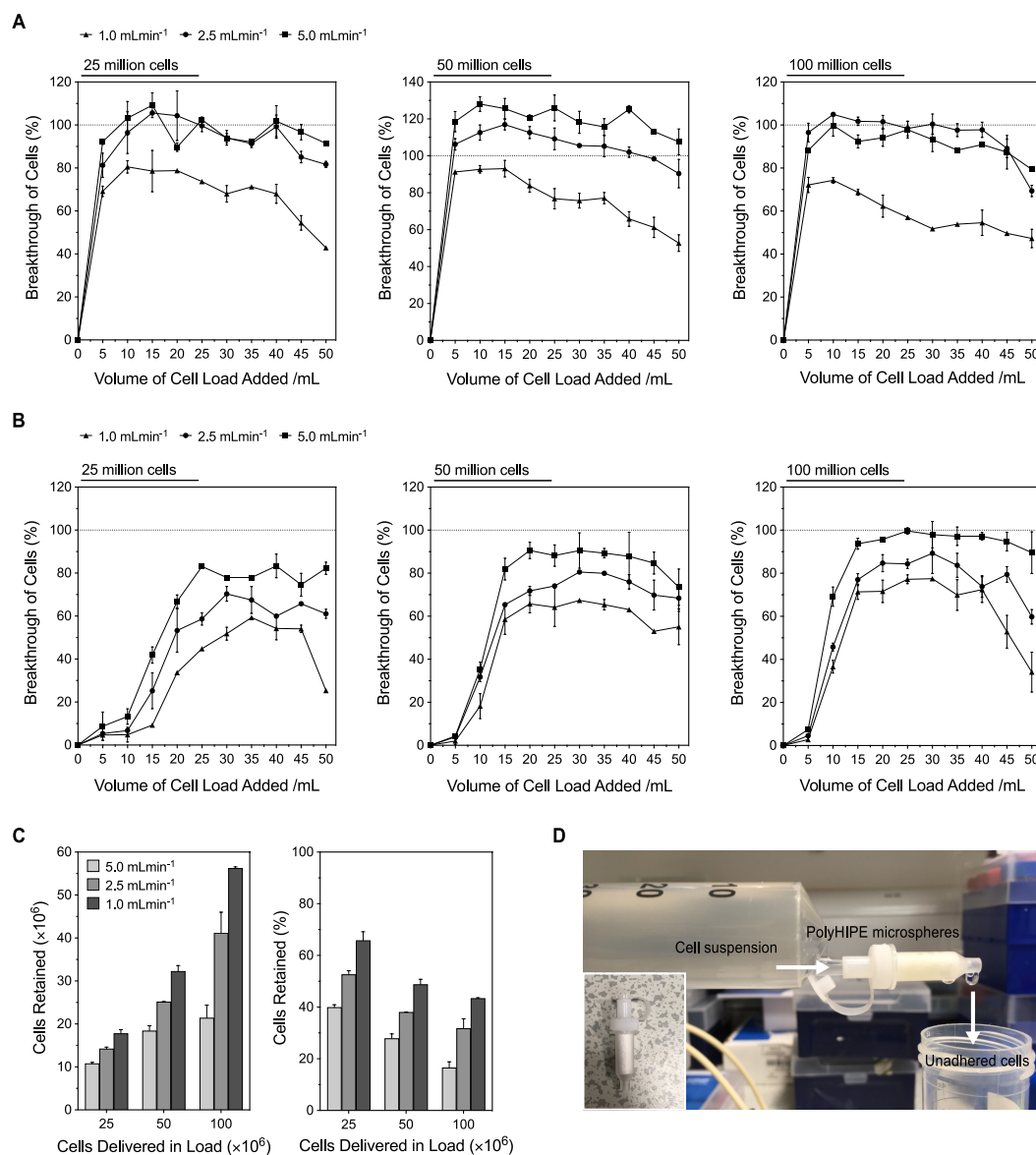
the passing cells were being retained upon the microspheres. This generally continued for the remainder of the loading schedule. For the  $1.0 \text{ mLmin}^{-1}$  flow rate, the breakthrough approached approximately 80 %, for all three cell loads, by the first 5 mL effluent. Interestingly, the breakthroughs then steadily decreased until the full 50 mL load had been delivered. This suggested, because of the relatively low flow rate, cells were likely getting entrapped within the packed-bed rather than physically adhered. The flushing of columns after delivering the 50 mL load, e.g. by using PBS or medium, was not attempted in this experiment.

Figure 5.12B shows the breakthrough of cells, as a percentage, for the loading of microspheres adsorbed with polyethylenimine. The retention of cells can now be observed, with the breakthrough percentage being initially less than that seen with uncoated microspheres, for all flow rates and cell loads. For each cell load amount, the flow rate dictated the breakthrough percentage for every 5 mL sample. This was as expected; the flow rate determined the residence time within the column, with a slower flow rate having a longer time and so allowing more chance of interaction between cells and microspheres. The residence time for  $1.0 \text{ mLmin}^{-1}$  was 1 min, for  $2.5 \text{ mLmin}^{-1}$  it was 24 s and for  $5 \text{ mLmin}^{-1}$  it was 12 s.

The breakthrough for each flow rate increased as the cell load was increased, e.g. for the 25 and 50 million load, no flow rate gave breakthroughs of 100 %, whilst for the 100 million load,  $5 \text{ mLmin}^{-1}$  did reach 100 % breakthrough by the delivery of 25 mL. For this higher cell load, 100 % breakthrough was maintained for the remainder of the delivery, suggesting saturation of the microspheres. With a greater number of cells, it was suggested there was increased competition for interaction and retainment between cells and microspheres, but whilst breakthrough may indeed be greater for these larger cell loads, the corresponding number of cells retained is also greater. It was anticipated that, as the volume of cells perfused through increased, the breakthrough for each 5 mL sample would likewise increase, as the microspheres become increasingly saturated with less available space for cells to adhere. This was indeed the case with a plateau effect being observed for all flow rates and cell loads. This plateauing was less prominent with the lower 25 million cell load, as there was likely more available space upon the microspheres for cells to adhere.

For ease of comparison, Figure 5.12C summarises the data for the final retainment of cells using polyethylenimine-adsorbed microspheres. Both the actual cells retained and the cells retained, as a percentage of the total cells delivered, are shown. For each of the three cell loads, the number of cells retained increased as the flow rate was decreased. The flow rate had a greater effect on the total number of cells retained when the cell load was higher.

As examples, for the cell load of 25 million, the difference in cells retained between the 1.0 and 5.0 mLmin<sup>-1</sup> flow rates was less than 10 million; for a cell load of 100 million, this difference was now over 30 million cells. This was not surprising, with a low cell load



**FIGURE 5.12 Breakthrough curves for CHO cells loaded onto PEI-adsorbed MAES polyHIPE microspheres.** CHO cell suspension containing either 25, 50 or 100 million cells were delivered at either 1.0, 2.5 or 5.0 mLmin<sup>-1</sup> flow rates through columns packed with 1 mL PEI-adsorbed microspheres. The number of cells in every 5 mL effluent was determined to calculate the percentage of cell breakthrough when using (A) uncoated microspheres and (B) PEI-adsorbed microspheres, with (C) showing the absolute number of cells retained and the cells retained (as a percentage of cells delivered) for PEI-adsorbed microspheres. (D) Photograph of a 1.0 mL column packed with microspheres attached to a syringe and being cell loaded (lower left inset: 1.0 mL column packed with microspheres and dried). Data represent mean  $\pm$  SD,  $n=2$  (biological duplicate).

resulting in less competition for potential microsphere interaction and thus meaning the flow rate had less of an effect. For a higher cell load, the flow rate had a greater effect, with cells likely now relying on longer residence times to interact successfully with the materials. This can be taken to mean a lower flow rate, and consequently a quicker loading time, can be used when loading small numbers of cells. The highest cell retainment achieved was approximately 55 million cells, using a 100 million load at a flow rate of  $1.0 \text{ mLmin}^{-1}$ . If this was indeed true, then it corresponds to be a concentration of 55 million cells per mL of microspheres.

The cells retained, as a percentage of total cells delivered, was interesting and shows that cells are not that easily retained. Indeed, for the 50 and 100 million cell loads, the majority of cells (50 % or greater) did not adhere and passed through the column, regardless of the flow rate employed. For the 25 million cell load, only when a flow rate of  $1.0 \text{ mLmin}^{-1}$  was used did the cells retained go above 60 %. There is clearly a need to prepare for cell loss and consequently increase the cell load to compensate for this.

Figure 5.12D shows the set up employed to obtain these data, with a column filled with microspheres being perfused with CHO cell suspension by the use of a 60 mL syringe and syringe pump. The set up was positioned so that the effluent, i.e. the suspended cells within medium which did not attach, was collected in a centrifuge tube. This tube would be swapped for a fresh one for every 5 mL collected, ensuring that the delivery was not periodically disrupted. For the  $5.0 \text{ mLmin}^{-1}$  flow rate, this swapping had to be performed quickly, with a collection of centrifuge tubes ready. The lower left inset photograph shows an example of polyHIPE microspheres filled and dried within one of these columns. The frit, also white, can be seen at the bottom and ensured no microsphere loss.

Microspheres were aspirated to visually observe if cells were indeed adhered, with this found to be the case. Figure 5.13 provides micrographs of retained cells. As expected, as the polyHIPEs employed here were 'deformed', i.e. microporous, cells appeared to be only adhered upon the surfaces of the materials. Only two syringe pumps were available, so the data presented here was the mean of a biological duplicate. Despite this, the results were fairly similar for each condition, with satisfactory error bars obtained, indicating reproducibility. Filling the columns with microspheres took several minutes. The easiest method involved twisting the column with one hand, whilst dispensing microspheres in dilute 1 mL suspensions using the other. This twisting ensured even settling with no air gaps. Using a dilute microsphere suspension also ensured no slurry formed on the inside of the tip as the materials were dispensed. Once a 1 mL bed had formed, the cap could be screwed on and the column attached to the syringe.

The technique of using columns and a syringe pump to actively force interaction between cells and microspheres has, as far as can be seen, never been reported in the literature. It was demonstrated here that cells can indeed be treated as a 'compound of interest' and retained via the use of a packed-bed of polyethylenimine-adsorbed microspheres. The trade-off between residence time within the column and retainment was soon apparent; the 1.0 mLmin<sup>-1</sup> flow rate took 50 min to deliver 50 mL of cell load, whilst the 5.0 mLmin<sup>-1</sup> flow rate only took 10 min. However, the lower flow rate achieved a greater retainment for all three cell loads tested. This may become a practicality issue with future operators of this system having to wait longer for a loading schedule to complete, before a culture can then be started. A more realistic system would likely require a compromise between effective retainment and quicker loading times. There is also the question of how long CHO cells can be within a suboptimal environment, such as a laminar flow hood, at room temperature without suitable buffering. For the 1.0 mLmin<sup>-1</sup> flow rate, which took 50 min, there was initial concerns regarding whether CHO cells would settle at the bottom of the syringe over time. However, this was not visually noticed and the full 50 mL volume was eventually delivered, so it was expected the entire cell amount would be passed through.

If the maximum retainment achieved, at 55 million cells per mL of microspheres, was correct then it would begin to give an indication of the potential of these microspheres for cell culture process intensification purposes. This value, however, is not entirely useful; for instance, 1 mL of microspheres would likely require at least 5 mL of medium for a culture, continuous or otherwise. The metric of 'effective cells per mL of medium' was suggested, where the number of cells per mL of microspheres would be translated into the number per mL of medium. This would mean, if 55 million cells were indeed retained on 1 mL of microspheres, and these microspheres were placed into 5 mL of medium, then the effective concentration would be 11 million cells per mL of medium. For reference, the maximum viable cell densities achieved during batch culture for the CHO-S IgG cell line used here is around 8 million cellmL<sup>-1</sup>. For fed-batch it may approach 15 million cellmL<sup>-1</sup>. The three ways to increase this proposed metric would be to either retain more cells, add more microspheres or reduce the volume of medium. Or even a combination of all three. As mentioned, there is likely a limit to how many mL of microspheres can be added to a relatively low volume of medium before a slurry is formed and the culture rendered unfeasible.

The 1.0 mL columns employed in the first cell loading experiment had capped ends. If the columns were held upright, these caps could be unscrewed and the microspheres gently aspirated out with a pipette. Even though 'plugging' the columns into a perfusion system was the eventual intention (see § 6.2.1), using a pipette gave a simple way of retrieving microspheres once loaded. To demonstrate adherent growth upon the microspheres, it was

decided to seed — rather than load — the microspheres, retrieve them via aspiration and inoculate into T-25 flasks with fresh medium. For this experiment, a biological triplicate was now performed, with microspheres seeded serially using one syringe pump.

Figure 5.13A shows the cells retained, as a percentage of the total delivered, for the seeding of uncoated microspheres and polyethylenimine-adsorbed microspheres. The seed, as 2.5 million cells, was delivered in a 10 mL suspension at a flow rate of 2.5 mLmin<sup>-1</sup>. With this now being a relatively low cell amount, over 90 % of cells were retained by the polyethylenimine-adsorbed microspheres. The uncoated microspheres retained under 20 %. Microspheres were retrieved and dispensed into T-25 flasks, medium added to 10 mL and the vessels placed in an incubator. On days 4 and 7, microspheres were decanted, washed with PBS to ensure only strongly adhered cells remained and a PrestoBlue assay performed to determine the number of cells upon the microspheres. Fluorescence, as discussed previously in Chapter 3, was used as a marker of cell viability and hence cell number. The uncoated microspheres gave little fluorescence for both time points, which agreed with the observation that a relatively low number of cells were adhered and thus little growth was achieved. The polyethylenimine-adsorbed microspheres did achieve sustained adherent growth, with a fluorescence of 3.5 on day 4 and nearing 6.0 on day 7.

Figure 5.13B shows representative micrographs for both microsphere types for days 0 (post-seed), 4 and 7. Due to their highly porous structures scattering light, PolyHIPE materials are a clean white colour. The ‘deformed’ microspheres employed in this work were no exception. Because of this light scattering, any microspheres viewed using an optical microscope will appear black, with cells only visible around the edges of the structures. It was decided to use Hoechst dyes to visualise cells, if any, adhered upon the central areas of the microspheres. Similar in function to DAPI, Hoechst dyes are employed to fluorescently stain the minor grooves of DNA. When shone with a light of an appropriate wavelength, the stains will emit blue fluorescence and enable cells, or more correctly the nuclei of the cells, to be easily distinguished upon surfaces or structures. The first two rows of micrographs shown are fluorescent images obtained after Hoechst staining; the colour was removed in these images due to suspected autofluorescence of the materials. If this was not done, stained cells were not easily seen; however, the top right inset has an example of a fluorescent micrograph with colour still kept. The bright white specks are stained nuclei of cells. For the polyethylenimine-adsorbed microspheres, the images clearly revealed cells adhered upon the central areas of the materials, with the majority of microspheres having a confluent layer of cells by day 7. The ‘blur’ seen around the edge of the microspheres is due to the limitations in the focusing of the camera. The image was focused on the centre of the microsphere to enable cells to be clearly observed at this location. For the uncoated microspheres,

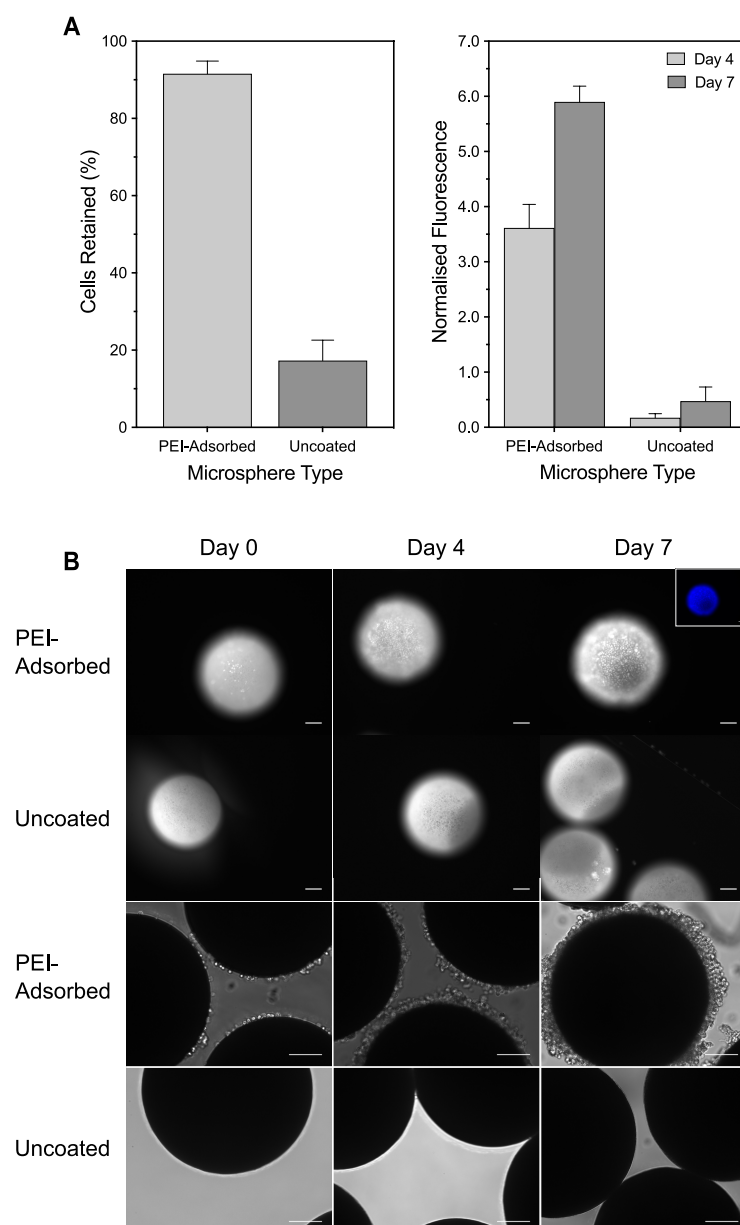


**FIGURE 5.13** **Microsphere CHO seeding and cell growth on PEI-adsorbed MAES polyHIPE microspheres in T-25 flasks.** CHO cells were seeded onto both uncoated and PEI-adsorbed microspheres by the use of a syringe pump with microspheres placed into T-25 flasks and incubated for 7 days. (A) shows the number of cells retained and (B) the adherent growth on the microspheres determined using PrestoBlue on days 4 and 7. (B) Fluorescent micrographs (colour not added), at 10 $\times$  magnification, were taken after adherent cells were stained with Hoechst and brightfield micrographs at 20 $\times$  magnification (top right inset: fluorescent micrograph, with colour added, to show the autofluorescence of the polyHIPE microspheres). Cells grew adherently on PEI-adsorbed microspheres and fully coated the majority of microspheres by day 7. Data represent mean  $\pm$  SD,  $n=3$  (biological triplicate). Scale bars for fluorescent and brightfield micrographs = 100  $\mu\text{m}$ .

the images revealed very few cells, although several clusters can be seen on day 7. Despite this, the fluorescence micrographs did reveal the microporous structure of the uncoated polyHIPEs.

The last two rows of micrographs shown are brightfield images, which revealed only the edges of the microspheres. Indeed, it was these types of image that were used extensively throughout the project to quickly assess the health of a microsphere culture by observing the edges of the materials. These brightfield images, along with the fluorescent micrographs, were used in combination to get a clearer understanding of adherent growth upon the microspheres. For the polyethylenimine-adsorbed microspheres, images obtained on day 1 revealed cells dotted around the structures. By day 4 there had been extensive growth, with most of the microspheres being 'surrounded' by adhered cells. On day 7, which was 3 days after a medium exchange (following the PrestoBlue assay), cells had grown on layers above each other and had begun to clump. This was a common observation with polyethylenimine-adsorbed microspheres; after becoming confluent upon the materials, cells would start clumping in masses as they continued to grow outwards. This would often result in microspheres with tumour-like growths extruding from particular areas of the materials. The exact health of the cells within these growths was not explicitly known, but microspheres giving high fluorescent values, as was the case here, always contained these cell masses. The brightfield micrographs obtained for the uncoated microspheres, as expected, revealed no adhered cells around the edges of the materials.

The loading of microspheres and the adherent growth upon the microspheres, with a static T-25 flask culture, were both demonstrated. A question was raised as to whether multiple columns could be loaded at once, i.e. a high throughput loading technique developed. Only two syringe pumps were available in the laboratory, with each having only a single slot for a syringe. Syringe pumps with multiple slots are available but these were not obtained. However, a peristaltic pump with a multidrive head was supplied. This head could allow up to 12 tubings to be inserted and acted upon at each. The rotational speed of the pump would act the same on all attached tubings, so a system could be operated where multiple tubings would deliver equal amount of volume at the same flow rate. An idea was to use this pump to load multiple columns simultaneously. The use of 2.5 mL columns, as opposed to 1.0 mL columns, was also discussed. By this time it was apparent that any future perfusion system developed for this project would employ either of these two columns (see § 6.2.1 for a discussion of the attempts made at perfusion using both of these column sizes).

The 2.5 mL columns, as with the 1.0 mL type, were polypropylene, autoclavable and came supplied with frits. The operator was, again, expected to fill the columns with a resin of

their choice for chromatography operations. As these columns would now be loaded using a pump, and not attached sideways to a syringe, they would have to be able to stand upright. Several attempts were made balancing columns against labware vessels or small pieces of equipment, but this proved cumbersome and often resulted in columns slipping or tipping and disrupting any on-going loading experiment. A bespoke stand, or a 'perfusion plate', had to be fabricated in-house.

Figure 5.14A shows a computer-aided design of the perfusion plate. The plate was laser cut as three components, two stands and a central section, using an acrylic sheet. Slots were cut into all components to allow them to slot together to create a free-standing structure. The central section had three attachment points on either side, each point designed to securely hold a single 2.5 mL column. The material used was not rigid and thus allowed these columns to snap securely in place by pushing. The plate was designed so that each column could comfortably have a stopcock on the top and the bottom, as well as associating tubings, with sufficient room to allow the operator to control the liquid flow within the columns. Figure 5.14B shows photographs of the fully assembled perfusion plate and the plate holding six 2.5 mL columns. Stopcocks and tubings were attached to give an indication of what a perfusion system, utilising these columns and the plate, may look like.

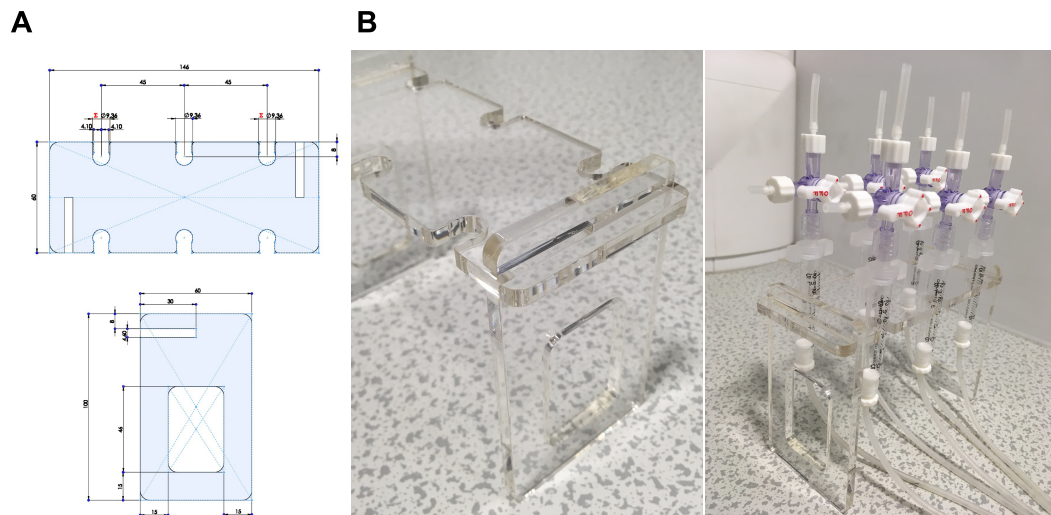


**FIGURE 5.14** Computer-aided design and laser cutting of the perfusion plate. An acrylic sheet was laser cut into three components (two stands and a central section) with slots to enable it to be easily assembled to form a free-standing 'perfusion plate' structure. It was designed to securely hold up to six 2.5 mL columns, with columns able to be snapped into place. Microspheres could be retained themselves within these columns, cell loaded and then perfused with medium in a continuous process. (A) shows the computer-aided design of the stand and the central section and (B) shows photographs of the finished plate, including with attached columns and associated parts, such as stopcocks and tubings.

The loading of 1 mL polyHIPE microspheres was performed, using these larger 2.5 mL columns and the peristaltic pump. PolyHIPEs fabricated using routine conditions were now tested, i.e. those under 300  $\mu\text{m}$ , as these would ultimately be used for any future attempt at perfusion culture. Figure 5.15B shows photographs of the system employed for the loading of three 1 mL polyHIPE beds. Cell load, gently agitated within a bottle, was pumped through the columns. Tubings, containing cells that did not attach, were directed to centrifuge tubes for later cell counting. The photographs show the system being tested on a laboratory bench. In actual experiments, labware would be autoclaved and equipment disinfected, with the system then placed inside a laminar flow hood to ensure aseptic loading. Cytopore, a commercial microcarrier, was supplied to compare with the performance of the polyethylenimine-adsorbed microspheres developed here. Cytopore is a dextran-based macroporous microcarrier, with a positive charge throughout its structure. It is intended as a substrate for adherent CHO cells in suspension systems. The use of Cytopore for perfusion CHO culture has been demonstrated (Goldman et al., 1998), though the authors added serum in the culture medium.

Two flow rates were tested; 0.5 and 1.0  $\text{mLmin}^{-1}$ . The loading was capped at a duration of 25 min, so for the former flow rate, a suspension of  $20 \times 10^6 \text{cellmL}^{-1}$  was delivered in 12.5 mL, whilst for the latter, a  $10 \times 10^6 \text{cellmL}^{-1}$  suspension was delivered in 25 mL. For both cases, 250 million cells would thus be delivered through the columns. To ensure weakly adhered cells were removed, medium was flushed through after loading, with 12.5 mL passed through for the 0.5  $\text{mLmin}^{-1}$  condition and 25 mL for the 1.0  $\text{mLmin}^{-1}$ . This was in contrast to the 1.0 mL column loading demonstrated previously, where flushing was not performed. At the end of the loading, all liquid within each centrifuge tube was mixed repeatedly and a cell count taken in technical triplicate. This was deducted from the initial load to determine the cells retained upon the microspheres.

Figure 5.15A shows the cells retained, in millions, for both the polyHIPE microspheres and the Cytopore microcarriers, at both flow rates. For 1.0  $\text{mLmin}^{-1}$ , the polyethylenimine-adsorbed polyHIPEs retained almost 60 million cells, whilst for Cytopore 80 million cells was retained. Decreasing the flow rate to 0.5  $\text{mLmin}^{-1}$ , as expected, increased the number of cells retained. PolyHIPE microspheres and Cytopore microcarriers now shared similar retention, with both retaining over 100 million cells, corresponding to  $1 \times 10^8$  cells per mL of microspheres for each.

The system had to be primed prior to cell loading. This was done using medium, with the stopcocks above and below each column used to manipulate the flows and control the height of liquid within the column. The loading was actually delivered into this primed

tubing, i.e. cells were delivered immediately after priming and thus the microspheres were already within medium before loading. For the polyHIPE microspheres, there was some aggregation as cells initially interacted with the materials, but this soon resolved itself. Both polyHIPE microspheres and Cytopore microcarriers turned progressively yellow as the loading was performed.

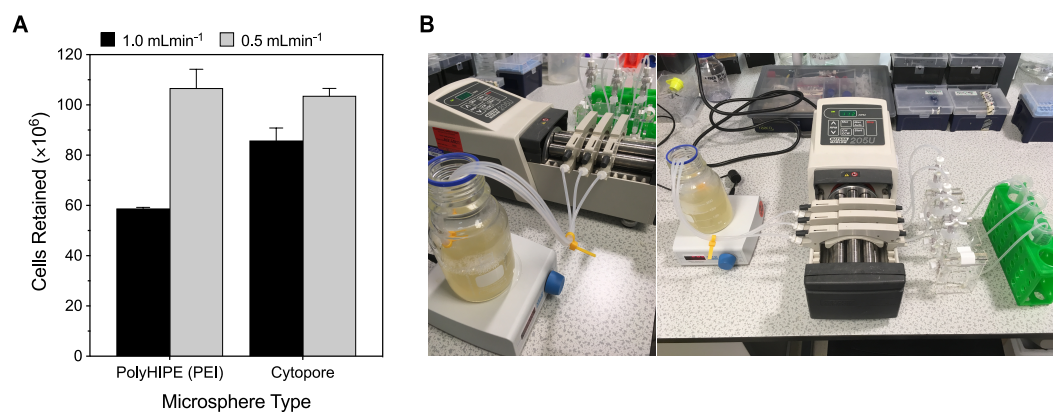


**FIGURE 5.15** Cell loading onto PEI-adsorbed MAES polyHIPE and Cytopore microspheres with the use of a multidrive peristaltic pump. 1 mL polyHIPE microspheres adsorbed with PEI and 1 mL Cytopore microcarriers were dispensed into 2.5 columns and attached to the cell loading rig. CHO-S IgG cells, at  $10$  or  $20 \times 10^6$  cellmL<sup>-1</sup> concentration, were then pumped through the packed beds within the columns at a  $0.5$  or  $1.0$  mLmin<sup>-1</sup> flow rate. Medium was flushed through to ensure weakly adhered cells were washed out. The number of cells in the effluent vessels were determined and the cells retained within each column calculated (A) with photographs (B) of the set up taken. Data represent mean  $\pm$  SD,  $n=3$  (biological triplicate).

The loading system demonstrated here was an extremely novel method of seeding cells onto microspheres. The use of Cytopore showed commercial microcarriers can too be loaded using this technique. Whilst using columns to force cells onto microspheres may seem technically excessive, the original idea was to then use the columns with a perfusion system, as mentioned previously. However, there may be times when the operator would wish to retrieve the loaded microspheres to transfer them to a culturing vessel. This was performed successfully with the  $1.0$  mL columns but attempting it with the  $2.5$  mL columns proved difficult.

After loading and flushing, the packed-bed of microspheres was just that — packed. Attempting to aspirate microsphere was challenging, with microspheres not readily taken up into the pipette tip. Forcefully dispensing medium did work, but this, as expected, appeared to detach cells off the microspheres. The retrieval of microspheres was eventually performed by perfusing medium from under the column, and so gently pushing microspheres up and out. Columns were tilted downwards with vessels positioned underneath to catch the released microspheres. This has been discussed further in § 6.1.2, where it was

attempted before a culture was started. This retrieval did, however, still lead to some cell loss.

#### *Confirmation of Retained Cells and Dissociation*

A method to determine the number of cells upon a particular volume of microspheres would be to simply dissociate the cells, separate the microspheres and perform a direct cell count. This was attempted, at numerous times in the project, using trypsin and other dissociation reagents first introduced in § 3.1.3. However, attempting any type of dissociation upon the polyethylenimine-absorbed microspheres resulted in severe aggregation. This was almost immediate upon exposure, e.g. after dispensing trypsin into a T-25 flask containing microspheres, and particularly apparent if microspheres were subsequently agitated.

The specific reagent used and conditions related to dissociation, such as DPBS washes and reagent pre-warming, did not appear to make much difference to this aggregation. Whilst dissociation did seem to occur, it required aspiration and dispensing of the microspheres to effectively happen. Cells were seen peeling off in part but the reagent alone was not sufficient. This was similar to how, in Chapter 3, plates and flasks would need to be tapped by hand to encourage dissociation of cells from polyethylenimine substrates. As mentioned, any agitation caused the microsphere to clump, making it difficult to further detach the cells and separate them from the materials.

There were several suggestions as to why this occurred. First, the dissociation reagent may be degrading the polyethylenimine substrate, with the sudden change in electrostatic charge causing the repulsion to fail and neighbouring microspheres to clump. Second, the cells might have themselves taken up the polyethylenimine (it is used, of course, elsewhere as a transfection reagent) and so once the cells are dissociated, the microspheres are left to aggregate. While this could be true, dissociation was first attempted immediately following cell loading, within 1.0 mL columns, using the syringe pump method. It was here that aggregation was first observed. Trypsin was perfused through the microspheres, and a medium flush then performed to encourage the detached cells to wash out in the effluent. It was here that the column began to leak from the cap, due to back pressure associated with the newly formed microsphere clumps. It was highly unlikely all polyethylenimine had been taken up by the retained cells in that short period between cell loading and the attempt at dissociation.

Because of this aggregation, the number of cells retained by the polyHIPE microspheres was never directly counted in the work presented here. The true numbers of cells retained,

---

or at least confirmed independently, remained unknown. This is a major caveat which should be remembered when reviewing all the cell loading data, both in this chapter and in Chapter 6. It is a major area of future work.

### 5.2.3 AMBR15 BIOREACTOR CELL LOADING

The loading of cells onto microspheres, using both a syringe pump and a multidrive peristaltic pump, was demonstrated previously. Whilst it was believed this was successful in ensuring the saturation of a set volume of microspheres, there exists processing scenarios where the use of columns and the requirement to retrieve microspheres would not be feasible. This includes bigger operations, such as those using spinner flasks or large-scale bioreactors, where the use of loading in situ may instead be required. To achieve this, a common technique used with commercial microcarriers, namely intermittent agitation, would need to be performed with the polyHIPE microspheres developed here.

The following experiment was carried out at CPI in the National Biologics Manufacturing Centre in Darlington, UK. CPI had an ambr15 unit available to use for this project. The ambr15 is a high throughput bioreactor system, housing up to 48 parallel reactors, with an integrated liquid handler allowing medium to be added or removed from any vessel at any time. Each reactor is single-use, with a working volume range of 10–15 mL and contains a magnetically stirred impeller. A pH and DO sensor ensures parameters can be automatically read and controlled by the unit. Each vessel has an entry point for a pipette to aspirate or dispense liquid. The ambr15 is used to test multiple conditions in parallel using scaled-down volumes and consequently enables a range of relevant processing data to be rapidly obtained prior to scale up.

The task here was to demonstrate a seeding technique common with microcarrier culture. This technique, which is called intermittent agitation in this work, mixes microcarriers and cells for a defined period of time before mixing is stopped. During this time, cells and microcarriers begin to settle toward the bottom of the vessel, encouraging interaction — without any chance of being ‘pushed apart’ by agitation — and thus promoting attachment. Agitation is eventually resumed to ensure seeding homogeneity and the process is repeated, often for several hours, until a satisfactory number of cells have seeded. The progress of this technique can be monitored by aspirating a set volume of microcarrier-cell suspension and decanting the microcarriers. The cells left, which are those that have not yet attached, can then be measured to calculate the cells that have attached. Over time, the number of unattached cells should decrease, indicating successful attachment of cells to the microcarriers.

After seeding, the agitation rate may be increased and the culture started. A benefit of this technique is no retrieval of microspheres is needed, with all seeding occurring in the vessel in which the culture will eventually start. This can be attempted with the ambr, and it was decided to test cell loading using this intermittent spinning technique with the unit. The minimum agitation rate allowed was 300 rpm. This rate was chosen to operate for 12 min, followed by a 2 min with no agitation. Cell loads were chosen as 50, 100 and 200 million cells, added as 5 mL to 7 mL medium (containing 5 mL microspheres). A 12 mL volume was thus made. The ambr stopped agitating automatically every 12 min and restarted 2 min after. Every 0.5 hr, 1 mL from the vessels would be aspirated, and the operator would decant the microspheres and count the unattached cells on a ViCell. Thus, two cycles of 'start-stop' were performed before each reading.

Figure 5.16A shows the percentage of cells retained and the calculated cells (in million) retained per mL of microspheres during the 2 hr loading schedule. It also shows the effective cells (in million) per mL of medium, assuming 10 mL working volume is eventually used. The percentage of cells retained is determined by deducting the number of cells within the samples from the number added at the start of the loading schedule. The number of cells added were determined in technical triplicate, immediately prior to adding to the vessels. The majority of the cells, at 80 % retained, were loaded within the first 0.5 hr, for each of the three concentrations tested. For the next 3 readings, no considerable difference in unattached cells was observed, suggesting a saturation had occurred by the first reading. The cells (in million) retained per mL of microspheres assumed equal adherence amongst all microspheres. Calculated from the numbers of cells retained, again the cells per mL of microsphere reaches its maximum from the first reading. For the 50 million load, the cells per mL of microsphere approached 10 million; for the 100 million load, it was above 15 million and for the 200 million load, it was over 30 million.

Comparing data to that seen in § 5.2.2, the loading density is considerable lower with this intermittent agitation technique. It is argued the values here are likely more correct, as the cells not attached are quantified every 0.5 hr for 2 hr. As discussed previously, it is only possible to know how many cells are actually present on the microspheres by dissociating the cells and then counting them. The effective cell number per mL of medium (within 10 mL) is arguably the more important parameter, as it will ultimately affect the concentration of product within the medium and is related to the intensification of the process. The highest effective cell number per mL of medium achieved was over 15 million for the 200 million load. Adding more microspheres and/or reducing the medium would increase this metric. There is, of course, a limit to this; once a certain volume of microsphere is reached the system will become a slurry and agitation issues may occur. Figure 5.16B shows pho-

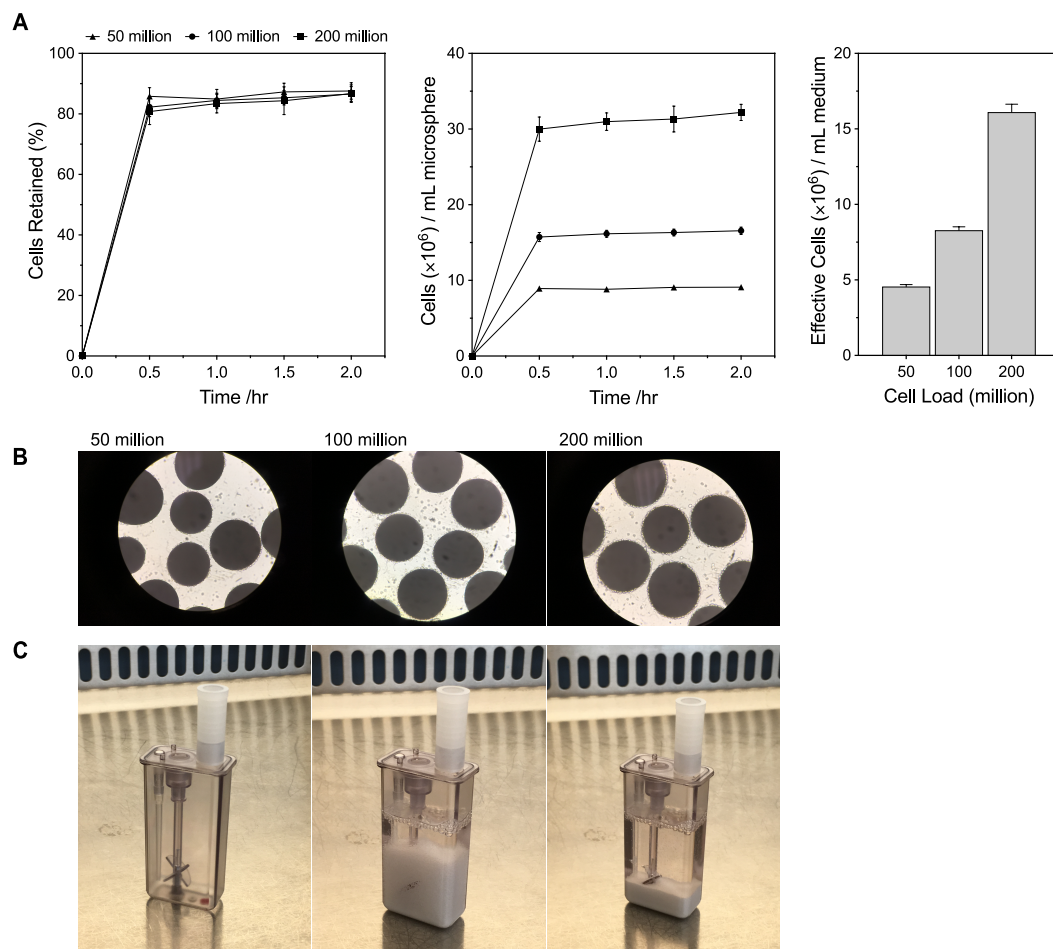


**FIGURE 5.16** Cell loading onto PEI-adsorbed MAES polyHIPE microspheres using ambr15 bioreactors. 5 mL PEI-adsorbed microspheres were dispensed into ambr15 bioreactors and allowed to settle to the bottom. 5 mL of either 50, 100 or 200 million cells was dispensed and the agitator set to 300 rpm. Every 30 min, until 2 hr, 1 mL suspension was aspirated, microspheres separated and unadhered cells quantified to determine cell retention. (A) shows the percentage of cells retained and cells / mL microsphere each 30 min, and the effective cell / mL medium if microspheres were placed into 10 mL medium, and (B) the loaded microspheres were visualised. (C) shows photographs of an empty ambr15 bioreactor, then unloaded microspheres in PBS within an ambr15 bioreactor to demonstrate their ability to settle via gravity after 2 min. Data represent mean  $\pm$  SD,  $n=3$  (biological triplicate).

photographs of microspheres under an optical microscope, after 2 hr, for each of the three loads tested. Visually more cells can be seen as the load was increased, indicating more cells were indeed attached.

The polyHIPE microspheres were compatible with the ambr15 vessels. There was some initial aggregation upon the impeller shaft, but this resolved itself after 30 min with the force of the agitation. There was no general aggregation on the inside walls of the vessels, although this proved to be an issue with Erlenmeyer flasks, as will be discussed in the next chapter. The agitation speed, once set at its minimum of 300 rpm, was sufficient to keep

the system homogenised. Each sample was 1 mL, with 2 mL thus removed after 2 hr. This was the reasoning behind a 12 mL starting volume, with 10 mL remaining for the culture after loading had completed.

The ambr15 is, by its physical design, a batch-wise operation. There is no means of modifying the system or the vessels (which come pre-sterilised in packs) to enable continual medium exchange. However, a pseudo-continuous operation where microspheres are allowed to settle via gravity, 'supernatant' removed and an equal volume of fresh medium added, can be carried out. Figure 5.16C shows photographs, as visual examples, of the ambr15 vessel and the polyHIPE microspheres. The first image shows an empty ambr15 vessel, the second shows 5 mL microspheres within 10 mL of PBS, once added, and the third shows the packed-bed that formed after 2 min of settling. This settling via gravity, and thus allowing medium to be exchanged without risk of cell loss, was the principle behind pseudo-continuous culture here. Pseudo-continuous culture was performed successfully prior to this visit to CPI with Erlenmeyer flasks, with the data presented in § 6.1.2. Readers are directed here now if they wish to learn about extended cultures involving manual medium exchange.

#### 5.2.4 CONCLUSIONS

The work in the second part of the chapter focused mainly upon cell loading, a technique where cells, at high densities, are forced to interact and become adhered to microspheres. The reasoning behind this was related to a suggestion that any continuous system eventually developed could be allowed to start immediately, i.e. cells are rapidly loaded, cooled to mild hypothermia and the process started for an indefinite period of time. Operators could then utilise the cells as they wish.

To achieve cell loading, microspheres were first dispensed into columns to allow the formation of packed-beds. Cells at high density were perfused through with the use of either a syringe or peristaltic pump, with the amount of cells in the effluent being determined. This was used to calculate the number of cells retained upon the microspheres. It was found that decreasing the flow rate led to greater cell retention due to, it was thought, the increased residence time of cells within the columns. Using 470  $\mu\text{m}$  microspheres and delivering 50 mL of 100 million cells at 1.0  $\text{mLmin}^{-1}$ , a total of 55 million cells per mL of microspheres were retained when using a syringe pump. This was improved by the use of 280  $\mu\text{m}$  microspheres, delivering 25 mL of 250 million cells at 0.5  $\text{mLmin}^{-1}$ , with over 100 million cells retained per mL of microspheres when using a peristaltic pump. Alongside these, a more typical intermittent agitation technique was also demonstrated using ambr15 vessels, with agitation set at 300 rpm for 12 min, followed by 2 min with no agitation, and so repeat-

ing for 2 hr. Using this method, where 10 mL microspheres were agitated with 200 million cells, a total of 30 million cells per mL of microsphere was achieved. This approach would likely be more suitable for larger-scale applications and follows similar methods already employed for microcarrier culture.

For the 1.0 mL columns, retrieval of loaded microspheres was technically simple, with the materials easily aspirated up with a pipette tip. This enabled them to be placed in T-flasks for a static growth culture demonstration. Indeed, cells grew readily upon the microspheres with full confluency seen by day 7. No considerable detachment was noted. The very nature of cell retention meant microspheres (adhered with cells) could be decanted on day 4 for a PrestoBlue assay and a medium exchange. For the 2.5 mL columns, retrieval was challenging, as the action of the pump had ensured a tight packed-bed. Aspiration with a pipette was not possible and another method was attempted, as described later in Chapter 6.

The use of cell loading has not been demonstrated in the literature, but it allows operators to rapidly saturate a retention device with the potential to immediately initiate a continuous culture. This has been demonstrated in the following chapter. While not suitable for every application, it may be a component of a future technology where cells, once grown to high densities, can rapidly be retained for on-demand continuous cultures.

This page intentionally left blank

---

# Chapter 6

---

## CONTINUOUS BIOPROCESSING SYSTEMS

---

### OVERVIEW

This chapter presents the results obtained towards the end of the project, which looked at the use of the newly developed cell retention device (polyHIPE microspheres adsorbed with a polyethylenimine substrate) in actual continuous bioprocessing systems. It is divided into two parts; (i) the demonstration of pseudo-continuous systems, whereby microspheres with attached cells were left to settle via gravity to allow periodic medium exchange by the operator and consequently mimic continuous culture, and (ii) attempts at actual perfusion culture, which involved continual medium exchange via a peristaltic pump. For the latter part, two designs were proposed and attempted; the first was a packed-bed system, where retained microspheres within columns had medium perfused through; the second was a spinner flask-based system, which instead placed microspheres within a modified spinner flask, with inlet and outlet tubings used for simultaneously medium entry and exit. This chapter contains highly experimental ideas and may be appealing to readers interested in the design and operation of bespoke continuous upstream systems.

### 6.1 INTRODUCTION TO PSEUDO-CONTINUOUS SYSTEMS

A frequently heard reason given by bioprocessing engineers for their reluctance to adopt continuous upstream processes is the perceived difficulty in operating the commercial systems available. Whether these views are justified or not is likely dependent upon the actual system used and the experience of those voicing their thoughts. A key advantage of using microspheres as a means of retaining cells is their versatility; potential users are not confined to pieces of specialised equipment and so they will not, strictly speaking, have to learn or be trained in these new operations. Microspheres are physically compatible with many familiar lab vessels, i.e. they can be directly added and used immediately, in exactly the same way as microcarriers are not restricted to any particular format.

A further advantage of using microspheres as a cell retention technology is their mode of retention. Microspheres, when coated with a sticky adhesion substrate, will physically adhere cells (as has been shown previously). This opens up the possibility of using a defined volume of loaded microspheres within a pseudo-continuous culture. Pseudo-continuous systems, sometimes referred to as mock- or semi-continuous, rely on manual exchange of medium by the operator, often at set intervals of a process, to mimic the effects of continu-

ous culture. This is in contrast to perfusion, or ‘true’ continuous operation, where medium is continually exchanged at a defined dilution rate by the use of a pumping mechanism. For pseudo-continuous operations, the operator must physically interact with the process, but it is technically simple to run; for perfusion, interaction is kept to a minimum, but the technical expertise required is far greater. For the retention of cells, the rationale for using microspheres becomes apparent when observing their ability to rapidly settle via gravity. This can be achieved by simply tilting the vessel in which they are themselves retained. As examples, microspheres within multiwell plates, T-flasks, or even larger shaking bottles will fall out of suspension when not agitated — this leaves cell-free medium, or “supernatant” as it were, available for removal by the operator. Adding an equal amount of fresh medium immediately after will constitute a medium exchange, without any loss in cells. Performing this exchange periodically effectively converts the culture into a pseudo-continuous operation; substrates are renewed, metabolites (including any product) are removed and the operation time can be vastly extended beyond that normally seen with batch, or even fed-batch, cultures.

Pseudo-continuous culture is simple to carry out. Unlike perfusion, no pumps or tubings are required and, when paired with microspheres, it can be performed using readily available labware vessels. It also introduces operators to extended cell culture, without any sub-culture, but does not involve the technical difficulty of perfusion. There are two immediate disadvantages, albeit minor ones; a 100 % medium exchange can never be achieved, with some liquid always having to remain each time in the vessel to keep the microspheres hydrated — although this can be overcome by serially performing a second or even a third medium exchange. These exchanges involve interaction between vessels and the operator. For a pseudo-continuous operation lasting several weeks, the risk of contamination is present.

Pseudo-continuous culture can be attempted right now in almost any laboratory working with cells, without the need for dedicated cell retention. Removing cells from vessels and performing centrifugation is a crude, but very effective, method of retaining cells. Supernatant (or spent medium in this instance) can be decanted, the cells resuspended in fresh medium and placed back into their original vessels for continuation of the process. The downside to this method, however, is the cumbersome transfer of cell suspension to and from centrifuge vessels, with the associated risk of contamination that this brings. Scalability is also an issue; scaling up these processes would demand the centrifugation of larger volumes, which is indeed possible but would require specialised centrifuge vessel holders once certain volumes are exceeded. In contrast, when cells are adhered to microspheres the rate of sedimentation via gravity can be a matter of several minutes, often less, with no

centrifugation needed. Medium exchange becomes a rapid, routine task with interaction kept to a minimum.

The main objective of the work presented in this chapter was to demonstrate both pseudo-continuous and perfusion operation in mild hypothermic conditions using the developed cell retention device. The specific objectives for the first part of this chapter were to; (i) ensure parameters useful for the analysis of pseudo-continuous and perfusion culture medium can be accurately measured within the laboratory, e.g. by the use of a Cedex Bio Analyzer unit; (ii) attempt pseudo-continuous culture of CHO cells with the developed cell retention device, i.e. microspheres adsorbed with polyethylenimine, by placing them in agitated Erlenmeyer flasks with periodic medium exchange, and (iii) optimise this pseudo-continuous operation, if possible, to keep CHO cells sustained at mild hypothermia, with continual production of IgG, for at least two weeks. The second part of this chapter looks at the design and assembly of two perfusion systems, with an attempt at true continuous operation using both of these systems.

#### 6.1.1 CEDEX BIO ANALYZER AND MILD HYPOTHERMIC CULTURE

The defining characteristic of any continuous upstream system is the vastly extended duration of the culture, with weeks without subculture or interaction between the system and the operator the norm. Problems of cell overgrowth, which may result in clogging or fouling of the retention device, are typically overcome by either shifting to mild hypothermic temperatures (to arrest culture growth) or via cell bleeding (where physiological temperatures are maintained but a portion of cells are periodically allowed to exit the system). The effluent medium of a continuous system, sometimes referred to as the perfusate, can be sampled daily and stored for later analysis. The determination of the concentration of metabolites, substrates and expressed product can subsequently be performed to deduce the health of the culture for each day of the operation. For clarity, metabolites are defined here as the products of metabolism and substrates as chemical species within culture medium; the former are produced by cells, the latter are consumed. Some species can act as both metabolite and substrate, such as lactate. Heterologous protein products, such as antibodies, are a form of metabolite — technically a secondary metabolite, as they are not involved in functions needed for cell survival. For cells that are retained internally, or those within physically closed devices that cannot be aseptically accessed, the analysis of metabolites and substrates within the perfusate can often be the only way to determine the health of retained cells and the state of the wider operation.

Countless commercial assays are available for the quantification of metabolites and substrates within culture medium. However, each of these assays typically only measures one

particular analyte, meaning multiple assays have to be performed, usually manually, for a full picture of a continuous culture to emerge. This is incredibly laborious and generally not cost-effective, but some dedicated units do exist that will automatically determine the concentration of an array of analytes from a single sample. Such units can thus eliminate the need to purchase multiple assay products and greatly streamline the required workflow. The Cedex Bio Analyzer, from Roche, is one such unit, and is capable of rapidly measuring the concentrations of many metabolites and substrates within cell culture medium. It is described as a low throughput device (to contrast with its larger, high throughput sister unit), with capability to handle eight discrete samples at a time — but for the objectives in this project this unit was entirely suitable.

The concentrations of glucose, L-glutamine, lactate and lactate dehydrogenase within perfusate can be measured to collectively reveal the general status of a continuous upstream operation. Whilst the intricacies of CHO metabolism are not, strictly speaking, within the scope of the work presented here, each of these analytes will be discussed to give context for the data that follow. It should be remembered CHO cells are, of course, mammalian, and the description of each of these analytes would generally be the same for all mammalian cells.

Glucose, a monosaccharide and carbon source, is the dominant supplier of energy for CHO cells, and indeed all living organisms. Glucose is thus a critical substrate, getting consumed within the culture as cells grow, and is supplied within CD CHO at around  $6 \text{ gL}^{-1}$ . It is first metabolised within glycolysis, an oxygen-independent pathway, to generate adenosine triphosphate (ATP) molecules. These molecules, informally called ‘energy currency’, are then used to fuel all cellular processes. In aerobic conditions, the end product of glycolysis, pyruvate, can subsequently be used within the citric acid cycle to further generate ATP. In anaerobic conditions, such as that felt by muscle cells of mammals during intense exercise, ATP is in high demand and so cells will typically respond by converting pyruvate into lactate and thus by-passing the citric acid cycle. This temporary reaction ensures the glycolysis pathway can be repeated quickly via the production of  $\text{NAD}^+$  cofactors, which help repeat this pathway.

Bizarrely, many immortalised mammalian cells, including CHO cell lines, will produce lactate via glycolysis even when abundant oxygen is present. This rewiring of metabolism, termed the Warburg effect after Otto Heinrich Warburg, was first observed in cancer cells (Liberti et al., 2016). The metabolism of glucose using glycolysis is highly inefficient — the majority of the potential energy is lost — yet it is considerably faster than the citric acid cycle and thus allows cells to quickly acquire energy for proliferation. As for the consequences

on CHO culture, glucose is rapidly consumed and lactate rapidly produced during periods of growth, such as that seen in the exponential phase of a culture. Lactate is thus a waste metabolite product arising from the inefficient use of glucose, with its concentration within medium increasing during cell culture. However, the presence of lactate is also detrimental to cell culture, causing a reduction in medium pH (which must be countered with base addition, affecting osmolarity) and having negative effect on growth and productivity (Fu et al., 2016). The regulation of lactate within CHO processes, in an effort to try alleviate these issues, is an active area of research (Buchsteiner et al., 2018; Konakovsky et al., 2016; Toussaint et al., 2016).

Glutamine (both a carbon and nitrogen source) is a non-essential amino acid, meaning its synthesis within mammalian cells is possible using glutamate and ammonia via glutamine synthetase. However, in rapidly proliferating cell lines such as CHO, L-glutamine (the naturally occurring enantiomer form) must be exogenously supplied via supplementation into the medium in order for cells to remain viable; in this case at  $8 \text{ mmolL}^{-1}$  for the CHO-S IgG cell line used here. The role of L-glutamine within CHO metabolism is critical, being utilised as an alternative energy source and a precursor in biosynthesis, amongst many others (Tannock et al., 1986). The conversion of glutamine into glutamate via glutaminase creates ammonia, a waste metabolite product. As with lactate, ammonia is not beneficial to cell culture and should be closely watched, although in this work the concentration of ammonia was not measured.

Lactate dehydrogenase is defined here incorrectly as a metabolite, though really it is an enzyme involved in the metabolism of pyruvate, and is measured solely within perfusate as an indirect marker of cell death. Cells undergoing necrosis lose membrane integrity and essentially leak their internal contents into surrounding medium; if lactate dehydrogenase, being an enzyme found in high amounts within cells, is detected then it can be presumed traumatic cell death has occurred. The measurement of lactate dehydrogenase as a means to detect cell death remains a widely used technique within cell culture processes (Chan et al., 2013).

The laboratory had an available Cedex Bio Analyzer. However, it was viewed as a relic from a previous project and had been lying dormant for several years. An initial task, before any form of continuous operation was attempted, was to revive the Cedex and ensure it could be trusted, once again, for actual experimental work. Maintenance was carried out and assay reagents for glucose, L-glutamine, lactate and lactate dehydrogenase obtained. Calibration and control samples were provided by Roche to ensure the Cedex would correctly measure the concentration of these four analytes.

---

Figure 6.1A shows graphs plotted with the three control values, as stated by Roche, against three concentrations, as measured by the Cedex. These three controls were measured for each of the four analytes. Regression lines were added and  $R^2$  values calculated. The tight fitting lines and high  $R^2$  data confirmed the successful calibration of the Cedex and demonstrated it could accurately measure these analytes. Serial dilutions of CD CHO medium were next prepared, with glucose and L-glutamine concentrations determined for each dilution, with a technical triplicate performed for each. Figure 6.1B shows ‘standard curves’ for both substrates, with undiluted CD CHO medium assigned an arbitrary value of 1.0, the first dilution then assigned 0.5, and so on. Plotting regression lines was used to confirm the ability of the Cedex in measuring decreasing concentrations of these two analytes. As with the controls, both gave a high  $R^2$  value and a tight fitting line, confirming that the unit could detect the dilutions correctly each time. The undiluted samples were corrected identified as  $6 \text{ gL}^{-1}$  and  $8.0 \text{ mmolL}^{-1}$ , for glucose and L-glutamine, respectively.

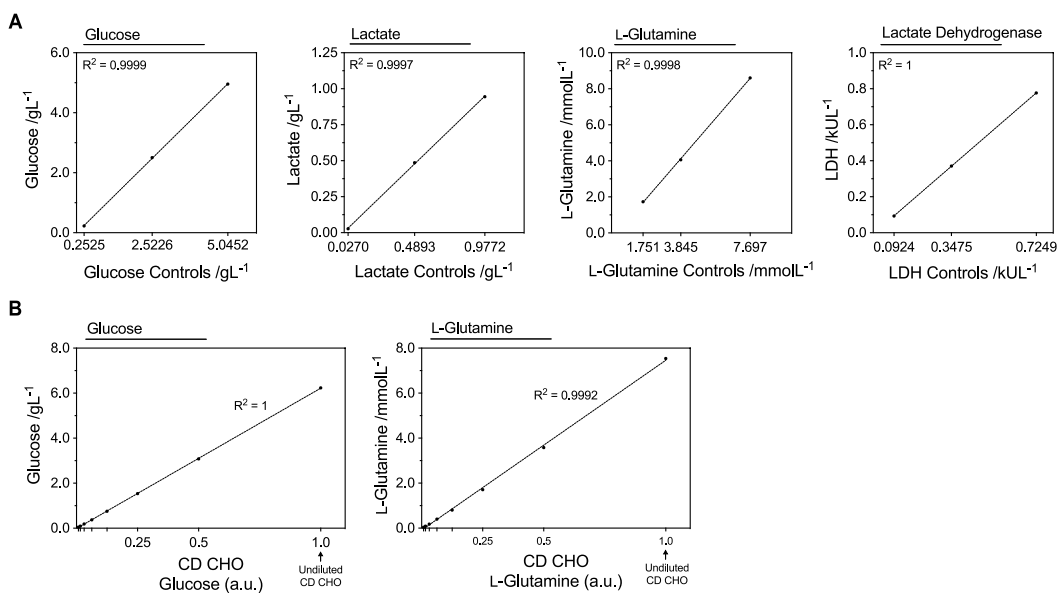


**FIGURE 6.1** Validation of the Cedex Bio Analyzer, using controls and serial dilutions. The Cedex Bio Analyzer was validated using (A) manufacturer-supplied controls for glucose, lactate, L-glutamine and lactate dehydrogenase, and (B) ‘standard curves’ for glucose and L-glutamine concentrations, using a serial dilution of CD CHO medium. For the two ‘standard curves’, the x-axis has arbitrary units, with 1 being undiluted medium, 0.5 the first dilution and so on. Lines shown are regression lines. For (A), data represent  $n=1$ ; for (B), data represent mean  $\pm$  SD,  $n=3$  (technical triplicate).

After seeing these data, the determination of these four analytes within actual cell culture medium using the Cedex was next. Figure 6.2A shows the daily viable cell density and viability of a suspension batch culture of CHO-S IgG cells in Erlenmeyer flasks. The culture had the typical lag, exponential, stationary and death phase growth curve, with an associ-

ated sudden drop in viability by day 8. Figure 6.2B shows the daily concentration of glucose, lactate, L-glutamine and lactate dehydrogenase, as measured by the newly calibrated Cedex, and can be used to complement the growth curve data obtained. The concentrations of glucose and L-glutamine, two key substrates within the CD CHO medium used here, remain high for the first two days of culture. As cells enter exponential phase, by day 3, these two began to get consumed with their levels dropping. This continued until day 5 and 6, when their concentrations approached zero. At this time, cells entered stationary phase with growth plateauing. Viability began to drop from day 7.

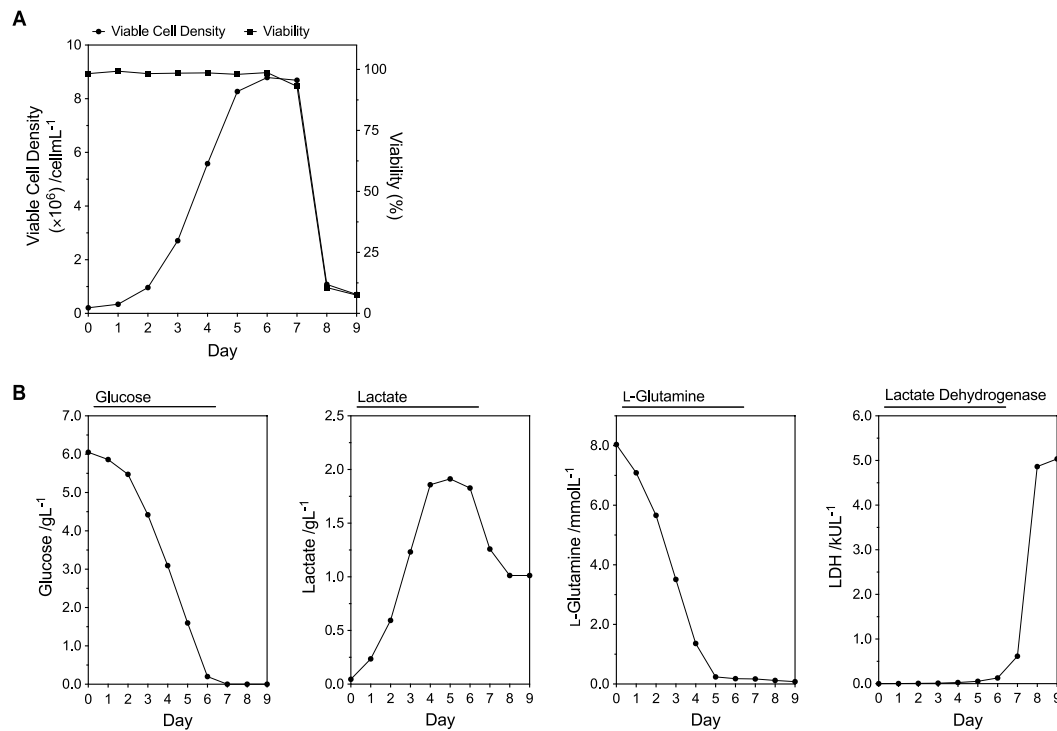


**FIGURE 6.2 Demonstration of the Cedex Bio Analyzer for determination of metabolites and substrates within actual cell culture medium.** A routine suspension culture using CHO-S IgG cells was performed, with (A) viable cell density and viability readings taken daily, and (B) glucose, lactate, L-glutamine and lactate dehydrogenase concentrations determined daily using the Cedex. Data represent  $n=1$ .

The concentration of lactate dehydrogenase, a marker of cell death, remained at an extremely low concentration until day 6, when it began to rise. By day 8, it had risen dramatically to almost reach  $8.0 \text{ kU L}^{-1}$ , corresponding to the sudden drop in cell viability as measured by the ViCell. Lactate was produced as biomass accumulated, rising rapidly during the exponential phase (as glycolysis was carried out), plateauing with stationary and then actually decreasing after day 6. This indicated consumption by the cells, before experiencing another plateau between days 8 and 9.

The data here were typical for CHO cells within batch culture and whilst not particularly interesting, demonstrated the accuracy of the Cedex unit. The decrease in lactate from day 6 was the result of the lactate metabolic shift or switch, which describes the phenomenon whereby CHO cells begin to consume rather than produce lactate, usually during late-stage culture. The exact causes of this metabolite change have been reviewed by Hartley et al. (2018), and include the result of glucose depletion, L-glutamine depletion and changes in pH, amongst others.

The use of mild hypothermia was always intended as a means to arrest the growth of CHO cells within the cell retention device. In § 3.1.4, cells adhered to polyethylenimine substrates within T-25 flasks were cultured at 37, 32 and 30 °C for 5 days, with cell growth and detachment measured and the daily concentrations of glucose, L-glutamine, lactate and lactate dehydrogenase determined. The samples from that experiment were stored and later analysed using the newly validated Cedex here. The data obtained from that experiment started to explore the effect of temperature on cell metabolism. Before attempting continuous culture with the use of microspheres, it was suggested the metabolic behaviour of CHO-S IgG cells within suspension batch culture, at mild hypothermia, be investigated. This was as to compare and contrast any effects which may arise later on in any continuous culture eventually attempted. As is the case with many industrial processes (particularly those operating as fed-batch), a biphasic culture was carried out by shifting the temperature from 37 °C to either 30 or 32 °C. In this instance, this shift was carried out on day 3 within a 9 day culture.

Figure 6.3A shows the viable cell densities and viabilities for each of the cultures from days 0 to 9. As with Fig. 6.3B and 6.3C, the black arrows on day 3 indicate the temperature shift from 37 to 30 or 32 °C. Before the temperature switch, all cultures had near-identical cell densities, with exponential phase beginning on day 2. The switch on day 3 had immediate effect on growth by the following day; those cultures remaining at 37 °C continued to accumulate biomass within the exponential phase, whilst those with reduced temperatures had considerably less growth. By day 5, cultures at 37 °C had entered stationary phase, whilst the viable cell density for those at 32 and 30 °C had plateaued and continued to do so until day 9. This demonstrated complete cell growth arrest by mild hypothermia. Regarding viabilities, cultures kept at 37 °C dropped to 50 % viability on day 7 before approaching 0 % by day 9. Viability for those shifted to 32 and 30 °C remained above 90 % until day 7, with a slight decrease observed on day 8. Interestingly, the viability of cultures at 32 °C approached 50 % by day 9, but those at 30 °C remained above 80 %.

Figure 6.3B shows the daily IgG titre and L-glutamine concentrations for each of the cul-

---

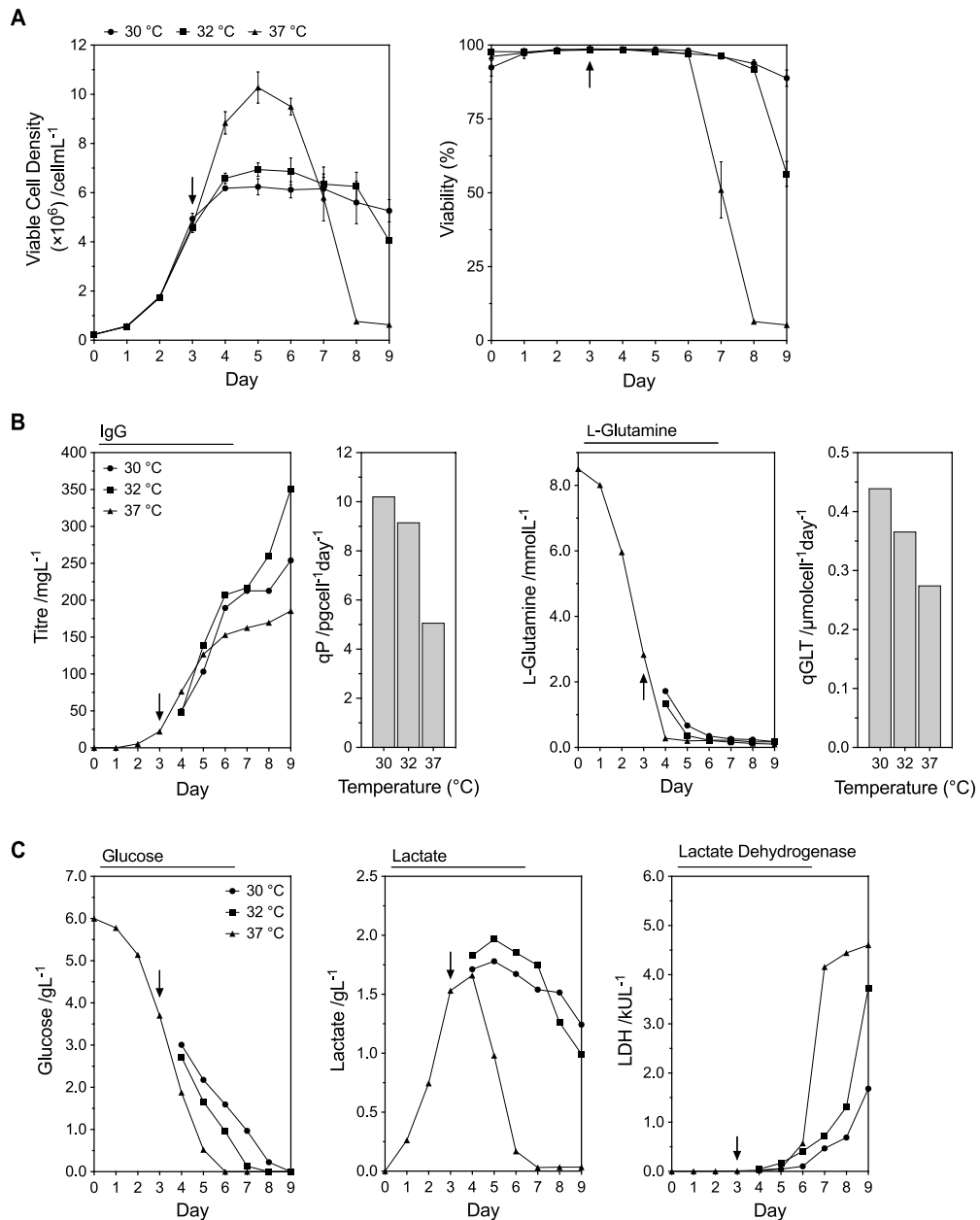


**FIGURE 6.3** Mild hypothermia of CHO cells using two temperatures within a biphasic culture, with daily determination of metabolites, substrates and IgG titre. A suspension batch culture of CHO-S IgG cells was performed using Erlenmeyer flasks, with a temperature shift to either 30 or 32 °C carried out on day 3 (black arrows). (A) viable cell density and viability readings were taken daily, (B) IgG titre and L-glutamine concentration was determined daily, with the cell-specific productivity (qP) and cell-specific L-glutamine consumption rate (qGLT) calculated between days 0 and 6, and (C) glucose, lactate and lactate dehydrogenase concentrations determined daily. During the first three days of culture, when all flasks were at 37 °C, metabolites, substrates and IgG was only determined for one set of flasks. For (A), data represent mean  $\pm$  SD,  $n=3$  (biological triplicate); for (B) and (C), data represent  $n=1$ .

tures; using these data the cell-specific productivities and cell-specific L-glutamine consumption rates were calculated between days 0 and 6. To save on consumable costs for this

particular experiment, only one flask for each condition was sampled for analysis and for the first 3 days, only one condition was measured as all parameters were considered constant. After day 3, the IgG titres were similar for all conditions and rose until day 6 when they began to plateau for cells kept at 37 °C. From this same day, the titre achieved by cells at 32 and 30 °C continued to rise, until day 8, when the titre for those at 32 °C started to surpass those at 30 °C. Cells cultured at 32 and 30 °C, from day 3, had cell-specific productivities almost twice that of the cells kept at 37 °C, between day 0 and 8. Cells switched to 30 °C achieved the highest at approximately 10 pgcell<sup>-1</sup>day<sup>-1</sup>. L-glutamine concentration dropped rapidly to around 4 mmolL<sup>-1</sup> and dropped further by day 4 for cells kept at 37 °C, with all available L-glutamine being consumed by every culture, regardless of temperature, by day 6. The cell-specific L-glutamine consumption rates revealed, as with the trend in productivity, an increase in consumption when temperatures were decreased. This matched the data seen previously in § 3.1.4, where CHO cells adhered to polyethylenimine substrates were exposed to mild hypothermic temperatures.

Figure 6.3C shows the daily glucose, lactate and lactate dehydrogenase for each of the cultures. The daily decrease in glucose concentration after day 3 was dependent upon the temperature of the culture, with cells at 37 °C experiencing the fastest drop, followed by those at 32 °C and those at 30 °C. By day 6, all glucose was consumed for cells at 37 °C; for cells at 32 °C this occurred by day 8 and for those at 30 °C by day 9. The lactate profile was interesting; by day 5 the lactate shift had occurred for cultures at 37 °C, with all available lactate rapidly consumed by day 7. This matched with a similar depletion in both glucose and L-glutamine and corresponded to the rapid drop in viability seen with cells at 37 °C. For cells at mild hypothermia, a lactate shift still occurred but only from day 6 and with a smaller daily decrease in lactate concentration, although cultures at 30 °C had the highest lactate concentration by day 9. For lactate dehydrogenase, a marker of cell necrosis, all conditions saw some increases by day 6, but cells at 37 °C experienced a dramatic increase by day 7, which began to plateau as the culture viability dropped. Cells shifted to 32 and 30 °C also saw steady increases in lactate dehydrogenase concentrations, with those at 32 °C giving higher readings than those at 30 °C. This complemented with the earlier observation that cells at 30 °C remained relatively more viable for the entire duration of the culture.

It is known that reducing the temperature of a mammalian cell culture has consequential effects on the progression of the cells through the cell cycle (Rieder et al., 2002). A downward shift in temperature is typically used to severely reduce the specific growth rate of the culture by arresting cells in the G<sub>0</sub>/G<sub>1</sub> phase of the cell cycle. The consequent boost in cell-specific productivity is considered a major benefit. This inverse relationship between growth rate and productivity is widely recognised for mammalian cell lines. Be-

cause of this relationship (cells must stop growing for productivity to increase), industrial processes typically rely on a biphasic approach, i.e. begin a culture at 37 °C for a defined duration to enable sufficient biomass is generated, before switching to a mild hypothermic temperature to boost productivity for the remainder of the culture. The extent of this effect, with respect to CHO cell production, appears to be highly empirical and depends ultimately upon the product expressed, the cell line used and the temperature ultimately applied (Becerra et al., 2012). The relationship between growth rate and productivity is not, strictly speaking, beneficial to a process; an operator cannot have both a high growth rate and a high productivity and must choose one over the other. Whilst biphasic cultures are a workable solution, others have attempted to ‘decouple’ growth rate and productivity by adapting cells to grow in hypothermic conditions, i.e. achieve normal growth rates with an increase in productivity (Fox et al., 2005; Sunley et al., 2008).

The switch to mild hypothermia in order to arrest cell growth has been demonstrated here for the CHO-S IgG cell line. A biphasic culture was performed, with cells first cultured at 37 °C for 3 days in order to increase cell concentration before switching to 32 or 30 °C. The choice of the third day post-seeding was largely to highlight the expected arrest in growth (when compared to the cells that remained at 37 °C); for a production process a shift on days 4 or 5 would be more appropriate to first achieve a greater biomass. This in turn would increase the product amount ultimately harvested. The boost in cell-specific productivity observed, between days 0 and 6, was not a surprise and obeyed the inverse relationship between specific cell growth and product output.

It can by now be appreciated that, if mild hypothermia was employed with a continuous culture, the cells would remain at a near constant concentration for the entire duration, with no clogging of the retention device. This would enable the process to be vastly extended, critically without any detrimental effect on the health of the cells or the integrity of the retention technology. The product, likewise, would be continually made with the ability to retrieve and process it within the exiting medium.

The increase in cell-specific L-glutamine consumption was intriguing, suggesting a change in metabolism as temperature was decreased — although this increased uptake appeared not to encourage cell growth. Yoon et al. (2002) similarly reported an increase in cell-specific L-glutamine consumption after performing a switch to 30 and 33 °C for an adherent CHO culture, with 30 °C once again yielding the highest specific consumption. Bizarrely, the same authors later performed similar experiments using the same cell line, but instead reported a decrease in L-glutamine consumption (Yoon et al., 2004). The only obvious differences that could be seen was, in the later report, cells were cultured in suspension rather

than adherently and switched now to 32.5 °C. This suggests the effect may in part be process-dependent.

### 6.1.2 PSEUDO-CONTINUOUS SYSTEMS USING ERLLENMEYER FLASKS

It was decided that pseudo-continuous culture of CHO cells, as opposed to perfusion culture, would be first attempted using the newly developed, microsphere-based cell retention device. Unlike the perfusion systems explored later on in the work, no dedicated equipment such as peristaltic pumps, tubings or medium tanks had to be obtained in order to attempt any pseudo-continuous culture. The specific vessel type chosen was the single-use Erlenmeyer flask, which possessed a cap containing a 0.2 µm filter for gaseous exchange. These were the same vessels used for routine cell passaging within the laboratory and so were readily available for use. It was decided cell loading would be carried out, as demonstrated in § 5.2.2, to seed the microspheres prior to continuous culture, i.e. 2.5 mL columns each containing 1 mL microspheres would be perfused with CHO cells at high viable cell densities. The microspheres, once loaded and washed through with medium, would then be retrieved from the columns and placed into fresh medium within the Erlenmeyer flasks. Agitating these flasks using orbitally-shaken incubators at mild hypothermic temperatures would then commence. The lack of impellers would also eliminate any potential shear arising from agitation.

The culturing of microspheres within Erlenmeyer flasks had never been attempted within the laboratory. Literature reports on microcarrier usage frequently employ spinner flasks (Gupta et al., 2016; Rafiq et al., 2016; Ismadi et al., 2014) as culturing vessels, with a central impeller (usually magnetically driven) used to keep microcarriers within suspension. As a consequence of using different — and simpler — vessels, there were numerous unknowns regarding certain process parameters. This included the rotational speed of the shaker within the incubator, the specific temperature needed to arrest cell growth (and to avoid possible detachment of cells from microspheres at these low temperatures), and the frequency of the medium exchanges. As with any first attempt, several issues arose which were not entirely foreseen, with these being discussed alongside the data below. Current CHO fed-batch processes within the laboratory could currently run for 2 weeks before a harvest was performed. Because of this, the duration of any continuous process (pseudo or perfusion) within the work here was always expected to exceed this.

For this first attempt, cell loading was performed using a flow rate of 0.5 mLmin<sup>-1</sup>. The cells retained, calculating by deducting the cells in the effluent from the cells delivered, was an average of approximately 125 million per column, or per 1 mL of microspheres. Retrieval was performed by flushing the microspheres up from the bottom of the column

through the top into a centrifuge tube by the use of fresh medium at  $1 \text{ mLmin}^{-1}$ . Microspheres were pushed out as a slurry, shaped like a cylinder, but resuspended readily once excess medium was added. Finally, microspheres were strained and flushed back into fresh medium. The number of cells lost during this retrieval was determined to be approximately 20 million, leaving over 100 million per 1 mL of microspheres. Microspheres were placed into Erlenmeyer flasks and a 25 day pseudo-continuous culture started.

Figure 6.4A shows the daily concentration of dead and viable cells within suspension, i.e. the cells detached from the microspheres, as well as the daily viability of these cells and the daily IgG titre for the process. It must be stressed that these cell densities are not the density of cells retained upon the microspheres, but rather detached cells suspended within the supernatant. Because of the nature of continuous processing, samples were taken daily without fear of excessive medium loss. Black arrows with dashed lines indicate 100 % medium exchange on that particular day. The data obtained on these particular days came from samples taken immediately before the medium exchange took place. Values on the top indicate the temperatures used during specific periods of the culture. To take a daily sample, or even perform a medium exchange, flasks were removed from the incubator and physically tilted to allow microspheres to settle. The eventual microsphere-free supernatant was then either sampled, or exchanged with an equal amount of fresh medium. Letting microspheres settle was simple to perform, and took under 2 minutes for a loose pellet to form. Using this method meant that, unless microspheres were decanted, it was impossible to exchange 100 % of the medium in a single medium exchange. To overcome this, 80 % medium was exchanged, with this then repeated twice (by gently resuspending microspheres and letting them settle once again). Initial medium exchanges performed in this experiment indeed only performed one 80 % exchange, but by the end of the process three exchanges were carried out to ensure complete renewal of substrates and removal of metabolites.

Samples taken on days 1 and 2, which was 24 and 48 hr after inoculating the vessels with loaded microspheres, gave a relatively high concentration of detached, but viable, cells. The concentration of dead cells, in comparison, was smaller. This was likely due to some cell detachment from microspheres once placed within the flasks, which was expected. The medium exchange on day 2 was performed to rid the flasks of any detached cells, so further observation on cell detachment could be carried out for the remainder of the culture. From day 5, medium was exchanged every 5 days until day 20. The concentration of viable and dead detached cells followed an expected pattern; 24 hr after the day when a medium exchange had been performed the concentration of both started low, before starting to rise steadily each day until the next exchange. These rises became more apparent from day 10. The ratio of viable to dead cells may reveal information regarding cell detachment, i.e. the

---

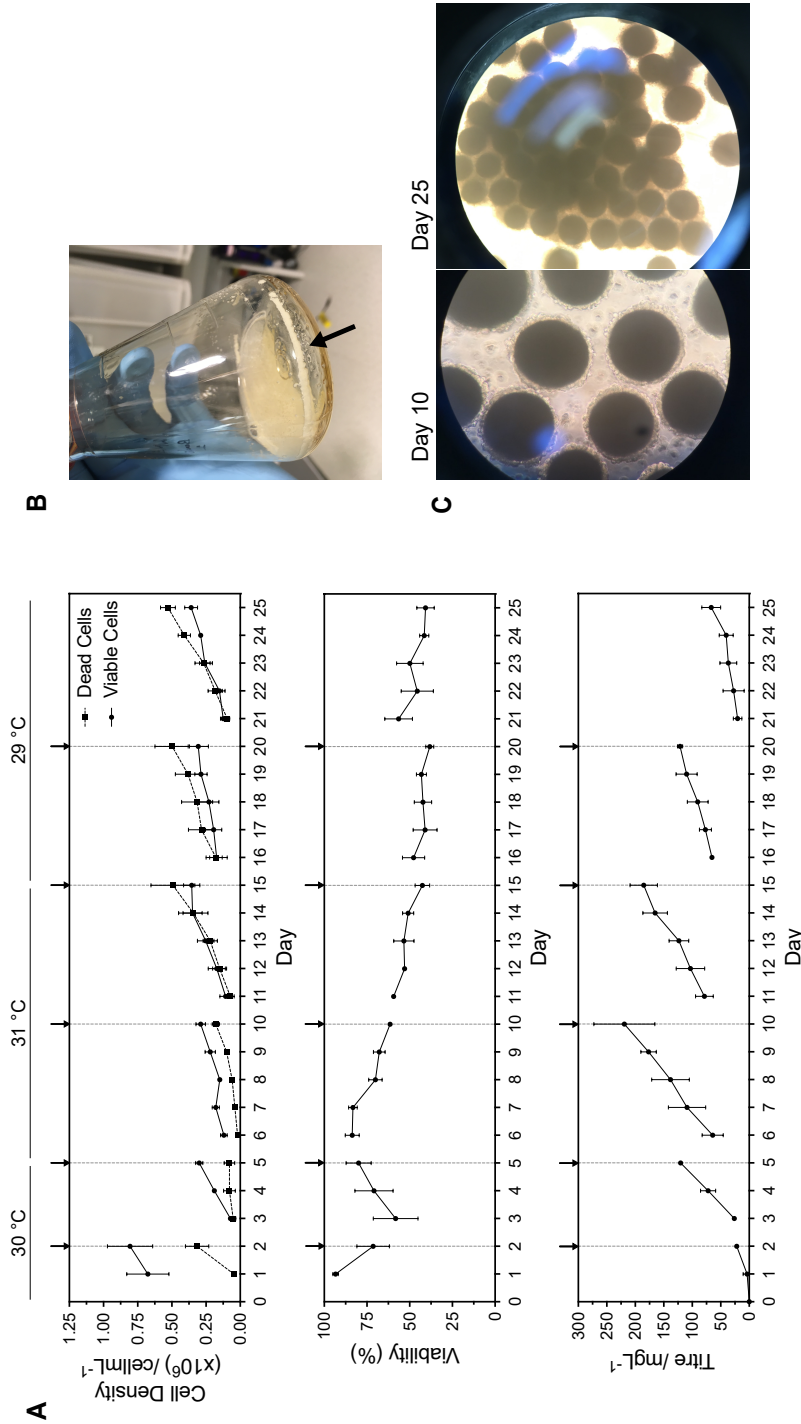


**FIGURE 6.4** First attempt at pseudo-continuous culture of CHO cells using PEI-adsorbed polyHIPE microspheres for 25 days. CHO-S IgG cells were loaded onto 1 mL polyHIPE microspheres adsorbed with polyethylenimine, then dispensed into Erlenmeyer flasks with agitation set at a range of rotational speeds. Temperatures were varied throughout the culture. Each day, starting on day 1, supernatant was aspirated from flasks and (A) the number and viability of peeled cells determined and IgG titre determined. (B) shows a photograph of a flask shaken at a high rotational speed, with an accumulation of microspheres on the inside of the flask walls visible (black arrow), and (C) micrographs of microspheres on days 10 and 25. Black arrows and dashed lines on (A) indicate manual media exchanges by allowing microspheres, retaining cells, to first settle by gravity. The daily sample on media exchange days was taken before the medium was exchanged and not after; a gap has been left between these days and the days that follow it to show this. Data represent mean  $\pm$  SD, n=3 (biological triplicate).

possibility of viable cells peeling off due to non-optimal processing parameters, or the possibility that cells are dying on the microspheres and consequently peeling off. Cell density data between days 10 and 25 revealed the first recurring pattern, with similar cell detachment by the fifth day for three consecutive medium exchange cycles. These cyclic patterns, or data 'zig-zags', would become characteristic for this pseudo-continuous system and indeed would be observed in any similar system employing periodic medium exchange.

The daily viability data complemented the daily concentration of detached cells. Whilst viability remained high at the beginning (as mainly viable cells detached), from day 7 it began to steadily decrease until an average of about 50 % was reached and maintained for the remainder of the culture. The daily IgG titre was, arguably, the most relevant data for this process. The defining characteristic of continuous culture is the vastly extended operation time, and with that the continual expression of product. As was the case with the detached cells, a medium exchange removed IgG before it was produced again with each subsequent day. The maximum titre observed was on day 10, with  $250 \text{ mgL}^{-1}$  almost achieved. Interestingly, after this day (which was a medium exchange day), the titre still increased relative to the preceding day, but did not achieve the same final titre as the preceding cycle. Indeed, by day 25, a titre under  $100 \text{ mgL}^{-1}$  was achieved. This suggested a failing somewhere within the process and corresponded with earlier data regarding the number of dead cells detached from the microspheres. However, the relatively increases each day indicated cells were still present and still being productive.

One of the first observations within this experiment was the creation of a 'tide mark', or the sticking and aggregation of microspheres upon the inside wall of the flasks. Figure 6.4B shows a particularly striking example of this aggregation (indicated by the black arrow). This appeared to be related to the rotational speed of the orbital shaker within the incubator. The initial rotational speed employed was 70 rpm, with visual observation confirming that loaded microspheres were in adequate suspension within each flask. However, by the end of the first day individual microspheres had begun to stick upon the walls of each vessel, and by the end of day 2 this had expanded with considerable accumulation of microspheres now present. Transferring the remaining microspheres into fresh erlenmeyer flasks was performed. Reducing the rotation speed to 60 rpm appeared to rectify the problem; however, microspheres would continue to stick to the inside walls of each flask if they came into repeated contact with the walls. This tended to happen when flasks were carried to a laminar flood hood for sampling or medium exchange and as such, care was taken to keep microspheres within the central area of each flask whilst vessels were handled. This sticking was likely due to the 'stickiness' of loaded cells upon each microsphere, with the polycarbonate walls within each flask effectively acting as a substrate to the retained cells.

---

This issue is also seen when using microcarriers with glass spinner flasks and as such the chemical treatment of these vessels is recommended prior to culture, as is reported later in § 6.2.2.

The use of mild hypothermic temperatures within this first run revealed two observations; one beneficial to the project and the other detrimental. Maintaining the process at 30 and 31 °C did not appear to entirely arrest growth. It was clear that the weight of the microspheres increased as cells continued to populate the materials. This was first noticed during the third and fourth medium exchanges, when the time needed for the microspheres to settle within each flask began to decrease. It was also visually observed by both optical microscope and eye. Figure 6.4C shows micrographs of microspheres at days 10 and day 25. In addition to these images, a very small amount of microspheres were sampled each day and observed under a microscope. It was apparent by the middle of the culture that growth, albeit at a very slow rate, was still occurring. As first described in Chapter 5, cells grew upon each other as the culture progressed, with cellular masses and clumps eventually seen protruding outwards from each microsphere. Because of this continued growth, by the last medium cycle of the culture aggregates of microspheres had formed within the centre of each flask. This was unrelated to the vessel wall sticking as described earlier, but appeared to be combined CHO-microsphere masses. In some cases, these masses were made up of at least 20 microspheres, as can be seen in Fig. 6.4C on day 25. It was likely that adhered cells were forming linkages with neighbouring microspheres as they divided and as a result aggregates began to form. Increasing the rotational speed may prevent this from happening, but it may again cause the sticking of microspheres to the flask walls. An even cooler temperature than that attempted here may be required.

Whilst this growth was not desired — the intention was always for a high but constant viable cell concentration upon the microspheres throughout the process — it did confirm that cells would not detach in dramatic numbers from the materials whilst in cooler temperatures. This was in contrast to the data seen in Chapter 3, where the majority of CHO cells adhered to polyethylenimine substrates in T-flasks began to detach once the temperature was reduced to 30 °C. Two possible reasons were suggested for this not happening with polyethylenimine substrates on microspheres. The first was the effect of the microporous surface on cell retainment. It is generally known that cells appear to adhere and grow more favourable to microporous surfaces rather than solid ones. Despite the polyHIPeS being ‘deformed’, they are nevertheless composed of a highly interconnected microporous mesh, including at their surface where cells are adhered. The second is related to the actual temperature of the environment immediately surrounding the cells. Due to the observation that cells divided upon one another when adhered to polyethylenimine substrates on

microspheres, the thick layer of biomass may be a source of relatively high heat. This potentially could prevent the cells from having such drastic morphological changes which appeared to lead to eventual peeling.

For this run, daily samples taken were immediately frozen. All samples were thawed at a later date, after the end of the culture, for metabolite and substrate analysis. As explained at the beginning of this chapter, the profiling of metabolites and substrates will give a greater overview of the process and can often be the only means of assessing the status of a continuous culture. The analysis in this first attempt was not carried out daily, but it likely would be for established continuous processes so as to enable day-to-day assessment and process control. Figure 6.5 shows the daily glucose, L-glutamine, lactate and lactate dehydrogenase concentrations for medium within one flask in this first pseudo-continuous run. Recurring trends in metabolite and substrate concentrations can be seen, at least from day 5 for each analyte, demonstrating the principle of a pseudo-continuous culture. The decision to eventually choose 5 days for exchanging medium was based upon the time for a typical batch culture in Erlenmeyer flasks to reach stationary, i.e. become depleted of substrates.

Focusing upon the data from days 5 to 10, i.e. the third cycle, the concentration of glucose dropped to  $3 \text{ gL}^{-1}$  by the final day. For cycles after this, the final glucose concentration began to increase and was under  $5 \text{ gL}^{-1}$  by day 25, indicating again some failure within the process as less glucose was being consumed by the end of the process. The L-glutamine concentrations decreased dramatically and started to plateau at a low concentration (approaching  $1.0 \text{ mmolL}^{-1}$ ) by the end of the third cycle. The depletion of L-glutamine by the fifth day, when compared to glucose, was likely a result of changes in metabolism resulting from the reduced temperatures, as discussed in § 6.1.1. These data were the first indication that maintaining the process for 5 days without any medium exchange was too long — if the intention was to keep substrate concentrations high. The concentration of lactate each day, once again, had a recurring pattern with a steady increase between days 5 and 10 and days 10 and 15. However, beyond that the concentration began to plateau, suggesting reduced metabolism within the culture. Lactate dehydrogenase concentrations remained low until day 10, where it began to approach  $2 \text{ kUL}^{-1}$  by the fifth day of each subsequent cycle. This confirmed the higher ratio of dead to viable cells within suspension towards the latter half of the culture. It also suggested substrates (or at least L-glutamine) were not being renewed at a quick enough frequency to sustain the cells.

The changes in culture temperature — which was done in this run to check if cells would detach from microspheres under mild hypothermia — did not bring about any consequent changes in metabolite or substrate concentration. However, due to the sub-optimal con-

---

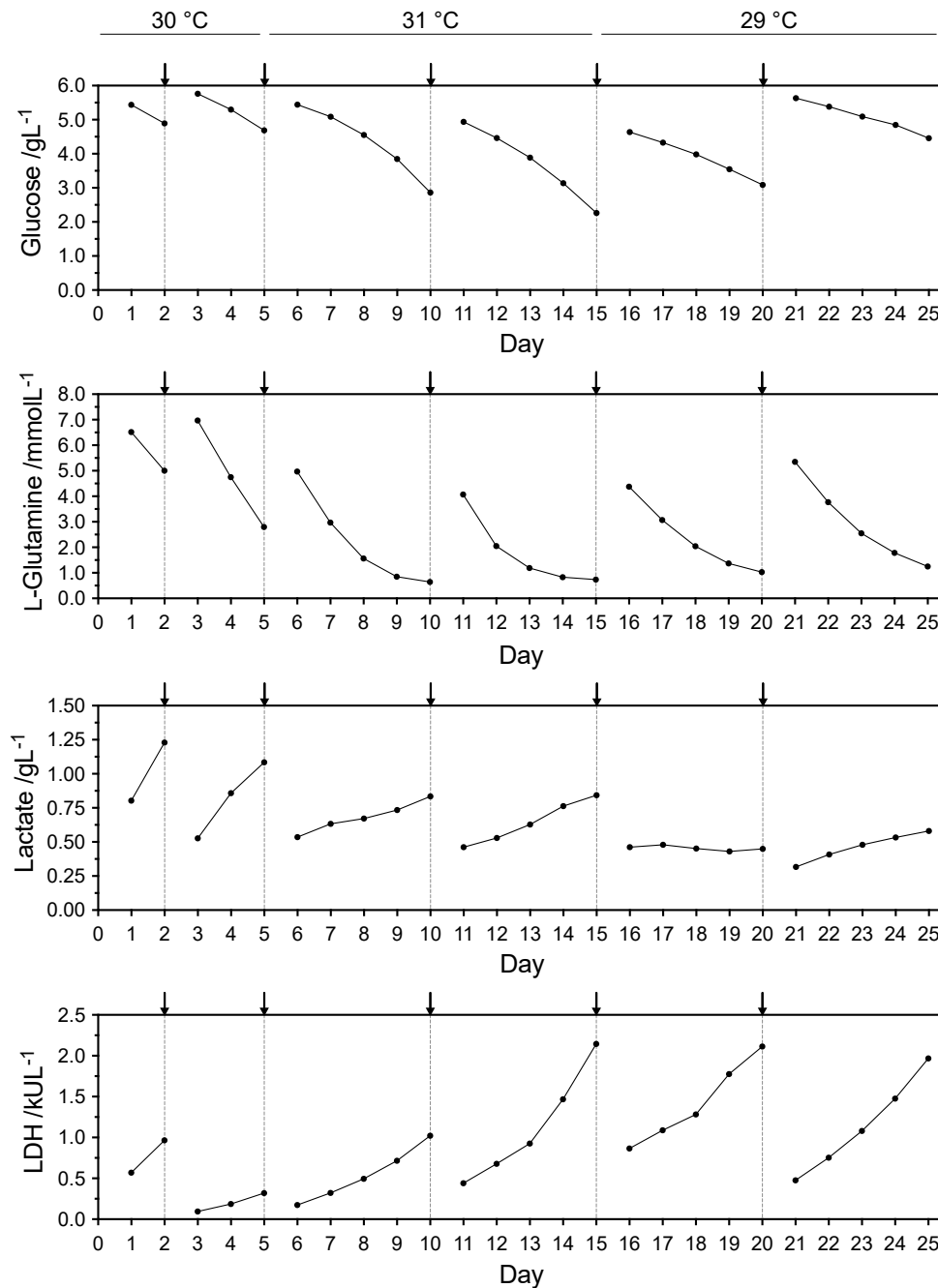


FIGURE 6.5 Metabolite and substrate analysis of the first attempt at pseudo-continuous culture of CHO cells using PEI-adsorbed polyHIPE microspheres for 25 days. During the same experiment as first shown in Fig. 6.4, glucose, L-glutamine, lactate and lactate dehydrogenase concentrations were determined daily between days 1 and 25. Data demonstrated the ability of manual medium exchanges to replenish substrates and remove metabolites. Black arrows and dashed lines indicate manual media exchanges by allowing microspheres, retaining cells, to first settle by gravity. The daily sample on media exchange days was taken before the medium was exchanged and not after; a gap has been left between these days and the days that follow it to show this. Data represent n=1.

ditions of the culture, the data obtained here were extremely crude and should not be over-analysed. The experiment was performed solely to determine the feasibility of using microspheres within Erlenmeyer flasks as a means to carry out simple pseudo-continuous culture. It had been demonstrated here that this was indeed possible, with no evidence of contamination, no dramatic peeling of cells and the continual production of IgG throughout the culture. The next step was to rectify any issues and re-attempt the process.

A second run was planned using the knowledge that had been gained from the first. Erlenmeyer flasks of 125 mL nominal value had been originally used, however the small circumferences of these vessels likely contributed to the sticking of microspheres upon the vessel walls. It was decided to use 250 mL Erlenmeyer flasks, keeping the volume the same at 20 mL, so as to ensure microsphere suspension was agitated around the centre within a greater area. Tests performed prior to this second attempt using non-loaded microspheres in these larger vessels indeed showed microspheres spreading out more evenly within the medium. A rotational speed of 45 rpm was found to be suitable.

For this second attempt, cell loading was performed again using a flow rate of  $0.5 \text{ mLmin}^{-1}$ . This time, 300 million cells were delivered, as opposed to the usual 250 million in the first attempt. The cells retained, calculated by deducting the cells in the effluent from the cells delivered, was an average of approximately 130 million per column, or per 1 mL of microspheres. Retrieval was performed again by flushing the microspheres up from the bottom of the column through the top into a centrifuge tube by the use of fresh medium at  $1 \text{ mLmin}^{-1}$ . The number of cells lost during this retrieval was determined to be approximately 50 million, considerably higher than last time, leaving over 75 million per 1 mL of microspheres. Microspheres were placed into Erlenmeyer flasks and a 31 day pseudo-continuous culture started.

Figure 6.6 shows the daily concentration of dead and viable cells within suspension, the daily viability of these cells and the daily IgG titre for the second attempt at pseudo-continuous culture. It must be stressed again that these daily cell densities are not the density of cells retained upon the microspheres, but detached cells in suspension within the supernatant. The values for cell density and viability, between days 18 and 22, were left blank because the data was lost, however the pattern can be envisaged if the data before and after is reviewed. The temperature of the culture was set at  $30 \text{ }^\circ\text{C}$  between days 0 and 4, and then changed to  $28 \text{ }^\circ\text{C}$  for the remainder of the culture. The rationale behind the initial high temperature was to encourage cells to spread upon the microspheres after cell loading. The switch to  $28 \text{ }^\circ\text{C}$ , the lowest ever attempted, would then attempt to arrest growth. Black arrows with dashed lines indicate 100 % medium exchange on that particular day,

---

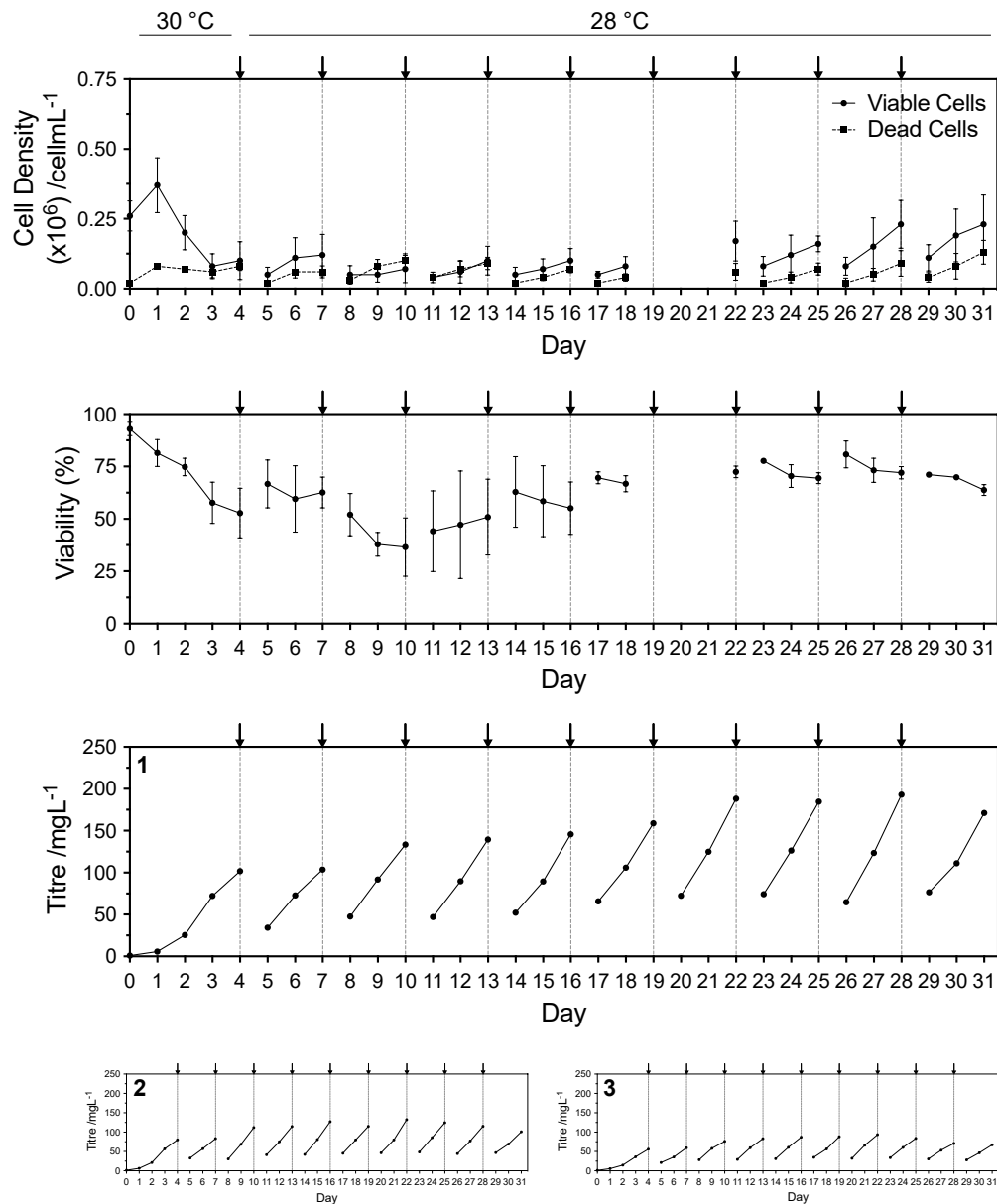


**FIGURE 6.6** Second attempt at pseudo-continuous culture of CHO cells using PEI-adsorbed polyHIPE microspheres for 31 days. CHO-S IgG cells were loaded onto 1 mL polyHIPE microspheres adsorbed with polyethylenimine, then dispensed into Erlenmeyer flasks with agitation set at 45 rpm. Temperature was kept at 30 °C for first 4 days, then 28 °C after for the remainder of the culture. Each day, starting on day 0, supernatant was aspirated from flasks and (A) the number and viability of peeled cells determined and IgG titre determined. Black arrows and dashed lines indicate manual media exchanges by allowing microspheres, retaining cells, to first settle by gravity. The daily sample on media exchange days was taken before the medium was exchanged and not after; a gap has been left between these days and the days that follow it to show this. Data represent mean  $\pm$  SD,  $n=3$  (biological triplicate). For IgG titre, individual sample data, as opposed to mean data, are shown to appreciate the cyclic pattern of antibody production. The values for cell density and viability, between days 18 and 22, were left blank because the data were lost.

with three 80 % medium exchanges carried out for every renewal from the beginning of the process. Medium was exchanged after the first 4 days, and then every 3 days for the remainder of the culture. The process was ended on day 31.

The data here were satisfactory. As with the first run, there was a considerable loss of viable cells on day 1, but this largely ceased by the second day. Unlike the first run, the number of viable cells that had peeled off mostly exceeded those of dead cells, with neither going above  $0.5 \times 10^6$  cellmL<sup>-1</sup> at any time in the culture. This was regarded as a positive outcome, revealing that those cells that had detached did not do so because of necrosis. The daily viabilities remained around 60 % by the end of each medium cycle and only went below 50 % at day 10.

Despite this experiment using a biological triplicate, there was obviously differences between each of the three samples, as can be seen with the size of the errors for the viability readings. For the IgG titre data, the mean was not calculated and instead the daily titre shown separately for each sample. Whilst the maximum titre achieved was different for each sample, together these data proved this second attempt was a partial success. It also demonstrated the potential of pseudo-continuous operation, i.e. a steady and recurring increase in product concentration for every day of each medium cycle. For samples 2 and 3, the last day of each cycle gave the same approximate titre for that particular flask, indicating a working pseudo-continuous culture. For sample 2, just over 100 mgL<sup>-1</sup> was achieved; whilst for sample 3, it was around 75 mgL<sup>-1</sup>. Interestingly, for sample 1 (the 'best' sample in terms of titre) the IgG titre began to increase over time; by day 7 (the last day of the first cycle at 28 °C), the titre was around 100 mgL<sup>-1</sup>, but by day 22 it had increased to over 150 mgL<sup>-1</sup> and achieved this same titre for the next two cycles. A first thought is the possibility of 'old' IgG remaining in the system, but three medium exchanges, of 80 % volume each, were carried out at the end of every cycle. It may present some evidence of sustained, but very slow, cell growth upon the microspheres.

Figure 6.7A shows micrographs of loaded microspheres at days 10, 20 and 30 from sample 1. There was indeed visual evidence of cell growth, even at 28 °C, though remembering each was taken 10 days apart, this growth was extremely slow. By day 30 some microspheres had aggregated due to the increased stickiness of the materials from over saturation with cells, though this was not on the scale seen in the first attempt. A rotational speed of 45 rpm was found to be sufficient in keeping microspheres suspended about the centre of the flask, with no microspheres sticking to the inside walls of the vessels. The photographs in Fig. 6.7B show an example of the sedimentation of microspheres when flasks were tilted. As with the first attempt, the colour of the microspheres turned from white to a golden-yellow

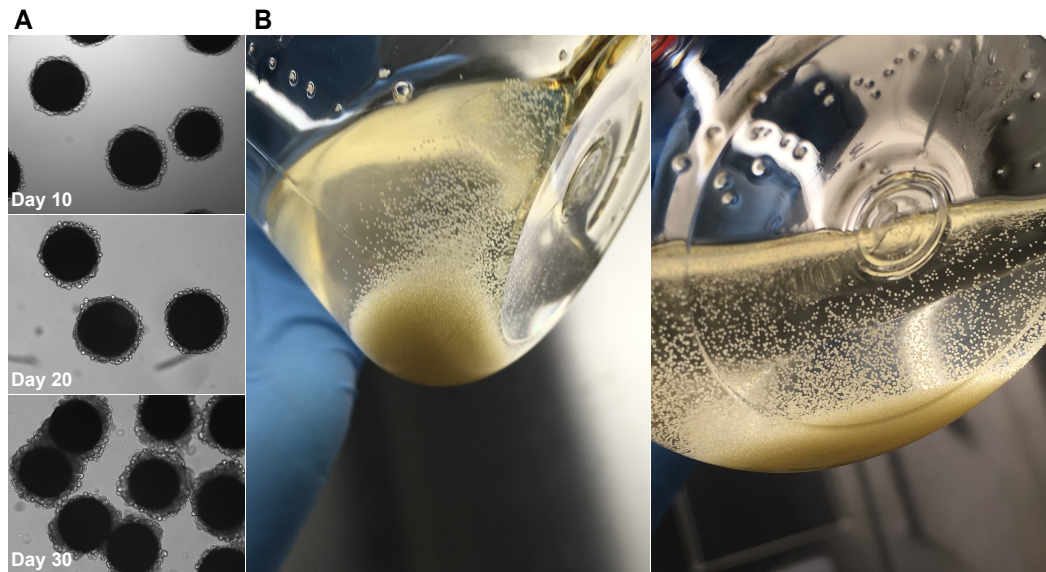


FIGURE 6.7 Micrographs and photographs of the second attempt at pseudo-continuous culture of CHO cells using PEI-adsorbed MAES polyHIPE microspheres for 31 days. (A) shows micrographs of microspheres on days 10, 20 and 30, with (B) photographs of microspheres, loaded with cells, settling within Erlenmeyer flasks.

after a week or so in culture.

Figure 6.8 shows the daily glucose, L-glutamine, lactate and lactate dehydrogenase concentrations within medium for sample 1. From day 4 onwards, the concentrations of glucose and L-glutamine had recurring 'zig-zag' patterns, indicating consistent consumption rates by the retained cells. The similarity in glucose between each cycle was particularly striking.

The concentration of L-glutamine likewise decreased to similar concentrations by the end of each cycle for the bulk of the culture. However, the concentration began to decrease further by the end of each cycle after day 19. Despite this, a medium exchange every 3 days appeared to be sufficient, with the concentrations of both substrates remaining comfortably high at the end of every cycle. The difference in the data between 30 and 28 °C is only apparent with the daily concentration of lactate. Between days 0 and 4, it approached 1.0 gL<sup>-1</sup> before beginning to plateau, indicating some cell growth. Once the temperature was switched to 28 °C, this concentration did not increase so steadily, with 0.5 gL<sup>-1</sup> or under being produced for the remainder of the culture. The concentration of lactate dehydrogenase remained low for the majority of the culture, only going beyond 0.5 kU L<sup>-1</sup> from day 16 onwards. Despite this increased concentration of lactate dehydrogenase towards the end of the culture, the IgG titre remained much the same at the end, indicating growth, or even some replacement, of cells was taking place.

The second attempt was considerably more successful than the first, with no major cell overgrowth, no microsphere sticking within the flasks and recurring patterns of IgG expression, metabolite production and substrate consumption for each cycle. The technique

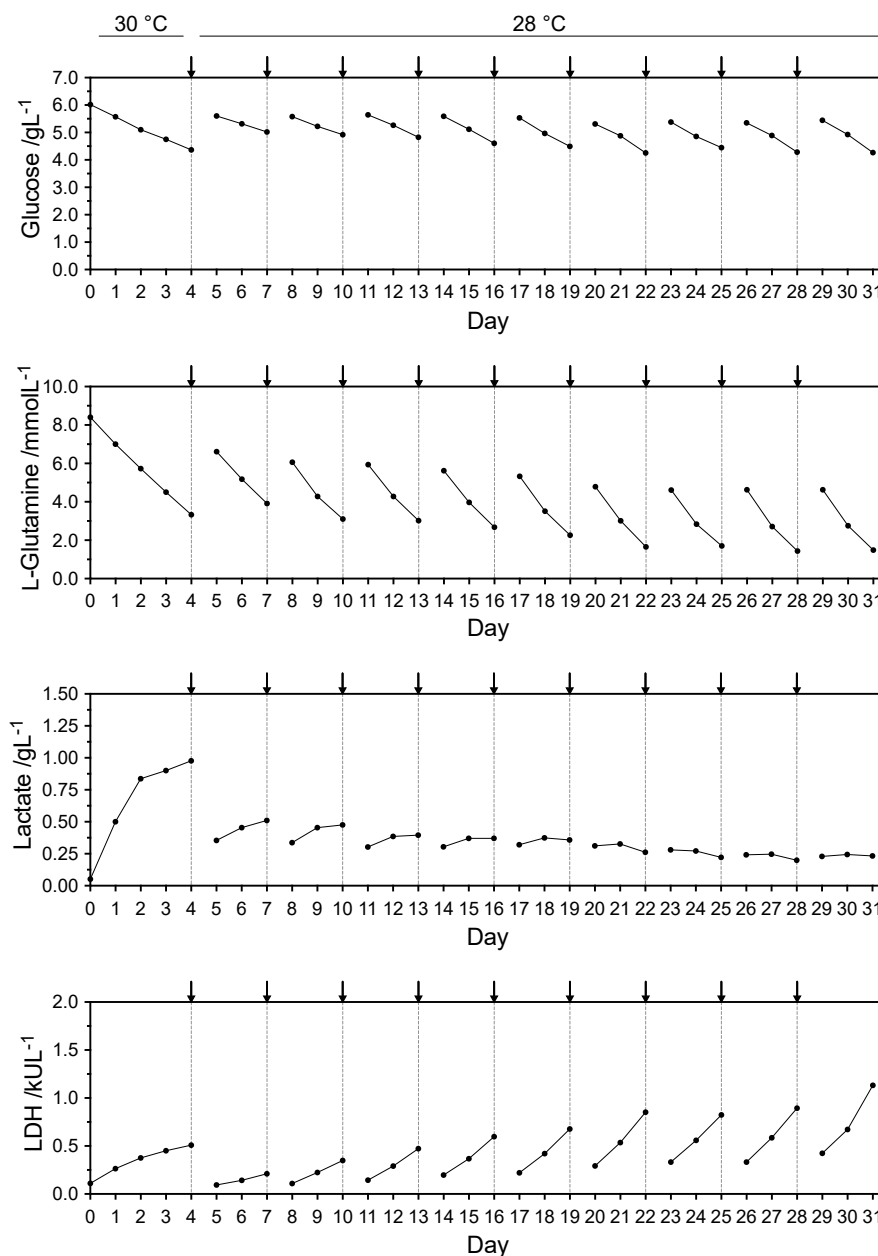


FIGURE 6.8 Metabolite and substrate analysis of the second attempt at pseudo-continuous culture of CHO cells using PEI-adsorbed polyHIPE microspheres for 31 days. During the same experiment as first shown in Fig. 6.6, glucose, L-glutamine, lactate and lactate dehydrogenase concentrations were determined daily between days 0 and 31. Black arrows and dashed lines indicate manual media exchanges by allowing microspheres, retaining cells, to first settle by gravity. The daily sample on media exchange days was taken before the medium was exchanged and not after; a gap has been left between these days and the days that follow it to show this. Data represent  $n=1$ , 'sample 1'.

of performing 80 % medium exchange multiple times to ensure a thorough exchange may be not be strictly necessary for future cultures, but it was done here to ensure the data between each cycle could be fairly compared. Of course, for the entire duration of 31 days, only 3 single-use Erlenmeyer flask were used. For a typical batch process with subculturing every 3–4 days, at least 8 flasks would have been consumed. The variability seen, when comparing all 3 samples, was likely the result of the microsphere retrieval method employed. The technique of pumping loaded microspheres back through the columns was not very controlled, and it was suggested cells were forcefully detached from random locations for each of the samples. This in turn may have affected which area of the microspheres were still populated and if growth did occur, the specific areas where cells would grow.

### 6.1.3 CONCLUSIONS

The work in the first part of the chapter focused upon learning how to routinely operate a Cedex Bio Analyzer, with the concentrations of glucose, L-glutamine, lactate and lactate dehydrogenase determined in a typical batch process and again in a biphasic mild hypothermic culture. Any data from the Cedex unit had to be trusted before any continuous process (which typically relies on metabolite and substrate profile within the exiting medium for culture assessment) was attempted. The Cedex worked as intended, with typical and expected data seen for batch CHO cultures. The switching to mild hypothermia, either at 30 or 32 °C, in a later experiment gave similar observations to those seen in literature reports; cells ceased growing and remained viable for longer than the cultures left at 37 °C. Cell-specific productivity also increased as did cell-specific L-glutamine consumption.

The data proved the use of cooler temperatures can generally extend the length of a batch process. When applied to continuous processing, it has the possibility to thus ensure any cell retention device does not become over saturated with cells. Whether mild hypothermia is performed after an initial growth phase, or whether it is begun from the start after high cell density loading, is dependent upon the particular process.

Pseudo-continuous culture, as opposed to perfusion culture, was attempted first. Mimicking continuous processes, this easier form of extended culture relies on manual exchange of medium at defined intervals. It can also be attempted without any prior expertise or specialised equipment. The decision to choose Erlenmeyer flasks as the vessel to retain the microspheres was based upon their immediate availability within the laboratory, and the equipment needed for shaking culture already being available, i.e. an orbitally shaking plate within an incubator. Tilting these flasks to one side simply allowed the microspheres, and thus the retained cells, to settle and so enabled rapid exchange of medium.

The first attempt determined the feasibility of using loaded microspheres, retained within Erlenmeyer flasks, as a pseudo-continuous system. It was generally a success, but several issues were encountered. The first related to the rotational speed of the orbital shaker; at higher speeds microspheres had a tendency to repeatedly hit the inside walls of the flasks. Over time cells appeared to interact with these surfaces and eventually stuck, causing microspheres to accumulate around the sides with associated aggregation. The second was the temperature of the culture, with 31, 30 and 29 °C being attempted. The choice of these temperatures was largely arbitrary, yet growth did still occur, albeit very slowly. By the end of the 25 days, however, microspheres had aggregated within the medium because of consistent cell growth. Despite this, the observation that cells did not detach, even at 29 °C, was surprising and highly beneficial for the aims of the project.

The second attempt rectified these issues, using a larger volume Erlenmeyer flask (to ensure microspheres did not hit the inside walls and were more evenly spread) with a suitable rotational speed. A temperature of 28 °C was maintained for the majority of the culture, with cell growth appearing to be considerably stunted. Despite differences between samples in this attempt, the principle of pseudo-continuous culture was demonstrated, with the IgG titre giving recurring patterns for each medium exchange cycle. The daily metabolite and substrate concentrations for one of the samples likewise showcased a cyclic process, corresponding to the periodic medium exchange.

The two experiments attempted here were largely done to investigate the potential of a simple pseudo-continuous system, using vessels and equipment available in most cell culture laboratories. The use of microspheres as a cell retention device, within shaking vessels, could not be found in the literature. However, these attempts were primarily focused upon the practical aspects of the processes, e.g. determining the correct values for parameters. It did not explore the potential benefits of continuous culture, such as process intensification.

However, there exists ways to attempt intensification in the future by increasing the ratio of microspheres (retained with cells) to medium, e.g. in these two attempts 1 mL microspheres was used with 20 mL medium, but up to 5 mL microspheres could likely be attempted with this same medium volume. This would be an easy way to boost the daily concentration of IgG, but the medium exchanges would likely have to be more frequent. As can be predicted, there would be a limit to this scaling, with a vessel full of microspheres likely requiring dedicated aeration and better agitation. Due to the inability to count the cells upon the microspheres, as discussed at the end of § 5.2.2, metrics such as cell-specific productivity and other useful quotients could not be determined in these two attempts, and this remains an area of future work.

## 6.2 INTRODUCTION TO CONTINUOUS SYSTEMS

The first part of this chapter demonstrated the use of microspheres as a cell retention device within Erlenmeyer flasks. Tilting the flasks to allow the microspheres, and the cells, to rapidly settle was performed periodically as a simple way to carry out manual medium exchange, and thus perform pseudo-continuous culture. True continuous culture, or perfusion, was always meant to be the end result of the work presented here. For bioprocessing, perfusion can be regarded as the most advanced form of cell culture, and enables the continual exchange of medium, via an automated pump, without any interaction from the operator. This has the potential to bring tremendous benefits, including hugely extended culture times, higher volumetric productivities, smaller-scale equipment, intensification of the process and even an improvement in the quality of expressed product. However, commercial perfusion systems are usually large-scale, expensive and not easily learnt without dedicated training. There thus exists a need to develop and demonstrate simpler perfusion systems.

The first part of this chapter explored the use of the Cedex Bio Analyzer for the determination of metabolites and substrates. It then demonstrated two attempts at pseudo-continuous culture using the microsphere-based cell retention device within Erlenmeyer flasks. The specific objectives for the second part of this chapter were to; (i) design and construct a perfusion system, using the in-house cell retention device, for the continuous culture of CHO cells, and simply (ii) demonstrate the use of this system.

### 6.2.1 PACKED-BED PERFUSION

From the very beginning of the project, ideas were suggested as to what particular format the proposed perfusion system should take. After the decision to use microspheres as a means of cell retention was made, one idea was to use a packed-bed operation. In this system, which was partly inspired by chromatography, microspheres would first settle within columns until a packed bed was formed. Cells would be loaded and the column attached to an inlet and outlet tubing to allow medium exchange through the column in a chosen direction. The eventual benefit of this system would be the potential to add multiple columns in parallel so as to create a plate-based perfusion platform.

Figure 6.9 shows a schematic detailing the proposed packed-bed perfusion system. For this operation, a column and retained microspheres would combine to form the cell retention device. It would be modular with planned capability to attach and detach columns as required. The fabrication of the perfusion plate, as first shown in § 5.2.2, was intended to be the part of this system and would securely hold columns upright. Every physical connec-

tion, e.g. between columns and tubings, would be luer-based, meaning compatibility with any item containing a luer fitting. This would also allow multiple vendors to supply the system and enable further items to be added in the future. The 1.0 and 2.5 mL columns, first introduced in Chapter 5, had luer fittings both at the top and bottom and so would be used again in this system.

Three main pieces of equipment would make up the system; a small refrigerator, a humidified, CO<sub>2</sub> incubator and a peristaltic pump. This pump acts as the central unit, connecting the refrigerator and incubator via tubings. The refrigerator would contain the chilled medium feed tank, whilst the incubator would contain a primed medium reserve tank and the cell retention device, i.e. columns holding the microspheres, as well as sampling tanks and an effluent tank. During normal operation, medium would exit the chilled medium feed tank, via the action of the pump, and enter the primed medium reserve tank. The medium within this tank would be agitated vigorously by a magnetic stirrer using a mixer underneath. The priming of medium would be necessary as any liquid entering would come from a chilled environment; it thus would have to be warmed and buffered before entering the cell retention device. In this instance, the cell retention device is external to the main vessel. The primed medium reserve tank would have a maximum working volume of 30 % of the nominal value and so would rely on headspace for gaseous exchange via two sterile filters. There would be no dedicated aeration or sparging to keep the operation technically simple.

Primed medium would exit the tank, leave the incubator via the pump and enter once again to perfuse through the columns and perform medium exchange. Once perfused through the columns, a three-way stopcock would be used to direct spent medium, or perfusate, to either a 1 L effluent tank or a 10 mL perfusate sampling tank. Each column would have its own sampling tank. During normal operation, these stopcocks would be set so as to allow medium from all of the columns to continually pool and go to the effluent tank but, once a day, they would be turned by the operator to re-direct perfusate to the sampling tanks. This perfusate is the medium directly leaving the retention device and can be analysed daily for peeled cells, IgG and metabolites and substrates. A cap with a septum would be used for each perfusate tank to allow aseptic entry via a needle. These septa caps will seal themselves after puncture and can be pierced repeatedly with a very low risk of contamination.

The pump used would be a multidrive unit, meaning all tubings would be connected onto a single head with identical flow rates. As a consequence, the flow of medium at any point in the system would be identical; thus, the rate of medium entering the primed media reserve

### Packed-Bed Perfusion Schematic

- ✓ Continuous perfusion operation (over 2 weeks, passage-free)
- ✓ Cells preloaded at high density (no need to wait for growth)
- ✓ Microsphere-based retention system, with animal origin-free adherence mechanism
- ✓ Aseptic injection and sampling points

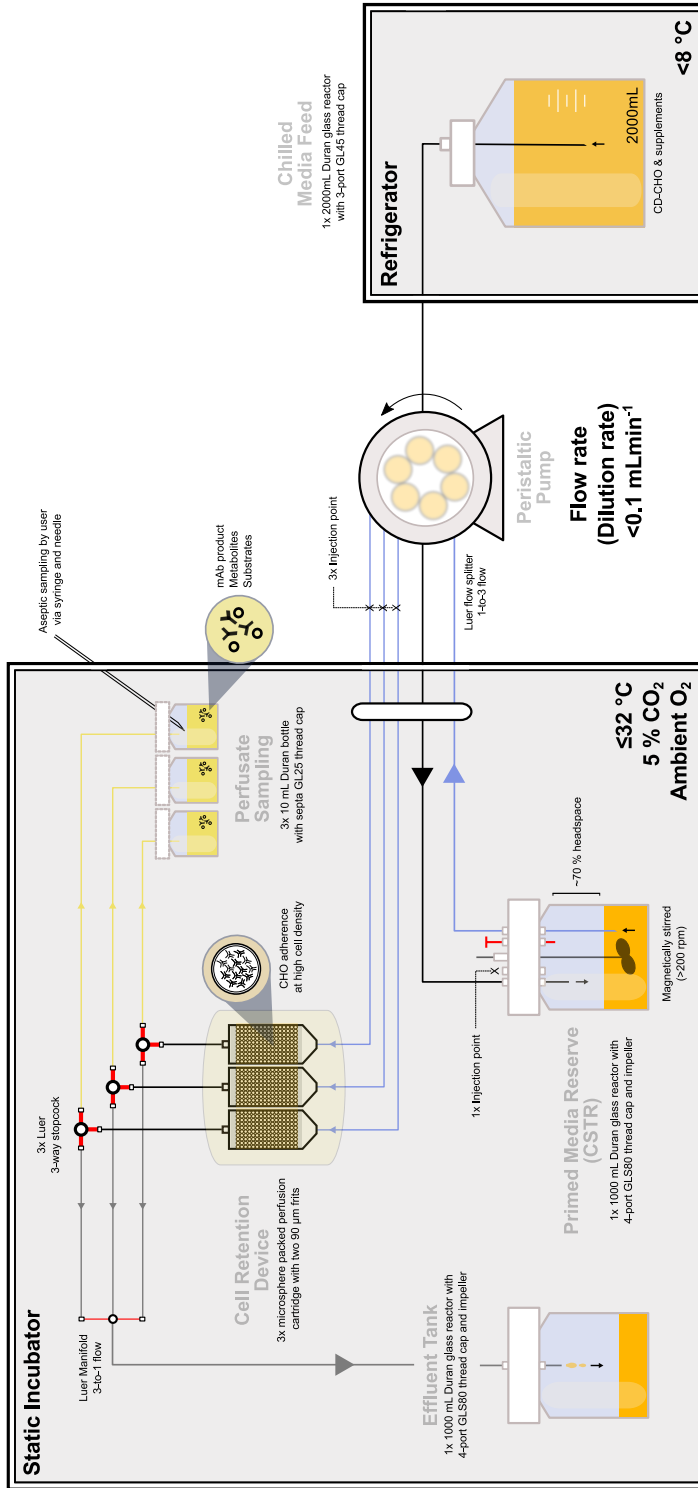


**FIGURE 6.9 Schematic detailing the packed-bed perfusion system.** The perfusion system first proposed was based upon a packed-bed design. Columns would be filled with PEI-adsorbed microspheres to form packed-bed environments. Microspheres would be loaded with cells and then connected to tubings, media tanks and a pump to create a continuous system. The pump would connect a refrigerated media feed tank to a media reserve, which would heat and buffer medium within a static incubator (set to mild hypothermia) before being delivered to the cells within each column. Perfusate would be sampled on-demand via the use of three-way stopcocks at the exit point of each column. An effluent tank would collect waste media. Lines represent tubing for medium flow. The system was to be designed and constructed entirely in-house.

tank would be equal to the rate of medium leaving. Likewise, the flow rate of the perfusate entering the effluent tank or the sampling tanks would also be the same. In theory, this would mean a steady state will form with the conditions of the medium within the primed media reserve tank eventually reaching and staying at some average profile. The flow rate would be kept low (certainly less than  $0.1 \text{ mLmin}^{-1}$ ) ensuring the residence time within the primed media reserve was long enough to heat and buffer the newly added medium.

The packed-bed design seemed ambitious but achievable, at least when using a single column as the cell retention device. A small 'drinks fridge' was supplied as the refrigerator and an incubator and peristaltic pump, with a multidrive head, obtained in-house. Silicon tubing was supplied with an internal diameter of 1.8 mm. This diameter was compatible with the head of the pump and could pass comfortably into and out of the incubator and refrigerator when they were both closed. The inner door of the incubator had a flexible lip, which would also allow the tubing in and out with no apparent effect on internal temperature or  $\text{CO}_2$  levels. One of the initial concerns was the use of electrical equipment within an humidified environment; it was because of this that the pump was placed outside of the incubator. A hermetically sealed magnetic stirrer, specifically designed for acidic, warm conditions was supplied solely for this work, with the primed medium reserve placed on top. This stirrer was attached to an external, analogue controller that set the stirrer speed. All tanks used were Duran bottles and autoclavable. GL caps were supplied with appropriate ports and silicon inserts to allow aseptic entry and exit of tubings. These had to be sized to allowing the specific tubings to fit aseptically.

All tanks required at least one sterile filter to ensure pressure equalisation and allow the pump to operate without any associated pressure. Luer fittings with barbed ends suitable for 1.8 mm tubings were obtained and used to attach these sterile filters to tubings via male-female connections. The material of the specific luer fittings employed were nylon and thus autoclavable. The stopcocks, supplied as single-use, could also be attached to tubings using these luer connections. The system was small enough to be split into particular segments, bagged up and then autoclaved. Everything was then re-assembled in a laminar flow hood, immediately prior to operation. Sterilise-in-place techniques were beyond the capability of the laboratory and could not be used in this instance.

Figure 6.10A shows an early example of the packed-bed design in operation, with the incubator, peristaltic pump and refrigerator shown. For initial attempts, 1.0 mL columns were used with a syringe pump employed to load cells, as first demonstrated in § 5.2.2. A dilution rate of  $0.25 \text{ }\mu\text{Lmin}^{-1}$  (corresponding to  $36 \text{ mLday}^{-1}$ ) was used. This was the lowest possible with the tubing and pump combination used. Figure 6.10B shows a photograph

of a single 1.0 column, filled with microspheres, being perfused within the system with the luer fittings and stopcock shown. The second photograph shows microspheres after 5 days in perfusion culture with evidence of microsphere discolouration, as was seen during the pseudo-continuous attempts.

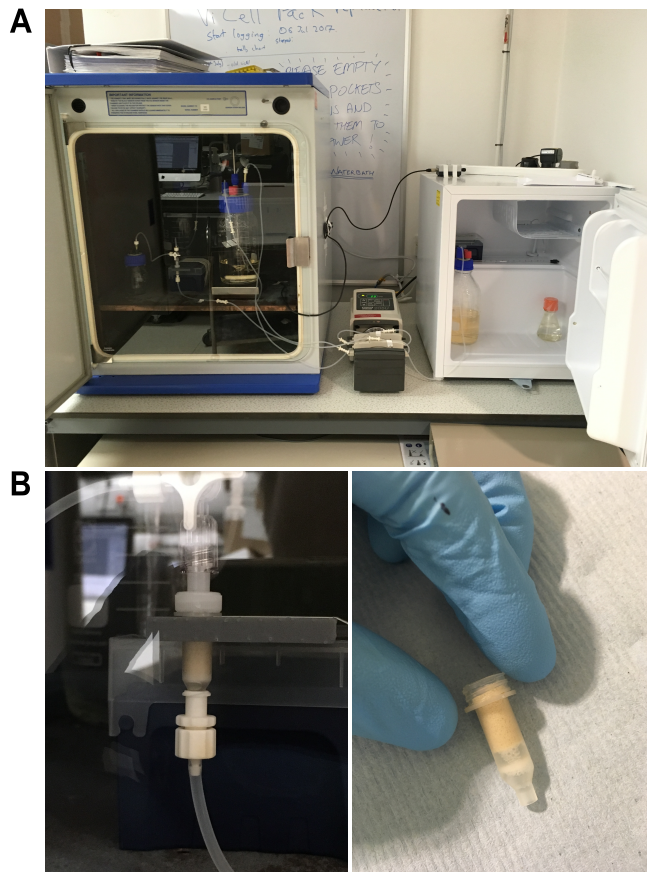


**FIGURE 6.10** Photographs of the packed-bed perfusion system using 1.0 mL columns. (A) shows the static incubator, pump and refrigerator filled with components as detailed in the schematic in Fig. 6.9, whilst (B) shows a 1.0 mL column in detail, filled with microspheres and being perfused upwards through the stopcock, and the same column after a week in culture. Microspheres were discoloured, from white to yellow-brown, from continual medium exposure.

The perfusate sampling system did work as intended, with a single-use needle and syringe being used to aspirate perfusate daily. Due to the slow dilution rate, it took approximately 1 hr to get 10 mL, which was regarded as a sufficient volume for analysis. The line immediately leading up to the sample tank was classed as dead volume and, when the system was not being sampled, would hold the medium sampled from the previous day. For each sample taken, this dead volume would first have to be directed through and collected separately before the actual sample was taken. This added 15 min to the sampling time. As a sterile filter could not be added to the septum, the cap was slightly loosened to ensure

perfusate was delivered without any associated pressure. Numerous attempts were made with this system, with each one providing new information on how to optimise the process. The first observation concerned the positioning of the outlet tubing in the primed media reserve tank. With the magnetic stirrer agitating the medium, the outlet tubing (submerged at first) would periodically flick up out of the liquid.

Whilst not an immediate cause of concern, over several days this disturbed the volume of medium within the tank to such an extent that the height of the liquid began to noticeably rise. It was soon apparent that the height of the volume within the tank could be used as an indicator of correct and continual medium flow around the system. An increasing medium volume was not desirable as it reduced the headspace available for gaseous exchange. There was also the possibility of air pockets forming within the outlet tubing. To overcome the flicking, the tubing was affixed to the inside wall of the tank with a piece of autoclave tape, just prior to autoclaving. Whilst this was cumbersome to achieve — imagine a ship-in-a-bottle — the tubing stayed securely down with the end remaining submerged in the medium for all subsequent attempts. A rigid, hollow rod, rather than flexible tubing, would be the optimal solution here but this was not pursued and the ad hoc solution kept.

A second observation concerned the temperature of the medium within the primed medium reserve tank. It was noticeably hotter than expected and it was later found that the magnetic stirrer plate was likewise hot upon touch. This plate, heated by the incubator, was transferring excess heat over to the tank and raising the temperature of the contained medium above that set by the incubator. An overnight test using a thermometer submerged in agitated medium confirmed this; when the incubator was programmed to 37 °C, the medium within the tank approached 40 °C. The lid of a 96-well plate was placed on top of the magnetic stirrer and the tank positioned upon that. This provided a small clearance of air, but still allowed the magnetism to drive the stirrer within the tank. A follow-up test confirmed the temperature now matched that set by the incubator.

A third observation concerned the direction of medium flow. It was originally intended to be upwards, i.e. the medium would flow from the bottom of the column through the microspheres and out the top. This was to allow the liquid to go against gravity and thus ensure the flow rate would be equal to that set by the pump. To achieve this, a frit had to be inserted from the top of the column after the microspheres were packed (and immediately before cell loading) to ensure no microsphere loss once medium exchange had commenced. It was a challenge to insert the frit and not accidentally crush the microspheres by pushing too far. To resolve this, attempts were also made to perfuse medium downwards, i.e. from the top of the column. It was noted, regardless of whether medium was perfused up or

---

down, that occasionally there were pockets of air within the packed-bed itself. At the low dilution rate used, these would not pass through the column. Flicking the column sides or manually agitating by hand was also not sufficient.

A fourth observation concerned leakage from the column itself. The bottom of these columns ended in a male luer. It was suspected the manufacturing process for these columns was not particularly robust, with these males often not fitting tightly with a corresponding female luer. In practice, this meant there was occasional leaking of medium as it entered or left the column (depending upon the direction of medium flow). In some instances, this led to contamination if an attempt was made to stop the leakage. Autoclaving female luers also seemed to weaken them, when used with this particular male luer, and further made the connection prone to leakage. An initial way to rectify this was to wash the specific female luer used in ethanol, although this was not ideal. Luer locks, which include a thread to screw fittings together, are a special form of fitting and help to ensure a secure connection. Standard luers, correctly called luer slips, are instead simply pushed together and connect via a tapered end. All male luers supplied for this system were luer lock to ensure total leak-free operation, except the male luers on the bottom of the 1.0 mL columns. The stopcock male luer attached to the column was also a luer lock, and as a result did not suffer from any leakage.

No trusted data could be obtained from the packed-bed perfusion attempts using the 1.0 mL columns. Whilst the issues surrounding the temperature of the primed medium reserve tank and the agitation of the outlet tubing were overcome, the problems arising from the use of the specific type of column remained, i.e. leaking with occasional trapped air pockets. A decision was made to retry the packed-bed system using the larger 2.5 mL columns. The main benefit of these columns was the male luer lock on the bottom end, meaning it could form a tighter, threaded connection with a female luer. The female luer on the top cap could, as with the 1.0 mL columns, connect to a male luer lock fitting on the stopcock. The circumference of these columns were also wider than the 1.0 mL version, meaning microspheres were not as tightly packed; indeed, 1 mL microspheres within a 2.5 mL column would float freely, almost in close suspension, when agitated manually. This allowed the columns to be agitated or flicked by hand to disrupt any air blockages.

An interesting question arose concerning the actual temperature of the medium immediately before it entered the column. Due to the slow dilution rate employed, the time spent by the primed medium on the outside of the incubator as it passed through the pump was around 20 min. This likely would cool the liquid down to ambient temperatures. A technique to reheat the medium, upon entering the incubator, was needed.

Figure 6.11A shows a photograph of the new set up, using a 2.5 mL column, during a test run outside of the incubator and refrigerator. It also shows coiled tubing, wrapped around a 15 mL centrifuge tube. This was the 're-warmer' unit and was positioned immediately before the column in the incubator. The residence time of the primed medium upon entering the incubator would be extended to roughly equal the time spent outside at ambient temperature. Any losses in temperature would thus be regained before passing through the column. Figure 6.11B shows a 2.5 mL column, filled with 1 mL microspheres, in perfusion operation. In this instance, the direction of medium was up through the column. The top stopcock can be seen connected to a perfusate sampling tank in one of its directions. The bottom stopcock was added so as to allow easy priming of the column after it had been connected, with a separate tubing (later removed) used to direct medium at a relatively fast flow rate.

The luer lock connection at the bottom of the 2.5 mL column did not leak during operation.

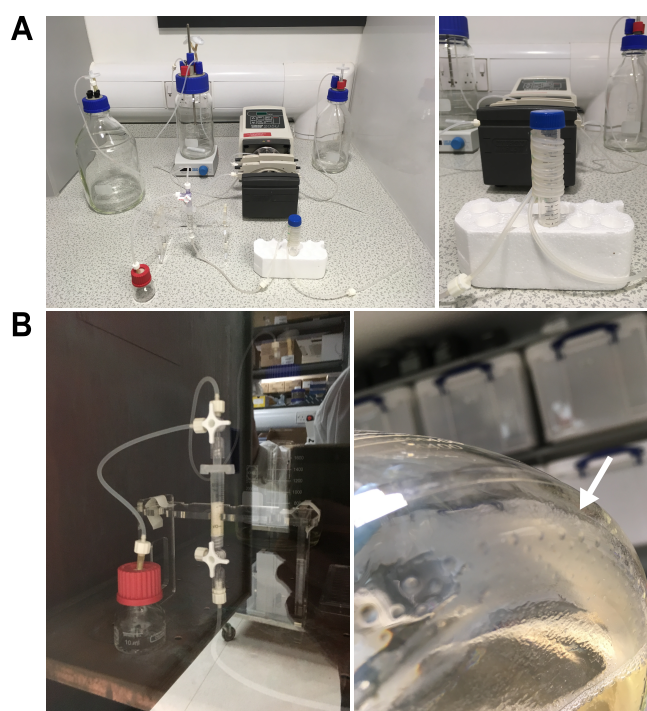


**FIGURE 6.II** Photographs of the packed-bed perfusion system using 2.5 mL columns. (A) shows the entire perfusion system connected outside of the static incubator and refrigerator (for clarity of the process), with a close up of the 're-warmer' component. (B) shows the new 2.5 mL column, with improved luer-lock connections. Initial attempts with the larger columns once again perfused medium upwards, but later tried perfusing downwards after observing leakage at the top of the column. Evidence of CHO accumulation in the effluent tank (white arrow) could be seen after an attempt at perfusion culture, indicating severe cell peeling off the microspheres during the process. The temperature of the CHO cells, within the cell retention device, was likely difficult to control due to the packed-bed environment.

Any air pockets, which tended to form during priming of the system, could be easily flicked or agitated by hand out of the columns with the flow of the medium. Microspheres did float through the column when the system was being primed, but eventually fell back down into a loose suspension towards the bottom when the usual dilution rate was restored. The frit at the top of the column could be inserted in the underside of the cap, meaning there were no risks of crushing microspheres as was the case previously. Frustratingly, it was soon apparent that the cap at the top of the column did sometimes leak. Unlike the 1.0 mL column, the cap did not screw into a thread, but rather was pushed on and slightly turned with small tabs to keep it in place. This meant, on certain 2.5 mL columns, there was some leakage of medium as it perfused through.

A piece of laboratory cleaning roll was gently brushed against the column directly under the cap to test for this leakage. To counter this, the direction of medium flow was once again reversed and directed down through the column. A small air gap was left at the top allowing liquid to drop down into the medium and microspheres below. There was a slight disturbance to the settled microspheres from the dripping but this was tolerable. The volume of the air gap could be decreased by simply turning 'off' the stopcock at the bottom and allowing extra medium to fill the column for several minutes. Having two stopcocks, one at the bottom and one at top, was found to be incredibly helpful in controlling the liquid level within the column.

Attempts to perfuse downwards, with all the other changes implemented, proved successful — at least in terms of medium flows within the physical system. There were no leakages, no air pockets, no visible contamination and the medium height stayed at a constant level within the primed media reserve tank. The last run performed using these improved techniques lasted about 10 days, but was stopped upon inspection of the effluent tank. Figure 6.11B shows visible build-up of CHO cells (as indicated by the white arrow) at the bottom of the effluent tank, near where the perfusate entered. At this point, the system was stopped and the microspheres visualised under a microscope. The cell retention device had failed with total detachment of cells. These cells were pumped into the effluent tank where they presumably accumulated over the course of the run.

Discussions brought up the idea that, due to the slow dilution rate, the temperature within the column was likely hot enough to allow growth. This was despite the initial concern that the temperature of the medium entering would be cool. The 'rewarmer' unit probably did ensure medium was warmed back to 30 °C (the temperature used for these processes) but the temperature within the microsphere bed may be far beyond that. Due to this and the continual supply of nutrients, there was likely rapid overgrowth with eventually de-

tachment.

Almost two months had been spent trying to get this design to operate correctly, with at least 10 attempts (some of which ended in contamination) made using either the 1.0 or 2.5 mL columns. No data was recorded for the vast majority of the runs, as the aims were to simply ensure the system would at least ‘work’ before committing to sample analysis. The temperature of the operation, as it currently stood, could not be reliably controlled and this may have caused the failure of the retention device in the final attempt. Increasing the dilution rate, so as to ensure cells would receive medium at a quicker rate and thus be cultured at the intended temperature, may have helped to overcome the suspected issue of cell heating with associated overgrowth. If this was performed, however, the medium usage would be too great for the work and would lead to higher cost, with the IgG product also being diluted. Updated criteria for the proposed perfusion system now required a more robust process, e.g. no potential for leakage or weak connections, and one where it would be certain the temperature of the cell retention device matched the temperature of the incubator. Alternative designs for the perfusion system were sought.

### 6.2.2 SPINNER FLASK-BASED PERFUSION

Once the packed-bed design was abandoned, discussions turned to what form the next design should take. It was suggested that Erlenmeyer flasks, retaining the microspheres in suspension as with the pseudo-continuous process, could be used again. Reusable glass Erlenmeyer flasks were commercially available with some having GL-style caps. These caps could have inserts for tubing to pass through. A very simple design, consisting of an inlet tubing for medium addition and an outlet tubing for medium exit, was suggested. The microspheres, loaded with cells, would be exposed to this exchange within the flask itself. This was essentially a chemostat system, whereby medium would be added and removed at the same rate. A steady state, in regards to process parameters, would be achieved and maintained via sufficient agitation of the incoming and outgoing medium. In this instance, and in contrast to the packed-bed design, the microspheres would become an internal cell retention device. Despite these differences, the principle of operation remained as detailed in Fig. 6.9, i.e. a pump would deliver medium from a chilled tank to a culturing vessel for eventual medium exchange. Perfusate would be directed to a waste tank or redirected as needed for sampling.

Whilst it had been demonstrated previously that Erlenmeyer flasks could be used to retain and agitate loaded microspheres, other vessels were explored to ensure more bioreactor-like mixing. As already stated, spinner flasks remain the most popular vessel type for microcarrier culture in the literature. Having a central shaft and impeller, these flasks are

capable of mixing microspheres in a similar fashion to that seen in larger-scale stirred tank reactors. The characteristic feature of a spinner flask is its two side arms, located opposite to one another with each possessing a threaded cap. It was proposed that one of these arms could secure the inlet tubing, whilst the other the outlet tubing. With medium entering and leaving the flask at the same rate, i.e. tubings were connected to the same pump, a chemostat would effectively be formed without too much technical expertise. Sufficient mixing provided by the impeller would ensure a homogenous environment, whilst a slow dilution rate would ensure the vessel is not exposed to cool medium too quickly, i.e. medium would slowly drip in from the inlet tubing.

This seemed achievable. It was also robust. There were no plastic caps or luer slips, with two access points for the inlet and outlet made using secure inserts within threaded caps. The rest of the system would remain as it was with the packed-bed design, as it was known to operate with no issues. The only concern was the potential loss of microspheres to the outlet tubing as medium was exchanged. An easy solution would be to ensure this tubing was touching the base of the flask with a sufficient agitation employed to deter microsphere loss. However, it was reasoned for extended processes, e.g. 3 weeks or more, there would eventually be some exiting of microspheres. Another solution looked at attaching a frit to the end of the outlet tubing, with a pore size smaller than that of the average diameter of the microspheres. Detached cells and medium could exit whilst microspheres are themselves retained internally. The frits used within both the 1.0 and 2.5 mL columns were supplied separately in packs and available in the laboratory. They had a 90  $\mu\text{m}$  porosity and could be autoclaved repeatedly. These very same frits could be used at the end of the outlet tubing. The only way to attach these frits to the tubing would be via a bespoke frit holder, which would have to be designed and fabricated in-house.

Figure 6.12A shows a technical drawing for a frit holder and models for the three frit holders eventually fabricated. The first two designs were for 'small' and 'large' frits; these corresponded to the physically smaller and larger frits that were available to use. These designs ended in a barb suitable for the tubing used in all the perfusion operations presented here. Several iterations were tested regarding the tapered opening, with this required to ensure a frit could be pushed in by hand and would stay securely in place. This frit holder, containing a frit, could then be attached to the end of the outlet tubing.

The third design was to make the frit holder universal. The barbed end, specific to the tubing here, was replaced with a female luer, meaning the frit could now be attached to any male luer fitting. This particular holder was made to be 'small', as it was decided a physically smaller frit holder may be beneficial within the flask. Figure 6.12B shows all

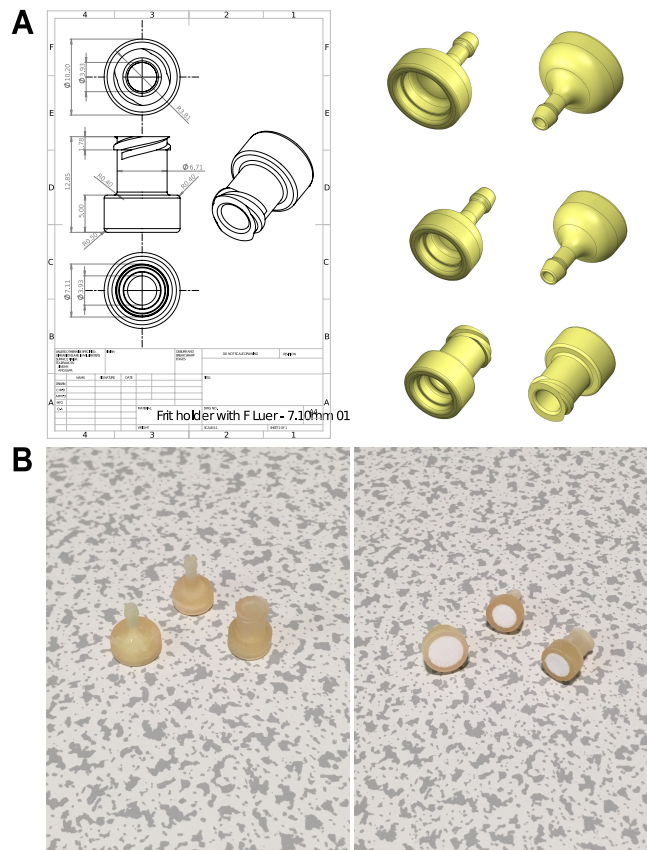
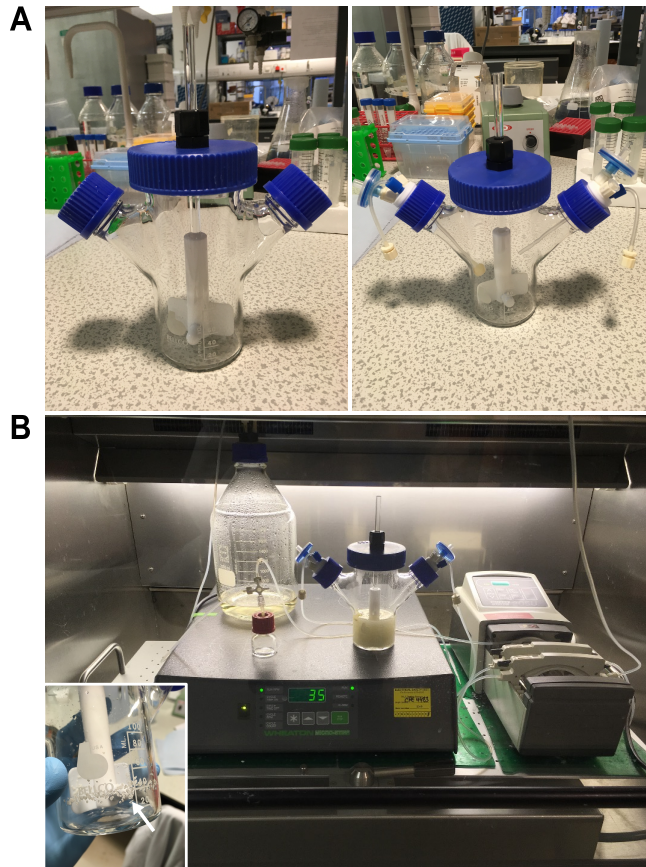


FIGURE 6.12 Computer-aided design and 3D printing of bespoke frit holders. (A) shows an example of a technical drawing, in this instance for the luer frit holder, as well as the model for each design, and (B) shows each of the holders after being 3D printed, and again after being inserted with polypropylene 90  $\mu\text{m}$  frits. Frit holders had a tapered opening and so allowed frits to be securely inserted. Both frit and frit holder were autoclavable.

three 3D-printed frit holders, before and after having their frits inserted. The particular resin used was capable of being autoclaved several times without any effect on its size, and so could be autoclaved within a spinner flask as part of a normal sterilisation protocol.

Figure 6.13A shows a spinner flask before and after modification to ready the vessel for continuous medium exchange. The outlet tubing can be seen within the left side arm, with the frit attached on the end. The inlet tubing can be seen within the right side arm. This tubing could be positioned anywhere, as long as medium would drop into the suspension below. The outlet tubing, however, had to be positioned so as to avoid the top of the impeller. This meant, in practice, the working volume would always have to 100 mL to ensure the frit was entirely submerged. There was little clearance between the walls of the vessel and the sides of the impeller. GL32 caps with three 1/4"-28 UNF(F) ports were supplied to replace the closed GL32 caps. These female ports could connect via a threaded connection to UNF(M), or male, fittings. UNF(M) to male luer adapters were supplied, which could

then attach to a female luer on a 0.2  $\mu\text{m}$  sterile filter. One filter was placed on each arm to ensure sufficient gaseous exchange. UNF(M) fittings with inserts suitable for the tubings used here were also attached to both caps. The inlet and outlet tubings could be aseptically secured through these inserts for entry into the flask.



**FIGURE 6.13** Photographs of the modified spinner flask and the spinner flask-based perfusion system. (A) first shows a standard 100 mL nominal glass spinner flask and then one which has been modified with suitable components to allow the continuous addition and removal of medium. GL caps with inserts, 0.2  $\mu\text{m}$  filter units and tubings were added to the spinner flask, including a bespoke frit on the outlet tubing. (B) shows the spinner flask-based perfusion in operation, with a pump delivering medium from a refrigerator into a spinner flask (lower left inset: evidence of microspheres sticking to inside wall of spinner flask before it was treated to render it hydrophobic, shown by white arrow). The microspheres, loaded with cells, were kept in suspension within the flask and prevented from exiting the vessel via the frit. The outlet tubing led to both a sample tank and a waste tank, with a stopcock used to direct the flow of effluent medium.

The use of a spinner flask, with a cell retention device that was now internal, meant the system was simpler and quicker to set up than the previous packed-bed design. Figure 6.13B shows the main section of the new system. A larger incubator was used, without humidification, so as to allow electrical equipment to be placed safely inside. The peristaltic pump

could thus be placed beside the spinner flask, meaning no exit and re-entry of tubings and eliminating the need to passively reheat medium. The refrigerator was placed above the incubator, with the tubing coming from the chilled media feed tank as before into the incubator. This tubing, along with the power supply leads, could fit behind the door of the incubator when closed without any effect on internal temperature or CO<sub>2</sub>.

A magnetic stirrer dedicated to spinner flask culture was sourced in the laboratory; this could achieve a low rotational speed appropriate for microsphere work. Initial testing determined 35–40 rpm to be a suitable speed for 10 mL microspheres within 100 mL medium. The metallic magnetic stirrer used previously was actually intended for chemical mixing within unusual environments and would not go below 200 rpm. The tubing leading to the perfusate sampling tank was eliminated by simply attaching the needle directly to the stopcock. This meant there was no longer any dead volume to remove prior to taking a sample. To further ensure swift sampling, a fresh, autoclaved perfusate sampling tank (with septum cap) was used each day. To switch the tanks, the needle would simply be lifted out of the old septum and reinserted into the new one. The septum of the new tank would be disinfected and allowed to dry prior to sampling to further minimise the risk of contamination. This technique ensured each sample was delivered into a fresh tank with no possibility of sample crossover each day.

The sole issue encountered during preliminary testing was, as with the Erlenmeyer flasks, the sticking of microspheres to the inside walls of the vessel. The lower left inset in Fig. 6.13B shows evidence of this, indicated by the white arrow. Being a widely known problem in microcarrier work, a solution was immediately found. A siliconizing reagent was supplied and added to the inside of the flask for several minutes, rendering the glass extremely hydrophobic. This coating was not affected by autoclaving and the issue was resolved.

The spinner flask, of course, could not be perfused through with a cell load as with the columns. The intermittent agitation technique, as first demonstrated using ambr15 vessels in § 5.2.3, was instead employed in this design. 10 mL microspheres were dispensed within 20 mL medium and to this 20 mL suspension containing 400 million cells was added. 20 mL medium was used as it was the lowest possible volume that 10 mL microspheres could be suspended in without a paste-like slurry forming. The intention was to keep the total volume used for cell loading as low as possible to encourage increased interaction between cells and microspheres. The spinner flask was agitated at 25 rpm for 15 min, 0 rpm for 2 min and then repeated. 1 mL samples were taken every 0.5 hr from the microsphere-cell suspension, the microspheres decanted and the supernatant then analysed for unattached cells. This meant, every 0.5 hr, two start-stop cycles had been completed.

Figure 6.14A shows the number of cells (in million) adhered to each mL of microsphere, and how this changed, during the 2 hr cell loading. These data assumed equal adherence to the total volume of microspheres. The maximum number of cells that could be adhered per mL of microspheres with this cell load was 40 million. There was some microsphere aggregation upon addition of the load, but this resolved itself within a few minutes upon agitation. As in § 5.2.3, a large proportion of cells were loaded by the first measurement at 0.5 hr, with 25 million cells adhered per mL of microspheres. The next measurement at 1.0 hr saw an increase to over 30 million cells, with the final two measurements remaining at this level. Approximately 30 million cells per mL of microspheres were thus retained using these conditions.

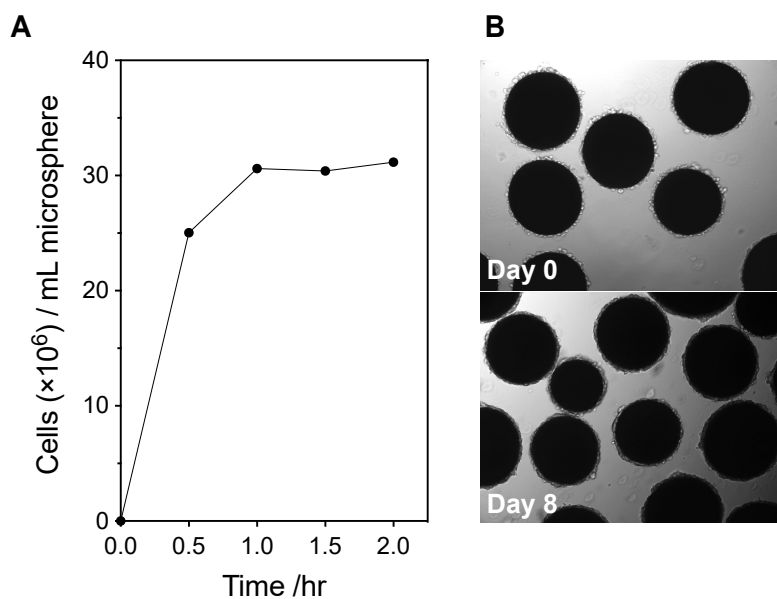


**FIGURE 6.14** Cells retained during intermittent agitation at the beginning of an attempt at the operation of the spinner flask-based perfusion system with visual evidence of adhered cells after 8 days. 10 mL polyHIPE microspheres adsorbed with polyethylenimine were added to CHO-S IgG cells, prepared to a density of  $20 \times 10^6 \text{ cell mL}^{-1}$ , within a spinner flask, with intermittent agitation for 2 hr. Every 0.5 hr, an aliquot was taken, the microspheres decanted and the cells not yet adhered determined, with (A) showing the number of cells adhered per mL of microsphere calculated each 0.5 hr. After this time, the unadhered cells were diluted out, and the spinner flask attached to the perfusion system with a dilution rate of 0.38 vvd. (B) shows cells adhered on microspheres after cell loading using this intermittent spinning technique and again on day 8 prior to cell pausing. Data represent  $n=1$ .

Fresh medium was added, the microspheres allowed to settle and the supernatant aspirated to cleanse out the unadhered cells. This was repeated twice, before a final addition of medium to increase the volume to 100 mL. The modified GL32 caps, with inserted tubings and sterile filters, replaced the closed caps used previously. These caps were loosened during loading to ensure gaseous exchange. The spinner flask was assembled together and

placed immediately in the incubator. The pump was set at  $25 \mu\text{Lmin}^{-1}$ , corresponding to a dilution rate of approximately 0.38 vvd; 38 % of the working volume would be exchanged every 24 hr. Samples were taken from the perfusate tank daily.

Figure 6.15 shows the daily glucose, L-glutamine, lactate, lactate dehydrogenase and IgG titre for the entire 35 day culture using the spinner flask-based perfusion system. It must be remembered the operation here was true continuous, i.e. the perfusate sample taken each day was the medium that had been pumped out of the spinner flask an hour prior to retrieving the sample. For the first 8 days, the temperature was kept at  $30^\circ\text{C}$ . The concentrations of glucose and L-glutamine, which were present in the medium at  $6 \text{ gL}^{-1}$  and  $8 \text{ mmolL}^{-1}$ , respectively, remained below these values for the first 8 days, with glucose steadily decreasing each day. For the same period, lactate was present within the medium and increased steadily, whilst lactate dehydrogenase was also present but its concentration remained low at under  $0.5 \text{ kUL}^{-1}$ . This was promising, as it showed cells were indeed present, metabolically active and generally viable within the system. A cell count of the perfusate sample using a ViCell was also performed daily, but no cells, dead or alive, were detected (data not shown).

As with lactate, the concentration of IgG will vary depending upon actual production and dilution rate. If the production of IgG is greater than the rate at which medium is exchanged, then the concentration will increase within the vessel over time. This happened here, between days 1 and 5, where IgG approached  $100 \text{ mgL}^{-1}$ , with a steady increase observed each day. For the titres after day 5, a separate ValitaTITER plate was used and the data obtained was not completely trusted, appearing to jump and drop at random points, which did not correlate with any of the process changes implemented.

Between days 8 and 9, the cell retention device was paused for 16 days (using similar principles as first presented in Chapter 4) by sealing the spinner flask and storing it at  $8^\circ\text{C}$ . The first 8 days were, surprisingly, fairly successful with regards to the physical system, with no leakages, no contamination and no observable cell detachment or microsphere loss. Figure 6.14B shows micrographs of microspheres at day 0 (immediately after the 2 hr loading protocol) and again at day 8. On the final day before pausing, cells appeared visually healthy upon the microspheres. Due to planned operator absence for 2 weeks, it was decided to pause the cells. Upon return, the operator would reattach the flask to the system and the culture would commence. This experiment was the first attempt using the spinner flask-based perfusion operation. It was carried out with the intention to perform later experiments, which explains the rationale behind the pausing here. The spinner flask was detached from the system, the tubing carefully removed and modified caps replaced with

closed ones. After 16 days, the tubings and tanks were autoclaved once more, the spinner flask reattached and the operation continued at 30 °C. Upon restarting the impeller there was evidence of microsphere aggregation, although after several hours the majority

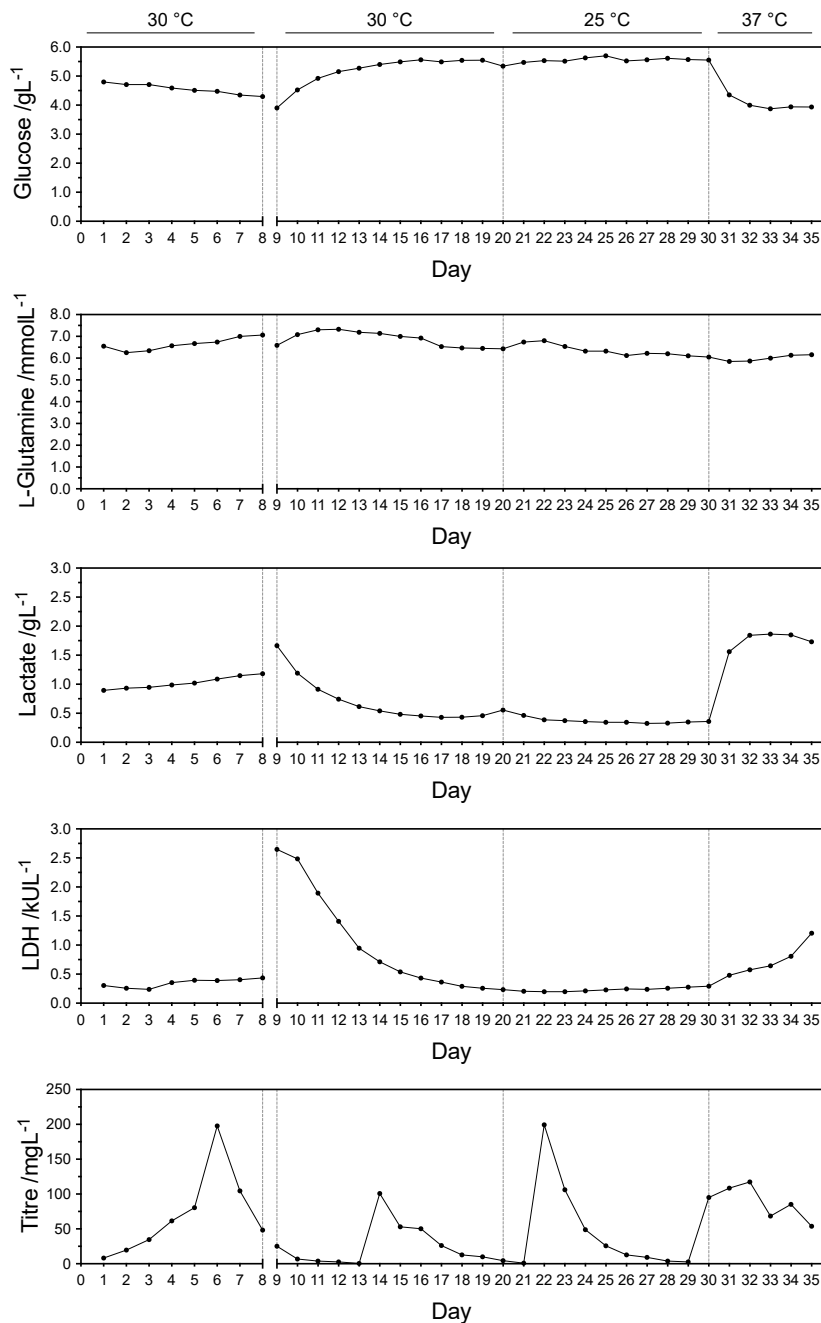


FIGURE 6.15 An attempt at the operation of the spinner flask-based perfusion system using a spinner flask and PEI-adsorbed polyHIPE microspheres for 35 days. A perfusate sample was taken daily, with glucose, l-glutamine, lactate, lactate dehydrogenase and IgG titre determined. Temperature of the culture was varied. Between day 8 and 9, the spinner flask was detached from the system and placed in a refrigerator at 8 °C for 16 days to pause the cells. This was performed due to absence of the operator for that time period. Data represent n=1.

of microspheres had resuspended.

Analytes were determined daily, once again, starting from this point. On day 9, the concentration of lactate dehydrogenase had increased to over  $2.5 \text{ kUL}^{-1}$ , indicating cell death from the pausing. Lactate had seemingly also increased in concentration, likely as a result of the medium not being perfused whilst the cells still remained metabolically active before the effects of pausing had occurred. Pausing for 16 days would likely never be tried in a real bioprocessing scenario, but it was decided to keep the system going to demonstrate the potential of this perfusion system. It was also thought it may give further insight into how the design could be improved.

The concentration of lactate dehydrogenase steadily decreased each day, from day 9 to day 20, showing how perfusion eventually dilutes an analyte if it is not being simultaneously produced. The same effect was seen with lactate, which after commencing medium exchange, likewise decreased. On the other hand, the glucose concentration increased slightly, suggesting reduced consumption and thus reduced metabolic activity, whilst L-glutamine remained at a steady concentration. Interestingly, by day 20 the height of the medium within the spinner flask had begun to rise. Just as with the primed medium reserve tank in the previous packed-bed system, a consistent medium height was dependent upon correct medium flow around the system. It was likely the frit itself had become increasingly clogged with cell debris as medium was exchanged. There was some accumulation of debris, in the effluent tank, directly under the point where the perfusate exited the outlet tubing. This debris, of course, being a result of cell death from the pausing between days 8 and 9. The system, unlike the packed-bed design, could be stopped easily and items changed. In this instance, an outlet tubing with a new frit and frit holder was inserted and the culture resumed. This solved the issue and the medium height stayed consistent for the remainder of the process.

The switch to  $25 \text{ }^\circ\text{C}$  on day 20 was simply to see if there would be any immediate cell detachment. There was, however, little apparent effect on any measured parameter and the system continued to operate largely as before. Finally, in a bid to demonstrate this system before ending the process, on day 30 the temperature was turned up to  $37 \text{ }^\circ\text{C}$ . A day after there was a drop in glucose and an increase in lactate concentrations, with both eventually plateauing. Lactate dehydrogenase also began to increase, but L-glutamine remained the same. These data suggest cells were likely starting to grow once again. Figure 6.16 shows the microspheres within the spinner flask on the final day of the culture. Discolouration had taken place. A photograph taken of several microspheres under an optical microscope revealed there were indeed cells still attached.



**FIGURE 6.16** Visual evidence of cell retention on microspheres at the end of the operation of the spinner flask-based perfusion system. A photograph of the spinner flask, with retained microspheres, on day 35, with evidence of some remaining adhered cells when viewed using an optical microscope.

The data presented here were obtained from the first attempt, with the system generally working in terms of operation and no immediate issues arising from normal use. The hypothermic storing of cells for 16 days would never usually be performed, but was attempted purely to see what would happen. It clearly had an effect on the system once perfusion operation was resumed, but the culture was kept running to check for any further issues in the design. Apart from the need to replace the frit (as a result of cell debris from the pausing) there was no other observable problems, demonstrating the potential for this particular design.

### 6.2.3 CONCLUSIONS

The work in the second part of the chapter attempted to carry out a perfusion culture using the cell retention device developed in the previous chapters. Perfusion is a true continuous process, enabling cells to be exposed to continual medium exchange without the need for operator interaction. This is in contrast to pseudo-continuous, where medium is exchanged periodically by an operator, as was demonstrated in the first part of this chapter. Whilst a perfusion system is considerably more challenging to get working, it can be argued that the benefits of continuous culture may only be fully realised with continual medium exchange.

Any system here had to be assembled in-house, technically simple to operate and have the potential to be scaled up or out in the future. Two designs were proposed. The first took inspiration from chromatography and considered whether a set volume of loaded microspheres could be employed within a column as a packed-bed and perfused through with medium. An incubator, a pump and a refrigerator would be used to first deliver chilled medium into a priming tank, before directing it through the columns for exchange. The advantage of this system was its potential to scale-out, with the idea of a plate-based platform containing an array of perfused columns being particularly appealing. No system in this format has been demonstrated in the literature. Whilst the components of the system were supplied and indeed connected together, numerous issues were quickly encountered when the process was actually attempted. Whilst a lot of these issues were overcome, it was likely the temperature within the packed-bed was greater than the mild hypothermic temperature set by the incubator. Ways to overcome this, such as increasing the flow rate, were not currently feasible with this work and so the design was abandoned.

The second design was inherently more simple, both in terms of practicality and of operation. Taking inspiration from a chemostat vessel (where medium is added and removed simultaneously at the same rate), a spinner flask was first obtained and modified to allow aseptic entry of two tubings. One tubing would act as the medium inlet, with the other the medium outlet. The issue of microsphere loss over time, via the outlet tubing, was overcome by the use of an attached frit. Using an intermittent agitation technique (typical for microcarrier seeding) to first load the microspheres with cells, an initial attempt was performed. No issues relating to the physical system arose. Due to interruption from a planned absence of the operator, the process was stopped and the spinner flask placed within a refrigerator for cell pausing for 16 days. Continuing the process clearly had an effect, yet the process was continued to demonstrate the feasibility of the actual design. Only one attempt could be carried out, yet the data observed was far more promising than any obtained for the first packed-bed design. The spinner flask-based design was simple to assemble and in terms of actual operation, appeared far more robust than the first packed-bed system. This spinner flask-based perfusion system should be pursued in any future work.

This page intentionally left blank

---

# Chapter 7

---

## CONCLUSIONS AND FUTURE WORK

---

### OVERVIEW

This chapter presents the main conclusions from the data obtained for this thesis, as well as a personal evaluation of the project. It ends by listing suggested future work for each of the results chapters, which some readers may find interesting if they wish to continue the aims of the work.

### 7.1 CONCLUSIONS AND EVALUATION

The project aimed to develop a cell retention device that would be compatible with both currently used suspension-adapted CHO cell lines and chemically defined medium. After this was achieved, the focus was upon demonstrating this bespoke cell retention technology within an associated pseudo-continuous and perfusion culture system. The lack of small-scale, inexpensive commercial perfusion equipment was the general rationale behind the work. The project largely achieved its aims, albeit with several compromises and many changes in research direction along the way.

Chapter 3 focused upon the search for an inexpensive, animal origin-free adhesion substrate. This substrate was destined for use as the chemical component of the in-house cell retention device. Three animal origin-free (and thus chemically defined) cationic polymers, namely poly-D-lysine, poly-L-ornithine and polyethylenimine, were selected and tested with suspension-adapted CHO cells. These were compared against four animal proteins, namely fibronectin, laminin, collagen and vitronectin, which were used as benchmark substrates. Polystyrene multiwell plates (of both tissue culture-treated and untreated types), glass plates and polystyrene T-flasks were all used as vessels for these experiments. The ability of polyethylenimine to rapidly and effectively adhere CHO cells was quickly realised early in the project. This finding was exciting; only two reports of polyethylenimine being used as an adhesion substrate could be found in the literature. It also satisfied the requirements for the desired adhesion substrate. For the work carried out in this chapter, and indeed for all the work in this project, serum products were never supplemented into the culture medium. It was thus shown that polyethylenimine, when adsorbed onto vessel surfaces, could be used to rapidly adhere suspension-adapted CHO cells without the need for animal origin products.

Chapter 4 focused upon the use of severe hypothermia for the storage of cells for prolonged periods, otherwise known as cell ‘pausing’, with an aim to complement work previously done by Hunt et al. (2005). It was proposed that the pausing of cells may be beneficial for any future cell retention device, or any associated technology, that may be developed in the project. Work was carried out to first determine the optimum pausing temperature by investigating the effect of pausing on viability when cells were stored at increasing time periods at a range of temperatures. It was found both 4 and 8 °C were sufficient for storing cells, i.e. with no observed growth and without any considerable drop in viability, even when stored for 8 days.

Regrowth of cells in suspension culture post-pausing was also attempted, with a decrease in cell growth observed when this pausing period was increased. However, a single sub-culture appeared to return cells back to normal growth patterns. Finally, cells adhered to fibronectin and polyethylenimine substrates were paused, with morphological changes imaged and observed. The storage of cells at hypothermic, rather than cryogenic, temperatures is widely reported in the literature — however it overwhelmingly is performed using cell therapy products, tissues or even whole transplants for the purpose of transportation. As far as could be found, only Hunt et al. (2005) has demonstrated the use of hypothermic storage for an immortalised cell line. The work here thus adds to this and further shows this technique may have some use in future bioprocesses.

Chapter 5 returned to the main objective of the project and focused upon the fabrication of polyHIPE microspheres. These would become the physical component of the cell retention device. The work in this chapter was heavily materials-based, and sought to adapt a current in-house microsphere fabrication system to the specific needs of the project. An acrylic monomer, MAES, was successfully incorporated into HIPEs and consequently cured polyHIPEs, with a TBO assay confirming the presence of its carboxyl groups within these materials. No literature on its use within polyHIPEs could be found. Particular carrier phases within the fabrication system were explored, including water, glycerol and PVA. The HIPE was also generated using water heated to 80 °C and the surfactant reduced from 10 to 1.25 %. All these modifications were attempted to ensure polyHIPE microspheres, containing MAES, would indeed be macroporous. This part of the project was considerably challenging, with any macroporous materials fabricated eventually collapsing. A compromise was eventually found, with 80 % glycerol carrier phase being employed to generate polyHIPE microspheres containing MAES with average diameters under 300 µm, however these materials had a microporous surface and were considered ‘deformed’.

Cell loading onto MAES polyHIPEs was attempted, using both 1.0 and 2.5 mL columns, to

rapidly adhered cells onto a packed-bed of microspheres. Loading was achieved by using a syringe or peristaltic pump to deliver a high cell density suspension through the columns. This forced cells and microspheres to interact and thus encouraged adherence. 1 mL of microspheres was found to retain 100 mill cells, although this was not independently confirmed and should be read with caution. In addition, microspheres were seeded within these columns before being retrieved and placed into T-25 flasks. Adherent growth upon the microspheres in a typical batch culture was then demonstrated.

Chapter 6 focused upon the design, construction and operation of several continuous upstream systems with the use of the microsphere-based cell retention technology developed. Attempts at pseudo-continuous were made by placing loaded microspheres within shaking Erlenmeyer flasks and manually exchanging medium periodically. A culture process in this style was performed for over 30 days; crucially, cells remained viable and productive throughout. Two main design were proposed for the perfusion system. The first, a packed-bed system, retained microspheres within columns and perfused medium through, with cells upon the microspheres consequently exposed to continual medium exchange. Whilst possible in theory, this system was fraught with practicality issues. Columns often leaked, tubings were not always secured and contaminations were frequent. When these issues were overcome and the process allowed to run, cells were observed to eventually peel off the microspheres, likely as a result of high temperatures within the columns. An increase in the dilution rate could overcome this, but the increased medium usage was not feasible.

The second design, a spinner flask-based perfusion system, was considerably more robust and involved placing microspheres into a spinner flask, itself with attached inlet and outlet tubings. The operation of this system was only attempted once, but it did not experience any leakage, tubing problems or contamination issues. The initial data from this one attempt were promising. Any future work should focus upon repeating the operation of this system.

#### *Personal Evaluation*

The project described in this thesis was extremely challenging; the practical skills that were required, the techniques and protocols that had to be developed and the amount of time spent in two laboratories was immense. The original aim of the work was the demonstration of an in-house perfusion system for 'continual cell line and process development', i.e. to employ the system to repeatedly perform transient transfections for cells continually maintained at a high density, and thus eliminate the need to subculture with the consequent downtime. However, by the middle of the project it was apparent this was far too ambitious and efforts changed to at least demonstrate that cells could be sustained within

a continuous process using a novel cell retention device.

The project by its very nature was multidisciplinary, with cell culture, materials science and process engineering having to be learnt, adapted and joined together for useful, trusted data to be obtained. The collaboration between the two departments demonstrated what can be achieved when expertise from different backgrounds come together to overcome or investigate a particular research problem. The work here was highly unique and, when taken together, was the 'first of its kind' within both laboratories. Indeed, continuous culture had certainly never been attempted within the cell culture team and many experiments began with no prior knowledge or experience. Despite this, the project was rewarding and encouraged a wide degree of flexibility and creativity. Contrary to most other doctoral projects, it did not explicitly aim to discover something or find an answer to a problem, but rather to create a technology and a process and demonstrate their uses.

## 7.2 FUTURE WORK

Whilst it is hoped the work presented in this thesis is of an expected quantity and quality, the project itself is by no means complete. Overcoming or demonstrating a particular piece of research work will always lead to further investigation. This project is no exception with the potential for much more data to be acquired. The final section of this thesis describes numerous areas of suggested research for future work, with ideas which may help readers who wish to continue the aims of the project. It is laid out using the title of each results chapter for easy reference, with questions asked to stimulate thought and discussion.

### **Adhesion Substrates**

Chapter 3 was successful for the early progression of the project, with a range of animal origin and chemically defined adhesion substrates employed to adhere suspension-adapted CHO cells. The realisation that polyethylenimine, presented as an inexpensive animal origin-free substrate, could adhere the same number of cells as costly animal origin proteins, was a key finding. Specific research questions which could be asked include;

*(i) What effect does the coating buffer have on the adsorption of particular substrates?*

This relates to the fact that substrates are dispensed upon surfaces using certain buffers so as to keep the pH at a defined value during adsorption. This helps to ensure correct and sufficient adsorption of substrate onto the base material. HBSS or water were used to adsorb all animal origin substrates in this work, whilst BBS or water were used for the three cationic polymers. Other buffers, or buffers kept at different pH values, could be tested to see if this does indeed affect adsorption rate. This relates more to surface chemistry research

and may not be totally relevant to the work presented here.

*(ii) Does trypsinisation affect the adhesion capability of adsorbed substrates?*

Exposing coated vessel surfaces to trypsin, or any other dissociation reagent, may begin to chemically strip these surfaces of their adsorbed substrates. If a vessel, such as a multiwell plate or T-flask, wanted to be re-used after the complete dissociation of cells, would the coating still be as effective in encouraging attachment and adherent growth of a fresh cell seed? Whilst the re-use of plates and flasks may seem unnecessary, given their low individual cost, this idea of ‘recycling’ coated materials came about when originally discussing the use of microspheres within a cell retention device. Put simply, microspheres could be packed within a column, seeded with cells and perfused for a period of time (as was attempted in Chapter 6). After this culture, cells could be dissociated via trypsin, retrieved and the column washed through with medium to retrieve the released cells. The microspheres left could then be re-seeded with a fresh batch of cells and the process repeated. If trypsin does indeed have an effect on the adsorbed coating, then there would be a limit to the number of cycles possible.

As was discussed previously, cells attached to polyethylenimine substrates upon microspheres could not be removed easily using trypsin due to severe aggregation of the microspheres. This was likely due to the action of trypsin upon polyethylenimine. Covalently linking polyethylenimine to microspheres may help rectify this issue and indeed enable microspheres to be re-used post-dissociation. However, a simple experiment to perform initially would be to adsorb substrates onto multiwell plate surfaces, adhere cells with eventual trypsinisation and then repeat to see if new cells will adhere.

*(iii) What other variants of polyethylenimine, or indeed other negatively-charged polymers, are available?*

The success of polyethylenimine was a surprise. As noted in Chapter 3, there exists other variants of polyethylenimine available to purchase. These variances differ in chemical structure, including in the ratios of primary and secondary amines and in the exact number present of each of these groups. Different molecular weights can also be purchased. What effect each of these has on encouraging the attachment of CHO cells remains to be seen.

### **Cell Pausing**

The data in Chapter 4 were obtained during a brief side project and as such there is plenty of potential for future work. This is especially true now that microspheres can indeed be

routinely used to adhere and retain CHO cells. Specific research questions which could be asked include;

*(i) Can rewarming previously paused detached cells cause them to reattach?*

Hunt et al. (2005) reported that warming culture flasks that had previously been used to pause cells resulted in cells, that had detached, to re-adhere. No other information was given, but this effect may be beneficial for long term pausing if the rewarming of vessels — without any immediate agitation or vigorous handling — ensures any detached cells are not lost in any subsequent process.

*(ii) What effect does pausing have on the potential regrowth of cells adhered to polyethylenimine substrates?*

This would follow the work done on the pausing of suspended cells and subsequent re-growth back in physiological temperatures. As with this work, attempts at awakening and regrowing paused adherent cells may not be immediately relevant to the project, but it may give interesting data and further develop the idea of cell pausing. It can be also be argued the pausing of adherent cells is far more beneficial for the purposes of this project, due to the potential pausing of the cell retention device.

*(iii) Can cells be loaded onto microspheres and immediately paused for defined periods without excessive cell loss?*

This question relates to the main potential use of cell pausing for this project, i.e. could operators use cell pausing as a means to store recently loaded cell retention devices? Whilst this would be more appropriate for the original method of cell loading (via use of a pump and columns with microspheres retained within), it could also be employed when using the more typical intermittent agitation technique. Spinner flasks containing microspheres that have recently been loaded could be placed into a refrigerator for hypothermic storage. The issue of cell detachment needs to be investigated, although rewarming before any agitation is initiated, as described above, may help cells re-attach.

### **PolyHIPE Microsphere Technology**

With regards to the microspheres ultimately used, the results obtained in Chapter 5 resulted in a compromise, although the data obtained when viewed together were very interesting. The effect of carrier phase, the orientation of the fabrication system and the conditions used during the generation of the HIPEs clearly had an effect on the polyHIPE microspheres fabricated. As such, the data obtained can be easily followed up, particularly by those with

an interest in materials science. The areas listed here look at both materials science-related questions and questions related to the loading of CHO cells. Specific research questions which can be asked include;

*(i) Is it possible to fabricate 'true' polyHIPE microspheres whilst still including MAES as a co-monomer?*

The rationale behind choosing polyHIPEs as a state of material to investigate was their macroporous structures. As was described in Chapter 5, the inclusion of MAES and the use of glycerol as a carrier phase prevented the fabrication of microspheres with these typical polyHIPE characteristics. This research question could investigate potential methods to keep MAES as a co-monomer but still achieve sufficient macroporosity within the fabricated structures. The use of polyethylenimine in combination with truly macroporous microspheres may enhance the capability of the cell retention technology considerably.

*(ii) Can the microsphere fabrication set up be altered to better control certain parameters?*

The use of the bespoke system for the fabrication of microspheres has been demonstrated in this work. This lab-scale fluidic system can be used to continuously manufacture microspheres with little to no input from the operator once the process has started. However, as reported in Chapter 5, the parameters involved in the fabrication process are not entirely understood. The viscosity of the HIPE, the flow rates of the HIPE and carrier phase, the position of the needle, as well as how they all interact with one another resulted in a process that was inherently complex, even when set parameters were kept constant.

The set up at present is *ad hoc*, and whilst it does indeed make microspheres, the construction of a microfluidic system would be highly beneficial. Such a system may have a dedicated injection point where the position of the needle is fixed each time. It may also have tubing with a much narrower internal diameter to ensure better manipulation of the HIPE and carrier phase. The viscosity of the HIPE could also be measured to see if there is an optimum window where microspheres with desired properties are easily fabricated.

*(iii) Can cells be dissociated successfully without severe aggregation of the microspheres?*

The aggregation of microspheres when exposed to trypsin was a major drawback for the project and one that was ignored while continuous culture work was attempted. An initial experiment should look at simply incubating the microspheres with trypsin, to see if microspheres aggregate even without cells adhered. With all that is currently known, it is expected using the carboxyl groups on the polyHIPE microspheres to indeed covalently

---

link polyethylenimine to the materials would likely rectify the issue of aggregation. It may also enable microspheres to be used again, as described previously.

*(iv) Do there exist methods, except dissociation, that can count the number of cells retained upon microspheres?*

The ability to directly count cells upon the microspheres remains the only way to truly know the concentration of cells within a process using microspheres. The inability to detach cells from microspheres resulted in particular parameters, such as cell-specific productivity, not being able to be determined for several experiments within this project. Possible ideas to count adhered cells include overcoming the aggregation of microspheres during trypsinisation and so enabling dissociation to be used for cell detachment and direct cell counting.

Alternatively, reagents such as PrestoBlue may be employed, although the extent to which mild hypothermia (which was used for all continuous processes in this work) affects cell metabolism (and hence the indirect measurement of viability) has to also be determined. The crystal violet staining method, where nuclei are first stained, extracted and then counted could likewise be attempted. This would first need to be validated when using polyHIPEs which, due to their porous nature, easily stain non-specifically.

### **Continuous Bioprocessing Systems**

Chapter 6 was the highlight of the project, with the data obtained the result of many streams of work finally coming together. It can be argued any future work would likely focus upon repeating, adapting or optimising the experiments that were carried out here. Specific research questions which could be asked include;

*(i) Can packed-bed perfusion system ever be made to work successfully?*

The use of a working packed-bed perfusion system would be beneficial for research and development purposes as it could allow multiple columns to be perfused simultaneously. Initial solutions should look at the temperature of the medium within the actual column as it perfuses through the cells, to ensure peeling does not occur. If a packed-bed perfusion system was achieved, the creation of a small-scale, high throughput perfusion system would finally be realised.

*(ii) Can the spinner flask-based perfusion system be optimised and adapted into a routine continuous process?*

This is the most relevant and pressing question asked here. Only one attempt was made

---

using the spinner flask-based perfusion system and, due to operation constraints at the time, the use of cell pausing far beyond what would normally be attempted was carried out. As such, any future work should try first to replicate what was attempted here without any hypothermic storage of cells. The advantage of the proposed spinner flask-based system is its scalability, with larger vessels also having ports where inlet and outlet tubings for medium renewal can be attached. These large-scale reactors would also enable dedicated aeration, more sophisticated agitation as well as the possibility for control of other critical parameters such as pH.

*(iii) Is a small-scale multi spinner flask-based perfusion system realistic and achievable?*

This is far beyond the scope of the project and would likely require a small team of researchers to achieve. Operating three or more spinner flasks using the spinner flask-based perfusion design would require a larger refrigerator, multiple or larger medium bottles and potentially more pumps. Although the multidrive pump, as was used in this work, may be suitable as it allows up to 12 lines. However, investigating and comparing the effect of different dilution rates would certainly require a dedicated pump for each flask.

*(iv) Will CHO cells be transfectable whilst retained on cells at mild hypothermic temperatures?*

Once routine perfusion culture is achieved, the discussion turns to potential applications. The perfusion system was always intended to be used as a means of rapidly and serially testing different genetic elements within vectors, without the downtime associated with batch-wise cell line development. If this testing was performed using a system capable of operating multiple, independent vessels in continuous culture, the data acquired, as well as the associated time and cost savings, could be immense. Investigations into the transfection of CHO cells within in-house developed continuous processes could very easily be an entire doctoral project.

This page intentionally left blank

---

## REFERENCES

---

*Listed in alphabetical order by surname of the first author*

Abd El-Mageed, A.I.A., Dyab, A.K.F., Mohamed, L.A., Taha, F. & Essawy, H.A. (2021) 'Suspension polymerization for fabrication of magnetic polystyrene microspheres stabilized with Hitenol BC-20', *Polymer Bulletin*, pp. 1–15.

Akay, G., Birch, M.A. & Bokhari, M.A. (2004) 'Microcellular polyHIPE polymer supports osteoblast growth and bone formation in vitro', *Biomaterials*, 25(18), pp. 3991–4000.

Ando, T. & Yonamoto, Y. (2015) 'In Situ EPR Detection of Reactive Oxygen Species in Adherent Cells Using Polylysine-Coated Glass Plate', *Applied Magnetic Resonance*, 46, pp. 977–986.

Anwar, A.R., Moqbel, R., Walsh, G.M., Kay, A.B. & Wardlaw, A.J. (1993) 'Adhesion to fibronectin prolongs eosinophil survival', *Journal of Experimental Medicine*, 177(3), pp. 839–843.

Arifin, M.A., Mel, M., Samsudin, N., Hashim, Y.Z.H., Salleh, H.M., Sopyan, I. & Nordin, N. (2016) 'Ultraviolet/ ozone treated polystyrene microcarriers for animal cell culture', *Journal of Chemical Technology & Biotechnology*, 91(10), pp. 2607–2619.

Audouin, F., Fox, M., Larragy, R., Clarke, P., Huang, J., O'Connor, B. & Heise, A. (2012) 'Polypeptide-Grafted Macroporous PolyHIPE by Surface-Initiated N-Carboxyanhydride (NCA) Polymerization as a Platform for Bioconjugation', *Macromolecules*, 45(15), pp. 6127–6135.

Awwad, S. & Angkawinitwong, U. (2018) 'Overview of Antibody Drug Delivery', *Pharmaceutics*, 10(3), pp. 83.

Baneyx, F. & Mujacic, M. (2004) 'Recombinant protein folding and misfolding in *Escherichia coli*', *Nature Biotechnology*, 22(11), pp. 1399–1408.

Bang, L.M. & Keating, G.M. (2004) 'Adalimumab: a review of its use in rheumatoid arthritis', *BioDrugs*, 18(2), pp. 121–139.

Barbetta, A., Cameron, N.R. & Cooper, S.J. (2000) 'High internal phase emulsions (HIPEs) containing divinylbenzene and 4-vinylbenzyl chloride and the morphology of the resulting PolyHIPE material', *Chemical Communications*, 3, pp. 221–222.

Barbetta, A., Dentini, M., Leandri, L., Ferraris G., Coletta, A. & Bernabei, M. (2009) 'Synthesis and characterization of porous glycidylmethacrylate–divinylbenzene monoliths using the high internal phase emulsion approach', *Reactive and Functional Polymers*, 69(9), pp. 724–736.

Barby, D. & Haq, Z. (1982) 'Low density porous cross-linked polymeric materials and their preparation', EP0060138A1.

Barnes, L.M., Bentley, C.M. & Dickson, A.J. (2000) 'Advances in animal cell recombinant protein production: GS-NS0 expression system', *Cytotechnology*, 32(2), pp. 109–123.

Barok, M., Joensuu, H. & Isola, J. (2014) 'Trastuzumab emtansine: mechanisms of action and drug resistance', *Breast Cancer Research*, 16(2), pp. 1–12.

---

Basson, N.J. (2000) 'Competition for glucose between *Candida albicans* and oral bacteria grown in mixed culture in a chemostat', *Journal of Medical Microbiology*, 49(11), pp. 969–975.

Bates, M.K., Phillips, D.S. & O'Bryan, J. (2011) 'Shaker Agitation Rate and Orbit Affect Growth of Cultured Bacteria', [online] Available at: <physiology.case.edu/media/eq\_manuals/eq\_manual\_Shaker\_Agitation\_Rate\_and\_Orbit\_Affect\_of\_Bacterial\_Growth.pdf> [Accessed 9 May 2020].

Becerra, S., Berrios, J., Osses, N. & Altamirano, C. (2012) 'Exploring the effect of mild hypothermia on CHO cell productivity', *Biochemical Engineering Journal*, 60, pp. 1–8.

Benson, J.M., Peritt, D., Scallon, B.J., Heavner, G.A., Shealy, D.J., Giles-Komar, J.M. & Mascelli, M.A. (2011) 'Discovery and mechanism of ustekinumab: a human monoclonal antibody targeting interleukin-12 and interleukin-23 for treatment of immune-mediated disorders', *mAbs*, 3(6), pp. 535–545.

Beveridge, T.J. (2001) 'Use of the Gram stain in microbiology', *Biotechnic & Histochemistry*, 76(3), pp. 111–118.

Bhumgara, Z. (1995) 'Polyhipe foam materials as filtration media', *Filtration & Separation*, 32(3), pp. 245–251.

Bleckwenn, N.A., Golding, H., Bentley, W.E. & Shiloach, J. (2005) 'Production of recombinant proteins by vaccinia virus in a microcarrier based mammalian cell perfusion bioreactor', *Biotechnology and Bioengineering*, 90(6), pp. 663–674.

Bokhari, M.A., Akay, G., Zhang, S. & Birch, M.A. (2005) 'The enhancement of osteoblast growth and differentiation in vitro on a peptide hydrogel-polyHIPE polymer hybrid material', *Biomaterials*, 26(25) pp. 5198–5208.

Bokhari, M., Carnachan, R.J., Cameron, N.R. & Przyborski, S.A. (2007b) 'Novel cell culture device enabling three-dimensional cell growth and improved cell function', *Biochemical and Biophysical Research Communications*, 354(4), pp. 1095–1100.

Bokhari, M., Carnachan, R.J., Przyborski, S.A. & Cameron, N.R. (2007a) 'Emulsion-templated porous polymers as scaffolds for three dimensional cell culture: effect of synthesis parameters on scaffold formation and homogeneity', *Journal of Materials Chemistry*, 17(38), pp. 4088–4094.

Bonham-Carter, J. & Shevitz, J. (2011) 'A Brief History of Perfusion Biomanufacturing', *Bio-Process International*, 9(9), pp. 24–30.

Bosco, B., Paillet, C., Amadeo, I., Mauro, L., Orti, E. & Forno, G. (2017) 'Alternating flow filtration as an alternative to internal spin filter based perfusion process: Impact on productivity and product quality', *Biotechnology Progress*, 33(4), pp. 1010–1014.

Boussif, O., Lezoualc'h, F., Zanta, M.A., Mergny, M.D., Scherman, D., Demeneix, B. & Behr, J.P. (1995) 'A versatile vector for gene and oligonucleotide transfer into cells in culture and in vivo: polyethylenimine', *Proceedings of the National Academy of Sciences of the United States of America*, 92(16), pp. 7297–7301.

Brunner, D., Frank, J., Appl, H., Schöffl, H., Pfaller, W. & Gstraunthaler, G. (2010) 'Serum-free cell culture: the serum-free media interactive online database', *ALTEX*, 27(1), pp. 53–62.

- 
- Buchsteiner, M., Quek, L., Gray, P. & Nielsen, L.K. (2018) 'Improving culture performance and antibody production in CHO cell culture processes by reducing the Warburg effect', *Biotechnology and Bioengineering*, 115(9), pp. 2315–2327.
- Bupathi, M., Ahn, D.H. & Bekaii-Saab, T. (2016) 'Spotlight on bevacizumab in metastatic colorectal cancer: patient selection and perspectives', *Gastrointestinal Cancer: Targets and Therapy*, 6, pp. 21–30.
- Busse, A. & Lüftner, D. (2019) 'What Does the Pipeline Promise about Upcoming Biosimilar Antibodies in Oncology?', *Breast Care (Basel)*, 14(1), pp. 10–16.
- Cai, Y., Xu, M., Yuan, M., Liu, Z. & Yuan, W. (2014) 'Developments in human growth hormone preparations: sustained-release, prolonged half-life, novel injection devices, and alternative delivery routes', *International Journal of Nanomedicine*, 9, pp. 3527–3538.
- Cameron, N.R. (2005) 'High internal phase emulsion templating as a route to well-defined porous polymers', *Polymer*, 46(5), pp. 1439–1449.
- Canavan, H.E., Cheng, X., Graham, D.J., Ratner, B.D. & Castner, D.G. (2005) 'Cell sheet detachment affects the extracellular matrix: a surface science study comparing thermal liftoff, enzymatic, and mechanical methods', *Journal of Biomedical Materials Research Part A*, 75(1), pp. 1–13.
- Casadevall, N. & Rossert, J. (2005). 'Importance of biologic follow-ons: experience with EPO', *Best Practice & Research Clinical Haematology*, 18(3), pp. 381–387.
- Chan, F.K., Moriwaki, K. & De Rosa, M.J. (2013) 'Detection of necrosis by release of lactate dehydrogenase activity', *Methods in Molecular Biology*, 979, pp. 65–70.
- Chang, C.N., Rey, M., Bochner, B., Heyneker, H. & Gray, G. (1987) 'High-level secretion of human growth hormone by *Escherichia coli*', *Gene*, 55(2–3), pp. 189–196.
- Chen, C., Wong, H.E. & Goudar, C.T. (2018) 'Upstream process intensification and continuous manufacturing', *Current Opinion in Chemical Engineering*, 22, pp. 191–198.
- Chen, G., Kawazoe, N. & Tateishi, T. (2008) 'Effects of ECM Proteins and Cationic Polymers on the Adhesion and Proliferation of Rat Islet Cells', *The Open Biotechnology Journal*, 2, pp. 133–137.
- Chen, J., Le, T.T.M. & Hsu, K. (2018) 'Application of PolyHIPE Membrane with Tricaprylmethylammonium Chloride for Cr(VI) Ion Separation: Parameters and Mechanism of Transport Relating to the Pore Structure', *Membranes*, 8(1), 11, pp. 1–17.
- Chheda, A.H. & Vernekar, M.R. (2015) 'A natural preservative -poly-L-lysine: Fermentative production and applications in food industry', *International Food Research Journal*, 22(1), pp. 23–30.
- Chiba, K., Kawakami, K. & Tohyama, K. (1998) 'Simultaneous evaluation of cell viability by neutral red, MTT and crystal violet staining assays of the same cells', *Toxicology in Vitro*, 12(3), pp. 251–258.
- Chong, V. (2016) 'Ranibizumab for the treatment of wet AMD: a summary of real-world studies', *Eye (London, England)*, 30(2), pp. 270–286.
- Choudhury, S., Fitzhenry, L., White, B. & Connolly, D. (2016) 'Polystyrene-co-Divinylbenzene PolyHIPE Monoliths in 1.0 mm Column Formats for Liquid Chromatography', *Materials*, 9(3), 212, pp. 1–14.

---

Clincke, M.F., Mölleryd, C., Zhang, Y., Lindskog, E., Walsh, K. & Chotteau, V. (2013) 'Very high density of CHO cells in perfusion by ATF or TFF in WAVE bioreactor™. Part I. Effect of the cell density on the process', *Biotechnology Progress*, 29(3), pp. 754–767.

Cohen, S., Chang, A., Boyer, H. & Helling, R. (1973) 'Construction of Biologically Functional Bacterial Plasmids In Vitro', *Proceedings of the National Academy of Sciences*, 70(11), pp. 3240–3244.

Collen, D. & Lijnen, H.R. (2004) 'Tissue-type plasminogen activator: a historical perspective and personal account', *Journal of Thrombosis and Haemostasis*, 2(4), pp. 541–546.

Correia, C., Koshkin, A., Carido, M., Espinha, N., Saric, T., Lima, P.A., Serra, M. & Alves, P.M. (2016) 'Effective Hypothermic Storage of Human Pluripotent Stem Cell-Derived Cardiomyocytes Compatible With Global Distribution of Cells for Clinical Applications and Toxicology Testing', *Stem Cells Translational Medicine*, 5(5), pp. 658–669.

Croughan, M.S., Konstantinov, K.B. & Cooney, C. (2015) 'The future of industrial bioprocessing: batch or continuous?', *Biotechnology and Bioengineering*, 112(4), pp. 648–651.

Cytiva (2020a) 'Cytopore - macroporous microcarriers', [online] Available at: <<https://cdn.cytivalifesciences.com/dmm3bwsv3/AssetStream.aspx?mediaformatid=10061&destinationid=10016&assetid=11791>> [Accessed 30 May 2021]

Cytiva (2020b) 'Cytopore - Instructions for Use', [online] Available at: <<https://cdn.cytivalifesciences.com/dmm3bwsv3/AssetStream.aspx?mediaformatid=10061&destinationid=10016&assetid=12636>> [Accessed 30 May 2021]

Czitrom, V. (1999) 'One-Factor-at-a-Time Versus Designed Experiments', *The American Statistician*, 53(2), pp. 126–131.

Deo, Y.M., Mahadevan, M.D. & Fuchs, R. (1996) 'Practical considerations in operation and scale-up of spin-filter based bioreactors for monoclonal antibody production', *Biotechnology Progress*, 12(1), pp. 57–64.

Desforges, A., Arpontet, M., Deleuze, H. & Mondain-Monval, O. (2002) 'Synthesis and functionalisation of polyHIPE® beads', *Reactive and Functional Polymers*, 53(2–3), pp. 183–192.

Dhara, V.G., Naik, H.M., Majewska, N.I. & Betenbaugh, M.J. (2018) 'Recombinant Antibody Production in CHO and NS0 Cells: Differences and Similarities', *BioDrugs*, 32(6), pp. 571–584.

Dikici, B.A., Sherborne, C., Reilly, G.C. & Claeysens, F. (2019) 'Emulsion templated scaffolds manufactured from photocurable polycaprolactone', *Polymer*, 175, pp. 243–254.

Dumont, J., Euwart, D., Mei, B., Estes, S. & Kshirsagar, R. (2016) 'Human cell lines for biopharmaceutical manufacturing: history, status, and future perspectives', *Critical Reviews in Biotechnology*, 36(6), pp. 1110–1122.

Ecker, D.M., Jones, S.D. & Levine, H.L. (2015) 'The therapeutic monoclonal antibody market', *mAbs*, 7(1), pp. 9–14.

Elshereef, A.A., Jochums, A., Lavrentieva, A., Stuckenberg, L., Scheper, T. & Solle, D. (2019) 'High cell density transient transfection of CHO cells for TGF- $\beta$ 1 expression', *Engineering in Life Sciences*, 19(11), pp. 730–740.

---

Fan, L., Frye, C.C., & Racher, A.J. (2013) 'The use of glutamine synthetase as a selection marker: recent advances in Chinese hamster ovary cell line generation processes', *Pharmaceutical Bioprocessing*, 1(5), pp. 487–502.

Feng, Y., Huang, S. & Teng, F. (2009) 'Controlled Particle Size and Synthesizing Mechanism of Microsphere of Poly(MMA-BuMA) Prepared by Emulsion Polymerization', *Polymer Journal*, 41(4), pp. 266–271.

Fields, W., Fowler, K., Hargreaves, V., Reeve, L. & Bombick, B. (2017) 'Development, qualification, validation and application of the neutral red uptake assay in Chinese Hamster Ovary (CHO) cells using a VITROCELL® VC10® smoke exposure system', *Toxicology in Vitro*, 40, pp. 144–152.

Fisher, A.C., Kanga, M.H., Agarabi, C., Brorson, K., Lee, S.L. & Yoon, S. (2019) 'The Current Scientific and Regulatory Landscape in Advancing Integrated Continuous Biopharmaceutical Manufacturing', *Trends in Biotechnology*, 37(3), pp. 253–267.

Foudazi, R. (2021) 'HIPes to PolyHIPes', *Reactive and Functional Polymers*, 164, 104917.

Fox, S.R., Yap, M.X., Yap, M.G.S. & Wang, D.I.C. (2005) 'Active hypothermic growth: a novel means for increasing total interferon production by Chinese hamster ovary cells', *Biotechnology and Applied Biochemistry*, 41(3), pp. 265–272.

Frampton, J.E. (2017) 'Golimumab: A Review in Inflammatory Arthritis', *BioDrugs*, 31(3), pp. 263–274.

Frieder, J., Kivelevitch, D. & Menter, A. (2018) 'Secukinumab: a review of the anti-IL-17A biologic for the treatment of psoriasis', *Therapeutic Advances in Chronic Disease*, 9(1), pp. 5–21.

Fu, T., Zhang, C., Jing, Y., Jiang, C., Li, Z., Wang, S., Ma, K., Zhang, D., Hou, S., Dai, J., Kou G. & Wang, H. (2016) 'Regulation of cell growth and apoptosis through lactate dehydrogenase C over-expression in Chinese hamster ovary cells', *Applied Microbiology and Biotechnology*, 100(11), pp. 5007–5016.

Gagliardi, T.M., Chelikani, R., Yang, Y., Tuozzolo, G. & Yuan, H. (2019) 'Development of a novel, high-throughput screening tool for efficient perfusion-based cell culture process development', *Biotechnology Progress*, 35(4), pp. 1–12.

Gajria, D. & Chandarlapaty, S. (2011) 'HER2-amplified breast cancer: mechanisms of trastuzumab resistance and novel targeted therapies', *Expert Review of Anticancer Therapy*, 11(2), pp. 263–275.

Gaynes, R. (2017) 'The Discovery of Penicillin—New Insights After More Than 75 Years of Clinical Use', *Emerging Infectious Diseases*, 23(5), pp. 849–853.

GE Healthcare Life Sciences (2013) 'Microcarrier Cell Culture: Principles and Methods', [online] Available at: <<https://www.cytivalifesciences.co.kr/wp-content/uploads/2020/04/AC-Microcarrier-cell-culture.pdf>> [Accessed 22 May 2021]

Gleede, T., Reisman, L., Rieger, E., Mbarushimana, P.C., Rugar, P.A. & Wurm, F.R. (2019) 'Aziridines and azetidines: building blocks for polyamines by anionic and cationic ring-opening polymerization', *Polymer Chemistry*, 10, 3257–3283.

Gokmen, M.T., Camp, W.V., Colver, P.J., Bon, S.A.F. & Prez, F.E.D. (2009) 'Fabrication of Porous "Clickable" Polymer Beads and Rods through Generation of High Internal Phase

---

Emulsion (HIPE) Droplets in a Simple Microfluidic Device', *Macromolecules*, 42(23), pp. 9289–9294.

Goldman, M.H., James, D.C., Rendall, M., Ison, A.P., Hoare, M. & Bull, A.T. (1998) 'Monitoring recombinant human interferon gamma N glycosylation during perfused fluidized bed and stirred tank batch culture of CHO cells', *Biotechnology and Bioengineering*, 60(5), pp. 596–607.

Grace, J.M. & Gerenser, L.J. (2003) 'Plasma Treatment of Polymers', *Journal of Dispersion Science and Technology*, 24(3–4), pp. 305–341.

Groth, T.H., Zlatanov, I. & Altankov, G. (1995) 'Adhesion of human peripheral lymphocytes on biomaterials preadsorbed with fibronectin and vitronectin', *Journal of Biomaterials Science, Polymer Edition*, 6(8), pp. 729–739.

Gstraunthaler G. (2003) 'Alternatives to the use of fetal bovine serum: serum-free cell culture', *ALTEX*, 20(4), pp. 275–281.

Gupta, P., Ismadi, M., Verma, P.J., Fouras, A., Jadhav, S., Bellare, J. & Hourigan, K. (2016) 'Optimization of agitation speed in spinner flask for microcarrier structural integrity and expansion of induced pluripotent stem cells', *Cytotechnology*, 68(1), pp. 45–59.

Hales, T., Adams, M., Bauer, G., Dang, T.D., Harrison, J., Hoang, L.T., Kaliszkyk, C., Margron, V., Mclaughlin, S., Nguyen, T.T., Nguyen, Q.T., Nipkow, T., Obua, S., Pleso, J., Rute, J., Solovyev, A., Ta, T.H.A., Tran, N.T., Trieu, T.D., Urban, J., Vu, K. & Zumkeller, R. (2017) 'A FORMAL PROOF OF THE KEPLER CONJECTURE', *Forum of Mathematics, Pi*, 5, e2, pp. 1–29.

Hanley, T.L. & Yiu, Z.Z.N. (2017) 'Role of IL-17 in plaque psoriasis: therapeutic potential of ixekizumab', *Therapeutics and Clinical Risk Management*, 13, pp. 315–323.

Harshman, L.C. & Srinivas, S. (2010) 'The bevacizumab experience in advanced renal cell carcinoma', *OncoTargets and Therapy*, 3, pp. 179–189.

Hartley, F., Walker, T., Chung, V. & Morten, K. (2018) 'Mechanisms driving the lactate switch in Chinese hamster ovary cells', *Biotechnology and Bioengineering*, 115(8), pp. 1890–1903.

Hayman, M.W., Smith, K.H., Cameron, N.R. & Przyborski, S.A. (2005) 'Growth of human stem cell-derived neurons on solid three-dimensional polymers', *Journal of Biochemical and Biophysical Methods*, 62(3), pp. 231–240.

Hayward, A.S., Eissa, A.M., Maltman, D.J., Sano, N., Przyborski, S.A. & Cameron, N.R. (2013a) 'Galactose-Functionalized PolyHIPE Scaffolds for Use in Routine Three Dimensional Culture of Mammalian Hepatocytes', *Biomacromolecules*, 14(12), pp. 4271–4277.

Hayward, A.S., Sano, N., Przyborski, S.A. & Cameron, N.R. (2013b) 'Acrylic Acid Functionalized PolyHIPE Scaffolds for Use in 3D Cell Culture', *Macromolecular Rapid Communications*, 34(23–24), pp. 1844–1849.

Hedner, U. & Lee, C.A. (2011) 'First 20 years with recombinant FVIIa (NovoSeven)', *Haemophilia*, 17(1), pp. 172–182.

Higel, F., Seidl, A., Sörgel, F. & Friess, W. (2016) 'N-glycosylation heterogeneity and the influence on structure, function and pharmacokinetics of monoclonal antibodies and Fc fusion proteins', *European Journal of Pharmaceutics and Biopharmaceutics*, 100, pp. 94–100.

- 
- Hong, J., Hong, C.K. & Shim, S.E. (2007) 'Synthesis of polystyrene microspheres by dispersion polymerization using poly(vinyl alcohol) as a steric stabilizer in aqueous alcohol media', *Colloids and Surfaces A: Physicochemical and Engineering Aspects*, 302(1–3), pp. 225–233.
- Hossler, P., Khattak, S.F. & Li, Z.J. (2009) 'Optimal and consistent protein glycosylation in mammalian cell culture', *Glycobiology*, 19(9), pp. 936–949.
- Huang, X., Dai, W. & Darzynkiewicz, Z. (2005) 'Enforced adhesion of hematopoietic cells to culture dish induces endomitosis and polyploidy', *Cell Cycle*, 4(6), pp. 801–805.
- Hughes, J. M., Budd, P. M., Tiede, K. & Lewis, J. (2014) 'Polymerized high internal phase emulsion monoliths for the chromatographic separation of engineered nanoparticles', *Journal of Applied Polymer Science*, 132(1), 41229, pp. 1–8.
- Hunt, L., Hacker, D.L., Grosjean, F., De Jesus, M., Uebersax, L., Jordan, M. & Wurm, F.M. (2005) 'Low-temperature pausing of cultivated mammalian cells', *Biotechnology and Bioengineering*, 89(2), pp. 157–163.
- Huš, S. & Krajnc, P. (2014) 'PolyHIPEs from Methyl methacrylate: Hierarchically structured microcellular polymers with exceptional mechanical properties', *Polymer*, 55(17), pp. 4420–4424.
- Ishii, K., Morii, N. & Yamashiro, H. (2019) 'Pertuzumab in the treatment of HER2-positive breast cancer: an evidence-based review of its safety, efficacy, and place in therapy', *Core Evidence*, 14, pp. 51–70.
- Ismadi, M., Gupta, P., Fouras, A., Verma, P., Jadhav, S., Bellare, J. & Hourigan, K. (2014) 'Flow characterization of a spinner flask for induced pluripotent stem cell culture application', *PLoS One*, 9(10), pp. 1–11.
- Jackson, J.M., Witek, M.A., Hupert, M.L., Brady, C., Pullagurla, S., Kamande, J., Aufforth, R.D., Tignanelli, C.J., Torphy, R.J., Yeh, J.J. & Soper, S.A. (2014a) 'UV activation of polymeric high aspect ratio microstructures: ramifications in antibody surface loading for circulating tumor cell selection', *Lab Chip*, 14(1), pp. 106–117.
- Jackson, J.M., Witek, M.A., Hupert, M.L., Brady, C., Pullagurla, S., Kamande, J., Aufforth, R.D., Tignanelli, C.J., Torphy, R.J., Yeh, J.J. & Soper, S.A. (2014b) 'UV activation of polymeric high aspect ratio microstructures: ramifications in antibody surface loading for circulating tumor cell selection – Supplemental Information', *Lab Chip*, 14(1), pp. 106–117. Jäger, V., Büssow, K., Wagner, A., Weber S., Hust, M., Frenzel, A. & Schirrmann T. (2013) 'High level transient production of recombinant antibodies and antibody fusion proteins in HEK293 cells', *BMC Biotechnology*, 13(52), pp. 1–20.
- Jebaramy, J., Ilanchelian, M. & Prabaha, S. (2009) 'Spectral Studies of Toluidine Blue O in the Presence of Sodium Dodecyl Sulfate', *Digest Journal of Nanomaterials and Biostructures*, 4(4), pp. 789–797.
- Jeon, C., Sekhon, S., Yan, D., Afifi, L., Nakamura, M. and Bhutani, T. (2017) 'Monoclonal antibodies inhibiting IL-12, -23, and -17 for the treatment of psoriasis', *Human Vaccines & Immunotherapeutics*, 13(10), pp. 2247–2259.
- Jerums, M. & Yang, X. (2005) 'Optimization of Cell Culture Media', *BioProcess International*, 30(8), pp. 20–23.
-

---

Jing, G., Yu, H., Wang, L., Shan, J., Huang, J., Abdin, Z., Zhao, Y. & Chen, Y. (2015) 'Synthesis and properties of polystyrene-based polyHIPEs reinforced with quadruple hydrogen bond functionality', *Journal of Polymer Research*, 22, 147, pp. 1–11.

Jinhua, L. & Guangyuan, Z. (2014) 'Polystyrene Microbeads by Dispersion Polymerization: Effect of Solvent on Particle Morphology', *International Journal of Polymer Science*, 2014, pp. 1–4.

Johnson, D.W., Sherborne, C., Didsbury, M.P., Pateman, C., Cameron, N.R. & Claeysens, F. (2013) 'Macrostructuring of Emulsion templated Porous Polymers by 3D Laser Patterning', *Advanced Materials*, 25, pp. 3178–3181.

Kalantar-Zadeh, K. (2017) 'History of Erythropoiesis-Stimulating Agents, the Development of Biosimilars, and the Future of Anemia Treatment in Nephrology', *American Journal of Nephrology*, 45(3), pp. 235–247.

Kam, L., Shain, W., Turner, J.N. & Bizios, R. (2001) 'Axonal outgrowth of hippocampal neurons on micro-scale networks of polylysine-conjugated laminin', *Biomaterials*, 22(10), pp. 1049–1054.

Kao, F.T. & Puck, T.T. (1968) 'Genetics of somatic mammalian cells, VII. Induction and isolation of nutritional mutants in Chinese hamster cells', *Proceedings of the National Academy of Sciences of the United States of America*, 60(4), pp. 1275–1281.

Kaplon, H. & Reichert, J.M. (2019) 'Antibodies to watch in 2019', *mAbs*, 11(2), pp. 219–238.

Karst, D.J., Scibona, E., Serra, E., Bielser, J., Souquet, J., Stettler, M., Broly, H., Soos, M., Morbidelli, M. & Villiger, T.K. (2017) 'Modulation and modeling of monoclonal antibody N-linked glycosylation in mammalian cell perfusion reactors', *Biotechnology and Bioengineering*, 114(9), pp. 1978–1990.

Karst, D.J., Steinebach, F., Soos, M. & Morbidelli, M. (2017) 'Process performance and product quality in an integrated continuous antibody production process', *Biotechnology and Bioengineering*, 114(2), pp. 298–307.

Keating, G.M. (2014) 'Bevacizumab: a review of its use in advanced cancer', *Drugs*, 74(16), pp. 1891–1925.

Kent, D., Rickwood, S. & Di Biase, S. (2017) 'Disruption and maturity: The next phase of biologics', [online] QuintilesIMS. Available at: <[https://www.iqvia.com/-/media/iqvia/pdfs/nemea/uk/disruption\\_and\\_maturity\\_the\\_next\\_phase\\_of\\_biologics.pdf](https://www.iqvia.com/-/media/iqvia/pdfs/nemea/uk/disruption_and_maturity_the_next_phase_of_biologics.pdf)> [Accessed 31 March 2020].

Khademhosseini, A., Suh, K.Y., Yang, J.M., Eng, G., Yeh, J., Levenberg, S. & Langer, R. (2004) 'Layer-by-layer deposition of hyaluronic acid and poly-L-lysine for patterned cell co-cultures', *Biomaterials*, 25(17), pp. 3583–3592.

Kimiz-Gebologlu, I., Gulce-Iz, S. & Biray-Avci, C. (2018) 'Monoclonal antibodies in cancer immunotherapy', *Molecular Biology Reports*, 45(6), pp. 2935–2940.

Kinch, M.S. (2015) 'An overview of FDA-approved biologics medicines', *Drug Discovery Today*, 20(4), pp. 393–398.

Knight, E., Murray, B., Carnachan, R. & Przyborski, S. (2011) 'Alvetex®: polystyrene scaffold technology for routine three dimensional cell culture', *Methods in Molecular Biology*, 695, pp. 323–340.

- 
- Kojima, C., Fusaoka-Nishioka, E., Imai, T., Nakahira, A. & Onodera, H. (2016) 'Dendrigraft polylysine coated-poly(glycolic acid) fibrous scaffolds for hippocampal neurons', *Journal of Biomedical Materials Research Part A*, 104(11), pp. 2744–2750.
- Koler, A., Paljevac, M., Cmager, N., Iskra, J., Kolar, M. & Krajnc, P. (2017) 'Poly(4-vinylpyridine) polyHIPEs as catalysts for cycloaddition click reaction', *Polymer*, 126, pp. 402–407.
- Konakovsky, V., Clemens, C., Müller, M.M., Bechmann, J., Berger, M., Schlatter, S. & Herwig, C. (2016) 'Metabolic Control in Mammalian Fed-Batch Cell Cultures for Reduced Lactic Acid Accumulation and Improved Process Robustness', *Bioengineering*, 3(1), 5, pp. 1–29.
- Konstantinov, K.B. & Cooney, C.L. (2014) 'White paper on continuous bioprocessing. May 20-21, 2014 Continuous Manufacturing Symposium', *Journal of Pharmaceutical Sciences*, 104(3), pp. 813–820.
- Krajnc, P., Brown, J.F. & Cameron, N.R. (2002) 'Monolithic Scavenger Resins by Amine Functionalizations of Poly(4-vinylbenzyl chloride-co-divinylbenzene) PolyHIPE Materials', *Organic Letters*, 4(15), pp. 2497–2500.
- Krajnc, P., Štefanec, D., Brown, J.F. & Cameron, N.R. (2005) 'Aryl acrylate based high internal phase emulsions as precursors for reactive monolithic polymer supports', *Journal of Polymer Science Part A: Polymer Chemistry*, 43(2), pp. 296–303.
- Kreye, S., Stahn, R., Nawrath, K., Goralczyk, V., Zoro, B. & Goletz, S. (2019) 'A novel scale-down mimic of perfusion cell culture using sedimentation in an automated microbioreactor (SAM)', *Biotechnology Progress*, 35(5), pp. 1–11.
- Kubota, T., Niwa, R., Satoh, M., Akinaga, S., Shitara, K. & Hanai, N. (2009) 'Engineered therapeutic antibodies with improved effector functions', *Cancer Science*, 100(9), pp. 1566–1572.
- Kunert, R. & Reinhart, D. (2016) 'Advances in recombinant antibody manufacturing', *Applied Microbiology and Biotechnology*, 100(8), pp. 3451–3461.
- Kwon, T., Prentice, H., Oliveira, J.D., Madziva, N., Warkiani, M.E., Hamel, J.P. & Han, J. (2017) 'Microfluidic Cell Retention Device for Perfusion of Mammalian Suspension Culture', *Scientific Reports*, 7, 6703, pp. 1–11.
- Lagassé, H.A.D., Alexaki, A., Simhadri, V.J., Katagiri, N.H., Jankowski, W., Sauna, Z.E. & Kimchi-Sarfaty, C. (2017) 'Recent advances in (therapeutic protein) drug development', *F1000Research*, 6, 113, pp. 1–17.
- Langer, E.S. (2011) 'Trends in Perfusion Bioreactors. The Next Revolution in Bioprocessing?', *BioProcess International*, 9(10), pp. 18–22.
- Langer, E.S. & Rader, R.A. (2014) 'Continuous Bioprocessing and Perfusion: Wider Adoption Coming as Bioprocessing Matures', *BioProcess Journal*, 13(1), pp. 43–49.
- Langford, C.R., Johnson, D.W. & Cameron, N.R. (2014) 'Chemical functionalization of emulsion-templated porous polymers by thiol-ene "click" chemistry', *Polymer Chemistry*, 5(21), pp. 6200–6206.
- Lapierre, F., Cameron, N.R. & Zhu, Y. (2015) 'Ready... set, flow: simple fabrication of microdroplet generators and their use in the synthesis of PolyHIPE microspheres', *Journal of Micromechanics and Microengineering*, 25(3), pp. 1–6.
-

---

Lauro S., Onesti C.E., Righini R. & Marchetti P. (2014) 'The use of bevacizumab in non-small cell lung cancer: an update', *Anticancer Research*, 34(4), pp. 1537–1545.

Lerman, M.J., Lembong, J., Muramoto, S., Gillen, G. & Fisher, J.P. (2018) 'The Evolution of Polystyrene as a Cell Culture Material', *Tissue Engineering Part B*, 24(5), pp. 359–372.

Lewis, N.E., Liu, X., Li, Y., Nagarajan, H., Yerganian, G., O'Brien, E., Bordbar, A., Roth, A.M., Rosenbloom, J., Bian, C., Xie, M., Chen, W., Li, N., Baycin-Hizal, D., Latif, H., Forster, J., Betenbaugh, M.J., Famili, I., Xu, X., Wang, J. & Palsson, B.O. (2013) 'Genomic landscapes of Chinese hamster ovary cell lines as revealed by the *Cricetulus griseus* draft genome', *Nature Biotechnology*, 31(8), pp. 759–765.

Liberti, M.V. & Locasale, J.W. (2016) 'The Warburg Effect: How Does it Benefit Cancer Cells?', *Trends in Biochemical Sciences*, 41(3), pp. 211–218.

Ligon, S.C., Husár, B., Wutzel, H., Holman, R. & Liska, R. (2014) 'Strategies to Reduce Oxygen Inhibition in Photoinduced Polymerization', *Chemical Reviews*, 114(1), pp. 557–589.

Lin, C. & Cheng, S. (2016) 'A review of omalizumab for the management of severe asthma', *Drug Design, Development and Therapy*, 10, pp. 2369–2378.

Lindsley, C. W. (2018) 'New 2017 Data and Statistics for Pharmaceutical Products', *ACS Chemical Neuroscience*, 9(7), pp. 1518–1519.

Lis, A.V., Schneider, K., Weber, J., Keasling, J.D., Jensen, M.K. & Klein, T. (2019) 'Exploring small-scale chemostats to scale up microbial processes: 3-hydroxypropionic acid production in *S. cerevisiae*', *Microbial Cell Factories*, 18(50), pp. 1–11.

Liumbruno G., Bennardello F., Lattanzio A., Piccoli P. & Rossetti G. (2009) 'Recommendations for the transfusion of plasma and platelets', *Blood Transfusion*, 7(2), pp. 132–150.

Lu, R., Hwang, Y., Liu, I., Lee, C., Tsai, H., Li H. and Wu, H. (2020) 'Development of therapeutic antibodies for the treatment of diseases', *Journal of Biomedical Science*, 27(1), pp. 1–30.

Lucey, B.P., Nelson-Rees, W.A. & Hutchins, G.M. (2009) 'Henrietta Lacks, HeLa cells, and cell culture contamination', *Archives of Pathology & Laboratory Medicine*, 133(8), pp. 1463–1467.

Ludwig, D.L. (2006) 'Mammalian Expression Cassette Engineering for High-Level Protein Production', *BioProcess International*, 4(5), S14–S23.

MacDonald, C., Finlay, D.B., Javed, A., Glass, M., Graham, E.S. (2014) 'Development of positive control tissue for in situ hybridisation using Alvetex scaffolds', *Journal of Neuroscience Methods*, 238, pp. 70–77.

Macek, B., Forchhammer, K., Hardouin, J., Weber-Ban, E., Grangeasse, C. & Mijakovic, I. (2019) 'Protein post-translational modifications in bacteria', *Nature Reviews Microbiology*, 17(11), pp. 651–664.

Macpherson, I. (1963) 'Characteristics of a Hamster Cell Clone Transformed by Polyoma Virus', *Journal of the National Cancer Institute*, 30(4), pp. 795–815.

Marks, L. (2012) 'The birth pangs of monoclonal antibody therapeutics', *mAbs*, 4(3), pp. 403–412.

- 
- Masterton, R.J. & Smales, C.M. (2014) 'The impact of process temperature on mammalian cell lines and the implications for the production of recombinant proteins in CHO cells', *Pharmaceutical Bioprocessing*, 2(1), pp. 49–61.
- Mazia, D., Schatten, G. & Sale, W. (1975) 'Adhesion of cells to surfaces coated with polylysine. Applications to electron microscopy', *Journal of Cell Biology*, 66(1), pp. 198–200.
- Mease, P.J. (2011) 'Certolizumab pegol in the treatment of rheumatoid arthritis: a comprehensive review of its clinical efficacy and safety', *Rheumatology (Oxford)*, 50(2), pp. 261–270.
- Mercier, A., Deleuze, H. & Mondain-Monval, O. (2000) 'Preparation and functionalization of (vinyl)polystyrene polyHIPE®: Short routes to binding functional groups through a dimethylene spacer', *Reactive and Functional Polymers*, 46(1), pp. 67–79.
- Miller, K.L. & Lanthier, M. (2015) 'Innovation in biologic new molecular entities: 1986–2014', *Nature Reviews Drug Discovery*, 14(2), pp. 83–83.
- Moglia, R.S., Holm, J.L., Sears, N.A., Wilson, C.J., Harrison, D.M. & Cosgriff-Hernandez, E. (2011) 'Injectable polyHIPEs as high-porosity bone grafts', *Biomacromolecules*, 12(10), pp. 3621–3628.
- Moglia, R., Whitely, M., Brooks, M., Robinson, J., Pishko, M., Cosgriff-Hernandez, E. (2014) 'Solvent-free fabrication of polyHIPE microspheres for controlled release of growth factors', *Macromolecular Rapid Communications*, 35(14), pp. 1301–1305.
- Mohan, V. (2002) 'Which Insulin to Use? Human or Animal?', *Current Science*, 83(12), pp. 1544–1547.
- Mondello, P., Cuzzocrea, S., Navarra, M. & Mian, M. (2016) '90 Y-ibritumomab tiuxetan: a nearly forgotten opportunity', *Oncotarget*, 7(7), pp. 7597–7609.
- Muhammed, Y. (2020) 'The Best IgG Subclass for the Development of Therapeutic Monoclonal Antibody Drugs and their Commercial Production: A Review', *Immunome Research*, 16(1), 173, pp. 1–12.
- Mulero, P., Midaglia, L. & Montalban, X. (2018) 'Ocrelizumab: a new milestone in multiple sclerosis therapy', *Therapeutic Advances in Neurological Disorders*, 11, pp. 1–6.
- Naranda, J., Sušec, M., Maver, U., Gradišnik, L., Gorenjak, M., Vukasovi, A., Ivkovi, A., Rupnik, M.S., Vogrin, M. & Krajnc, P. (2016) 'Polyester type polyHIPE scaffolds with an interconnected porous structure for cartilage regeneration', *Scientific Reports*, 6, 28695, pp. 1–11.
- Nelson, A. L. (2010) 'Antibody fragments: hope and hype', *mAbs*, 2(1), pp. 77–83.
- Nelson, P.N., Reynolds, G.M., Waldron, E.E., Ward, E., Giannopoulos, K. & Murray, P. G. (2000) 'Monoclonal antibodies', *Journal of Clinical Pathology*, 53(3), pp. 111–117.
- Neutelings, T., Lambert, C.A., Nusgens, B.V. & Colige, A.C. (2013) 'Effects of Mild Cold Shock (25 C) Followed by Warming Up at 37 C on the Cellular Stress Response', *PLoS One*, 8(7), pp. 1–15.
- O'Brien, S. & Österborg, A. (2010) 'Ofatumumab: a new CD20 monoclonal antibody therapy for B-cell chronic lymphocytic leukemia', *Clinical Lymphoma, Myeloma & Leukemia*, 10(5), pp. 361–368.
-

---

Owen, R., Sherborne, C., Paterson, T., Green, N.H., Reilly, G.C. & Claeysens, F. (2016) 'Emulsion templated scaffolds with tunable mechanical properties for bone tissue engineering', *Journal of the Mechanical Behavior of Biomedical Materials*, 54, pp. 159–172.

Pais, D.A.M., Carrondo, M.J.T., Alves, P.M. & Teixeira, A.P. (2014) 'Towards real-time monitoring of therapeutic protein quality in mammalian cell processes', *Current Opinion in Biotechnology*, 30, pp. 161–167.

Paterson, T. (2017) 'PolyHIPE Microspheres for Injectable Bone Tissue Engineering Applications', PhD thesis, The University of Sheffield, Sheffield.

Paterson, T.E., Gigliobianco, G., Sherborne, C., Green, N.H., Dugan, J.M., MacNeil, S., Reilly, G.C. & Claeysens, F. (2018) 'Porous microspheres support mesenchymal progenitor cell ingrowth and stimulate angiogenesis', *APL Bioengineering*, 2(2), 026103, pp. 1–19.

Petrenko, Y., Chudickova, M., Vackova, I., Groh, T., Kosnarova, E., Cejkova, J., Turnovcova, K., Petrenko, A., Syková, E. & Kubinova, S. (2019) 'Clinically Relevant Solution for the Hypothermic Storage and Transportation of Human Multipotent Mesenchymal Stromal Cells', *Stem Cells International*, 2019, pp. 1–11.

Poggioli, G., Laureti, S., Campieri, M., Pierangeli, F., Gionchetti, P., Ugolini, F., Gentilini, L., Bazzi, P., Rizzello, F. & Coscia, M. (2007) 'Infliximab in the treatment of Crohn's disease', *Therapeutics and Clinical Risk Management*, 3(2), pp. 301–308.

Pollock, J., Ho, S.V. & Farid, S.S. (2013) 'Fed-batch and perfusion culture processes: economic, environmental, and operational feasibility under uncertainty', *Biotechnology and Bioengineering*, 110(1), pp. 206–219.

Pribyl, J.G., Taylor-Pashow, K.M.L., Shehee, T.C. & Benicewicz, B.C. (2018) 'High-Capacity Poly(4-vinylpyridine) Grafted PolyHIPE Foams for Efficient Plutonium Separation and Purification', *ACS Omega*, 3(7), pp. 8181–8189.

Puck, T.T., Cieciura, S.J. & Robinson, A. (1958) 'Genetics of somatic mammalian cells. III. Long-term cultivation of euploid cells from human and animal subjects', *Journal of Experimental Medicine*, 108(6), pp. 945–956.

Pulko, I. & Krajnc, P. (2012) 'High Internal Phase Emulsion Templating – A Path To Hierarchically Porous Functional Polymers', *Macromolecular Rapid Communications*, 33, pp. 1731–1746.

Qi, Y., Yan, Z. & Huang, J. (2001) 'Chromatography on DEAE ion-exchange and Protein G affinity columns in tandem for the separation and purification of proteins', *Journal of Biochemical and Biophysical Methods*, 49(1–3), pp. 263–273.

Quianzon, C.C. & Cheikh, I. (2012) 'History of insulin', *Journal of Community Hospital Internal Medicine Perspectives*, 2(2), pp. 1–3.

Rafiq, Q.A., Coopman, K., Nienow, A.W. & Hewitt, C.J. (2016) 'Systematic microcarrier screening and agitated culture conditions improves human mesenchymal stem cell yield in bioreactors', *Biotechnology Journal*, 11(4), pp. 473–486.

Repetto, G., del Peso, A., Zurita, J.L. (2008) 'Neutral red uptake assay for the estimation of cell viability/cytotoxicity', *Nature Protocols*, 3(7), pp. 1125–1131.

---

Reprocell (2019a) 'Achieve Genuine 3D Cell Culture, Simply and Routinely', [online] Available at: <<https://www.reprocell.com/downloads/1550854126MM-ALVETEX-SYSTEMS-D001004-A4.pdf>> [Accessed 26 June 2020].

Reprocell (2019b) 'Maintenance of Intact Tissues Using Alvetex Strata', [online] Available at: <[https://www.reprocell.com/downloads/1536665607AN-ST-01\\_AppNote\\_Strata\\_01\\_A4\\_1.pdf](https://www.reprocell.com/downloads/1536665607AN-ST-01_AppNote_Strata_01_A4_1.pdf)> [Accessed 26 June 2020].

Reprocell (2019c) 'Reinnervate Perfusion Plate: Dynamic Circulation and Perfusion of Culture Medium Within a Multi-welled Plate', [online] Available at: <[https://www.reprocell.com/downloads/1536665334AN-SC-08\\_AppNote\\_Scaffold\\_08-A4.pdf](https://www.reprocell.com/downloads/1536665334AN-SC-08_AppNote_Scaffold_08-A4.pdf)> [Accessed 26 June 2020].

Reprocell (2019d) 'Example Protocol for the Culture of the CHO-K1 Cell Line on Alvetex™ Scaffold in Well Plate and Well Insert Formats', [online] Available at: <<https://www.reprocell.com/downloads/1555082708PR-ALVETEX-SCAFFOLD-D026002-US.pdf>> [Accessed 26 June 2020].

Reprocell (2019e) 'Alvetex™ Scaffold: Quick Start', [online] Available at: <<https://www.reprocell.com/downloads/1555077361PR-ALVETEX-SCAFFOLD-D001002-US.pdf>> [Accessed 26 June 2020].

Riedel, S. (2005) 'Edward Jenner and the History of Smallpox and Vaccination', *Baylor University Medical Center Proceedings*, 18(1), pp. 21–25.

Rieder, C.L. & Cole, R.W. (2002) 'Cold-Shock and the Mammalian Cell Cycle', *Cell Cycle*, 1(3), pp. 169–175.

Riley, T.R. & Riley, T.T. (2019) 'Profile of crizanlizumab and its potential in the prevention of pain crises in sickle cell disease: evidence to date', *Journal of Blood Medicine*, 10, pp. 307–311.

Robinson, N.J. (2017) 'Low-temperature pausing: an alternative short-term preservation method for use in cell therapies', PhD thesis, Loughborough University, Loughborough.

Robinson, N.J., Picken, A. & Coopman, K. (2014) 'Low temperature cell pausing: an alternative short-term preservation method for use in cell therapies including stem cell applications', *Biotechnology Letters*, 36(2), pp. 201–209.

Rodgers, K.R. & Chou, R.C. (2016) 'Therapeutic monoclonal antibodies and derivatives: Historical perspectives and future directions', *Biotechnology Advances*, 34(6), pp. 1149–1158.

Rodríguez-Hernández, J., Gatti, M. & Klok, H. (2003) 'Highly Branched Poly(l-lysine)', *Biomacromolecules*, 4(2), pp. 249–258.

Roobol, A., Carden, M.J., Newsam, R.J. & Smales, C.M. (2009) 'Biochemical insights into the mechanisms central to the response of mammalian cells to cold stress and subsequent rewarming', *The FEBS Journal*, 276(1), pp. 286–302. Rourou, S., van der Ark, A., van der Velden, T. & Kallel, H. (2009) 'Development of an animal-component free medium for vero cells culture', *Biotechnology Progress*, 25(6), pp. 1752–1761.

Rosser, M.P., Xia, W., Hartsell, S., McCaman, M., Zhu, Y., Wang, S., Harvey, S., Bringmann, P. & Cobb, R.R. (2005) 'Transient transfection of CHO-K1-S using serum-free medium in suspension: a rapid mammalian protein expression system', *Protein Expression & Purification*, 40(2), pp. 237–243.

- 
- Sart, S., Schneider, Y.J. & Agathos, S.N. (2009) 'Ear mesenchymal stem cells: an efficient adult multipotent cell population fit for rapid and scalable expansion', *Journal of Biotechnology*, 139(4), pp. 291–299.
- Schmidt, P.J. & Leacock, A.G. (2002) 'Forgotten transfusion history: John Leacock of Barbados', *BMJ*, 325(7378), pp. 1485–1487.
- Schmidt, S.R. (2017) 'Drivers, Opportunities, and Limits of Continuous Processing', *Bio-Process International*, 15(3), pp. 30–37.
- Schwab, M.G., Senkovska, I., Rose, M., Klein, N., Koch, M., Pahnke, J., Jonschker, G., Schmitz, B., Hirscherd, M. & Kaskel, S. (2009) 'High surface area polyHIPEs with hierarchical pore system', *Soft Matter*, 5(5), pp. 1055–1059.
- Shoae, M., Khorashadizadeh, M., Derakhshani, A., Safarnejad, M.R. & Safarpour, H. (2019) 'An overview of the current status of engineered therapeutic monoclonal antibodies', *International Pharmacy Acta*, 2(1), pp. 1–10.
- Shoulders, M.D. & Raines, R.T. (2009) 'Collagen structure and stability', *Annual Review of Biochemistry*, 78, pp. 929–958.
- Shaw, G., Morse, S., Ararat, M. & Graham, F.L. (2002) 'Preferential transformation of human neuronal cells by human adenoviruses and the origin of HEK 293 cells', *FASEB Journal*, 16(8), pp. 869–871.
- Shouval, D. (2003) 'Hepatitis B vaccines', *J Hepatol*, 39(Suppl. 1), pp. 70–76.
- Shukla, S.C., Singh, A., Pandey, A.K. & Mishra, A. 'Review on production and medical applications of  $\epsilon$ -polylysine', *Biochemical Engineering Journal*, 65, pp. 70–81.
- Shulman, M., Wilde, C.D. & Köhler, G. (1978) 'A better cell line for making hybridomas secreting specific antibodies', *Nature*, 276(5685), pp. 269–270.
- Siddiqui, M.A. & Scott, L.J. (2005) 'Infliximab: a review of its use in Crohn's disease and rheumatoid arthritis', *Drugs*, 65(15), pp. 2179–2208.
- Silverstein, M.S., Tai, H., Sergienko, A., Lumelsky, Y. & Pavlovsky, S. (2005) 'PolyHIPE: IPNs, hybrids, nanoscale porosity, silica monoliths and ICP-based sensors', *Polymer*, 46(17), pp. 6682–6694.
- Singh, A., Yadav, R.K. & Srivastava, A. (2009) 'Synthesis of resole-type phenolic beads from phenol and formaldehyde by suspension polymerization technique', *Journal of Applied Polymer Science*, 112, pp. 1005–1011.
- Smith, I., Haag, M., Ugbode, C., Tams, D., Rattray, M., Przyborski, S., Bithell, A., Whalley, B.J. (2015) 'Neuronal-glia populations form functional networks in a biocompatible 3D scaffold', *Neuroscience Letters*, 609, pp. 198–202.
- Spiegel, R.J., Spicehandler, J.R., Jacobs, S.L. & Oden, E.M. (1986) 'Low incidence of serum neutralizing factors in patients receiving recombinant alfa-2b interferon (intron a)', *The American Journal of Medicine*, 80(2), pp. 223–228.
- Starzyk, K., Richards, S., Yee, J., Smith, S.E. & Kingma W. (2007) 'The long-term international safety experience of imiglucerase therapy for Gaucher disease', *Molecular Genetics and Metabolism*, 90(2), pp. 157–163.

- 
- Steger, K., Brady, J., Wang, W., Duskin, M., Donato, K. & Peshwa, M. (2015) 'CHO-S antibody titers >1 gram/liter using flow electroporation-mediated transient gene expression followed by rapid migration to high-yield stable cell lines', *Journal of Biomolecular Screening*, 20(4), pp. 545–551.
- Sun, P., Yang, S., Sun, X., Wang, Y., Jia, Y., Shang, P., Tian, H., Li, G., Li, R., Zhang, X. & Nie, C. (2019) 'Preparation of PolyHIPE Scaffolds for 3D Cell Culture and the Application in Cytotoxicity Evaluation of Cigarette Smoke', *Polymers*, 11(6), 959, pp. 1–13.
- Sunley, K., Tharmalingam, T. & Butler, M. (2008) 'CHO cells adapted to hypothermic growth produce high yields of recombinant beta-interferon', *Biotechnology Progress*, 24(4), pp. 898–906.
- Tanaka, T., Hishitani, Y. & Ogata, A. (2014) 'Monoclonal antibodies in rheumatoid arthritis: comparative effectiveness of tocilizumab with tumor necrosis factor inhibitors', *Biologics: Targets and Therapy*, 8, pp. 141–153.
- Tannock, I.F., Steele, D. & Roberts, J. (1986) 'Influence of reduced concentration of L-glutamine on growth and viability of cells in monolayer, in spheroids, and in experimental tumours', *British Journal of Cancer*, 54(5), pp. 733–741.
- Tharmalingam, T., Sunley, K., Spearman, M. & Butler, M. (2011) 'Enhanced production of human recombinant proteins from CHO cells grown to high densities in macroporous microcarriers', *Molecular Biotechnology*, 49(3), pp. 263–276.
- Thompson, B., Clifford, J., Jenns, M., Smith, A., Field, R., Nayyar, K. & James, D.C. (2017) 'High-throughput quantitation of Fc-containing recombinant proteins in cell culture supernatant by fluorescence polarization spectroscopy', *Analytical Biochemistry*, 534, pp. 49–55.
- Thompson, L.H. & Baker, R.M. (1973) 'Isolation of Mutants of Cultured Mammalian Cells', *Methods in Cell Biology*, 6, pp. 209–281.
- Tjio, J.H. & Puck, T.T. (1958) 'Genetics of somatic mammalian cells. II. Chromosomal constitution of cells in tissue culture', *Journal of Experimental Medicine*, 108(2), pp. 259–268.
- Tobinai, K., Klein, C., Oya, N. & Fingerle-Rowson, G. (2017) 'A Review of Obinutuzumab (GA101), a Novel Type II Anti-CD20 Monoclonal Antibody, for the Treatment of Patients with B-Cell Malignancies', *Advances in Therapy*, 34(2), pp. 324–356.
- Toussaint, C., Henry, O. & Durocher, Y. (2016) 'Metabolic engineering of CHO cells to alter lactate metabolism during fed-batch cultures', *Journal of Biotechnology*, 217, pp. 122–131.
- Tunc, Y., Hasirci, N. & Ulubayram, K. (2012) 'Synthesis of Emulsion-Templated Acrylic-Based Porous Polymers: From Brittle to Elastomeric', *Soft Materials*, 10(4), pp. 449–461.
- Ueda, M.J. & Takeichi, M. (1976) 'Two Mechanisms in Cell Adhesion Revealed by Effects of Divalent Cations', *Cell Structure and Function*, 1, pp. 377–388.
- Ugbode, C.I., Hirst, W.D. & Rattray, M. (2016) 'Astrocytes Grown in Alvetex® Three Dimensional Scaffolds Retain a Non-reactive Phenotype', *Neurochemical Research*, 41(8), pp. 1857–1867.
- Urlaub, G., Käs, E., Carothers, A.M. & Chasin, L.A. (1983) 'Deletion of the diploid dihydrofolate reductase locus from cultured mammalian cells', *Cell*, 33(2), pp. 405–412.
- Urquhart, L. (2018) 'Market watch: Top drugs and companies by sales in 2017', *Nature Reviews Drug Discovery*, 17(4), pp. 232.

---

Urquhart, L. (2019) 'Top drugs and companies by sales in 2018', *Nature Reviews Drug Discovery*, 18, pp. 245.

Urquhart, L. (2020) 'Top companies and drugs by sales in 2019', *Nature Reviews Drug Discovery*, 19(4), pp. 228.

van der Valk, J., Mellor, D., Brands, R., Fischer, R., Gruber, F., Gstraunthaler, G., Hellebrekers, L., Hyllner, J., Jonker, F.H., Prieto, P., Thalen, M. & Baumans, V. (2004) 'The humane collection of fetal bovine serum and possibilities for serum-free cell and tissue culture', *Toxicology in Vitro*, 18(1), pp. 1–12.

van Wezel, A.L. (1967) 'Growth of Cell-strains and Primary Cells on Micro-carriers in Homogeneous Culture', *Nature*, 216(5110), pp. 64–65.

Vancha, A.R., Govindaraju, S., Parsa, K.V., Jasti, M., González-García, M. & Ballester, R.P. (2004) 'Use of polyethyleneimine polymer in cell culture as attachment factor and lipofection enhancer', *BMC Biotechnology*, 4(23), pp. 1–12.

Vanz, A.L.S., Renard, G., Palma, M.S., Chies, J.M., Dalmora, S.L., Basso, L.A. & Santos, D.S. (2008) 'Human granulocyte colony stimulating factor (hG-CSF): cloning, overexpression, purification and characterization', *Microbial Cell Factories*, 7(13), pp. 1–12.

Vergara, M., Becerra, S., Berrios, J., Osses, N., Reyes, J., Rodríguez-Moyá, M., Gonzalez, R. & Altamirano, C. (2014) 'Differential Effect of Culture Temperature and Specific Growth Rate on CHO Cell Behavior in Chemostat Culture', *PLoS One*, 9(4), pp. 1–6.

Vleggeert-Lankamp, C.L., Pêgo, A.P., Lakke, E.A., Deenen, M., Marani, E. & Thomeer, R.T. (2004) 'Adhesion and proliferation of human Schwann cells on adhesive coatings', *Biomaterials*, 25(14), pp. 2741–2751.

Voisard, D., Meuwly, F., Ruffieux, P.A., Baer, G. & Kadouri, A. (2003) 'Potential of cell retention techniques for large-scale high-density perfusion culture of suspended mammalian cells', *Biotechnology and Bioengineering*, 82(7), pp. 751–765.

Vulto, A.G. & Jaquez, O.A. (2017) 'The process defines the product: what really matters in biosimilar design and production?', *Rheumatology*, 56(S4), iv14–iv29.

Walsh, G. (2018) 'Biopharmaceutical benchmarks 2018', *Nature Biotechnology*, 36(12), pp. 1136–1145.

Walsh, G. & Jefferis, R. (2006) 'Post-translational modifications in the context of therapeutic proteins', *Nature Biotechnology*, 24(10), pp. 1241–1252.

Wang, A.J., Paterson, T., Owen, R., Sherborne, C., Dugan, J., Li, J. & Claeysens, F. (2016) 'Photocurable high internal phase emulsions (HIPEs) containing hydroxyapatite for additive manufacture of tissue engineering scaffolds with multi-scale porosity', *Materials Science and Engineering C*, 67, pp. 51–58.

Wang, B., Prinsen, P., Wang, H., Bai, Z., Wang, H., Luque, R., Xuan, J. (2017) 'Macroporous materials: microfluidic fabrication, functionalization and applications', *Chemical Society Reviews*, 46(3), pp. 855–914.

Wang, W., Singh, S., Zeng, D.L., King, K. & Nema, S. (2007) 'Antibody structure, instability, and formulation', *Journal of Pharmaceutical Sciences*, 96(1), pp. 1–26.

---

Wang, X., Yang, L., Cao, W., Ying, H., Chen, K. & Ouyang, P. (2016) 'Efficient Production of Enantiopure d-Lysine from l-Lysine by a Two-Enzyme Cascade System', *Catalysts*, 6(11), 168, pp. 1–12.

Wei, Y., Sun, X., Xia, X., Cui, F., He, Y., Liu, B., & Xu, Q. (2009) 'Hyaluronic Acid Hydrogel Modified with Nogo-66 Receptor Antibody and Poly(L-Lysine) Enhancement of Adherence and Survival of Primary Hippocampal Neurons', *Journal of Bioactive and Compatible Polymers*, 24(3), pp. 205–219.

Weinberg, W.C., Frazier-Jessen, M.R., Wu, W.J., Weir, A., Hartsough, M., Keegan, P. & Fuchs, C. (2005) 'Development and regulation of monoclonal antibody products: challenges and opportunities', *Cancer and Metastasis Reviews*, 24(4), pp. 569–584.

White, G.C. (2010) 'Hemophilia: an amazing 35-year journey from the depths of HIV to the threshold of cure', *Transactions of the American Clinical and Climatological Association*, 121, pp. 61–75.

Whitely, M., Rodriguez-Rivera, G., Waldron, C., Mohiuddin, S., Cereceres, S., Sears, N., Ray, N. & Cosgriff-Hernandez, E. (2019) 'Porous PolyHIPE microspheres for protein delivery from an injectable bone graft', *Acta Biomaterialia*, 93, pp. 169–179.

Whitford, W.G. (2015) 'Single-use perfusion bioreactors support continuous biomanufacturing', *Pharmaceutical Bioprocessing*, 3(1), pp. 75–93.

Whitford, W.G. & Cadwell, J.J.S. (2009) 'Interest in Hollow-Fiber Perfusion Bioreactors Is Growing', *BioProcess International*, 7, pp. 54–63.

Woodward, R.T., Jobbe-Duval, A., Marchesini, S., Anthony, D.B., Petit, C. & Bismarck, A. (2017) 'Hypercrosslinked polyHIPEs as precursors to designable, hierarchically porous carbon foams', *Polymer*, 115, pp. 146–153.

Wu, R., Menner, A. & Bismarck, A. (2013) 'Macroporous polymers made from medium internal phase emulsion templates: Effect of emulsion formulation on the pore structure of polyMIPes', *Polymer*, 54(21), pp. 5511–5517.

Xie, L., Pilbrough, W., Metallo, C., Zhong, T., Pikus, L., Leung, J., Auninš, J.G. & Zhou, W. (2002) 'Serum-free suspension cultivation of PER.C6(R) cells and recombinant adenovirus production under different pH conditions', *Biotechnology and Bioengineering*, 80(5), pp. 569–579.

Xu, J., Rehmann, M.S., Xu, M., Zheng, S., Hill, C., He, Q., Borys, M.C. & Li, Z.J. (2020). 'Development of an intensified fed-batch production platform with doubled titers using N-1 perfusion seed for cell culture manufacturing', *Bioresources and Bioprocessing*, 7, 17, pp. 1–16.

Xu, M., McCanna, D.J. & Sivak, J.G. (2015) 'Use of the viability reagent PrestoBlue in comparison with alamarBlue and MTT to assess the viability of human corneal epithelial cells', *Journal of Pharmacological and Toxicological Methods*, 71, pp. 1–7.

Xu, W., Sun, F., Liu, J., Li, X. & Zhang, F. (2015) 'Polymerization of Dicyclopentadiene/Styrene in PolyHIPE', *Materials Science Forum*, 815, pp. 562–567.

Xu, Y., Hoshi, Y. & Ober, C.K. (2011) 'Photo-switchable polyelectrolyte brush for dual protein patterning', *Journal of Materials Chemistry*, 21(36), pp. 13789–13792.

- 
- Xue, W., Mizukami, I., Todd III, R.F. & Petty, H.R. (1997) 'Urokinase-Type Plasminogen Activator Receptors Associate with and  $\alpha_5\beta_1$  Integrins of Fibrosarcoma Cells: Dependence on Extracellular Matrix Components', *Cancer Research*, 57, pp. 1682–1689.
- Yabannavar, V.M., Singh, V. & Connelly, N.V. (1992) 'Mammalian cell retention in a spin-filter perfusion bioreactor', *Biotechnology and Bioengineering*, 40, pp. 925–933.
- Yang, H.S., Jeon, O., Bhang, S.H., Lee, S. & Kim, B. (2010) 'Suspension culture of mammalian cells using thermosensitive microcarrier that allows cell detachment without proteolytic enzyme treatment', *Cell Transplantation*, 19(9), pp. 1123–1132.
- Yang, X., Tan, L., Xia, L., Wood, C.D. & Tan, B. (2015) 'Hierarchical Porous Polystyrene Monoliths from PolyHIPE', *Macromolecular Rapid Communications*, 36(17), pp. 1553–1558.
- Yannuzzi, N.A. & Freund, K.B. (2019) 'Brolicizumab: evidence to date in the treatment of neovascular age-related macular degeneration', *Clinical Ophthalmology*, 13, pp. 1323–1329.
- Yavin, E. & Yavin, Z. (1974) 'Attachment and culture of dissociated cells from rat embryo cerebral hemispheres on polylysine-coated surface', *Journal of Cell Biology*, 62(2), pp. 540–546.
- Yoo, E.M., Chintalacheruvu, K.R., Penichet, M.L. & Morrison, S.L. (2002) 'Myeloma expression systems', *Journal of Immunological Methods*, 261(1–2), pp. 1–20.
- Yoon, S.K., Kim, S.H., Song, J.Y. & Lee, G.M. (2006) 'Biphasic culture strategy for enhancing volumetric erythropoietin productivity of Chinese hamster ovary cells', *Enzyme and Microbial Technology*, 39(3), pp. 362–365.
- Zamani, L., Lundqvist, M., Zhang, Y., Aberg, M., Edfors, F., Bidkhorji, G., Lindahl, A., Mie, A., Mardinoglu, A., Field, R., Turner, R., Rockberg, J. & Chotteau, V. (2018) 'High Cell Density Perfusion Culture has a Maintained Exoproteome and Metabolome', *Biotechnology Journal*, 13(10), pp. 1–11.
- Zeiger, A.S., Hinton, B. & Van Vliet, K.J. (2013) 'Why the dish makes a difference: quantitative comparison of polystyrene culture surfaces', *Acta Biomaterialia*, 9(7), pp. 7354–7361.
- Zhang, H. & Cooper, A.I. (2005) 'Synthesis and applications of emulsion-templated porous materials', *Soft Matter*, 1(2), pp. 107–113.
- Zhang, J. & Robinson, D. (2005) 'Development of Animal-free, Protein-Free and Chemically-Defined Media for NS0 Cell Culture', *Cytotechnology*, 48(1–3), pp. 59–74.
- Zhang, T., Sanguramath, R.A., Israel, S. & Silverstein, M.S. (2019) 'Emulsion Templating: Porous Polymers and Beyond', *Macromolecules*, 52(15), pp. 5445–5479.
- Zhang, Y., Stobbe, P., Silvander, C.O. & Chotteau, V. (2015) 'Very high cell density perfusion of CHO cells anchored in a non-woven matrix-based bioreactor', *Journal of Biotechnology*, 213, pp. 28–41.
- Zhao, L., Fu, H., Zhou, W. & Hu, W. (2015) 'Advances in process monitoring tools for cell culture bioprocesses', *Engineering in Life Sciences*, 15, pp. 459–468.
- Zheng, K., Bantog, C. & Bayer, R. (2011) 'The impact of glycosylation on monoclonal antibody conformation and stability', *mAbs*, 3(6), pp. 568–576.

---

Zhu, J. (2012) 'Mammalian cell protein expression for biopharmaceutical production', *Biotechnology Advances*, 30(5), pp. 1158–1170.

Zhu, J., Wooh, J.W., Hou, J.J., Hughes, B.S., Gray, P.P. & Munro, T.P. (2012) 'Recombinant human albumin supports single cell cloning of CHO cells in chemically defined media', *Biotechnology Progress*, 28(3), pp. 887–891.

Zou, L., Lai, H., Zhou, Q. & Xiao, F. (2011) 'Lasting controversy on ranibizumab and bevacizumab', *Theranostics*, 1, pp. 395–402.

Zydney, A.L. (2016) 'Continuous downstream processing for high value biological products: A Review', *Biotechnology and Bioengineering*, 113(3), pp. 465–475.